This document is:

Pons, S., ed. *Proceedings of the 5th International Conference on Cold Fusion*. 1995, IMRA Europe, Sophia Antipolis Cedex, France: Monte-Carlo, Monaco. 640.

The printed book is in one volume, but this version has been split into two parts to facilitate downloading.

This is Part 1, cover page to page 200:

http://lenr-canr.org/acrobat/PonsSproceeding.pdf

Part 2, page 201 to page 640, is here:

http://lenr-canr.org/acrobat/PonsSproceedinga.pdf

PROCEEDINGS OF THE 5TH INTERNATIONAL CONFERENCE ON COLD FUSION

ICCF-5
April 9-13, 1995
Hotel Loews
Monte-Carlo, Monaco

Proceedings of the 5th International Conference on Cold Fusion

April 9-13, 1995
Monte-Carlo, Monaco

International Conference on Cold Fusion 5
Valbonne FRANCE

Published by
International Conference on Cold Fusion 5, Valbonne FRANCE

Printed in FRANCE

ORDERING INFORMATION

Copies of these Proceedings may be ordered from:

International Conference on Cold Fusion 5
IMRA Europe, SA
Centre Scientifique
BP 213
06904 SOPHIA ANTIPOLIS CEDEX
FRANCE
(33) 93 95 73 37 Tel (33) 93 95 73 30 Fax

PREFACE

The 5th International Conference on Cold Fusion was held at the Loew's Hotel complex in Monte Carlo, Monaco, April 9-13, 1995. The previous meetings were convened at Salt Lake City, Utah (USA, 1990), Como (Italy, 1991), Nagoya (Japan, 1992), and Maui (Hawaii, USA, 1994). The International Advisory Board elected at its meeting in Monaco to hold the 6th Conference in Hokkaido, Japan, in 1996.

There were over 200 registered participants at this Conference representing 15 countries: 67 from the United States, 51 from France, 47 from Japan, 38 from Italy, 5 from Russia, 4 from Canada, 4 from Germany, 3 from England, 1 from China, 1 from India, 2 from Spain, 1 from Hong Kong, 1 from Korea, 1 from the Netherlands, and 2 from Switzerland.

The Volume is divided thematically into 6 sections following the order in which the papers were presented at the Conference: Introduction and Overviews, Calorimetry and Excess Power, Nuclear Measurements, Theory and Modelling, Cathode Loading and Materials, and New Developments. The oral presentations were held in single sessions, which were followed by poster sessions. The Conference Program was organized around 14 special and plenary lectures, 44 oral presentations, and 132 poster presentations. The tasks of planning and organizing the scientific program, selecting the papers presented, and inviting of all the speakers and presenters were undertaken by Dr. Martin Fleischmann and Dr. David Thompson, to whom the ICCF5 Association is indebted.

We have published in these Proceedings the manuscripts that were received from the various authors following their presentation at the meeting. We apologize for not publishing the many manuscripts which were submitted to us for publication which were either (a) submitted by persons not present at the Conference, or (b) were far outside the designated manuscript length, or (c) were in addition to the allotted number of presentations allowed to the author, or (d) were markedly different from the actual paper(s) presented at the meeting.

New results reporting the generation of excess enthalpy in heavy water electrolytic cells continue to be reported. Significant new results were presented from workers in ENEA, Frascati, IMRA Europe, the United States and many Japanese laboratories including the NHE efforts.

Of special experimental interest were many of the papers dealing with the successes in achieving especially high levels of loading of hydrogen / deuterium into the palladium - palladium alloy lattice. There were several experimental techniques discussed for achieving high loading ratios, as well as papers dealing with the advantages of considering particular metallurgical properties of the cathode materials used. Reproducibly high loading ratios is clearly one of the most important technological problems that has faced the community, and it is gratifying to see that there is a significant amount of good work being undertaken in this area.

The theoretical contributions continued to represent a significant fraction of the total contributions made. While several consistencies are beginning to become evident in the work of several of the theorists, there remains significant disparity in the conclusions of others. Proposals of "New Physics" and new views of the atom continue to be a popular approach to explain several of the observed phenomena of

cold fusion, while others continue to seek to apply new boundary conditions and assumptions in order to be able to predict experimental observations using more "conventional" approaches.

The Organizing Committee was disappointed that several invited key researchers were not able to attend this particular Conference for personal or technical reasons. We look forward to hearing the latest results of all these researchers at ICCF6 in Hokkaido in 1996.

We gratefully acknowledge and thank the sponsors of ICCF5, without whose generous financial contributions the meeting would not have been possible. The sponsors were (in alphabetical order): AISIN SEIKI CO. LTD., AISIN AW CO., LTD., AGA, S.A., CEGELEC, S.A., ENECO, INC., NIPPON TELEPHONE AND TELEGRAPH, NOVOLEC, S.A., RIBER, S.A., SETERAM, S.A., RADIOMETER ANALYTIQUE, S.A., and TECHNOVA, INC.

The Organizing Committee thanks especially the volunteers who undertook the very difficult task of organization and management of the details of the Conference: Alexandra Carvalho, Jacqueline Chirio, Claudia Bartolomeo, Veronique Guillon, Gerardo Larramona, Carina Lopes, Monique LeRoux, Jacques Payet, Yumiko Payet, Sheila Pons, Jeanne Roulette, and Thierry Roulette. Without their very capable assistance, the meeting would have not been possible.

Organizing Committee
S. Pons
November 1995

Members of the International Advisory Committee:

J.P. Biberian (France)
J. O'M. Bockris (USA)
M. Fleischmann (UK)
H. Ikegami (Japan)
K. Kunimatsu (Japan)
X.Z. Li (China)
M. McKubre (USA)
S. Pons (France)
G. Preparata (Italy)
C. Sanchez (Spain)
F. Scaramuzzi (Italy)
M. Srinivasan (India)
A. Takahashi (Japan)
D. Thompson (UK)
J. Vigier (France)

Proceedings of the 5th International Conference on Cold Fusion - ICCF5

Table of Contents

Session 1 - Introduction

Session 2 - Calorimetry and Excess Power

Session 3 - Nuclear Measurements and Instrumentation

Session 4 - Theory and Modelling

Session 5 - Cathode Loading and Materials

Session 6 - New Developments, Approaches and Systems

Session 1

Introduction

Fifth International Conference on Cold Fusion
9-13 April, 1995 - Monte Carlo, Monaco
ICCF5 ©1995

Status of "Cold Fusion"

Edmund STORMS
270 Hyde Park Estates
Santa Fe, NM 87501

Abstract

A selection of experimental evidence supporting the "cold fusion" effect is evaluated. In addition, an effort is made to show why these observations can be considered real and correct. The total evidence set strongly demonstrates a new phenomenon worthy of potential technological development.

1. Introduction

Six years have passed since the modern era of chemically assisted nuclear reactions (aka "cold fusion") was started by Profs. Stanley Pons and Martin Fleischmann (then at the University of Utah)[1]. During this time, criticisms made by skeptics have been taken seriously, errors have been reduced or eliminated, and a wide variety of studies have been done using modern equipment in many countries.[2] As a result, the early problem of reproducing the effect has been largely eliminated, a rich assortment of nuclear products has been found, and theoretical explanations are blossoming like flowers after a long delayed rain. Ten different methods are known to initiate nuclear reactions of various types in a variety of chemical environments. The boundaries of a new field of science are gradually being extended into territory guaranteed to challenge the imagination.

The problem now is more psychological than scientific. In spite of this new and improved information, general skepticism about the effect continues within the scientific community. This attitude has limited the availability of financial support, reduced publication options, and required excessive effort to demonstrate the reality of the effect. In addition, resolution of the many conflicting explanations requires a consensus about what is known to be true and correct. I will show what I believe is known about a few selected aspects of the field. Hopefully, this will lead a discussion toward agreement about what is actually known rather than what fits a particular explanation or what provides justification for rejecting the phenomenon.

Only work reported before ICCF-5 is included. Papers at ICCF-5 show how several of the ongoing studies are maturing toward an understanding that will eventually produce an acceptable explanation and make commercialization possible. Although information is still inadequate, it is safe to conclude that conventional theo-

ries are no longer adequate to explain the observations and that a clean and inexhaustible source of potentially useful energy has been discovered.

2. Anomalous Claims

Table 1 lists the major indicators of what is normally called "Cold Fusion". Note the wide variety of manifestations and wide range of implied nuclear reaction rates. The first three manifestations clearly have the greater rates and, therefore, greater technological importance. Items 4, 5, and 6 are important to demonstrate a variety of possible nuclear reactions and to understand the nuclear mechanisms. While the observed quantities are too small to explain the excess energy, few if any measurements have been done while significant energy was being generated. Neutron emission, the 7^{th} item, is very insignificant even during energy generation. While we can be thankful that the various radiation fluxes are small, the use of such measurements for diagnostic purposes has been frustrating and unconvincing to some people.

These manifestations do not appear to be strongly coupled because they frequently occur at different times and under different conditions. Therefore, different chemical environments apparently trigger different nuclear reactions. This important realization complicates any explanation.

TABLE 1

INDICATORS OF THE "Cold Fusion" EFFECT

Estimated rate of implied nuclear reaction shown

1. Excess energy (10^{10}-10^{14} /sec)
2. Helium (0.5-1.0 x energy rate)
3. Tritium (10^{7}-10^{8}/sec)

4. Nonradioactive isotopes
5. Charged particles including strange particles
6. Prompt and delayed gamma
7. Neutron (10-100/sec excluding bursts)

Because fusion is only one of the apparent nuclear reactions, the phenomenon is overdue for a name change. Table 2 lists a number of suggestions. It is still too early to achieve universal agreement. The name listed last, normally used by skeptics, is no longer appropriate because many characteristics of this value judgment are no longer operating. The phenomenon is becoming more reproducible and is growing in magnitude as techniques are improved. This term is appropriate only when the opposite experience is encountered.

3. Discussion

Before discussing the first three indicators listed in Table 1, it is worth discussing neutron emission.

3.1 Neutron Emission

Over 300 attempts to measure neutron emission have been published. About 1/3 have claimed a signal sufficient to be considered significant. Regardless of expectations based on experience obtained from hot fusion environments, very few neutrons are generated during cold fusion. A few of these neutrons appear to

---

TABLE 2

"Cold Fusion" aka

Chemically Assisted Nuclear Reactions (CANR)
Lattice Assisted Nuclear Transformations (LANT)
Lattice Induced Nuclear Chemistry (LINC)
Nuclear Energy in an Atomic Lattice (NEAL)
Catalyzed Nuclear Reactions (CNR)
Solid-State Nuclear Reactions (SSNR)
New Hydrogen Energy (NHE)
Pathological Science (PS)

---

have energy near 2.5 MeV [3; 4; 5; 6; 7; 8; 9], a value consistent with a fusion origin. A few others have energies up to about 7 MeV[10; 11; 12; 13] which require a more exotic explanation. Occasionally, bursts of neutrons are seen having a high average rate but containing a relatively small number of particles. These bursts might result from rare fractofusion events.[14]

Although the complete data set strongly suggests the existence of neutron producing reactions, the numbers are too small to have any important relationship to energy or tritium production. This experience does not preclude novel neutron transfer reactions, but it does show that important neutron generating reactions are not part of the general "cold fusion" effect.

3.2 Tritium

Of those products giving evidence for the existence of significant nuclear reaction, tritium stands well above the rest in magnitude and in the number of successful studies. Tritium is produced in quantities that are well outside of any conventional explanation, and that are occasionally well above levels that could be caused by potential contamination. Production rates of 10^7-10^8 atoms/sec have been achieved in small, laboratory-sized cells, giving as many as 10^{15} atoms before the experiment was terminated. At least 6 different methods have succeeded as shown in Table 3.

There is no reason to believe these are the only methods or that this rate is the upper limit. If a method could be scaled-up to generate 10^{12} atoms/sec, such tritium production would become very cost effective without having to deal with the many radioactive products associated with present techniques.

Tritium production occurs in different chemical/physical environments than does heat production. This fact is very important in demonstrating the broad range of possible nuclear-active conditions (NAC) and in arriving at a correct explanation for the general effect.

Failure to detect 14 MeV neutrons from secondary fusion during tritium generation has caused uncertainty as to how the tritium can be produced at energies less than the required ≈25 keV needed to avoid this reaction. Proposed solutions to this

---

TABLE 3

METHODS USED TO PRODUCE TRITIUM

Pd as a cathode in D_2O-based electrolyte.[15; 16; 17; 18; 19; 20]
Ni as a cathode in H_2O-based electrolyte.[21; 22]
Low-voltage discharge involving Pd electrodes in low pressure D_2.[23]
Low-voltage discharge involving Pd electrodes in high pressure D_2.[23]
Rapid gas release from Pd upon heating.[23]
Gas loading of Ti with high pressure D_2 followed by temperature change.[24; 25]

---

problem still do not have universal agreement although plausible theories are now being developed.

Why should we believe such tritium has been produced by "cold fusion"? Only two errors are possible. Either the presence of tritium is misdiagnosed or it is present but results from contamination. Five different methods have been used to detect tritium, all giving positive evidence in different studies. Most skeptics now admit that anomalous tritium is present. The next question is, Where does the tritium come from? Two sources are possible; either from the environment or from tritium dissolved in the palladium cathode. Let's examine environmental tritium first.

Although an open cell can absorb tritium-water from the surrounding atmosphere, this option is not available to sealed cells in which tritium has also been found. In addition, large amounts of tritium-water are not normally present in the environment. Even tritium laboratories work very hard to keep the tritium level low. However, if it is present, its entry into the cell would have a constant rate determined by the size of the opening in the container and the ambient concentration. The mechanism is well understood from much general experience, and it has been applied to the cold fusion configuration by exposing a typical cell to a high-tritium environment.[26]

Tritium has yet to be detected in commercial palladium.[27] Nevertheless, tritium that might be present has well-known characteristics.[28] Such tritium quick-

ly leaves the metal and appears in the evolving gas during normal cathodic electrolysis. It does not enter the electrolyte where anomalous tritium is found, in this case only after a long delay. This behavior not only demonstrates that anomalous tritium does not result from previously-dissolved tritium, but it also shows that the nuclear-active environment is not within the bulk material when the electrolytic method is used. In addition, tritium has been produced by gas-loading various metals followed by a temperature change. The nature of the metal has a large effect on this process.[23; 29] These considerations will be addressed using an electrolytic study as an example.

Chien et al. [15] at Texas A& M electrolyzed two cells at the same time, in the same room, using the same construction materials. One cell produced tritium in the electrolyte and the other did not. Both pieces of palladium were prepurified. The early behavior is shown in Fig. 1. At each current-voltage increase, the tritium production rate increased to a new, constant value. This behavior can not be explained by assuming the presence of environmental tritium or contaminated palladium for the following reasons.

For the sake of argument, we will first assume the tritium came from the environment. Environmental tritium could have entered the open cell along with the observed normal-water uptake. Measurements of the normal-water content of the cell allow calculation of the tritium concentration in the air required to produce the observed tritium increase in the cell. Within a factor of three, 20 $\mu Ci/m^3$ would be required in the surrounding air to produce the maximum apparent generation rate of 1×10^8 atoms/sec within the cell. This concentration triggers the evacuation alarms in the tritium laboratories at LANL. Skeptics would have us believe that this concentration exists at Texas A & M, that it fluctuates in concert with current changes, and that it enters only one cell while ignoring the other one.

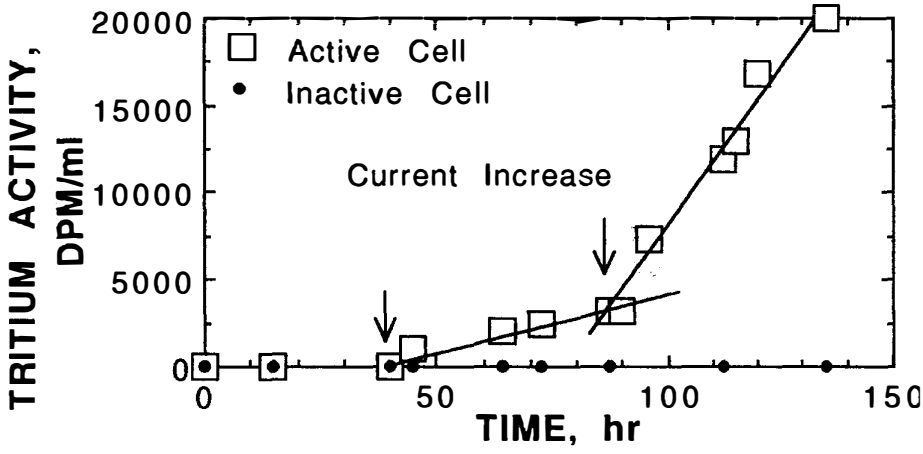

FIGURE 1. Change in tritium content of D_2O electrolyte caused by change in cell current/voltage during electrolysis during early part of study. Tritium concentration is given as disintegrations per minute (DPM). Background is 20 DPM.

Possible tritium in the palladium was eliminated by pre-analyzing the metal. This was done by sweeping any tritium out during anodic electrolysis (a process known to remove tritium along with all other hydrogen isotopes[28]) and by analyzing the palladium for ^3He, the tritium decay product. The absence of ^3He shows that the anomalous tritium was not present in the palladium during prior years. The absence of tritium after anodic electrolysis shows that it was not dissolved in the palladium immediately before the experiment. Only pre-analyzed, hence pre-purified, palladium was used for the experiment.

If the tritium found in this cell, or that claimed in more than ten other well-documented studies, can not be rationally explained as contamination, the existence of a completely unexpected nuclear reaction must be acknowledged.

3.3 Helium Production

Of the nuclear products, only ^4He has been found in sufficient quantity to roughly account for the observed excess energy. Most helium is found in the gas with lesser amounts being retained by the metal.[15; 30; 31; 32; 33; 34; 35] Charged particles similar to energetic helium emission (α-particles) have also been detected when suitable detectors were in place.[36; 37; 38; 39; 40; 41] Therefore, this product appears to be a major part or perhaps all of the sought for nuclear ash required to explain energy production.

Two studies stand out in demonstrating the helium/energy relationship.[42; 43] Space limitations allow the showing of only one. The first measurement of helium in the evolved gas is provided by Miles and Bush[42]. Eight gas samples taken in Pyrex flasks during heat production were found to contain helium while six control cells showed no helium. Because glass was used to contain the gas, the results might have resulted from diffusion of helium through the glass. In response to these concerns, the investigators measured the diffusion rate of helium through glass, When corrections were made, excess helium remained in the flasks. Another study was launched using metal flasks. These results are shown in Figure 2. Although the errors are large, the measured helium is close to that expected from the $d + d = {}^4He +$ 23.8 MeV fusion reaction and well above measurements made using a H_2O-based electrolyte in a control study. A study recently reported by Bush et al.[44], done at SRI (Stanford Research International), shows the same trend.

Possible errors include helium that might leak into the system along with air. If all of the collected gas were replaced by normal air, a helium concentration of 6 ppm would be expected. Even though such total replacement is impossible, a large random variation in measured values would be expected if a leak had been present. Absence of helium during the control studies and the absence of these large random variations during active measurements strongly indicate that the measured helium does not result from a leak.

Many other studies have shown that helium observed in the gas does not reside initially in the palladium. Even if helium were present, electrolytic action would not remove it.[45] This fact is important to the understanding of where the helium-producing region might be located. Clearly this region is not within the bulk

material and must be much less than 10 μm from a surface.[45] Otherwise, most of the helium would be retained by the palladium, which is contrary to experience. Other factors such as local heating by the nuclear reaction or presently unknown properties of the nuclear-active environment might also contribute to a greater than expected helium release.

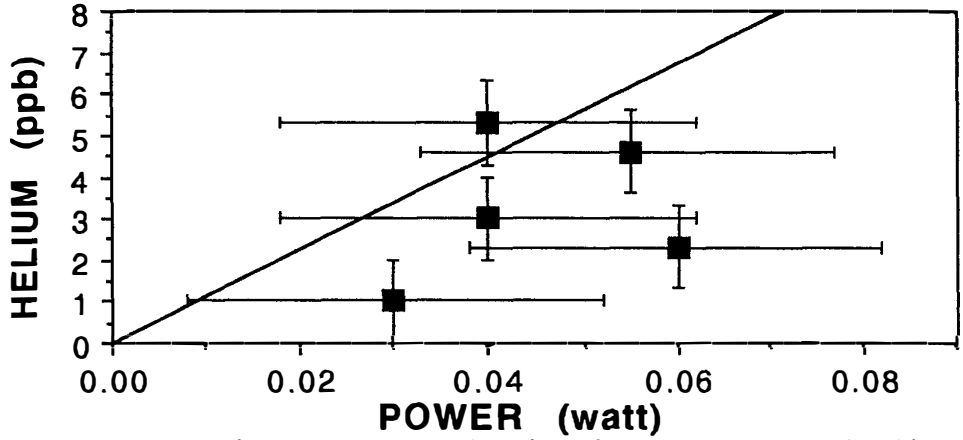

FIGURE 2. Helium produced as a function of excess power. Relationship based on d+d=He+23.8 MeV shown as line. The helium concentration results from a constant current of 500 ma held for a constant time. Collection was done using a metal system.

3.4 Excess Energy Production

More than 120 studies of energy production have been published with about 1/3 being successful. Table 4 lists the claimed successful methods. These can be grouped into four major categories: Gas Reaction, Electrolytic Reaction, Ion Discharge, and Bubble Generation. Only a few of many possible citations are listed for the first two items listed in the table. McKubre et al. at SRI have made the most complete study of the first method.

TABLE 4

METHODS CLAIMED TO PRODUCE EXCESS ENERGY

1. Electrolysis of D_2O-based electrolyte using a Pd cathode.[46]
2. Electrolysis of H_2O-based electrolyte using a Ni cathode.[47; 48]
3. Electrolysis of KCl-LiCl+ D electrolyte using a Pd anode.[49]
4. Current passed through $Sr(CeNbY)O_3$ in D_2.[50]
5. Gas discharge using Pd electrodes in hydrogen.[51]
6. Gas discharge using Pd electrodes in deuterium.[52; 40]
7. Gas reaction with Ni under special conditions.[53]
8. Enhanced reaction involving D_2O using an acoustic field.[35]
9. Enhanced reaction in H_2O using microbubble formation.[54]
10. Gas-loading of finely divided palladium.[55]

Of these techniques, electrolysis of D_2O using a palladium cathode—the so-called Pons-Fleischmann Effect—has been given the greater attention. Table 5 summarizes the results and how often a particular experimental approach was used. All cases included in this table claim power production rates well above the stated error and sensitivity of the respective calorimeter. Use of closed, sealed cells or testing for recombination eliminates uncertain recombination as an error in 19 cases. Six studies were calibrated using electrolytic power as well as Joule heat supplied by an internal resistor. This dual method effectively tests the calorimeter using a known chemical reaction, eliminates most suggested errors, and demonstrates that the calorimeter does not have an unexpected bias.

TABLE 5

SUMMARY OF RESULTS FOR THE PONS-FLEISCHMANN EFFECT

Measured Excess Values Shown
Power Range: 0.015 to 130 Watt
Energy Range: 0.06 to 200 MJ

Number of cells of the following type:
Closed and sealed: 12
Checked for recombination: 7
Used blank: 20
Stirred or not needed: 13
Dual calibration: 6

Several important variables required to initiate the Pons-Fleischmann Effect have been found. Figure 3 shows how cell current affects power production. A critical current generally between 100 and 200 ma/cm^2 is required to initiate the effect. Once initiated, power production increases in an apparently linear fashion as the current is increased. Increased current causes a larger average deuterium concentration in the palladium because the unavoidable loss from cracks is overcome to a greater extent. In general, a larger D/Pd ratio results in a greater heat production rate because, perhaps, a greater fraction of the hydride has been converted to the nuclear-active state (NAS).

A combination of observations have suggested the location of the nuclear-active sites. Studies using thin (≈5 μm) palladium hydride films on silver[56] show a similar energy production rate compared to bulk hydride. Simple diffusion theory combined with the observed dynamic loading process[28] show that the highest D/Pd ratio exists at the electrolyzing surface. Therefore, this region is proposed to be the site of the heat-producing reaction. Because most of the helium is found in the gas rather than in the cathode, the helium-producing reaction must also be very near the surface.

It is important to realize that it is the current, not the voltage that creates the measured average composition. The observed overvoltage is created by the resulting surface composition required to maintain the average.

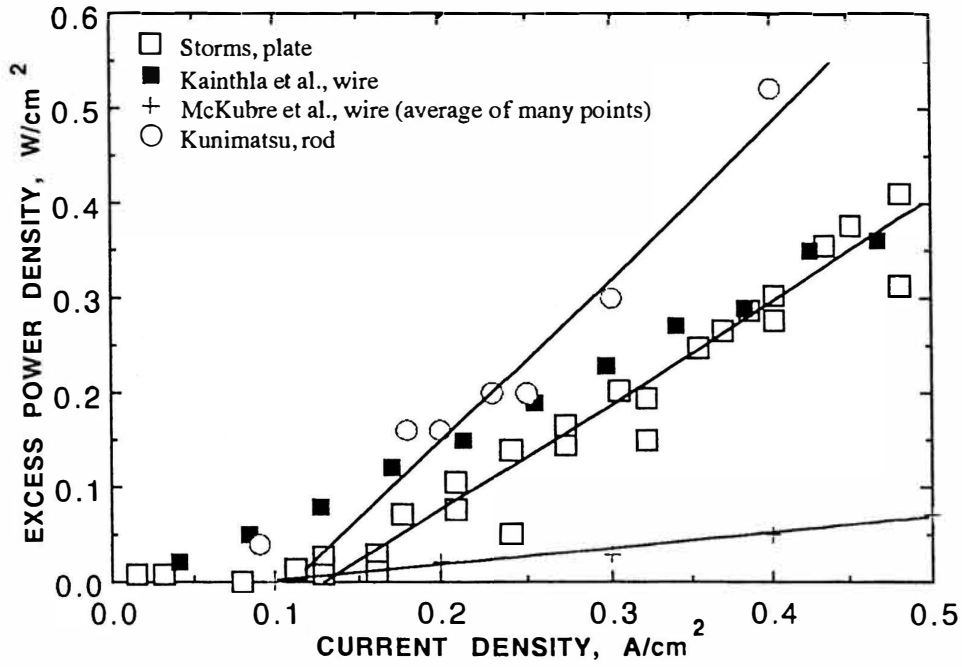

FIGURE 3. Comparison between excess power production and applied current.

In addition to a high D/Pd ratio, other, less well-defined conditions must be met.[57] Creation of these conditions generally requires many hours after a suitable composition has been achieved. One of these conditions seems to be the introduction of sufficient energy, from various sources, into the lattice.[58] The situation suggests the need to initiate an endothermic phase change in order to achieve the NAS. Regardless of the explanation, difficulty in creating this special environment has caused acceptance to be limited and has slowed technological and theoretical progress. Therefore, the mechanism for creating the NAS as well as the resulting crystal structure need to be better understood.

Several other, less well understood methods should be acknowledged. Bubbles that collapse next to a metal surface are possibly a common factor involved in several energy generation methods. Stringham and George[35] use an ultrasonic generator (20 kHz) to produce bubbles in D_2O that, when collapsed against palladium or titanium, generate significant heat and helium. Griggs[54] generates bubbles in H_2O using a special aluminum rotor driven by a 100 hp motor. Although large amounts of excess energy are produced in the latter study, no nuclear products have yet been identified. This search needs to be intensified.

Arata et al.[55] have generated significant energy after exposing finely divid-

ed palladium (palladium-black) to pressurized deuterium gas generated by electrolysis. This technique has the potential to be very useful and needs further study.

A few (at least 9) studies have claimed excess energy by electrolyzing H_2O containing various carbonate salts, mainly K_2CO_3, using a high-surface-area nickel cathode.[2; 47] Evidence for a transmutation reaction involving a proton addition to the nucleus of the electrolytic salt has been published.[21; 48] These claims indicate that the coulomb barrier is not as formidable as claimed by conventional theories.

4. Conclusions

The number of methods claimed to generate energy and nuclear products is growing along with the magnitude of effects. While some of the claims are hard to believe or inadequately supported, an objective evaluation of all claims clearly shows the occurrence of a new phenomenon having enormous potential.

Technological development and a clear understanding are handicapped by the difficulty in creating the special, nuclear-active state (NAS). Therefore, this problem needs special attention. The NAS in the Pd-D system appears not to include the normal β-PdD phase, but another structure requiring energy for its formation. Furthermore, the NAC is located only in a very narrow layer near the electrolyzing surface when it is formed by electrolysis. Its formation is controlled by the applied current and energy from various sources, with the electrode over-voltage being determined by the resulting composition of the surface. This environment must be better understood before an explanation can be accepted or total reproducibility can be achieved.

The large variety of observed nuclear reactions involving high-Z elements strongly suggests the presence of a very efficient process for overcoming the coulomb barrier. Therefore, theoreticians need to concentrate on the general process rather than trying to explain only the fusion reaction in palladium. Absence of significant high-energy radiation, both X-ray and γ-ray, strongly suggests a novel process for coupling energy to the lattice.

5. Acknowledgments

The author would like to thank ENECO for supporting the effort required to make this paper possible.

Reference

[1] Fleischmann, M., S. Pons and M. Hawkins "Electrochemically Induced Nuclear Fusion of Deuterium", *J. Electroanal. Chem.*, **261**, 301 (1989) : see also *ibid* **263**, 187 (1989).

[2] Storms, E. K., "Critical Review of the 'Cold Fusion' Effect", Submitted to *Phys. Rev. B* (1995).

[3] Arata, Y., and Y.C. Zhang, "Achievement of Intense 'Cold' Fusion Reaction", *Japan Acad. Ser. B* **66**, 1 (1990); *Fusion Technol.* **18** , 95 (1990). See also: ibid, ""Cold" Fusion in a Complex Cathode", *Frontiers of Cold Fusion*, Nagoya Japan, October 21-25, 1992, p. 441. Universal Academy Press, Inc.,Tokyo (1993).

[4] Bertin, A., M. Bruschi, M. Capponi, S. DeCastro, U. Marconi, C. Moroni, M. Piccinini, N. Semprini-Cesari, A. Trombini, A. Vitale, A. Zoccoli, S.E. Jones, J.B. Czirr, G.L. Jensen, and E.P. Palmer, "Experi-

mental Evidence of Cold Nuclear Fusion in a Measurement Under the Gran Sasso Massif", *Il Nuovo Cimento* **101**, 997 (1989). See also: Bertin, A., M. Bruschi, M. Capponi, S. De Castro, U. Marconi, C. Moroni, M. Piccinini, N. Semprini-Cesari, A. Trombini, A. Vitale, A. Zoccoli, S.E. Jones, J.B. Czirr, G.L. Jensen, and E.P. Palmer, "First Experimental Results at the Gran Sasso Laboratory on Cold Nuclear Fusion in Titanium Electrodes", *J. Fusion Energy* **9** [2], 209 (1990).

[5] Bittner, M. , A. Meister, D. Seeliger, R. Schwierz and P. Wüstner, "Observation of d-d Fusion Neutrons During Degassing of Deuterium-Loaded Palladium", *Fusion Technol.* **23**, 346 (1993).

[6] Agnello, M. E. Botta, T. Bressani, D. Calvo, A. Feliciello, P. Gianotti, F. Iazzi, C. Lamberti, B. Minetti, and A. Zecchina, "Measurement of 2.5 MeV Neutron Emission from Ti/D and Pd/D Systems", *Frontiers of Cold Fusion*, Nagoya Japan, October 21-25, 1992, p. 433. Universal Academy Press, Inc., Tokyo (1993).

[7] Jones, S. E., E. P. Palmer, J. B. Czirr, D. L. Decker, G. L. Jensen, J. M. Thorne, S. F. Taylor and J. Rafelski, "Observation of Cold Nuclear Fusion in Condensed Matter", *Nature* **338**, 737 (1989).

[8] Hongyu, Z., W. Chenlin, R. Yanin, F. Guoying, Y. Hua, Z. Weidong, W. Dachun, H. Ming, L. Shuzen, H. Zhuen, W. Zhongda, Y. Runhu, L, Zhenghao, and R. Guoxiao, "Some Results on Cold Fusion Research", *The Science of Cold Fusion*, Vol. 33, Como, Italy, June 29–July 4, 1991, p. 49. Societa Italiana di Fisica, Bologna (1991).

[9] Shani, G., C. Cohen, A. Grayevsky, and A Brokman, "Evidence for a Background Neutron Enhanced Fusion in Deuterium Absorbed Palladium", *Solid State Comm.* **72** [1], 53 (1989).

[10] McKee, J. S. C., G. R. Smith, J. J. G. Durocher, C. B. Kwok, H. L. Johnston, M. S. Mathur, J. K. Mayer, A. Mirzai, Y. H. Yeo, K. S. Sharma, and G. Williams, "Neutron Emission from Low-Energy Deuteron Injection of Deuteron-Implanted Metal Foils (Pd, Ti, and In)", *Anomalous Nuclear Effects in Deuterium/Solid Systems*, Provo, UT, Oct. 22-23, 1990, p. 275. American Institute of Physics, NY (1991).

[11] Nakada, M., T. Kusunoki, and Okamoto, "Energy of the Neutrons Emitted in Heavy Water Electrolysis", *Frontiers of Cold Fusion*, Nagoya Japan, October 21-25, 1992, p. 173. Universal Academy Press, Inc.,Tokyo (1993).

[12] Okamoto, M., Y. Yoshinaga, M. Aida, and T. Kusunoki, "Excess Heat Generation, Voltage Deviation, and Neutron Emission in D_2O-LiOD Systems", *Proc. Fourth International Conference on Cold Fusion*,(EPRI TR-104188-V2), Lahaina, Maui, Dec. 6-9, 1993, p. 3. Electric Power Research Institute, Palo Alto (1994).

[13] Takahashi, A., T. Takeuchi, T. Iida, and M. Watanabe, "Neutron Spectra from D_2O-Pd Cells with Pulsed Electrolysis", *Anomalous Nuclear Effects in Deuterium/Solid Systems*, Provo, UT, Oct. 22-23, 1990, p. 323. American Institute of Physics, NY (1991). *Ibid*, "Short Note ; Emission of 2.45 MeV and Higher Energy Neutrons from D_2O-Pd Cell Under Biased-Pulse Electrolysis", *J. Nucl. Sci. Tech.* **27**, 663 (1990); Takahashi, A., T. Iida, T. Takeuchi, A. Mega, S. Yoshida, and M. Watanabe, "Neutron Spectra and Controllability by PdD/electrolysis Cell With Low-High Current Pulse Operation", *The Science of Cold Fusion*, Vol. 33, Como, Italy, June 29--July 4, 1991, p. 93. Societa Italiana di Fisica, Bologna (1991).

[14] AbuTaha, A. F., "Cold Fusion-The Heat Mechanism", *J. Fusion Energy* **9** [3], 345 (1990).
Bagnulo, L. H., "Crack-fusion: a Plausible Explanation of Cold Fusion", *The Science of Cold Fusion*, Vol. 33, Como, Italy, June 29--July 4, 1991, p. 267. Societa Italiana di Fisica, Bologna (1991).
Chechin, V. A., V. A. Tsarev, P. I. Golubnichyi, A. D. Philonenko, and A. A. Tsarik, "Fracto-Acceleration Model of Cold Nuclear Fusion", *Anomalous Nuclear Effects in Deuterium/Solid Systems*, Provo, UT, Oct. 22-23, 1990, p.686. American Institute of Physics, NY (1991).

Derjaguin, B. V., A.G. Lipson, V.A. Kluev, D.M. Sakov and Y.P. Toporov, "Titanium Fracture Yields Neutrons?", *Nature* **341**, 492 (1989).

Dickinson, J. T., L. C. Jensen, S. C. Langford, R. R. Ryan, and E. Garcia, "Fracto-Emission From Deuterated Titanium: Supporting Evidence for a Fracto-Fusion Mechanism", *J. Mater. Res.* **5** [1], 109 (1990).

Golubnichii, P. I., V. A. Kurakin, A. D. Filonenko, V. A. Tsarev, and A. A. Tsarik, "A Possible Mechanism for Cold Nuclear Fusion", *Sov. Phys. Dokl.* **34**, 628 (1989).

Kühne, R. W., "The Possible Hot Nature of Cold Fusion", *Fusion Technol.* **25**, 198 (1994).

Kühne, R. W. and R. E. Sioda, "An Extended Micro Hot Fusion Model for Burst Activity in Deuterated Solids", *Fusion Technol.* **27**, 187 (1995).

Lipson, A. G., D. M. Sakov, V. A. Klyuev, B. V. Deryagin, and Yu. P. Toporov, "Neutron Emission During the Mechanical Treatment of Titanium in the Presence of Deuterated Substances", *JETP Lett.* **49** [11], 675 (1989).

Mayer, F. J., J. S. King, and J. R. Reitz, "Nuclear Fusion From Crack-Generated Particle Acceleration", *J. Fusion Energy* **9** [3], 269 (1990).

Preparata, G., "Fractofusion Revisted", *Anomalous Nuclear Effects in Deuterium/Solid Systems*, Provo, UT, Oct. 22-23, 1990, p. 840. American Institute of Physics, NY (1991).

Shirakawa, T., M. Fujii, M. Chiba, K. Sueki, T. Ikebe, S. Yamaoka, H. Miura, T. Watanabe, T. Hirose, H. Nakahara, and M. Utsumi, "Particle Acceleration and Neutron Emission in a Fracture Process of a Piezoelectric Material", *Proc. Fourth International Conference on Cold Fusion*,(EPRI TR-104188-V3), Lahaina, Maui, Dec. 6-9, 1993, p. 6. Electric Power Research Institute, Palo Alto (1994).

Takeda, T. and T. Takizuka, "Fractofusion Mechanism", *J. Phys. Soc. Japan* **58** [9], 3073 (1989).

Yasui, K., "Fractofusion Mechanism", *Frontiers of Cold Fusion*, Nagoya Japan, October 21-25, 1992, p. 605. Universal Academy Press, Inc. Tokyo (1993).

Zhang, W-X, "Possibility of Phase Transitions Inducing Cold Fusion in Palladium/Deuterium Systems", *Fusion Technol.* **21**, 82 (1992).

[15] Chien, C-C., D. Hodko, Z. Minevski, and J. O'M. Bockris, "On an Electrode Producing Massive Quantities of Tritium and Helium", *J. Electroanal. Chem.* **338**, 189 (1992).

[16] Chêne, J. and A. M. Brass, "Tritium Production During the Cathode Discharge of Deuterium on Palladium", *J. Electroanal. Chem.* **280**, 199 (1990).

[17] Iyengar, P. K., M. Srinivasan, S.K. Kikka, A. Shyam, et. al., "Bhabha Atomic Research Centre Studies in Cold Fusion", *Fusion Technol.* **18** , 32 (1990). See also: Iyengar, P. K., and M. Srinivasan, "Overview of BARC Studies in Cold Fusion", *Proc. of The First Annual Conference on Cold Fusion*, March 28-31, 1990, Salt Lake City, Utah, p. 62, National Cold Fusion Insitute, Salt Lake City (1990).

[18] Storms, E. and C. L. Talcott, "Electrolytic Tritium Production", *Fusion Technol.* **17**, 680 (1990).

[19] Szpak, S., P. A. Mosier-Boss, and J. J. Smith, "Reliable Procedure for the Initiation of the Fleischmann-Pons Effect", *The Science of Cold Fusion*, Vol. 33, Como, Italy, June 29--July 4, 1991, p. 87. Societa Italiana di Fisica, Bologna (1991).

[20] Will, F. G., K. Cedzynska, and D. C. Linton, "Tritium Generation in Palladium Cathodes With High Deuterium Loading", *Proc. Fourth International Conference on Cold Fusion*,(EPRI TR-104188-V1), Lahaina, Maui, Dec. 6-9, 1993, p. 8. Electric Power Research Institute, Palo Alto (1994).

[21] Notoya, R. and M. Enyo, "Excess Heat Production during Electrolysis of H_2O on Ni, Au, Ag, and Sn Electrodes in Alkaline Media", *Frontiers of Cold Fusion*, Nagoya Japan, October 21-25, 1992, p. 421.

Universal Academy Press, Inc., Tokyo (1993). See also: Notoya, R., "Alkali-Hydrogen Cold Fusion Accompanied with Tritium", *Proc. Fourth International Conference on Cold Fusion*,(EPRI TR-104188-V3), Lahaina, Maui, Dec. 6-9, 1993, p. 1. Electric Power Research Institute, Palo Alto (1994). Notoya, R., Y. Noya, and T. Ohnishi, "Tritium Generation and Large Excess Heat Evolution by Electrolysis in Light and Heavy Water-Potassium Carbonate Solutions with Nickel Electrodes", *Fusion Technology* **26**, 179 (1994); Notoya, R., "Cold Fusion by Electrolysis in a Light Water-Potassium Carbonate Solution With a Nickel Electrode", *Fusion Technol.* **24**, 202 (1993).

[22] Ramamurthy, H., M. Srinivasan, U. K. Mukherjee, and P. Adi Babu, "Further Studies on Excess Heat Generation in Ni-H_2O Electrolytic Cells", *Proc. Fourth International Conference on Cold Fusion*,(EPRI TR-104188-V2), Lahaina, Maui, Dec. 6-9, 1993, , p. 15. Electric Power Research Institute, Palo Alto (1994). See also: Sankaranarayanan, M. Srinivasan, M. Bajpai, and D. Gupta, "Investigation of Low Level Tritium Generation in Ni-H_2O Electrolytic Cells", ibid, Vol. 3, p. 3.

[23] Claytor, T. N, D. G. Tuggle, H. O. Menlove, P. A. Seeger, W. R. Doty, and R. K. Rohwer, "Tritium and Neutron Measurements From Deuterated Pd-Si", *Anomalous Nuclear Effects in Deuterium/Solid Systems*, Provo, UT, Oct. 22-23, 1990, p. 467. American Institute of Physics, NY (1991). See also: Claytor, T. N., D. G. Tuggle, and H. O. Menlove, "Tritium Generation and Neutron Measurements in Pd-Si Under High Deuterium Gas Pressure", *The Science of Cold Fusion*, Vol. 33, Como, Italy, June 29--July 4, 1991, p. 395. Societa Italiana di Fisica, Bologna (1991). Claytor, T. N., D. G. Tuggle, and S. F. Taylor, "Evolution of Tritium from Deuterided Palladium Subject to High Electrical Currents", *Frontiers of Cold Fusion*, Nagoya Japan, October 21-25, 1992, p. 217. Universal Academy Press, Inc. Tokyo (1993). Taylor, S. F. , T. N. Claytor, D. G. Tuggle, and S. E. Jones, "Search for Neutrons from Deuterated Palladium Subject to High Electric Currents", *Proc. Fourth International Conference on Cold Fusion*,(EPRI TR-104188-V3), Lahaina, Maui, Dec. 6-9, 1993, p. 17. Electric Power Research Institute, Palo Alto (1994). Tuggle, D. G., T. N. Claytor, and S. F. Taylor, "Tritium Evolution from Various Morphologies of Palladium", *Proc. Fourth International Conference on Cold Fusion*,(EPRI TR-104188-V1), Lahaina, Maui, Dec. 6-9, 1993, p. 7. Electric Power Research Institute, Palo Alto (1994).

[24] D'Amato, F., A. De Ninno, F. Scaramuzzi, P. Zeppa, C. Pontorieri, and F. Lanza, "Search for Nuclear Phenomena by the Interaction Between Titanium and Deuterium", *Proc. of The First Annual Conference on Cold Fusion*, March 28-31, 1990, Salt Lake City, Utah, p. 170. National Cold Fusion Insitute, Salt Lake City (1990). See also: De Ninno, A., F. Scaramuzzi, A. Frattolillo, S. Migliori, F. Lanza, S. Scaglione, P. Zeppa, and C. Pontorieri, "The Production of Neutrons and Tritium in the Deuterium Gas-Titanium Interaction", *The Science of Cold Fusion*, Vol. 33, Como, Italy, June 29--July 4, 1991, p. 129. Societa Italiana di Fisica, Bologna (1991).

[25] Srinivasan, M., A. Shyam, T. C. Kaushik, R. K. Rout, L. V. Kulkarni, M. S. Krishnan, S. K. Malhotra, V. G. Nagvenkar, and P. K. Iyengar, "Observation of Tritium in Gas/Plasma Loaded Titanium Samples", *Anomalous Nuclear Effects in Deuterium/Solid Systems*, Provo, UT, Oct. 22-23, 1990, p. 514. American Institute of Physics, NY (1991).

[26] Storms, E., "Review of Experimental Observations About the Cold Fusion Effect", *Fusion Technol.* **20**, 433 (1991).

[27] Cedzynska, K., and F. G. Will, "Closed-System Analysis of Tritium in Palladium", *Fusion Technol.* **22**, 156 (1992). Cedzynska, K., S. C. Barrowes, H. E. Bergeson, L. C. Knight, and F. G. Will, "Tritium Analysis in Palladium with an Open System Analytical Procedure", *Fusion Technol.* **20**, 108 (1991).

[28] Storms, E. and C. Talcott-Storms, "The Effect of Hydriding on the Physical Structure of Palladium and on the Release of Contained Tritium", *Fusion Technol.* **20**, 246 (1991).

[29] Srinivasan, M., A. Shyam, T. C. Kaushik, R. K. Rout, L. V. Kulkarni, M. S. Krishnan, S. K. Malhotra, V. G. Nagvenkar, and P. K. Iyengar, "Observation of Tritium in Gas/Plasma Loaded Titanium Samples", *Anomalous Nuclear Effects in Deuterium/Solid Systems*, Provo, UT, Oct. 22-23, 1990, p. 514. American Institute of Physics, NY (1991).

[30] Morrey, J. R., M. W. Caffee, H. Farrar, IV, N. J. Hoffman, G. B. Hudson, R. H. Jones, M. D. Kurz, J. Lupton, B. M. Oliver, B. V. Ruiz, J. F. Wacker, and A. Van , "Measurements of Helium in Electrolyzed Palladium", *Fusion Technol.* **18**, 659 (1990).

[31] Liaw, B. Y., P-L. Tao, and B. E. Liebert, "Helium Analysis of Palladium Electrodes After Molten Salt Electrolysis", *Fusion Technol.* **23**, 92 (1993).

[32] Savvatimova, I., Y. Kucherov, and A. Karabut, "Cathode Material Change after Deuterium Glow Discharge Experiments", *Proc. Fourth International Conference on Cold Fusion*,(EPRI TR-104188-V3), Lahaina, Maui, Dec. 6-9, 1993, p. 16. Electric Power Research Institute, Palo Alto (1994).

[33] Yamaguchi, E. and T. Nishioka, "Cold Nuclear Fusion Induced by Controlled Out-Diffusion of Deuterons in Palladium", *Japan. J. Appl. Phys.*, Part 2 Letters, 29, [4], L666 (1990) . ibid, "Direct Evidence for Nuclear Fusion Reactions in Deuterated Palladium", *Frontiers of Cold Fusion*, Nagoya Japan, Oct. 21-25, 1992, p. 179. Universal Academy Press, Inc., Tokyo (1993). *Ibid,* "Nuclear Fusion Induced by the Controlled Out-Transport of Deuterons in Palladium", *Anomalous Nuclear Effects in Deuterium/Solid Systems*, Provo, UT, Oct. 22-23, 1990, p. 354. American Institute of Physics, NY (1991).

[34] Zhang, Q. F., Q. Q. Gou, Z. H. Zhu, B. L. Xio, J. M. Lou, F. S. Liu, J. X. S., Y. G. Ning, H. Xie, and Z. G. Wang, "The Detection of 4-He in Ti-Cathode on Cold Fusion", *Frontiers of Cold Fusion*, Nagoya, Japan, Oct. 21-25, 1992, p. 531. Universal Academy Press, Inc., Tokyo (1993).

[35] Stringhan, R. and R. George, presented at Fourth International Conf. on Cold Fusion, Lahaina, Maui, Dec. 6-9, 1993. Not published in proceedings. Contact E-Quest Sciences, P. O. Box 60642, Palo Alto, CA 94036 for more information. See also: ibid, "Cavitation Induced Micro-Fusion Solid State Production of Heat, ^{3}He, and ^{4}He", submitted to *Science*, 1995.

[36] Cecil, F. E., H. Liu, D. Beddingfield, and C. S. Galovich, "Observation of Charged-Particle Bursts from Deuterium-Loaded Thin-Titanium Foils", *Anomalous Nuclear Effects in Deuterium/Solid Systems*, Provo, UT, Oct. 22-23, 1990, p. 375. American Institute of Physics, NY (1991). See also: Cecil, F., D. Ferg, T. Furtak, C. Mader, J. A. McNeil, and D. L. Williamson, "Study of Energetic Charged Particles from Thin Deuterated Palladium Foils Subject to High Current Densities", *J. Fusion Energy* **9** [2], 195 (1990).

[37] Dong, S. Y., K. L. Wang, Y. Y. Feng, L. Chang, C. M. Luo, R. Y. Hu, P. L. Zhou, D. W. Mo, Y. F. Zhu, C. L. Song, Y. T. Chen, M. Y. Yao, C. Ren, Q. K. Chen, and X. Z. Li , "Precursors to "Cold Fusion" Phenomenon and the Detection of Energetic Charged Particles in Deuterium/Solid Systems", *Fusion Technol.* **20**, 330 (1991).

[38] Iida, T., M. Fukuhara, H. Miyazaki, Y. Sueyoshi, Sunarno, J. Datemichi, and A. Takahashi, "Deuteron Fusion Experiment with Ti and Pd Foils Implanted with Deuterium Beams", *Frontiers of Cold Fusion*, Nagoya Japan, October 21-25, 1992, p. 201. Universal Academy Press, Inc., Tokyo (1993).

[39] Kamada, K., "Electron Impact H-H and D-D Fusions in Molecules Embedded in Al.", *Frontiers of Cold Fusion*, Nagoya Japan, Oct. 21-25, 1992, p. 551. Universal Academy Press, Inc., Tokyo (1993).

[40] Karabut, A. B., Ya. R. Kucherov, and I. B. Savvatimova, "Nuclear Product Ratio for Glow Discharge in

Deuterium", *Phys. Lett.* A **170** (1992) 265; Karabut, A. B., Y. R. Kucherov, and I. B. Savvatimova, "Possible Nuclear Reactions Mechanisms at Glow Discharge in Deuterium", *Frontiers of Cold Fusion*, Nagoya, Japan, Oct. 21-25, 1992, p. 165. Universal Academy Press, Inc., Tokyo (1993). Savvatimova, I., Y. Kucherov, and A. Karabut, "Cathode Material Change after Deuterium Glow Discharge Experiments", *Proc. Fourth International Conference on Cold Fusion*, (EPRI TR-104188-V3), Lahaina, Maui, Dec. 6-9, 1993, p. 16. Electric Power Research Institute, Palo Alto (1994).

[41] Yamaguchi, E. and T. Nishioka, "Direct Evidence for Nuclear Fusion Reactions in Deuterated Palladium", *Frontiers of Cold Fusion*, Nagoya, Japan, Oct. 21-25, 1992, p. 179. Universal Academy Press, Inc. Tokyo (1993).

[42] Bush, B. F., J. J. Lagowski, M. H. Miles, and G. S. Ostrom, "Helium Production During the Electrolysis of D_2O in Cold Fusion", *J. Electroanal. Chem.* **304**, 271 (1991); and Miles, M. H., B. Bush, and J. J. Lagowski, "Anomalous Effects Involving Excess Power, Radiation, and Helium Production During D_2O Electrolysis Using Palladium Cathodes", *Fusion Technol.* **25**, 478 (1994). Miles, M. H. and B. F. Bush, "Heat and Helium Measurements in Deuterated Palladium", *Proc. Fourth International Conference on Cold Fusion*,(EPRI TR-104188-V2), Lahaina, Maui, Dec. 6-9, 1993, p. 6. Electric Power Research Institute, Palo Alto (1994).

[43] Gozzi, D., P. L. Cignini, M. Tomellini, S. Frullani, F. Garibaldi, F. Ghio, M. Jodice and G. M. Urciuoli, "Multicell Experiments for Searching Time-Related Events in Cold Fusion", *The Science of Cold Fusion*, Vol. 33, Como, Italy, June 29--July 4, 1991, p. 21. Societa Italiana di Fisica, Bologna (1991). See also: Gozzi, D., P.L. Cignini, L. Petrucci, M. Tomellini, and G. De Maria, "Evidences for Associated Heat Generation and Nuclear Products Release in Pd Heavy-Water Electrolysis", *Il Nuovo Cimento* **103**, 143 (1990). Gozzi, D., R. Caputo, P. L. Cignini, M. Tomellini, G. Gigli, G. Balducci, E. Cisbani, S. Frullani, F. Garibaldi, M. Jodice, and Urciuoli, "Helium-4 Quantitative Measurements in the Gas Phase of Cold Fusion Electrochemical Cells", *Proc. Fourth International Conference on Cold Fusion*, (EPRI TR-104188-V1), Lahaina, Maui, Dec. 6-9, 1993, p. 6. Electric Power Research Institute, Palo Alto (1994).; See : *Ibid*, p. 2.

[44] Bush, B. F., J. J. Lagowski, and M. H. Miles, "Nuclear Products Commensurate with Energy Generated During D_2O Electrolysis at Palladium Cathodes: Quantitative Analysis", 209th American Chemical Society, Anaheim, CA, April 2-6, 1995.

[45] Abell, G. C., L. K. Matson, and R. H. Steinmeyer, "Helium Release From Aged Palladium Tritide", *Phys. Rev.* **41**, 1220 (1990).

[46] McKubre, M. C. H., S. Crouch-Baker, R. C. Rocha-Filho, S. I. Smedley, F. L. Tanzella, T. O. Passell, and J. Santucci, " Isothermal Flow Calorimetric Investigations of the D/Pd and H/Pd Systems", *J. Electroanal. Chem.* **368**, 55 (1994). See also: McKubre, M, B. Bush, S. Crouch-Baker, A. Hauser, N. Jevtic, S. Smedley, M. Srinivasan, F. Tanzella, M. Williams, and S. Wing, "Loading, Calorimeteric and Nuclear Investigation of the D/Pd System", *Proc. Fourth International Conference on Cold Fusion*,(EPRI TR-104188-V1), Lahaina, Maui, Dec. 6-9, 1993, p. 5. Electric Power Research Institute, Palo Alto (1994). McKubre, M. C. H., R. C. Rocha-Filho, S. Smedley, F. Tanzella, J. Chao, B. Chexal, T. Passell, and J. Santucci, "Calorimetry and Electrochemistry in the D/Pd System", *Proc. of The First Annual Conference on Cold Fusion*, Mar. 28-31, 1990, Salt Lake City, Utah, p. 20, National Cold Fusion Insitute, Salt Lake City (1990). McKubre, M. C. H., R. Rocha-Filho, S. I. Smedley, F. L. Tanzella, S. Crouch-Baker, T. O. Passell, and J. Santucci, "Isothermal Flow Calorimetric Investigations of the D/Pd System", *The Science of Cold Fusion*, Vol. 33, Como, Italy, June 29--July 4, 1991, p. 419. Societa Italiana di Fisica, Bologna (1991). McKubre, M. C. H., S. Crouch-Baker, A. M. Riley, S. I. Smedley and F. L. Tanzella, "Excess Power

Observations in Electrochemical Studies of the D/Pd System; The Influence of Loading", *Frontiers of Cold Fusion*, Nagoya, Japan, Oct. 21-25, 1992, p. 5, Universal Academy Press, Inc., Tokyo (1993).

[47] Mills, R. and S. P. Kneizys, "Excess Heat Production by the Electrolysis of an Aqueous Potassium Carbonate Electrolyte and the Implications for Cold Fusion", *Fusion Technol.* **20**, 65 (1991). See also: Mills, R. L., W. R. Good, and R. M. Shaubach, "Dihydrino Molecule Identification", *Fusion Technol.* **25**, 103 (1994).

[48] Bush, R. T. and R. D. Eagleton, "Calorimetric Studies for Several Light Water Electrolytic Cells With Nickel Fibrex Cathodes and Electrolytes with Alkali Salts of Potassium, Rubidium, and Cesium", *Proc. Fourth International Conference on Cold Fusion*,(EPRI TR-104188-V2), Lahaina, Maui, Dec. 6-9, 1993, p. 13. Electric Power Research Institute, Palo Alto (1994).

[49] Liaw, B. Y., P-L. Tao, P. Turner, and B. Liebert. "Elevated Temperature Excess Heat Production Using Molten-Salt Electrochemical Techniques", *Special Sym. Proc. Cold Fusion.*, 8th World Hydrogen Energy Conf., Honolulu, HI, July 22-27, 1990, p. 47. Hawaii Natural Energy Institute, Honolulu (1990).

[50] Mizuno, T., M. Enyo, T. Akimoto, and K. Azumi, "Anomalous Heat Evolution from $SrCeO_3$-Type Proton Conductors during Absorption/Desorption in Alternate Electric Field", *Proc. Fourth International Conference on Cold Fusion*, (EPRI TR-104188-V2), Lahaina, Maui, Dec. 6-9, 1993, p. 14. Electric Power Research Institute, Palo Alto (1994).

[51] Dufour, J., J. Foos, and J. P. Millot, "Cold Fusion by Sparking in Hydrogen Isotopes. Energy Balances and Search for Fusion By-products. A Strategy to Prove the Reality of Cold Fusion", *Proc. Fourth International Conference on Cold Fusion*,(EPRI TR-104188-V1), Lahaina, Maui, Dec. 6-9, 1993, p. 9. Electric Power Research Institute, Palo Alto (1994).

[52] Dufour, J., "Cold Fusion by Sparking in Hydrogen Isotopes", *Fusion Technol.* **24**, 205 (1993).

[53] Focard, S., R. Habel, and F. Piantelli, "Anomalous Heat Production in Ni-H Systems", *Il Nuovo Cimento* **107A**, 163 (1994).

[54] Griggs, J. L., "A Brief Introduction to the Hydrosonic Pump and the Associated "Excess Energy" Phenomenon", *Proc. Fourth International Conference on Cold Fusion*,(EPRI TR-104188-V4), Lahaina, Maui, Dec. 6-9, 1993, p. 43. Electric Power Research Institute, Palo Alto (1994). U. S. Patent # 5,188,090, Feb. 23, 1993. "Apparatus for Heating Fluids". Contact Hydro Dynamics, 8 Redmond Court, Rome, GA 30165 for more information.

[55] Arata, Y., and Y-C. Zhang, "A New Energy Caused by "Spillover-Deuterium"", *Proc. Japan Acad.*, **70**, Ser. B, 106 (1994).

[56] Studies carried out by Bush et al. (Cal. Poly and LANL) but not yet published.

[57] Storms, E., "How to Produce the Pons-Fleischmann Effect", *Fusion Technol.* (1995).

[58] Bockris, J., R. Sundaresan, D. Letts, and Z. Minevski, "Triggering of Heat and Sub-Surface Changes in Pd-D System", *Proc. Fourth International Conference on Cold Fusion*,(EPRI TR-104188-V2), Lahaina, Maui, Dec. 6-9, 1993, p. 1. Electric Power Research Institute, Palo Alto (1994).

Session 2

Calorimetry and Excess Power

Fifth International Conference on Cold Fusion
9-13 April, 1995 - Monte Carlo, Monaco
ICCF5 ©1995

Concerning Reproducibility of Excess Power Production

M. C. H. McKUBRE, S. CROUCH-BAKER, A. K. HAUSER,
S. I. SMEDLEY, F. L. TANZELLA, M. S. WILLIAMS, S. S. WING
SRI INTERNATIONAL
Menlo Park, CA 94025 (USA)

Abstract

An apparent irreproducibility in the production of an, as yet, anomalous excess power from Pd cathodes electrochemically loaded with D can be associated with irreproducibility in the attainment of several necessary starting conditions. Of these, the threshold loading (D/Pd atomic ratio) has received the most attention. A statistical analysis is presented of the results of 176 experiments intended to test the means of establishing reproducible control over D/Pd loading. A set of variables are examined, and procedures identified which permit the attainment of loading above the threshold necessary for excess heat production.

Calorimetric results from two experiments are presented and analyzed. A mathematical function is identified which correlates closely with the time evolution of excess power. An important element of this correlation is the measured rate of change of the cathode resistivity. We have interpreted the resistance change as indicating the presence of an oscillation or "breathing" of the cathode loading induced by a flux of deuterons through the cathode/electrolyte interface.

The observed functionality of excess power with deuteron flux above a loading threshold, conforms closely with theoretical predictions.

1. Introduction

Six years have passed since publication of the defining paper of Fleischmann, Pons and Hawkins.[1] In this time, scientific progress has been made to resolve issues that were quickly, and easily, anticipated. The resolution of some important issues has been accompanied by a slow, somewhat unsteady, but certain growth in the field of science which has come to be called "cold fusion".

At the time of that publication, few would have suspected after six years of study, that the field revealed would have survived, but not thrived. This surprising situation has come about because, in restraint of progress, stand two technically challenging problems:

i) Irreproducibility. This is not, as some have argued, an irreproducibility of results. It is a difficulty in achieving reproducible starting conditions for comparative experiments.

ii) Scarcity of energetic (nuclear) products. It is quite clear that the nuclear product(s) quantitatively associated with excess heat, if there is one, is not an energetic particle, or penetrating radiation, or a radioactive isotope; this makes the search very difficult.

In this paper, an attempt is made to address the first of these difficulties, with specific attention to the reproducible attainment of positive heat excess in the D/Pd system, under electrochemical conditions.

2. Necessary Conditions

We need first to identify the experimental starting condition thought, or observed, to be associated the phenomenon under study. In a series of papers SRI[2-7] and others[8,9] have attempted to define and quantify the variables associated with apparent excess heat production. These are:

i) Loading. The D/Pd loading seemed, at the outset, to be a likely controlling variable; this has clearly been shown to be the case. The loading is relatively easily measured; the attainment and maintenance of high loading (D/Pd $\geq$ 0.9), is not easily controlled. Independent experiments at SRI[4] and IMRA-Japan[8] have demonstrated a roughly parabolic functionality between excess power and loading above a loading threshold of D/Pd ~ 0.84 $\pm$ 0.02. In order to achieve appreciable (and measurable) power excess, loadings much higher than the threshold are needed (D/Pd $\geq$ 0.9 and preferably $\geq$ 0.95). Several other factors also are necessary.

ii) Current Density. In an electrochemical experiment, current density affects loading. In addition to this expected, but complex, functionality, the interfacial current density also directly affects the rate of excess heat production. In experiments performed under nearly isothermal conditions at nearly constant loading, a linear dependence of excess power is observed with increasing current density above the threshold value. Unlike the loading threshold, the current density threshold displays considerable variability ranging from ~ 100 to ~ 400 mA cm^{-2} in different experiments, or in the same experiments, at different times.

iii) Initiation. Many authors have reported a delay in the onset of excess heat production. Even after the loading and current density thresholds have been usefully exceeded, excess heat is (generally) not observed until a significant time has elapsed, on the order of 300 h for 1-4 mm dia. Pd wires. It is apparent that some initiation process must occur, presumably within the Pd lattice. At this stage, the origin is unclear.

iv) Disequilibrium. It has long been suspected that a flux of deuterium atoms through the interface is needed in addition to high deuterium atom loading, to produce measurable excess power. Recently theoretical arguments have been advanced to support the conjecture that flux, combined with high loading are necessary for excess heat or nuclear product formation. In this paper, we present experimental evidence of this, and attempt to quantify the role of deuterium interfacial flux in excess power production.

3. Loading

The attainment of high D/Pd loading is critical to the appearance of excess power. We previously have presented evidence[2-7] that, in every case that we have observed in a calorimeter, where a cathode achieved a maximum loading of D/Pd ≥ 0.95 while meeting criteria (ii) and (iii) above, excess power was measured ($P_{xs} > 0$). For cathodes achieving maximum loadings $0.90 \leq D/Pd < 0.95$, approximately half exhibited $P_{xs} > 0$. In only one case for which the maximum loading was less than 0.90, have we observed $P_{xs} > 0$. This case will be discussed later in this paper, as it is instructive.

Attainment of these high loadings, while clearly critical, is neither usual, nor can it be achieved reproducibly. An analysis is presented here of the results of 214 experiments, both loading and calorimetric, representing 200,416 hours of experiment operation (or 23 experiment-years). All experiments employed Pd cathodes, and loading was measured using a four terminal resistance method.[3,7,10]

From this set of 214 experiments, the data from 38 have been excluded by reason of poor resistance measurement, premature failure, or suspected compromise, leaving 177,640 hours of reliable data, (20 experiment-years). The following Tables show the material sources, electrolytes and additives employed.

Table 1. Metal Sources

Engelhard			Various		
E1	32*	Engelhard Lot #1	AE	1	AECL**
E2	24	Engelhard Lot #2	AM	4	Aithaca Metals
E3	38	Engelhard Lot #3	IB	4	Ingot Block - cast
E4	4	Engelhard Lot #4	JM	40	Johnson Matthey
E5	15	Engelhard Lot #5	NL	5	NRL†
E-	6	Engelhard 1mm	ZR	1	Zone Refined

* Number of experiments

**AECL Atomic Energy of Canada Ltd (Cast, High Purity)

†NRL Naval Research Laboratories (High Purity). 30 and 600 μ grain sizes.

Table 2. Electrolytes, Additives and Variables

Electrolytes			Additives††		Variables
3	0.5 D_2SO_4	D	71	None	Additive
6	0.5 Li_2SO_4	D	68	Al	Annealing
158	1.0 LiOD	D	10	Ni†††	Cathode machining
2	0.3 M LiCl	D	6	B	Diameter
1	0.1 M LiOD	D	6	Cu	Experiment length
1	0.5 Li_2SO_4	H	6	Poison*	Metal source
4	1.0 LiOH	H	3	Si**	
1	0.1 M LiOH	H	2	Be	

* Additional series of experiments were performed specifically to test the effects of classical hydrogen recombination poisons and the effect of their concentrations. The results of these have not been included in this data set.

** All experiments were performed in quartz vessels and/or with quartz structures in the electrolyte. Si, was therefore present in increasing amounts as this element dissolved. For these three cases, additional Si was added as SiO_2 dissolved in electrolyte.

†† For the 176 cases analyzed here, when present, additive concentrations were ~ 200 ppm.

††† These 10 experiments employed Ni anodes not additives.

Each experiment has been characterized by the maximum loading attained by the cathode, at any time during the experiment (the average experiment length was 1009 hours). Twelve approximately equal groups were defined, according to the mean loadings shown in Table 3. An exhaustive analysis of these results is presented elsewhere.[11] The purpose here is to focus attention on those variables that strongly influence loading; this we can do with a relatively simple analysis.

The results in Table 3 show great dispersion, with a significant number of experiments achieving a maximum loading of only 0.74 (just beyond the maximum in R/R°), while an equal number apparently exceed 1.0 (R/R° ≤ 1.5 on the right hand side of the maximum). At this point, it is worth remembering that the experiments analyzed here represent our "best efforts" to attain high loading; 57% of all experiments reported in Table 3 achieved our stated target of 0.9.

Table 3. Maximum Loading

Group	Mean	#	Quartile	Group	Mean	#	Quartile
1	0.74	14	4	7	0.92	13	2
2	0.75	13	4	8	0.93	1	2
3	0.83	18	4	9	0.94	15	2
4	0.87	14	3	10	0.95	13	1
5	0.89	13	3	11	0.96	16	1
6	0.90	16	3	12	1.02	14	1

We are interested in the variables, of those examined, which affect the attainment of high loading. We have divided the results into quartiles. Very roughly, we are interested in the correlation between the experimental variables, and attainment of the first (preferably) or first and second quartiles. In Table 4 we indicate the variable, the number of experiments in that set, the percentage attaining the first quartile, and the percentage attaining the first or second quartile.

Table 4. Variables Affecting Loading

		Quartiles	
Pd Lot Variation:	#	First	First or Second
E1	32	53%	78%
E2	24	29%	67%
E3	38	26%	42%
Not {E1,E2,E3}	82	12%	38%
E5	15	13%	80%
JM	40	18%	35%
Additives:			
Al	68	34%	57%
Ni	10	0%	0%
None	71	17%	48%
Physical Variables:			
Machined	39	36%	77%
d<0.25 cm	42	14%	26%
t>1009 h	70	34%	63%

Table 4 reveals a striking variation between Pd samples, even in lots from the same manufacturer. For Engelhard Lot#1 (E1), 53 % loaded into the first quartile while 78 % reached the first two quartiles. Whatever property this material had (or, critical flaw it did not have), there was less of it in subsequent lots, which exhibited generally inferior behavior.

For various samples from Johnson Matthey (JM), the pattern is not so clear. On average, these materials performed poorly (although better than other samples in the not {E1, E2, E3} set). The distribution for all JM samples is, however, bimodal, exhibiting a peak in Group 5 and another in Group 12.

For the effect of additives, only Al and Ni were sampled in statistically significant numbers. For Al, the effect is moderately strong and positive; for Ni (in this cases as an anode, not an additive) the effect is strong and deleterious. The set with no additives {None} loaded less well, on average, than those with deliberate additives.

In the final category, strong effects are seen for machining, cathode diameter, and experiment duration. "Machined" refers to those cathodes for which the outer surface was removed mechanically, by a cutting tool, in a lathe. In this process, the radius (of a 1/8" or 3mm diameter) cathode was reduced by ~ 0.1mm (respectively to 3mm or 2.8mm diameter), in a single pass of the cutting tool. This process appears to be beneficial in removing surface inclusions and mechanical defects, and in promoting loading.

In our experiments, smaller diameter wires ($d < 0.25$ cm) have not loaded, on average, as well as cathode 2.8 mm in diameter and larger. It should be noted that none of the smaller diameter wires were machined prior to electrolysis.

The final variable, duration of experiment, needs to be interpreted with care. Experiments longer than average ($t > 1009$ h) correlate with high loading. This reflects two factors. Cathodes which initially load poorly (fourth quartile) tend not to respond with better loading following anodic stripping or chemical addition, and these experiments often were terminated early. Cathodes which initially load at least into the third quartile, often display increased loading after anodic stripping cycles with or without chemical addition. This improvement may continue in several sequential loading cycles, each of which may require 200-400 hours. Such experiments tend to be longer than average and to result in better than average loading.

4. Metallurgical Variables in Loading

It is clear from Table 4, that the metal, itself, plays a role in determining the maximum loading. One might propose, as a hypothesis, that a difficulty in attaining reproducible starting conditions, in this case threshold loading, is due in large part to an uncontrolled variable contained within the Pd stock. Anticipating this possibility, the 176 cathodes analyzed in this paper were all prepared from moderate to high purity Pd. All were subjected to a similar annealing process (800-850°C for 2-3 hours, in low O_2 Ar, vacuum, or D_2 gas). With only one or two exceptions, all were etched with aqua regia (appropriately light or heavy) after machining and annealing. These procedures were intended to assert a uniform bulk and surface condition on the cathodes; nevertheless, significant variability was encountered between and within Pd lots.

Several important questions are raised in this analysis:

i) What is the characteristic of a "good" material?
ii) What is the uncontrolled parameter?
iii) How can we control this parameter to yield consistently high loading?
iv) How can we maximize the loading for a "good" Pd sample?
v) Does this procedure work to optimize loading in "poor" Pd samples?

We can begin to answer some of these questions by further analysis of our loading data base. Examining Table 4 we see that the parameters associated with the attainment of high loading are: Metal Source; Machining; {Annealing}; {Etching}; {1M LiOD} + Al addition. { } is a parameter employed, but not tested statistically. At this point, it is worth noting that a significant variable, the presence of dissolved silicate in solution, has also not been tested in this data set. Previous experiments[12] have indicated that Si is critical for the attainment of high loading. In all of the experiments described here this species was provided adventitiously by dissolution of quartz components of the electrochemical cell.

We can therefore propose a "best" procedure to achieve loading, based on the set of parameters examined. In this procedure one would:

[0) Select a suitable material]
1) Machine the outer surface to remove surface inclusions and damage.
2) Anneal at low oxygen partial pressure, in the temperature range 800-850°C, for 2-3 hours.
3) Etch cathode (plus Pt contact wires) in freshly prepared (heavy) aqua regia, for 5-10 seconds.
4) Electrolyze in 1 M LiOD, freshly prepared (in a H_2O free environment), by the reaction of D_2O with high purity Li.
5) After electrolyte preparation, and shortly before electrolysis, include in the electrolyte a small piece of high purity Al foil, sufficient to yield 200 ppm when dissolved.

The results are shown in Table 5 for experiments in which this enumerated procedure was followed.

Table 5. "Best Procedure" for Loading

	#	Quartiles	
Procedures 1-4 (No additive)		**First**	**First or Second**
E1	11	27%	55%
E2-4	6	33%	83%
Other	10	10%	80%
All	27	23%	69%
Procedures 1-5 (Al additive)			
E1	8	88%	100%
E2-4	4	100%	100%
Other	9	22%	78%
All	21	62%	90%
Procedures 2-5 (No machine)			
E2-4	26	23%	50%

While the selection constraints are severe, and the numbers in each category are small, a clear pattern emerges. Without the addition of Al, Procedures 1-4 show a small benefit for the Engelhard samples but no significant effect for other samples. In the presence of Al, however, following Procedures 1-5 yields a striking and useful result for Engelhard samples, and a beneficial effect for all metal samples.

We cannot generally assess the influence of machining as all E1 samples were machined before use. Procedures 2-5 (with Al, no machining), results in no significant improvement in maximum loading for the set of Engelhard samples {E2-4}.

From the analysis presented here, one may conclude that surface machining, and the addition of Al to the electrolyte both are important in concert, but that neither has a strong influence, alone. This concerted action, or synergism, benefits both the "good" loading materials, specifically early Engelhard Lots, and other generally more difficult to load Pd samples. In the light of this discovery, we must focus attention on the underlying mechanisms of loading, in order to reveal the hidden variable which influences the reproducibility of loading.

5. Other Issues of Reproducibility

The D/Pd loading is clearly a critical element in attaining the conditions that have been shown to be necessary for excess heat production. In the past six years, the issue of loading, and its reproducible attainment for both the D/Pd and H/Pd systems, has been studied extensively and with renewed vigor. Our understanding, however, remains poor. Furthermore, other parameters have been shown to be critical for the reproducible attainment of excess power: interfacial current density; time delay or initiation. In neither case is the role of these variables, or the process(es) that they engender, understood. Either may contribute significantly to an (apparent) irreproducibility of effect.

Recent experimental results have indicated a significant mathematical correlation between the rate of excess heat production, and the rate of change of the Pd cathode resistance. This effect, if not monitored, may constitute another important factor in (apparent) irreproducibility. If monitored and understood this phenomenon may yield information about fundamental processes and the underlying mechanism of excess heat production.

We measure cathode resistance, using a four-terminal method[3,7,10], to monitor D/Pd loading. Two parameters importantly control the resistance of palladium: hydrogen isotope loading, and temperature. In the experiments to be discussed, we observed a periodic variation in Pd resistance with fundamental period ~ 2 hours (~ 10^{-4} Hz), the amplitude of which appeared to correlate directly with the magnitude of the excess power being measured simultaneously in a mass flow calorimeter.[6,7]

If we accept that R/R° and P_{xs} both are measured accurately, then, as an explanation for this correlation we offer two hypotheses:

i) The observed excess heat is sourced at one or more small regions within the cathode. Because of the small volumes, local heating of the cathode produces resistance fluctuations which are observed at effectively constant loading. In this hypothesis, the excess power is the "cause", and the resistance the "effect". Periodicity of the resistance (perhaps induced by local de-loading following local heating) should be

associated in this model with a periodicity in excess power with the same frequency. Such an effect is indeed, observed.

ii) One can propose an alternative hypothesis in which resistance fluctuations reflect the "cause" with excess power the "effect". Unless the source of excess heat is extremely localized, at the levels of average excess power observed (1-5 W cm^{-3}) one would expect changes in local temperature insufficient to cause a detectable resistance variation. In which case one must look to a change in loading to cause a change in resistance. Bulk loading changes by adsorption/desorption processes at the cathode/electrolyte interface; this is accompanied by a flux of deuterons orthogonal to, and through the interface. The rate of change of average loading ($\delta x/\delta t$) is thus related to the deuteron flux.

There has been a suggestion[13] that, above a critical loading threshold, the rate of excess heat production should be related to the deuteron flux (*i.e.* ~ $\delta x/\delta t$). For this reason we have chosen to analyze our data in terms of hypothesis (ii). It should, however, be remembered that an alternative hypothesis exists which is consistent with the experimental evidence so far obtained.

6. Results

Figure 1 presents the current density, loading and excess power, measured by the methods previously described,[2-7] for a 1 mm dia., 10 cm long Pd cathode. The palladium was obtained from Johnson Matthey, and was formed into the shape of a horizontal "lasso", and annealed by our normal procedure.[7] The electrolyte was 1.0M LiOD containing 200 ppm Al at the outset. Sufficient Cu was added, dissolved in LiOD, 156 hours before the data shown in Figure 1, to make the concentration ~ 3 ppm in the electrolyte.

Figure 1 shows, initially, the normal response of a cell producing excess power: P_{xs} rising with increasing current density and loading above threshold values. After ~ 2 days, however, the characteristic of P_{xs} at constant current density and (generally) decreasing loading, is unexpectedly dynamic. Furthermore excess power was observed in this cell at an unusually low maximum loading (D/Pd ≈ 0.88).

Examining closely the loading plotted in Figure 1 we see that this too is unexpectedly dynamic. For the first and last 24 hours shown, the amplitude of the variation in x is small, in the period around 608 h intermediate, but for the rest of the time the average loading shows a significant variation about the mean, with standard deviation ~ ± 0.002. These periods of greater dynamism in x correlate with those for which $P_{xs} > 0$.

Figure 1b shows in detail the period of transition between low and modest excess power after 608 hours of electrolysis. While the frequency of the oscillation in loading does not change significantly, during the time of increasing P_{xs} (at t > 620h), the amplitude of this oscillation increases by a factor of 3 or more. When converted to a flux the rate of change of net loading could be accommodated by an adsorption and desorption current density, of ~ 0.1 - 1 mA cm^{-2}.

Understanding that considerable approximation is involved, we will propose a simplified predictive function for P_{xs}, and test this against the time series data. Figure 2 shows the excess power data from Figure 1a compared to the test function,

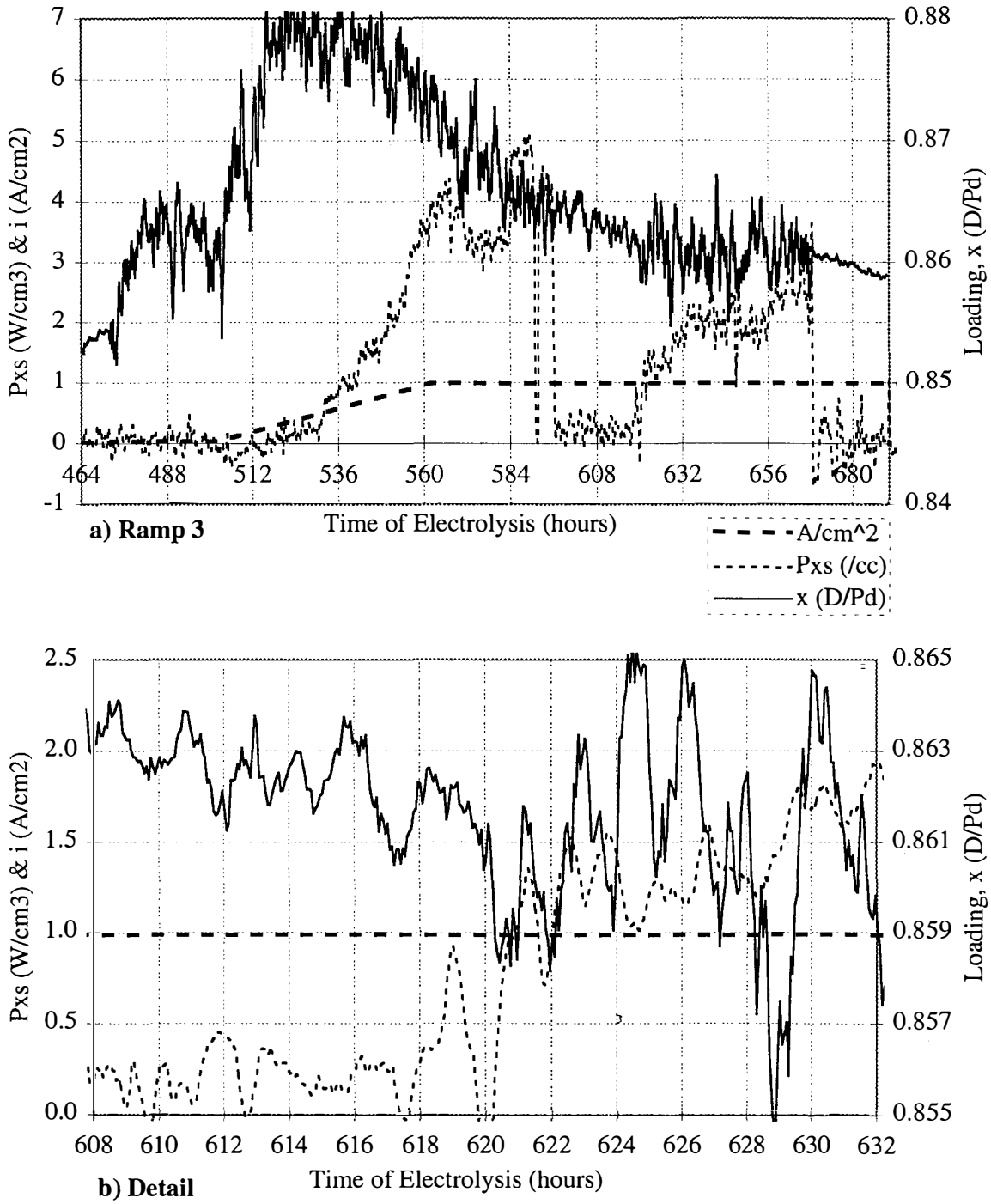

Figure 1 M4 Excess Power Current Density and Loading

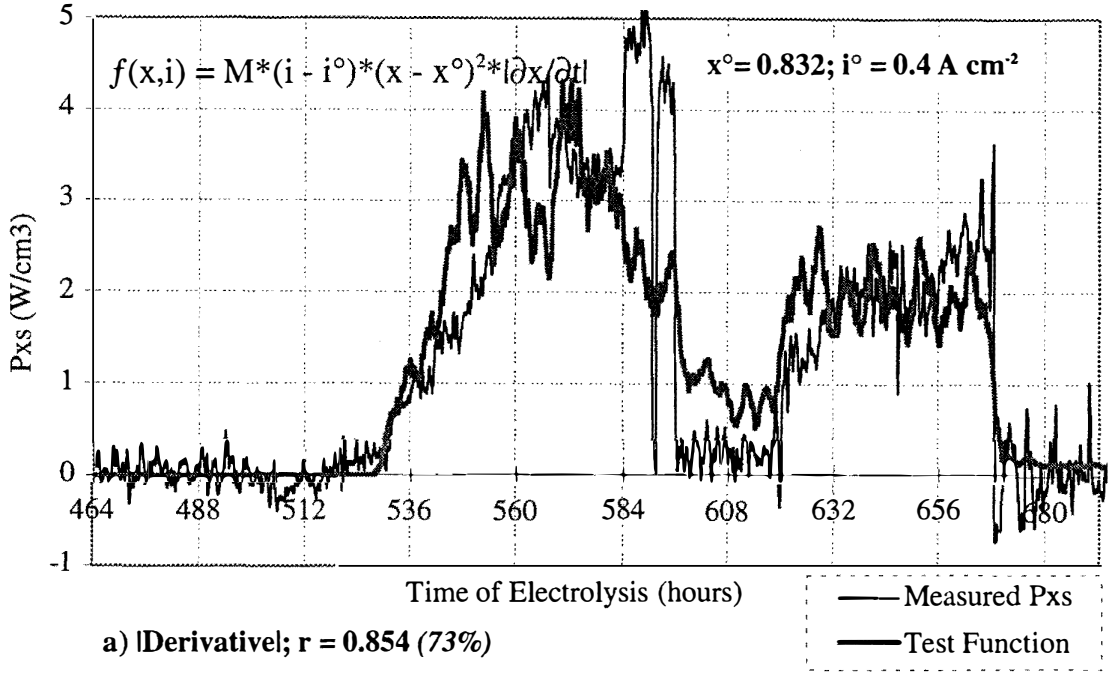

a) |Derivative|; r = 0.854 *(73%)*

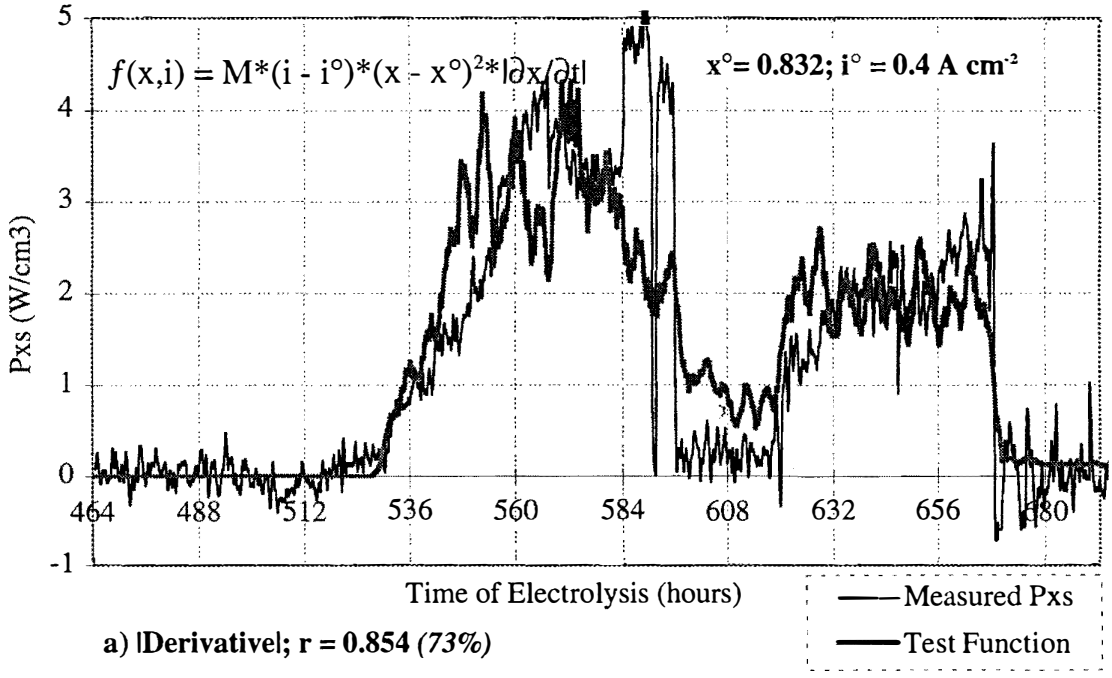

a) |Derivative|; r = 0.854 *(73%)*

Figure 2 M4 Excess Power and Fit Functions

$$P_{xs.test} = M\ (i - i^{\circ})\ (x - x^{\circ})^2\ |\delta x/\delta t|$$

The term $|\delta x/\delta t|$ assumes the importance of flux to be independent of sign, and gives no weight to a steady state flux. The proportionality constant, M, was determined to be 2.33×10^5 in order to set the two functions $P_{xs}(t)$ and $P_{xs.test}(t)$ to equal energy. The threshold values, x° and i° were determined by maximizing the correlation between these two functions. For the two data sets shown in Figure 2, the correlation coefficient, r = 0.854, with $x^{\circ} = 0.832$ and $i^{\circ} = 0.4$ A cm^{-2}

A value of 0.854 indicates that ~ 73% of the excess power is related linearly to our test function. Other variables may be involved (the test function is not complete) or the coefficients may not be precisely right or the component variables strictly independent (the test function is not completely correct); this is nevertheless a remarkable degree of correlation when the approximations and implications involved in generating the test function are considered.

A factor not taken into account in the simple correlation function is the possibility of temporal displacement between the two data sets. If one imagines that the test function is a generating function and the measured excess power is the response (that our test function is causal) then one might expect $P_{xs}(t)$ to be delayed with respect to $P_{xs.test}(t)$, and to have large amplitude (high frequency) features somewhat smoothed. Close inspection of Figure 2 reveals that this may indeed be the case; an analysis of the cross correlation function will be presented elsewhere, together with a more rigorous description of the treatment of the variable $|\delta x/\delta t|$.

Important questions are raised by the apparent success of our test function:

i) how generally applicable is this function?
ii) is the function predictive or responsive to other (possibly hidden) variables?
iii) can the function be used to explain the appearance of excess power in some experiments and its non-appearance in others.
iv) can the function variables be used to induce controllable excess power?
v) what can this function teach us about the phenomenon under test?

On the question of general applicability, we are limited in our choice of comparative experiments. It would be desirable to select reference experiments having the same cathode geometry and dimension as the M4 cathode. Very few of our experiments have been performed with 1 mm wires, and none, previously, with the "lasso" geometry employed in M4. In practice, we are more constrained in our choice by the need for high data quality in resistance measurements, so that random measurement errors are not introduced into the values of $\delta x/\delta t$. Simply because the signal-to-noise ratio for 1 mm wires is better than the 3 or 4 mm diameter wires more typically (and successfully) employed, we are reduced in our selection of comparative experiments to one only: C1.

Experiment C1 has been described previously.[4] Figure 3a presents the loading and current density data for the first current ramp of C1. As for M4, the loading inferred from the measured resistance initially shows little perturbation, first decreasing with time at low current density, then increasing with the current ramp. Some time after initiation of the current ramp, an oscillation appears in x, which builds in amplitude. Figure 3b

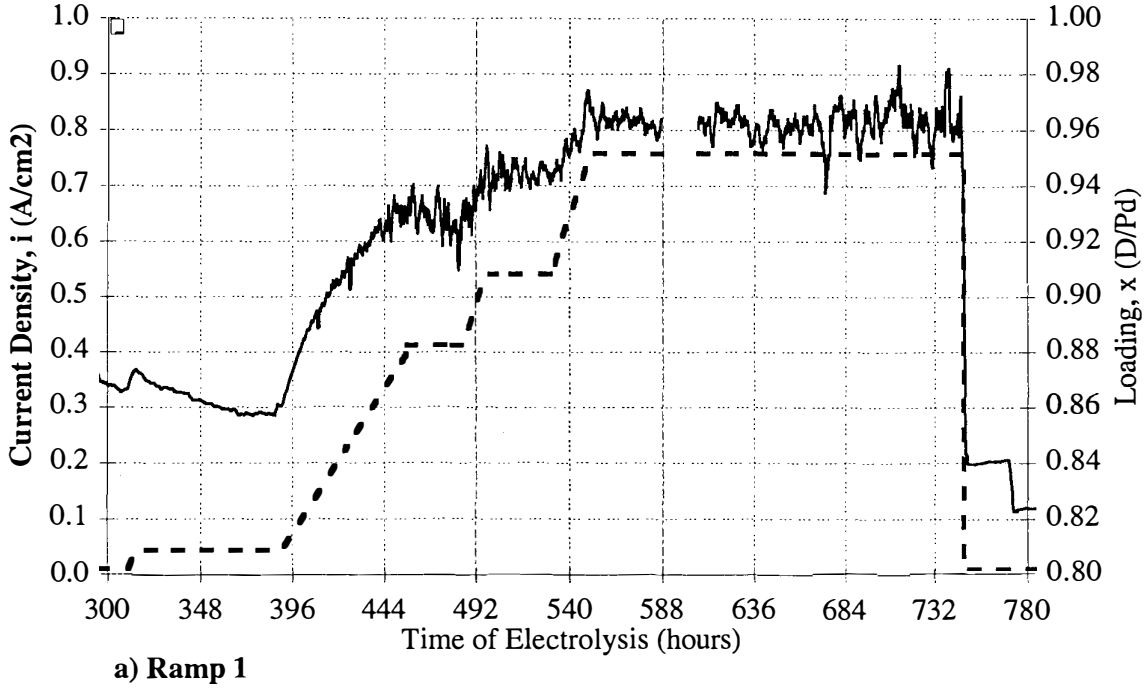

a) Ramp 1

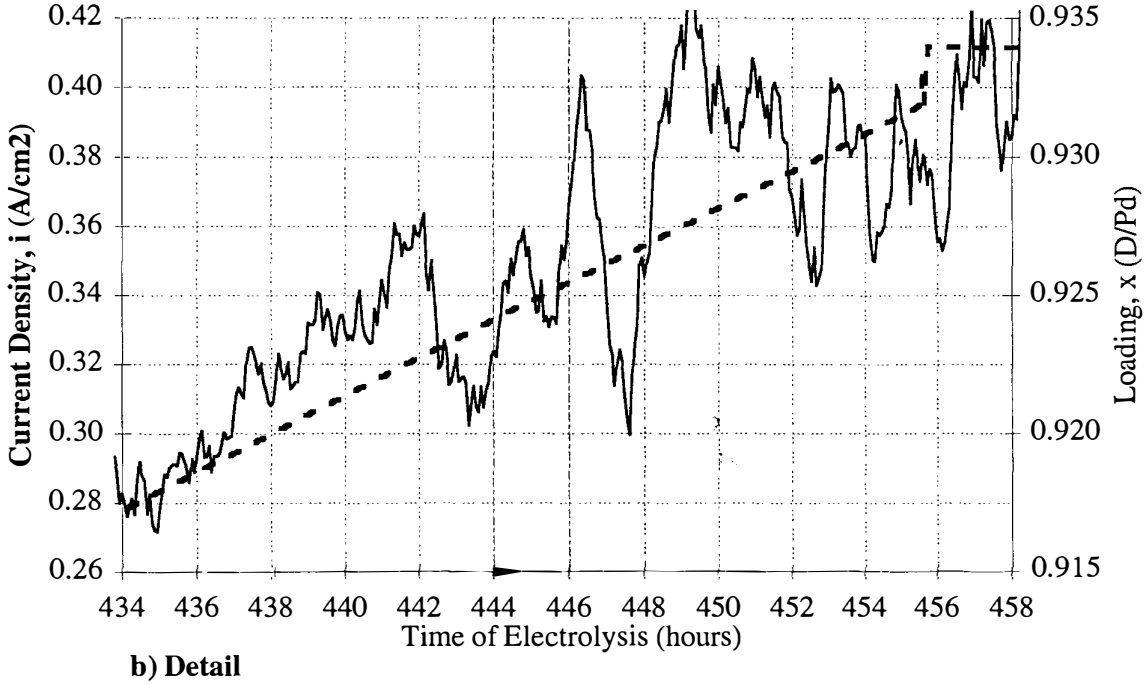

b) Detail

Figure 3 C1 Current Density (A/cm2) & Loading (D/Pd)

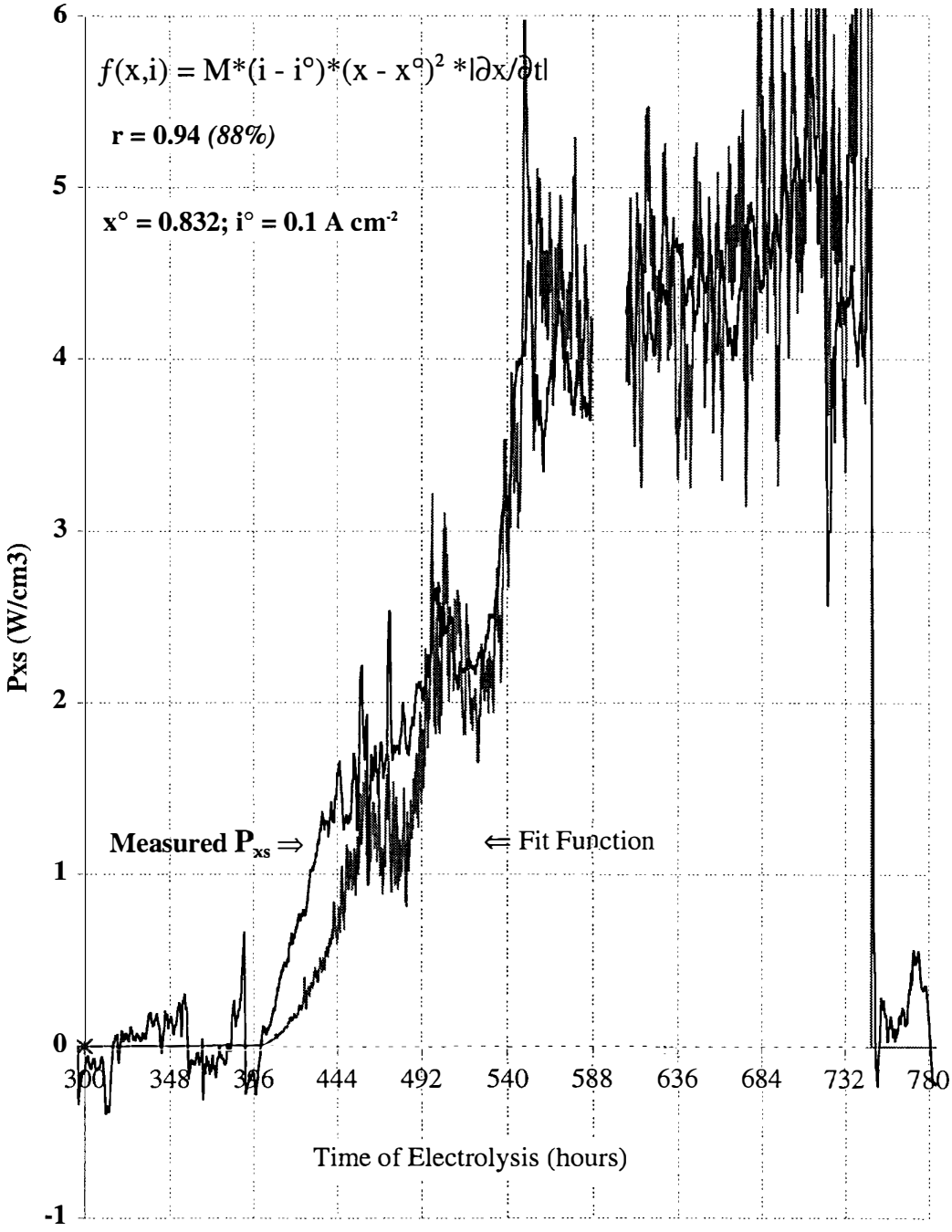

Figure 4 C1 Excess Power and Fit Function

shows a 24 hour detail in the vicinity of 444 h. While generally increasing with increasing current density, before 442 h the loading shows small fluctuation. After ~ 442h the loading exhibits a superimposed somewhat sinusoidal oscillation of period ~2h, as seen for M4. Perhaps significantly, the rate of increase in loading with increasing current density decreases at this point, suggesting the initiation of a transient de-loading (desorption) process, superimposed on the steady state loading.

Figure 4 shows the excess power measured during C1; ramp 1, compared to the test function employed previously for the M4 data (Figure 2). In this case, the value of x° was chosen to be the same as previously used for the M4 data (0.832); this value is also consistent with the number found by direct regression of P_{xs} vs. $(x - x^\circ)^2$. The maximum correlation is, however, found with a significantly lower current density threshold for C1 (0.1 A cm^{-2}) than for M4 (0.4 A cm^{-2}). For the two data sets shown in Figure 4, the correlation coefficient r = 0.94, with $x^\circ = 0.832$ and $i^\circ = 0.100$ A cm^{-2}. This correlation suggests that 88% of the function $P_{xs.test}(t)$ is reflected linearly in $P_{xs}(t)$.

7. Discussions and Conclusions

We have demonstrated a mathematical correlation between excess power and the product of three variables: the excess current density, $(i-i^\circ)$; the excess loading, squared, $(x-x^\circ)^2$; the rate of change of the Pd cathode resistance. While we have demonstrated this correlation only for two experiments, M4 and C1, we have no reason to suppose that this correlation is not general. In one of two possible interpretations we have associated the rate of change of resistance with the rate of change of cathode deuterium loading, $\delta x/\delta t$, at constant temperature.

In terms of the "excess" parameters, there is little difference in the maximum value, $(i_{max} - i^\circ)$ between experiments M4 and C1. Although the threshold value for M4 is much higher, the current density obtained in experiment M4; ramp 3, also was higher, and the exponent of 1 makes this not a strong variable. A significant difference does exist in the maximum "excess loading" variable, $(x_{max} - x^\circ)^2$. Due to the higher loading attained, this variable for C1 exceeded that for M4 by nearly an order of magnitude.

This latter observation is exceedingly important. Assuming that we can, as seems reasonable, use our test function as a predictor or, at least diagnostic for P_{xs}, then we need to pay close attention to the variables which give rise to large increases in the magnitude of the test function. An order of magnitude is the difference between indiscernible levels of excess power (~ 50 mW), and an interesting effect. This focuses attention on the need to obtain loadings as high as possible, above the threshold, as the parabolic dependence has greater power in amplifying the effect.

In the M4 and C1 experiments, the observed excess power densities and excess current densities were very similar. In order to achieve this result in terms of our multiplicative test function, the order of magnitude lower excess loading in M4 must be compensated for by a similar increase in the flux variable, $\delta x/\delta t$. In terms of hypothesis (ii), therefore, it is only the adventitious presence of a large deuteron flux that has promoted the excess power in experiment M4 from an insubstantial level at the low maximum loading achieved, to significant levels.

It is important to recognize that in neither experiment, M4 or C1, was an attempt made to maximize $\delta x/\delta t$. Quite the contrary. Both experiments were operated at constant (or slowly changing) currents, temperatures, and gas pressures; the three variables most

likely to influence loading. What fluctuation in loading did occur, and in both cases it was significant and varied, occurred apparently spontaneously; we observed the effect, we did not control it.

Nevertheless, if our hypothesis is correct, it may prove advantageous to understand the role of deuteron flux, and the means by which this can be stimulated without net de-loading, as a means to understand the phenomenon of excess power generation.

To this point we have treated the data statistically, and empirically. The functionality of our excess power test function can, however, be discussed in terms of at least one of the theories proposed for "cold fusion" phenomena. Hagelstein[13] has proposed that a phonon laser operates to initiate solid state neutron transfer, and to couple the nuclear energy produced, to the lattice, as heat. The details of this model are presented in Reference 13, and in preceding papers cited therein. This model makes two predictions that are relevant in the discussion:

i) No excess power will be observed at deuterium loadings below that at which the partial molar enthalpy change for desorption becomes exothermic.
ii) The rate of excess heat release (excess power) will increase with the desorption flux.

The first (threshold) criterion establishes the point at which a phonon laser may begin to operate. In an accompanying paper[14] we have attempted to define the position of this loading threshold based on literature data for the Pd-D system. By extrapolating the literature data at lower loadings, we estimate that the threshold value for the exothermic desorption of deuterium from palladium to be $0.83 \leq x^{\circ} \leq 0.85$. A value closely in accord with our observed value of $x^{\circ} \approx 0.832$.

The second (flux) criterion is associated with the rate of phonon excitation. This flux can be measured as the rate of change of the average loading; in the Hagelstein model only the desorption flux plays a role. In our empirical function we have employed $|\delta x/\delta t|$. For a symmetric loading/de-loading cycle (*i.e.* no dc term) the average value of $|\delta x/\delta t|$ is simply twice the average value of the desorption component alone, so that our observed correlation would be unchanged, and consistent with the Hagelstein model prediction.

A great deal more needs to be said about our results, the correlation analysis, and the relationship of these to the Hagelstein model predictions. We need to consider the time-scales of the various processes, the relationship of the observed transient net flux to the atomic scale process of a heterogeneous surface, and any possible role that a steady state flux may play. A related topic of importance is the relationship between the endothermic/exothermic transition surveyed by Crouch-Baker[14] to the phonon laser threshold predicted by Hagelstein[13], particularly as these affect the onset of thermal positive feedback, observed calorimetrically by Pons and Fleischmann.[15]

Despite our incomplete understanding, we are encouraged to see, perhaps for the first time in this field, the suggestion of a synthesis and consensus of theory and experiment.

Acknowledgments

The financial support provided by the Institute of Applied Energy and the New Energy and Industrial Technology Development Organization (Japan) and the Electric Power Research Institute (U.S.A.) is gratefully acknowledged.

References

1. M. Fleischmann, S. Pons and M. Hawkins, "Electrochemically Induced Nuclear Fusion of Deuterium", *J. Electroanalytical Chem*, **261** p. 301-308, (1989).

2. M. McKubre, R. Rocha-Filho, S. Smedley, F. Tanzella, J. Chao, B. Chexal, T. Passell, and J. Santucci "Calorimetry and Electrochemistry in the D/Pd System" in *Proceedings of the First Annual Conference on Cold Fusion*, National Cold Fusion Institute, Salt Lake City, UT, 1990, p. 20.

3. M. McKubre, R. Rocha-Filho, S. Smedley, F. Tanzella, S. Crouch-Baker, T. Passell, and J. Santucci "Isothermal Flow Calorimetric Investigations of the D/Pd System" in *The Science of Cold Fusion,*, Eds. T. Bressani, E. Del Giudice, and G. Preparata, Conference Proceedings Vol. 33, Italian Physical Society, Bologna, 1992, p. 419.

4. M. McKubre, S. Crouch-Baker, A. Riley, S. Smedley and F. Tanzella "Excess Power Observations in Electrochemical Studies of the D/Pd System: Proceedings of 3rd International Conference on Cold Fusion, *"Frontiers of Cold Fusion"*, ed. H. Ikegami, Universal Academy Press, Inc., Tokyo p. 139 (1993).

5. M. McKubre, S. Crouch-Baker, S. Smedley and F. Tanzella, "An Overview of Calorimetric Studies on the D/Pd System, at SRI; May 1989 to October 1993. Proceedings of the Russian Conference on Cold Fusion (RCCF), Abrau Durso, September 1993.

6. M. McKubre, S. Crouch-Baker, A. Hauser, N. Jevtic, S. Smedley, M. Srinivasan, T. Passell and F. Tanzella, "Loading, Calorimetric and Nuclear Investigation of the D/Pd System", Presented at the Fourth International Conference on Cold Fusion, Maui Hawaii (1993).

7. M. McKubre, S. Crouch-Baker, R. Rocha-Filho, S. Smedley, F. Tanzella, T. Passell, and J. Santucci "Isothermal Flow Calorimetric Investigations of the D/Pd System" *J. Electroanalytical. Chem.*, **368** (1994) p. 55

8. K. Kunimatsu, "Deuterium Loading Ratio and Excess Heat Generation", Proceedings of 3rd International Conference on Cold Fusion, *"Frontiers of Cold Fusion"*, ed. H. Ikegami, Universal Academy Press, Inc., Tokyo p. 139 (1993).

9. N. Hasegawa and N. Hayakawa, "Observation of Excess Heat During Electrolysis of 1M LiOD in a Fuel Cell Type Closed Cell", Proceedings of the 4th International Conference on Cold Fusion, Maui Hawaii (1993).

10. D. Macdonald, M. McKubre, A. Scott and P. Wentrcek, "Continuous *In-Situ* Method for the Measurement of Dissolved Hydrogen in High Temperature Aqueous Systems", I&EC Fundamentals **20**, p. 290, (1981).

11. M. McKubre, S. Crouch-Baker, A. Hauser, N. Jevtic, S. I. Smedley, F. L. Tanzella, M. Williams, S. Wing, "Development of Energy Production Systems from Heat Produced in Deuterated Metals", Final Report on EPRI Contract 3170-23, (1995).

12. M. McKubre, S. Crouch-Baker, S. Smedley, F. Tanzella, M. Maly-Schreiber, R. Rocha-Filho, P. Searson, J. Pronko and D. Kohler, "Development of Advanced Concepts for Nuclear Processes in Deuterated Metals", Final Report on EPRI Contract 3170-01, (1994).

13. P. Hagelstein, "An Update on Neutron Transfer Reactions", Proceedings of the Fifth International Conference on Cold Fusion, Monte Carlo (1995).

14. S. Crouch-Baker, M. McKubre, and F. Tanzella, "Some Thermodynamic Properties of the H(D)-Pd System", Proceedings of the Fifth International Conference on Cold Fusion, Monte Carlo (1995).

15. S. Pons and M. Fleischmann, "More About Positive Feedback, More About Boiling", Proceedings of the Fifth International Conference on Cold Fusion, Monte Carlo (1995).

Fifth International Conference on Cold Fusion
9-13 April, 1995 - Monte Carlo, Monaco
ICCF5 ©1995

Power Excess Production in Electrolysis Experiments at ENEA Frascati

L. Bertalot[1], A. De Ninno[2], F. De Marco[1], A. La Barbera[3], F. Scaramuzzi[4], V. Violante[1]

(1) ENEA, Dip. Energia, Settore Fusione, Centro Ricerche Frascati, C.P. 65 - 00044 Frascati, Italy
(2) ENEA/INN/FIS, same address
(3) ENEA/INN/NUMA, same address
(4) ENEA/ERG, same address

Abstract

Continuing the research activity on heat excess detection during the electrolysis of heavy water with palladium (Pd) cathodes, previously reported at ICCF3 and ICCF4, new experiments have been performed with success. In one of them it was also possible to correlate the power excess production with other parameters of the experiment: its description will be the subject of this communication.

1. Introduction

Many types of experiments are enlisted under the name of "Cold Fusion" (CF), following the first one performed by Fleischmann and Pons (1). Among them, the measurement of the production of heat in excess during the electrolysis of heavy water with a palladium (Pd) cathode has been more extensively investigated, and a substantial progress has been produced.

In the past years we have performed two campaigns of measurements of this type, which have produced positive results: i.e., they have allowed us to detect heat in excess during extended periods of time (up to tens of hours) with values largely above the sensitivity of the apparatus (by 1 to 2 orders of magnitude). We have chosen a particular geometry, in which the cathode is a flat Pd electrode of circular shape, in contact on one side with the electrolytic solution, and on the other side with a vacuum-tight ambient, in which the pressure of the deuterium gas permeating through the metal could be measured: in this way we have also been able to get information helpful to the comprehension of the dynamics of D in Pd during the electrolysis (2). The evaluation of the D/Pd ratio with resistivity measurements was not possible with this apparatus, because of its unfavourable geometry. We have thus decided to perform a new experiment, aimed to learning how to measure the D/Pd ratio through the resistivity of the cathode. In order to do so, we have changed the geometry of the electrolytic cell, by using a cathode in the form of a thin Pd cylinder

and the anode in the shape of a Pd hollow cylinder, surrounding the cathode.

In the first attempt the aim of our experiment was not reached. On the other side, the experiment was particularly successful as far as the production of heat in excess is concerned, and for the possibility of correlating the heat production with other parameters of the experiment, noticeably the difference of potential between anode and cathode (which in the following we will call the voltage V): this correlation can in our opinion help understanding the phenomena at the basis of the heat excess production.

2. The experiment

The current in the electrolytic cell was started on March 21, 1994, and was shut down on May 9, after 50 days. In this period heat excess was observed in three occasions, each one lasting more than one day. In this chapter we will describe, in the order: the cell, the calorimetry, and the results.

2a. The cell

The cell, with the exception of the shape of the electrodes, is of the same type described in reference (2). Anyway, we will outline here its main features (see Fig.1). It is made out of Pyrex glass, with a substantially tight Teflon cap: it contains ≈ 250 cm^3 of high purity heavy water. The electrolyte used is LiOD, and the molarity has been changed during the experiment from 0.1 M to 0.5 M. The cathode is a Pd solid cylinder, 2 mm in diameter, with a useful length (the length facing the anode) of 2 cm. The anode is a Pd hollow cylinder, 2 cm high, 0.5 mm thick and 8mm inner diameter. The electrolytic current is fed with a constant-current power supply, and both the current and the voltage are continuously monitored: since the voltage is subjected to abrupt changes due to the production and detachment of gas bubbles at the surface of the electrodes, its signal is recorded across an RC circuit, with a constant time of $\approx$10 s, long with respect to the characteristic times of the quoted changes, short with respect to the characteristic times of the heat transfer processes. The electrodes are connected to the external circuit by spot-welding to them nickel conductors. The gases evolved at the electrodes (O_2 and D_2) are conveyed through a Teflon pipe outside of the cell, and the gas flow is measured

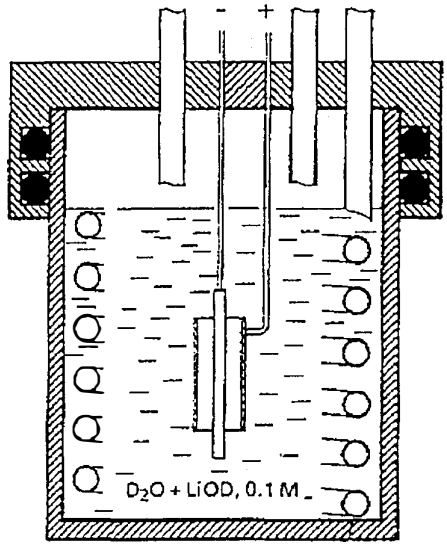

Fig.1 Schematic view of the apparatus: cathode and anode of the electrolytic cell are shown. In the coil presented in section water flows for calorimetry.

every few hours, in order to check it against the value of the cell current, thus confirming the efficiency of the electrolysis: values between 95% (at low currents) and 100% (at high currents) are always obtained. At intervals, depending on the current intensity, fresh heavy water must be added in order to compensate for the electrolysed water. Before starting the experiment, both the electrodes have been cleaned with organic solvents, and then degassed by bringing them to the temperature of ≈ 200°C under vacuum for about an hour. Assembling and charging heavy water has been performed in an inert atmosphere of argon.

2b. Calorimetry

Also the calorimetry is in principle the same as in reference (2); anyway, it will be described here. The cell, contained in a glass dewar, is placed inside a large styrofoam box, in which the temperature is kept constant to better than 0.5°C with the help of a source of heat (an electric bulb) and a source of cold (a coil in which water from the tap is circulated): the latter is substantially at constant temperature, while the bulb is activated by a thermoregulator led by a thermometer placed in the box. A fan assures that the maximum temperature difference inside the box is lower than 0.5°C. The main feature of the calorimeter is a Pyrex glass coil immersed in the cell, as shown in Fig.1, in which water is circulated. The heat exchange between the circulating water and the liquid in the cell acts in such a way as to extract most of the power produced in the cell, in the following called the output power. We evaluate that a large percentage (of the order of 95%) of the power produced is extracted in this way, the remaining fraction being dissipated (mostly by convection in the liquid to its free surface and then by conduction/convection and by radiation) to the outside world. Care is taken that the water enters always at the same temperature (within 0.1°C) and is circulated with a constant flow. The former feature is obtained by using a thermoregulated water source, while the latter is pursued by having the water circulated by free fall from an upper container to a lower one: then, it is sent back to the upper container by a pump. The water flow rate is however checked every few hours and it results constant within 1% along the whole experiment. Two thermocouples are placed at the inlet and at the outlet of the circulating water to the cell, and are connected in a differential mode (by short-circuiting two leads together, and measuring the difference of potential between the two remaining leads). This circuit gives directly the difference of temperature between these two points (ΔT), which is a monotonous function of the power output, and by calibration is found to be substantially linear for powers lower than 30 W. Note that the use of a water-circulating coil extended to all the height of the cell guarantees that the measured value of the power output is averaged on the whole volume of the cell. The calorimeter is calibrated by producing a known power in the cell and measuring the ΔT. This has been done by using an electrical resistor immersed in the same position in which the cathode will be placed, and dissipating in it a known Joule power. The calibration has been made at different starting temperatures, between 20° and 50°C, for different molarities of the solution, and for powers ranging up to 50 W.

In order to calculate the power excess, the power input is subtracted from the power produced in the cell, i.e., the power output. The former is obtained by the formula:

$$P_{in} = (V - 1.54)\ I \text{ watts}$$

with V in volts and I in amperes (the constant 1.54 volts takes into account the energy spent by the current to electrolyse the water). The power output is obtained, as said before, through the measurement of the temperature difference T between the

inlet and the outlet of the circulating water in the cell, with the help of the calibration curves obtained previously. We evaluated the overall error in the measurement of the excess power to be well within 100 mW, at all power output levels.

2c. The results

Fig.2 shows a summary of the results, expressed as the time evolution of the experiment: only the last, most relevant, 22 days are shown. Two quantities are reported: the excess power P, measured as described before and expressed in watts (scale on the left), and the voltage V, measured in volts (scale on the right). The abscissa is the time t, measured in days, from 28, corresponding to April 18, to 50, corresponding to May 9. The basic temperature chosen for the experiment was 30°C. The molarity was increased on the 10th day from the initial 0.1 M to 0.5 M. The maximum current of 2 A was applied on the 30th day, the previous value being 1.2 A.

The first episode of power excess production started on the 30th day, and was hardly noticeable: the power excess grows very slowly, reaching the value of about 200 mW on the 32nd day, when the addition of heavy water in the cell shuts the excess power down. But another productive period starts soon after, lasting 5 days, with power excess increasing up to about 700 mW, ending on the 37th day, when another refilling - this time not with pure water, but with a 0.5 M solution preheated at the cell temperature - destroys it again. No heat excess is produced in the following 5 days. In order to "stimulate" the system, on the 43rd day we invert the current in the cell for 30 seconds, interchanging cathode and anode in the circuit. After 1.5 days another period of excess power production is initiated: this time it will

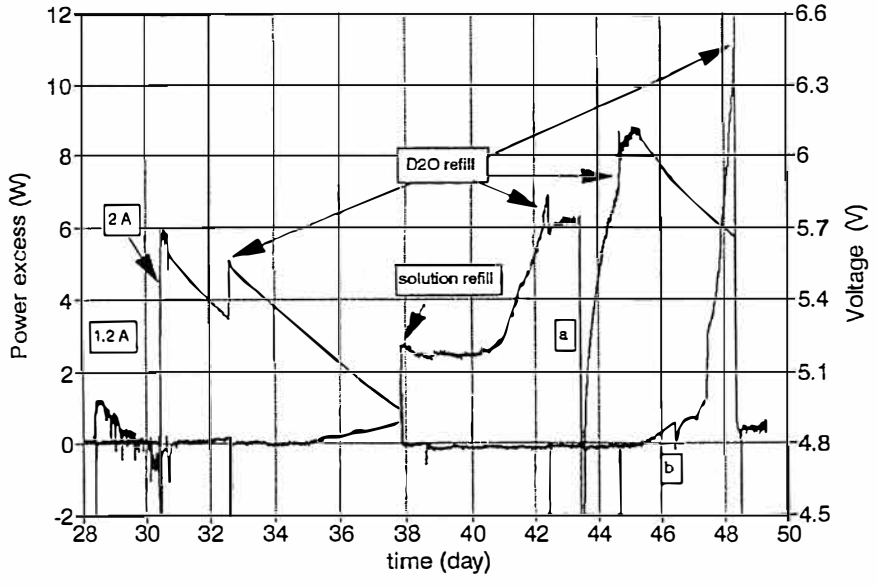

Fig.2 The rsults obtained during the last 22 days of the experiment. Letter a refers to the inversion of current described in the text. Letter b refers to the 10-s short-circuit produced on the 46th day.

last about 3 days, the excess power will grow almost exponentially, eventually reaching the value of 11 W. Note that the power input at that moment was 8 W. Once more the undelayable addition of heavy water shuts the cell down, and this time forever.

On the 46th day, while doing a check on the circuit, we unwillingly short-circuited the cell for about 10 seconds. This is not visible on the voltage, but had a quite dramatic effect on the power production: it looks as if the system is less efficient in producing heat for about one day, then goes back rapidly to the previous trend. Without this episode, one could claim that the increase in power excess production was a real exponential as a function of time. Anyway, we think that this episode is quite instructive, and we will go back to it when commenting the results.

The exam of the voltage behavior is quite interesting in this experiment. In particular, we notice an apparent "change of mode" exhibited by the voltage whenever a power excess production is in course. The signal, that in the absence of power excess is rather noisy, with oscillations within about 0.03 volt, becomes abruptly quiet, and takes on a very regular trend, consisting in a decrease of the voltage as a function of time. The passage from the noisy to the quiet mode can be seen twice: on the 30th day and on the 45th day. The latter is shown with an expanded scale in Fig.3. In next chapter a possible interpretation of this phenomenon will be presented.

The end of the experiment was determined by the enormous increase of V produced after the last refilling on the 48th day: the value went up to about 13 volts. We interpret this as a consequence of the substantial destruction of the anode, consumed by 50 days of electrolysis (which was confirmed by the inspection of the electrolytic cell performed at the end of the experiment).

3. Comments on the results

3a. Is there a phase transition?

In the description of the results we have shown that there seems to be a correlation between the appearance of heat excess and the "mode" of the voltage V as a function of time. The first mode that we envisage is characterised by a random oscillation of the voltage, within about 0.03 volt, and a general trend in time, increasing and decreasing, the latter not always clearly correlated to the various operations performed on the apparatus: this has been the mode of the first 30 days, and of the 7 days between the 38th and the 45th. In the second mode, quoted before, present when heat in excess is produced, the noise is strongly reduced and the general trend of the voltage is a regular decrease: this can be explained, also quantitatively, by the consumption of water, at constant amount of electrolyte, and thus with increasing molarity, produced by the electrolysis.

The extended graph of the voltage as a function of time in the vicinity of the change of mode (Fig.3) emphasizes the noise reduction: it reminds visually the occurrence of a phase transition, mostly for the abruptness of the commutation between the two modes. We have tried to imagine an empirical and qualitative explanation of what happens. We imagine that during the electrolysis, once the deuterium has been charged in the cathode, gaseous D_2 is formed on its surface. What one would expect is that the molecules so formed organise themselves in tiny bubbles of gas, which grow slowly, still remaining attached to the surface, until they reach a convenient size, such that the buoyant force due to the Archimedes principle exceeds the sticking force of the bubble to the surface: then, the bubble detaches itself and moves to the surface of the liquid. During the growing phase, the bubble

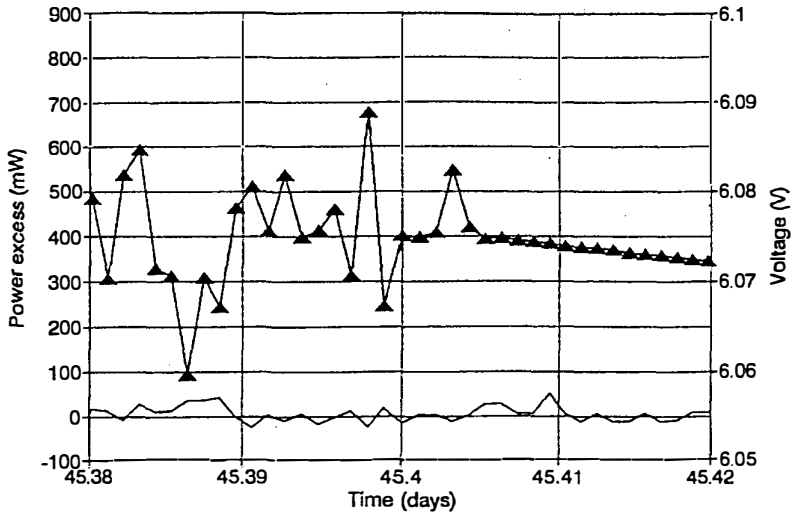

Fig.3 An enlarged detail of Fig.2, showing the change of mode of the voltage V on the 45th day.

represents an increasing electrical impedance to the current: thus, at constant current, this means that the applied voltage has to continuously increase. When the bubble detaches itself from the cathode and flies to the surface, there is an abrupt decrease of the electrical impedance of the cell, and thus a decrease of the voltage. Each bubble, thus, produces in time a tiny saw-tooth shaped variation of the voltage. What we see on the left side of Fig.3 is presumably the average effect of many bubbles which are growing and eventually detaching themselves from the cathode surface: the use of an RC filter on the V-measuring circuit has only the effect of reducing the voltage changes produced by this phenomenon. In order to explain why, on the right side of Fig.3, the oscillation disappears, we can imagine that, for some unknown reason, the bubbles are no more allowed to grow, and the gas is leaving the surface of the cathode with much smaller bubbles. Since the buoyant force cannot be altered, the only explanation is that the sticking force is much smaller. This could be due to some disturbance coming from the inside of the cathode, which alters it. The fact that this passage from one mode to the other is so abrupt as shown in Fig.3 substantiates the hypothesis that we could be dealing with a phase transition in the PdD_x lattice, characterised by the set up of some kind of field (phonons?) within the lattice.

We have been looking into our previous experiments (2), to see whether this change of mode accompanied the appearance of heat excess production, and we had a confirmation, even though less dramatic. Anyway, we must remember that in the previous experiments, as quoted above, we used a planar geometry for the electrodes. The contribution of the cathode potential to the build-up of the voltage V is much more relevant in a cylindrical geometry with a thin inner electrode (the cathode), as that used in the present experiment, than in a planar geometry. Thus, it is to be expected that the phenomenon is more evident in the present configuration.

3b. Surface or bulk?

Since the first days of CF the question of whether the observed phenomena, whatever they were, were taking place on the surface or in the bulk of the system has been put and extensively discussed. For the heat excess phenomena, their depend-

ence on the D/Pd ratio is a clear indication that the bulk of the PdD_x system is involved. Nevertheless, the relevance of the surface, for example to the D-charging, is out of discussion. The argument is not a straightforward one, and more research is required to address it, and give it an answer, provided that a simple answer does exist.

However, in our experiment there are two episodes, already quoted in chapter 2, that could contribute to this discussion, and we want to point them out. On the 43th day (see Fig.2) we inverted for 30 seconds the current in the electrolytic cell. The effect was much more dramatic than expected. It took almost one day for the voltage to go back to the original value. The second episode took place on the 46th day, while producing excess power. We short-circuited the cell for 10 seconds, and, if we accept the hypothesis of the exponential growth of the power excess, again it took one day to resume its original trend, with a dramatic recovery at the end of the day, consisting in the increase of 2 W in half an hour. Keeping in mind the order of magnitude of the coefficient of diffusion, even at the high levels expected at high D/Pd ratios, such short perturbations should affect only the first few monolayers of the system, and this is enough to produce a big change in its behaviour. This seems to indicate the relevant role that the first layers of the charged cathode have on the observed phenomena.

4. Conclusions

It seems to us that the experiment reported here constitutes a strong confirmation of the reality of CF, at least for what concerns the production of heat in electrolytic cells with heavy water and Pd cathode. Many open problems remain, such as the nature of the energy produced, the existence of a phase transition, whether the phenomenon takes place in the bulk or on the surface of the cathode, and so on: we have tried to outline some of them in Chapter 3. They will be addressed in our next experiments, starting with the measurement of the D/Pd ratio in real time. Other implementations to our experiment will be realised, the most important of which consists in analysing the gases evolving from the cell, mostly D_2 and O_2, in order to check for the presence of the helium isotopes, that would provide an evidence for the nuclear nature of the heat. A field that should be thoroughly investigated concerns the material science properties of the PdD_x system, with the aim of evaluating the meaningful parameters for a reproducible charging of D in Pd at high D/Pd ratios.

Acknowledgements

The experiment described here would not have been possible without the skill and dedication of the technicians operating in our Group: Mr. Domenico Lecci, Mr. Giuseppe Lollobattista and Mr. Fabrizio Marini. To them goes our deep appreciation.

References

1. M. Fleischmann, S. Pons, and M. Hawkins, "Electrochemically Induced Nuclear Fusion of Deuterium", J. Electroanal. Chem., **301** (1989)
2. L. Bertalot, F. De Marco, A. de Ninno, A. La Barbera, F. Scaramuzzi, V. Violante, P. Zeppa, "Study of Deuterium Charging in Palladium by the Electrolysis of Heavy Water: Search for Heat Excess and Nuclear Ashes", Frontiers od Cold Fusion, Proceedings of ICCF3, Editor H. Ikegami, Universal Academy Press Inc., Tokyo, pag. 353 (1993);
L. Bertalot, F. De Marco, A. De Ninno, R. Felici, A. La Barbera, F. Scaramuzzi, V. Violante, "Behavior of a Pd Membrane During Deuterium Electrochemical Loading: Excess Heat Production", presented at ICCF4, Maui, Hawaii, USA, December 1994

Fifth International Conference on Cold Fusion
9-13 April, 1995 - Monte Carlo, Monaco
ICCF5 ©1995

Anomalous heat evolution of deuteron implanted Al on electron bombardment

K. Kamada, H. Kinoshita[1] and H. Takahashi[1]
National Institute for Fusion Science, Nagoya,
464-01 Japan.
[1]Department of Engineering, Hokkaido University,
Sapporo, 062 Japan

Abstract

Anomalous heat evolution was observed in deuteron implanted Al foils on 175 keV electron bombardment. Local regions with linear dimension of several 100nm showed simultaneous transformation from single crystalline to polycrystalline structure instantaneously on the electron bombardment, indicating the temperature rise up to more than melting point of Al from room temperature. The amount of energy evolved was more than 180MeV for each transformed region. The transformation was never observed in proton implanted Al foils. The heat evolution was presumed to be due to a nuclear reaction in D_2 molecular collections.

1. Introduction

In a previous paper [1], one of the authors (K.K.) reported an anomalous particle emission phenomenon from H_3^+ or D_3^+ implanted Al foil on 200 or 400keV electron bombardment. In the paper, the author presumed that fusion reactions to take place not only between deuterons but also between hydrogenes, which were embedded in the so called "Tunnel Structure" (T.S.), created in sub-surface layers of Al on the implantations. (The results will be supplemented by more detailed experiments and also by theoretical considerations in a recent paper [2].)One of the prominent features of this phenomenon was that it is not due to the energetic collisions between reacting particles. This was derived in the paper [1] from the calculation on the fusion reaction rate between knocked-on deuterons, produced by the electron bombardment, and embedded deuterons. In the present state of our knowledge, we cannot present any conclusive mechanism of the phenomenon, but the author presumes that β disintegration of proton on capturing secondary electron in highly ionized hydrogen or deuteron plasma of nearly solid state density may play a fundamental role in some aspect of the phenomenon.

In the present paper, a direct observation of this anomalous phenomenon via heat evolution leading to very local melting of deuterium implanted Al on 175 keV electron bombardment is reported. The direct observation was made by the transmission electron microscope (TEM), which at the same time served as an electron accelerator.

2. Experiment

We first implanted Al specimens with 25 keV D_2^+ ions. The specimens were prepared beforehand so as to enable TEM observations after the implantation. They were polished chemically from Al disk with 5^{mm} diameter

and 0.1mm thick using TENUPOLE chemical polishing machine. The purity of the Al was 99.99%, and the specimens were annealed at 400℃ for 3 hours before the polishing. After the polishing they have wedge shape with average thickness of more than 1 μ m over an area of about 1mm diameter and have a small hole of about 0.1mm diameter in the central part of each specimen.

The fluence of the implanted deuteron was chosen around 5×10^{17} D^+/cm^2, since below this amount of fluence only a bubble structure is formed in the sub-surface layer of Al foil, and above that so called "Tunnel Structure" (T.S.) is produced [3].

The density of the implanted deuterium in the T.S., $1 \times 10^{22} D_2 cm^{-3}$, was also estimated from the same kind of experiment measuring the implanted amount of hydrogen during and after the implantation at room temperature [2,3]. Again from these experiments, the implanted deuterium are presumed to situate at about 100nm depth from the implanted surface. As a consequence, more than ten times of the implanted depth remains unimplanted beneath the T.S..

3. Experimental results

Two micrographs of Fig.1 show the typical examples of TEM observations taken on the Al specimens implanted with hydrogen, (a), and with deuteron, (b), respectively. Regions of brighter contrast in both micrographs are the T.S. regions, where Al atoms are lacked and, instead, hydrogen or deuterium molecules are contained. In the micrograph (b), we can observe several areas, like the one indicated by an arrow, where something looks like microcrystallites are concentrated. These speckled areas appear instantaneously with the focusing of electron beam for the observation with a brighter contrast. They are not inherent to the implanted Al originally, but are attributable to the electron beam focusing effect. Before the focusing, when looking for the area to be observed with less focused beam, we can never observe such speckled areas. Further, these speckled areas can never be observable in hydrogen implanted Al under exactly the same experimental conditions with the deuteron implanted case. (So far we have done several ten times of the hydrogen implantation experiment.) This is readily seen in the micrograph (a) of Fig.1. To observe the speckled area, there is a region of optimum fluence of deuteron ions, which produce the microstructure like those shown in Fig.1. For lower fluence than that in the optimum region, we observe only bubble structures and never observe the speckled area, and for higher fluence, we observe, in addition to the T.S. structure, the bubble structure again but never observe the speckled area.

For crystallographic investigation of the speckled areas, selected area electron diffraction was tried on about 500nm area surrounding the speckled area. Those inserted in Fig.1 show the diffraction patterns taken on the areas seen in the micrographs. One should pay attention that (b-1) in Fig.1 (b), which was taken at the speckled area, clearly demonstrates the polycrystalline pattern with co-central spotty circular rings. On the other hand, the diffraction patterns from the normal areas, (a-1) and (b-2), show only usual Bragg spots showing single crystalline Al. So far we have observed five polycrystalline rings from several speckled areas of different specimens. The lattice constants corresponding to the rings are tabulated in Table 1, together with the lattice constants and planes inhirent to Al.

To confirm the correspondence between the polycrystalline rings and the speckled area, dark field images were taken using several spots on the rings. Fig.3 (a) shows the bright field image of the speckled area with the diffraction rings, and (b) shows the dark field image of the same area taken with several diffraction spots on the rings. They show evidently that the polycrystalline spots originate from several parts of the speckled area, which appear brighter in (b).

The appearance of the speckled areas on the electron beam focusing is so rapid that we could not follow the detailed process of the appearance during the observation. However, after the appearance the images change rather gradually as seen in Fig.3. In this figure, (a) was taken in roughly 10 seconds or so after the appearance, and (b) and (c) were taken sequentially in less than 60 seconds after (a). These micrographs show rather gradual polycrystallization, judging from the growth of small crystallites as seen in (b) and (c), and the gradual change of equal thickness fringes as shown by an arrow. The change of the equal thickness fringes is presumed due to the thermal conditions around the region. The image did not change anymore after (c).

These observations indicate a rapid melting and gradual crystallization, which is rather conceivable if we assume that the reactions in D_2 collections occurred suddenly and was maintained for a short time, evolving the large amount of heat.

In addition to the above observations, we tried stereographic observations of the speckled region with change of the tilt angle of about 6 to 8 degrees to indentify the depth of the layer in which the polycrystals are laying. As a result, we found that they are contained within the surface layer of the specimen with thickness of about 100nm above the T.S..

The experimental results described above clearly show that the speckled areas appeared on the electron bombardment is due to the local transformation from single crystalline to polycrystalline Al.

As far as the present authors are aware, the transformation from single crystalline to polycrystalline structure of Al metal with purity of 99.99% or above can never be achieved without melting and subsequent rapid solidification. One might inquire that the melting may induce evaporation of Al in high vacuum of electron microscope. However, the evaporation of Al on the melting does not take place usually due to the firm protection of the melt surface by the oxide film even after the chemical etching.

Now we evaluate the amount of the heat evolution necessary for the observed local melting. We know already that the implanted deuterium molecules aggergate at the depth of around 100nm from a surface on the implantation of 25 keV D_2^+, referring to the previous experiment with 25 keV H_2^+ [3]. From our observations so far undertaken, the extent of the transformed region occupies, on the average, $1 \times 10^{-9} cm^2$ of the surface. Taking the cover thickness of Al on the T.S. as 100nm, weight of Al contained in the polycrystalline transformation becomes $2.7 \times 10^{-14} g$. The heat necessary to raise the temperature of this amount of Al from 300K to melting point 933K is $q = 633 \times 0.25 \times 2.4 \times 10^{-14} = 4.3 \times 10^{-12}$ cal, where the specific heat of Al in this temperature range is 0.25 cal/g · K. The latent heat of melting of Al is 2.58×10^3 cal/mol [4], which gives the total latent heat for the melting of the above amount of Al $L = 2.58 \times 10^3 \times 2.7 \times 10^{-14}/27 = 2.58 \times 10^{-12}$ cal. Therefore, the whole heat necessary for the melting becomes,

averaging on the several transformed regions, $Q = q + L = 6.9 \times 10^{-12}$ cal = 180 MeV for each transformed region.

Here, we would like to mention that the above estimation of the energy evolution could be smaller than that of whole energy evolved, since we have totally neglected the heat conduction though Al specimen. As mentioned before, the bottom side of the specimen below the T.S. is far thicker than the top side. So, a large amount of heat evolved in the D_2 collections in T.S. is presumed to flow out of the specimen though the thick bottom part to the specimen holder. Therefore, the heat responsible for the melting of the top area of the specimen must be a part of the whole heat evolution.

4. Discussions

One of the authors (K.K.) has published a short paper [1] describing the particle emission from implanted Al on the electron bombardment. The present experimental results have close similarities with this particle emission experiment in two aspects. First of all, it is requisite to focus the electron beam to observe both the polycrystalline transformation and the particle emission. Secondly, the optimum implantation fluence around $5 \times 10^{17} D^+/cm^2$ is common in both experiments. Neither lower nor higher fluence does produce the heat evolution and the particle emission as well. we have to keep the fluence within roughly $\pm 10\%$ around the above value. However, the difference of the two kinds of experiment is that in the present experiment we could never observe the heat evolution in hydrogen implanted case, and, on the other hand, in the particle emission experiment, we could observed the particle emission in both hydrogen and deuterium implanted cases. We presume that though the reactions in deuterium are accompanied with the heat evolution, the reactions in hydrogens, on the other hand, could be such as not accompaning heat evolution. The two reactions are not necessarily the same reactions at all.

Here, we like to add that the primary electrons with energy around 200 keV has little interactions with the embedded deuterium, and hydrogen as well, in the present experimental conditions. However, internal secondary electrons produced in Al due to the primary electron bombardment have strong inelastic interactions with the deuterium leading to the ionization of them. In justification of this model, this interaction is capable of explaning the dependence of the phenomenon on both the electron beam focusing and the microstructure in the subsurface layer which are described above. These points will be discussed fully in [2].

In a subsequent paper [5], we will discuss more fully on possible heating mechanisms based on solid state properities of Al, such as the insulating effect of the T.S. on the electron bombardment, difference of implantation depth of hydrogen and deuterium, and the decrease of melting point of the thin Al surface layer. However, we can show experimentally and theoretically that these mechanisms do not contribute to the observed melting. Further, we can show that the mean kinetic energy of the embedded deuterous in the T.S. possibly acquired by some mechanism, whatever it may be chemical or nuclear nature, must be more than 30eV to melt the surface layer.

These considerations strongly suggest the presence of some kind of nuclear reactions in the present situation.

Reference

[1] K. Kamada ; Jpn. J. Appl. Phys. 31 L1289 (1992)
[2] K. Kamada, M. Nakajima, M. Ogawa, T. Goto and H. Kakihana; Proc. 7th Int. Conf. on Emerging Nuclear Energy System(ICENES'93), p168 Sept.1993.
[3] K. Kamada, A. Sagara, H. Kinoshita and H. Takahashi; Rad. Effects 103 119 (1987): K. Kamada ; J. Nucl. Mater. 169 141 (1989).
[4] from American Institute of Physics Handbook, 3rd edition, McGraw Hill, New York, 1972.
[5] submitting.

Figure captions

Fig.1 Transmission electron micrographs of hydrogen, (a), and deuterium, (b), implanted Al. An example of the polycrystallized area on the electron bombardment is shown by an arrow in (b). Selected area diffraction patterns taken on normal T.S. area, (a-1) and (b-2), and that taken on the polycrystallized area, (b-1), are inserted.

Fig.2 Bright field, (a), and dark field, (b), images taken on the polycrystallized area in a deuterium implanted Al. The dark field image was taken with several diffraction spots on the circular rings of the inserted selcted area diffraction pattern.

Fig.3 Sequential TEM micrographs of the same area of a derterium implanted Al, which were taken in less than 60 seconds after the appearance of the speckled area. (a) was taken in less than 10 second, then (b) and (c) were taken in less than 60 seconds sequentially after (a).

able 1 Lattice constants of the polycrystalline aggregates determined y electron diffraction with the camera length L=570mm and the wavelength f electron $\lambda = 2.99 \times 10^{-3}$nm. Lattice constants and corresponding lattice lanes of Al are shown together for reference purpose.

ing	d_{obs}(A)	d_{obs}(A)	d_{obs}(A)	d_{obs}(A)	d_{obs}(A)(hkl)
1	2.4024	2.3976	2.3549	2.3385	2.338(111)
2	2.0366	2.0609	2.0287	-	2.024(200)
3	1.4570	1.4511	1.4505	-	1.431(220)
4	1.2473	1.2398	1.2213	-	1.221(331)
5	0.9266	-	-	-	0.9289(331)

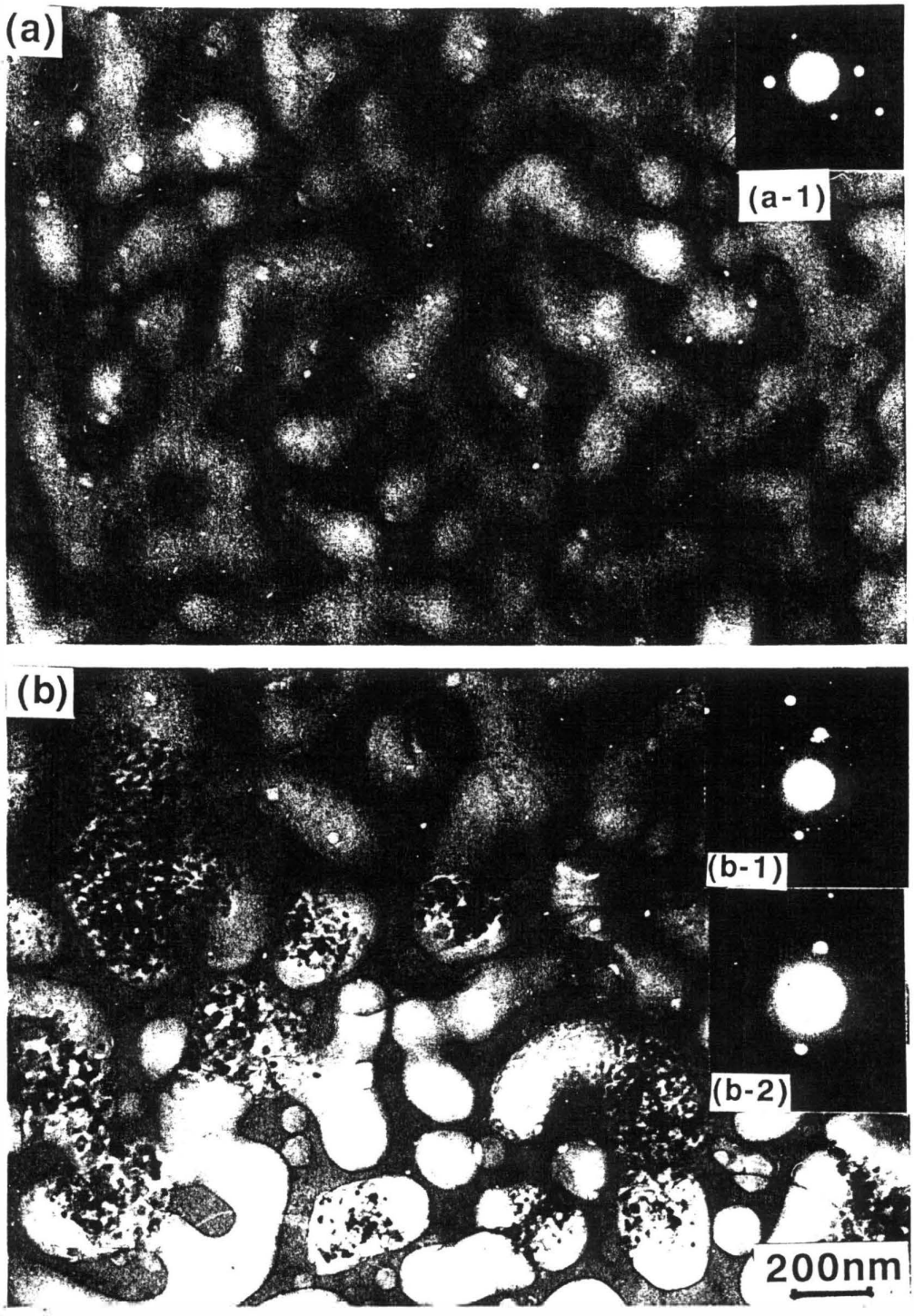

Kamada Fig. 1

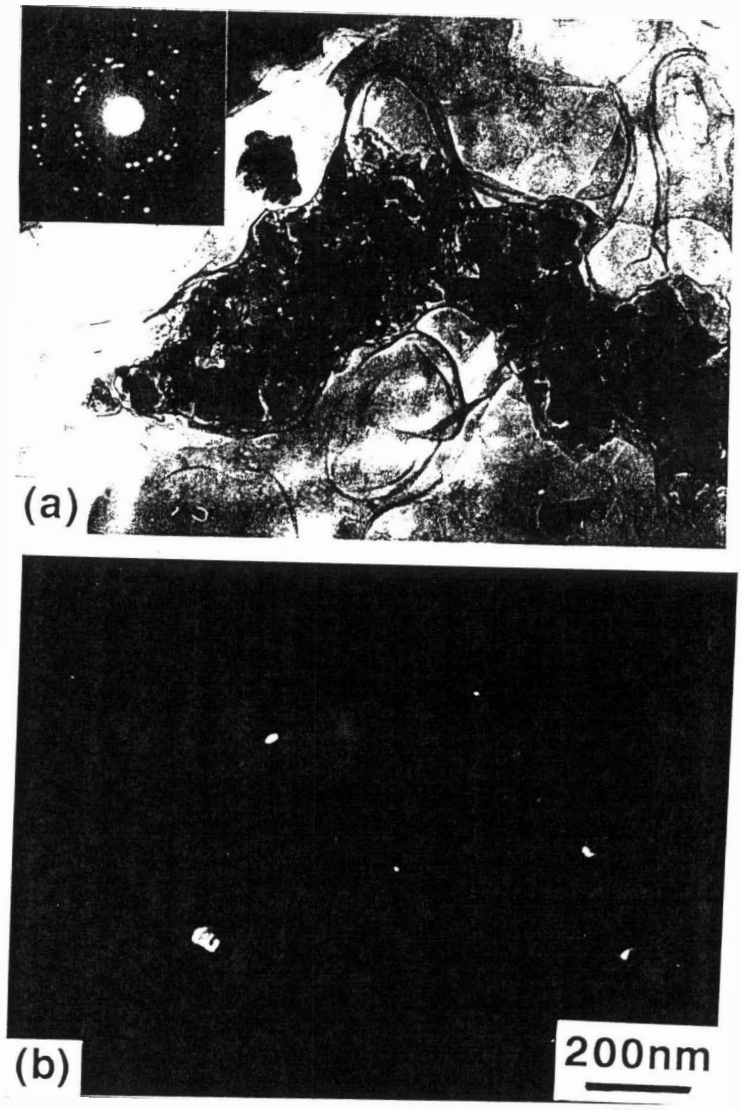

Kamada Fig. 2

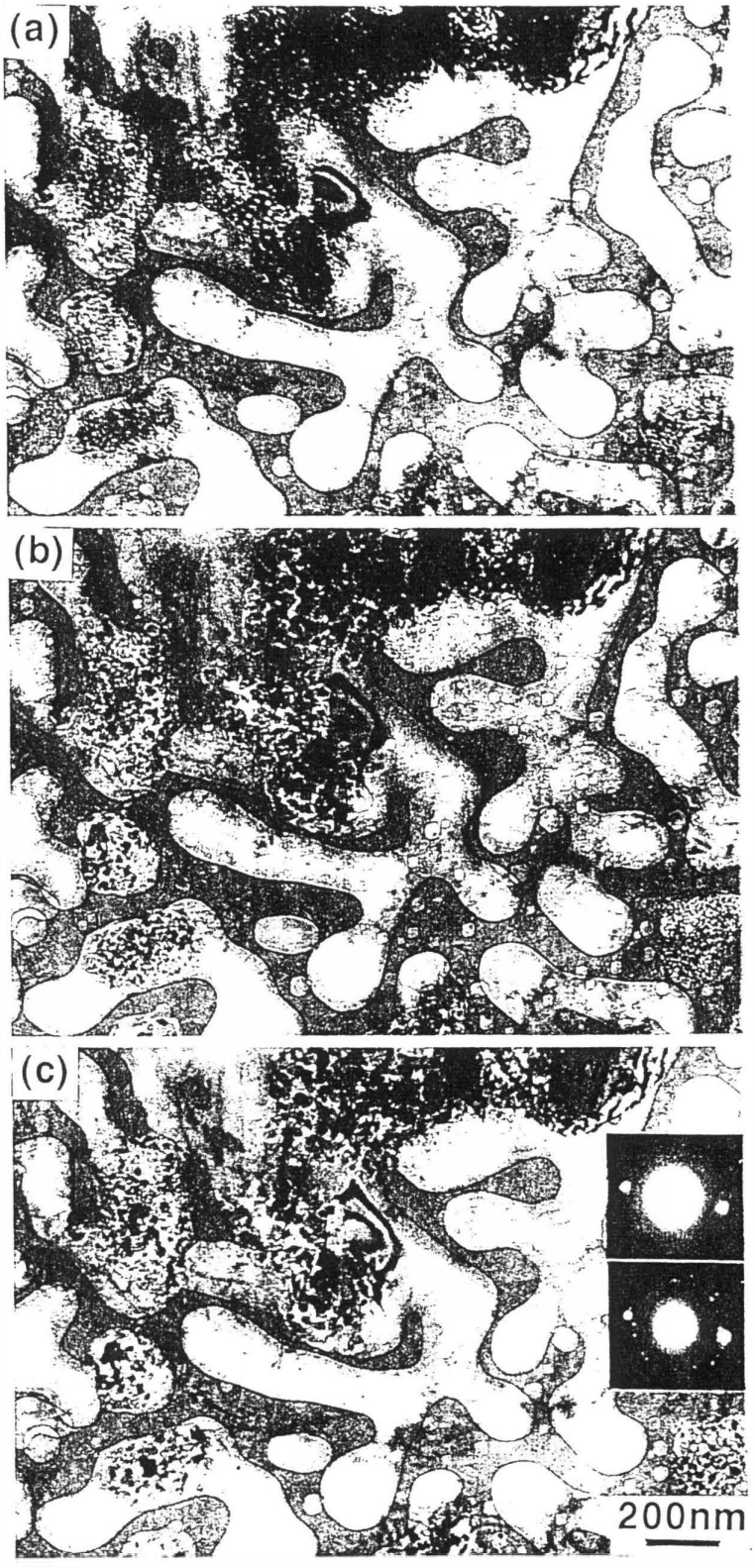

Kamada Fig. 3

Fifth International Conference on Cold Fusion
9-13 April, 1995 - Monte Carlo, Monaco
ICCF5 ©1995

Excess Heat Measurement in $AlLaO_3$ Doped with Deuterium

Jean-Paul BIBERIAN
Département de Physique, Faculté des Sciences de Luminy,
70 Route Léon Lachamp,
13288 Marseilles Cédex 9, France

Abstract:

We show evidence that solid state electrolytes can be used successfully in "cold fusion" experiments. We describe in this work that $LaAlO_3$ single crystals loaded with deuterium produce excess heat up to 10 times the amount of electrical power applied. No significant amount of neutrons has been detected.

1. Introduction

Since the public announcement of the discovery of "cold fusion" in 1989 by Fleischmann et al. ([1]), most of the experimental research work has been done in liquid electrolytes. However, as soon as 1989, Forrat ([2]) patented a solid state electrolytic device, with the reaction in the electrolyte. He proposes a process catalyzed by nascent muonic like atoms in polyvalent vacancies compensated by H^+ or D^+ ions in refractory oxides. Mizuno et al. ([3]) have shown that large quantities of excess heat could be generated in perovskite ceramics in deuterium atmosphere when a slowly varying current is passed through the sample.

It is the purpose of this work to repeat this early work, and to determine the characteristics of the reaction in a better controlled environment.

2. Theoretical point of view

Oxides with the perovskite structure are excellent proton conductors, when metal atoms are replaced by protons ([4,5]). They are therefore a good choice for "cold fusion" experiments. In this work we have used $LaAlO_3$ single crystals. Figure 1a shows the unit cell of the stoichiometric lanthanum aluminum oxide. The structure is composed of a lanthanum atom at each corner of the cubic unit cell, an aluminum atom at the center, and an oxygen atom at the center of each face. An alternative description is shown in figure 1b, with an aluminum atom at each corner, a lanthanum atom at the center, and oxygen atoms in the middle of each side.

If a lanthanum vacancy is created (V center or p type semiconductor), the unit cell is shown in figure 1c. Since lanthanum is trivalent, three protons (or deuterons) can replace one lanthanum ion as shown in figure 1d. When a negative voltage is applied, more protons (deuterons) are attracted and can fill up the vacancy.

Figure 1e shows the structure of the cell with interstitial deuterium. Five protons can be placed in a single lanthanum vacancy. The density of deuterons is then close to that of liquid deuterium.

Intrinsic lanthanum aluminum is transparent. When lanthanum vacancies are present, it becomes red (the maximum vacancy concentration being 5%). When vacancies are filled with deuterium, the crystal becomes transparent again ([4,5]).

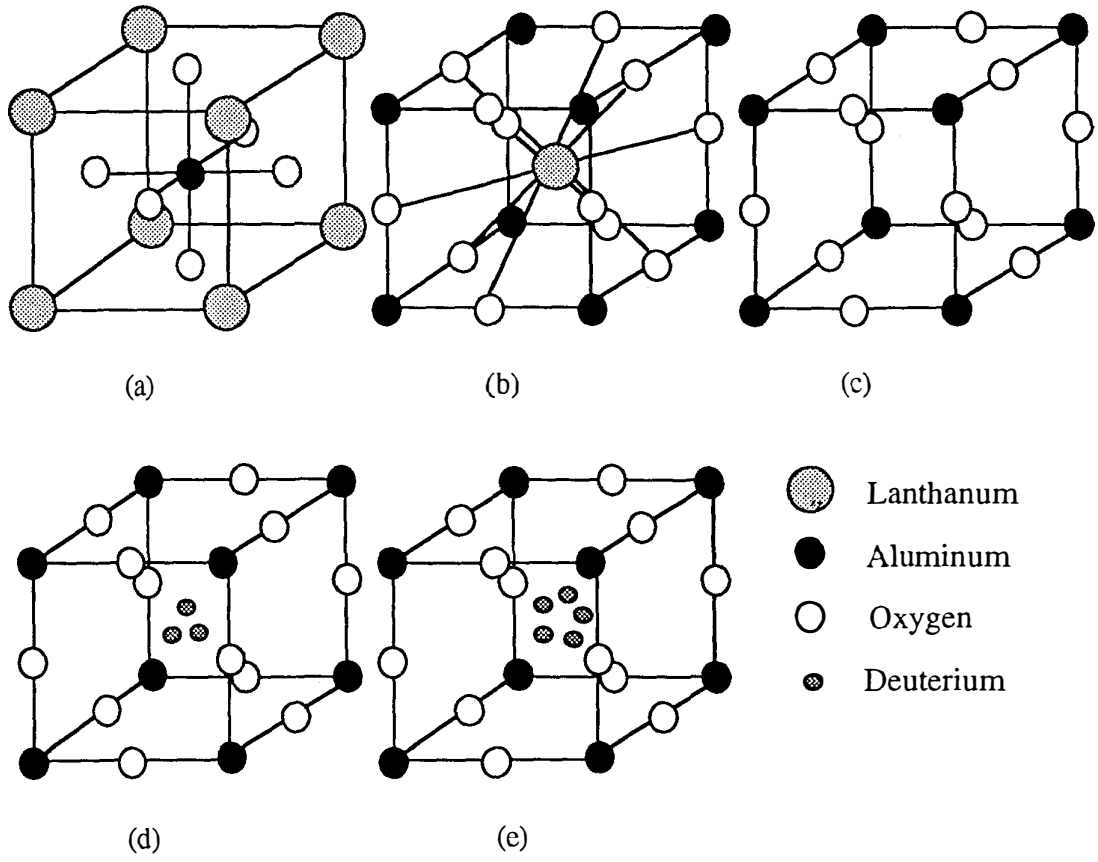

Figure 1

The $LaAlO_3$ perovskite type unit cell. a) The intrinsic unit cell with Lanthanum atoms at the corners and Aluminum at center. b) Same cell with Aluminum at corners and Lanthanum at center. c) Cell with Lanthanum missing creating a V center. d) Cell with Lanthanum replaced by 3 deuterons to compensate vacancies. e) Cell with Lanthanum replaced by 5 deuterons forming F centers.

When the crystal is heated in an hydrogen (deuterium) atmosphere, protons (deuterons) diffuse in the crystal. If a voltage is applied on two faces of the crystal, protons (deuterons) diffuse towards the cathode. Three zones develop, as shown in figure 2. The cathode side has excess interstitial deuterium, so that it becomes blue, (F centers), as described in figure 1e. The middle section is white, because it is stoichiometric, the lanthanum vacancies have been filled by three hydrogen (deuterium) atoms as in figure 1d. The anode side is red because it has lanthanum vacancies as in figure 1c (V centers).

Numerous such crystals can be used as proton conductors, however rare earth aluminates are very well suited because aluminum and lanthanum are both solely trivalent. $AlLaO_3$ proton conductivity has been extensively studied for fuel cell applications ([4]).

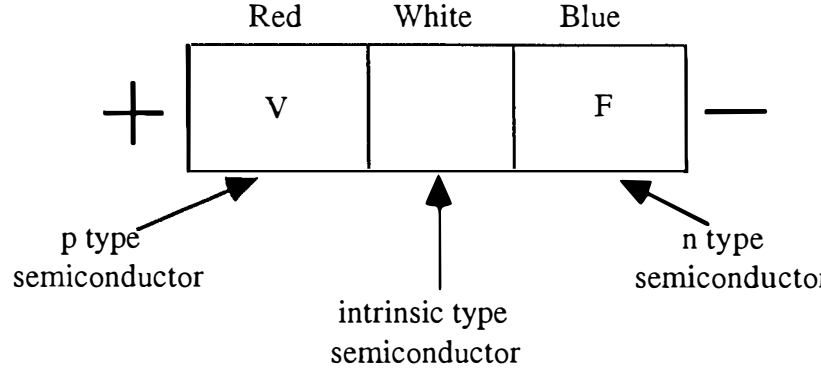

Figure 2

When a voltage is applied through the sample at high temperature in an hydrogen (deuterium) atmosphere, the anode becomes red, because of depletion in proton (deuteron) contents, the cathode becomes blue due to proton (deuteron) enrichment, and the middle returns white because the vacancies are neutralized by the protons (deuterons).

The structure of the intrinsic aluminum lanthanate is:

$$Al^{3+}La^{3+}O_3^{6-}$$

and the crystal appears white.

A crystal with 5% vacancies will be red and will have the following structure:

$$Al^{3+}La_{0.95}^{2.85+}O_3^{5.85-}$$

When the crystal is heated in a deuterium or hydrogen atmosphere, ions diffuse in the sample and vacancies are occupied by the deuterium ions, and consequently the crystal recovers its intrinsic white color. The structure of the crystal is now:

$$Al^{3+}La_{0.95}^{2.85+}D_{0.15}^{0.15}O_3^{6-}$$

After application of a voltage an F zone appears at the cathode with the composition:

$$Al^{3+}La^{2.85+}D^{0.2}O_3^{6.05-}$$

Therefore, when a voltage is applied through the sample at high temperature in an hydrogen (deuterium) atmosphere, the anode becomes red, because of depletion in proton (deuteron) contents, the cathode becomes blue due to proton (deuteron) enrichment, and the middle returns white because the vacancies are neutralized by the protons (deuterons) as shown in figure 2.

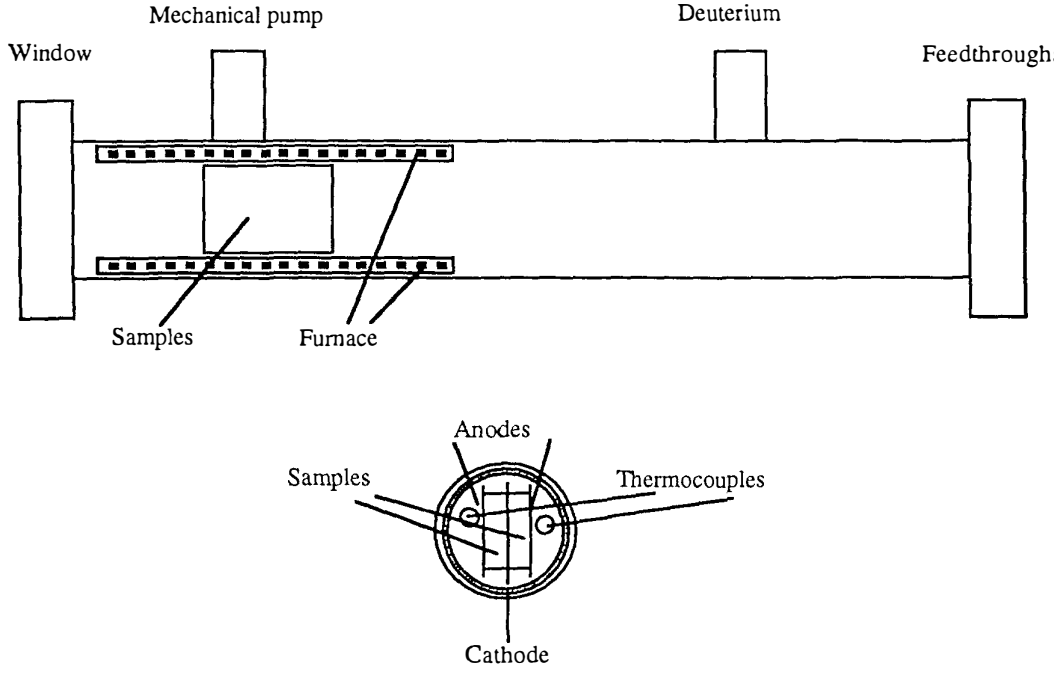

Figure 3

Schematic of the experimental setup. The samples are sandwiched between two palladium foils. They are heated by a cylindrical furnace. Two thermocouples measure temperatures near the sample. A glass window allows viewing of the sample, and a gauge monitors pressure. The cylindrical chamber is 35 mm in diameter and 300 mm long.

3. Experimental set up

The samples we have used are $LaAlO_3$ single crystals with unknown amounts of vacancies, but probably less than 5 %, and in some cases doped with rare earth metals. They have been prepared in the sixties by the flame fusion process. They are cut with a diamond saw: 4 cm^2 in area and 3 mm thick. The first experiments have been conducted with a thin film of gold sputtered on each side. In one occurrence, when the crystal has been heated at high temperature (500-600 C), the gold layer dissolved in the crystal, so later bare crystals were used successfully.

Figure 3 shows a schematic of the experimental set-up. The system is a 300 mm stainless steel tube 35 mm in diameter, positioned horizontally The crystals are sandwiched with 100 μm thick palladium foils. Two chromel-alumel thermocouples measure the ambient temperature near the sample. A window at the other end of the tube allows viewing the sample. A gauge is used for crude measurement of the pressure in the chamber.

The sample is positioned at 250 mm from the flange, so that the feedthroughs do not warm up significantly. A palladium foil is used as cathode between two identical wafers cut from the same crystal rod. Two palladium foils used as anodes are then placed symmetrically on the other faces of the crystals. These two anodes are hold together by a molybdenum clamp. The symmetric design has the advantage of eliminating the problem of the mechanical attachment of the electrodes without producing a short circuit.

Temperature is measured two ways: on one hand, two chromel-alumel thermocouples are positioned in the ambient deuterium gas surrounding the crystal. And on the other hand temperature is deduced from measuring the resistivity of the tungsten wire used in the furnace heater. This resistance has been first calibrated against the two thermocouples, and shown to behave linearly with temperature in the whole temperature range. The advantage of using this second type of temperature measurement is that it is an average temperature and not a local measurement as with thermocouples.

All measurements are made with a PC based data acquisition system. The heating power of the furnace is maintained constant by regulating the applied voltage.

A helium-3 neutron detector is positioned 30 cm from the sample, and its measurements are recorded at all times. An internal source inside the detector produces a signal at a frequency of 0.534. Therefore any neutron emission from the sample should add to this signal.

4. Experimental procedure

The crystals are first heated in air to remove any hydrogen present. After that crystals are red indicating the presence of lanthanum vacancies. It is then heated in deuterium for several hours at about 800 °C. At this point crystals turn white.

Crystals are placed in pairs in order to simplify the attachment as described in the above section. The stainless steel chamber is evacuated using a mechanical pump down to a pressure of 10^{-2} torr. Deuterium is subsequently introduced at about atmospheric pressure. Power of the furnace is raised slowly, without passing current through the crystals. After a few hours, when the desired temperature is reached, and remains stable,

a voltage is applied through the crystal. This is done with four 120 Volts power supplies mounted in series. To avoid any power surge in the crystal when the current is applied, we use the current limitation mode.

Blank experiments have been performed in a similar way, but with a virgin crystal, without any deuterium. We can therefore compare directly data obtained with samples loaded with deuterium and blanks experiments.

5. Experimental results

A blank experiment is shown in figure 4. Sample temperature is deduced from the measurement of the resistance of the furnace. The furnace power is 150 Watts, producing a sample temperature of 545 °C. The electrochemical power is 250 mW (250 V, 1 mA). The temperature rise is 0.5 K.

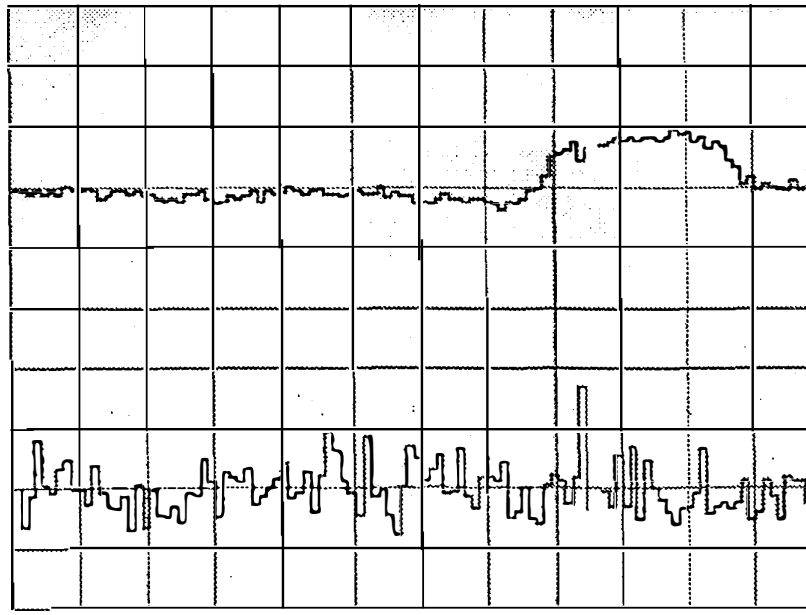

Figure 4
Blank experiment. Top curve: temperature, bottom curve: neutron counter.
Time: full scale 120 minutes. Temperature: full range 5 K.

Figure 5 shows similar curves, but the crystals are doped with an unknown amount of praseodymium, and loaded with deuterium. The furnace power is 150 Watts, and the electrochemical power is 50 mW (250 V, 0.2 mA). The temperature rise is 1 K, and corresponds to 500 mW. The excess energy gain is therefore 10.

The lower curves in figures 4 and 5 represent the neutron counts, and show no sign of increase. However in one occasion a very slight increase 0.1 counts/sec has been measured. We cannot exclude that this signal is due to noise, because further experimentation has shown that the detector is very sensitive to noise.

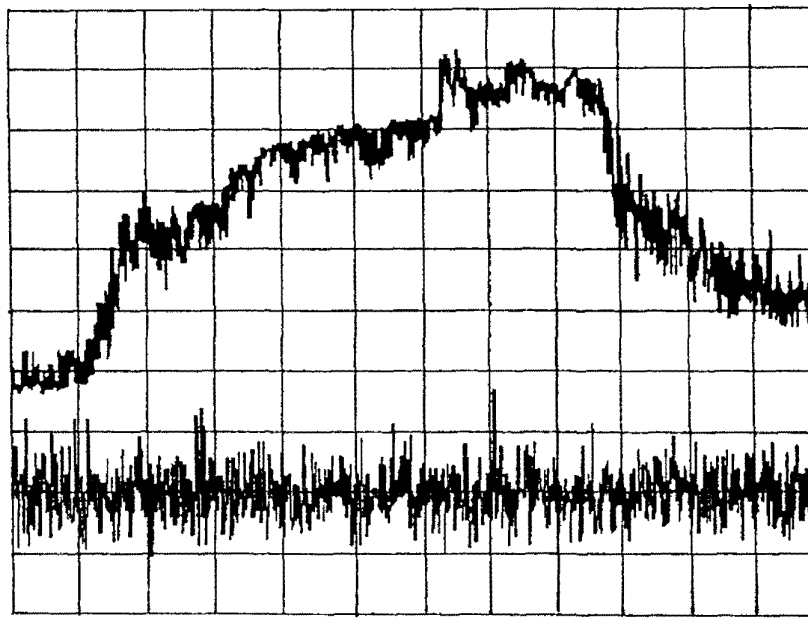

Figure 5
Experiment in deuterium. Top curve: temperature, bottom curve: neutron counter. Time: full scale 18 hours. Temperature: full range 5 K.

An interesting observation is the potential difference between anode and cathode when the voltage generator is disconnected. Values of up to 1.9 Volts have been measured. This indicates that upon application of the initial voltage through the crystal, there is a non-uniform distribution of the deuterium inside the crystal. This voltage decreases with a time constant in the 5 to 10 minutes range.

6. Discussion

A comparison between temperature curves of figure 4 and 5 shows that in the blank experiment, temperature increase is achieved in 3 or 4 minutes, whereas with the active sample the temperature rise happens after at least one hour. This indicates that during the process of passing current through the sample, there is probably diffusion of deuterium inside the crystals.

Experiments have been carried out in a closed cell. So if we assume that all the deuterium molecules have reacted somehow, we obtain an energy of 10 eV per molecule. This is not possible because after the experiment is stopped, there is still plenty of deuterium.

We therefore believe that the reaction mechanism is either nuclear in origin, (in which case it corresponds to unknown reactions since observed fusion ashes lie below the threshold needed to explain the observed heat) or to a new quantum chemistry.

Mizuno et al. ([3]) have observed similar effects with a SrCeO3 ceramics , that have the same perovskite structure. However, they observe a much larger excess heat of

the order of 10^4, at 300 to 400 °C! The main difference is probably the structure of the sample. We have used a single crystal , whereas Mizuno et al. have used a ceramic that has a polycrystalline structure with grain boundaries.

7. Conclusion

We have shown that excess heat is observed when a current is passed through a lanthanum aluminum oxide crystal with lanthanum vacancies in a deuterium atmosphere. The amount of excess heat has been determined to be up to 10 times the electric power passed through the sample.

We cannot exclude low level neutron emission, but at this point noise can still be the cause of the small signal increase observed.

Solid state electrolytes are excellent candidates for future applications because they operate at much higher temperature than liquid electrolytes. This should make it much easier to generate electricity. Also because of the closed cell configuration, and the possibility of working at low deuterium pressure, it would be possible to measure helium-4 production with an excellent accuracy.

Acknowledgments

I would like to thanks: Yves Grange now at the Commissariat a l'Energie Atomique in France for providing me with the samples, Francis Forrat for all the support he gave me to understand and succeed in this work, Huntington Laboratories for their technical support, and my children Mélanie and Gabriel in collecting data during the first successful experiment.

References

1. M. Fleischmann, S. Pons and M. Hawkins,
J. Electroanal. Chem. **261** (1989) 301.

2. F. Forrat,
Patents numbers: F 89 07703 and F 90 08360

3 T. Mizuno, M. Enyo, T. Akimoto and K. Azumi, I
ICCF-4, Maui, Hawaii, 1993.

4- F. Forrat, G. Dauge, P. Trévoux, G. Danner and M. Christen,
C.R. Acad. Sc. Paris, **259** (1964) 2813.

5 F. Forrat, R. Jansen, P. Trévoux,
C.R. Acad. Sc. Paris, **256** (1963) 1271.

Fifth International Conference on Cold Fusion
9-13 April, 1995 - Monte Carlo, Monaco
ICCF5 ©1995

High power μs pulsed electrolysis using palladium wires: evidence for a possible "phase" transition under deuterium overloaded conditions and related excess heat.

Francesco CELANI*, Antonio SPALLONE*,Paolo TRIPODI*,
Alessandra PETROCCHI*, Daniele Di GIOACCHINO*
Paolo MARINI**, Vittorio Di STEFANO**
Sandro PACE***, Alfredo MANCINI****,

* INFN, Laboratori Nazionali di Frascati, via E.Fermi 40, 00044 Frascati (Italy).

**EURESIS, v. Lero 40, 00144 Roma

***Dipartimento di Fisica, Universita` di Salerno, 84081 Salerno (Italy)

****ORIM S.R.L., via Concordia 65, 62100 Macerata (Italy)

Abstract

In this paper we describe an electrolytic experiment aimed at reaching high deuterium concentration gradients in palladium wires, using the electromigration effect.
We will describe the selection criteria of experimental parameters and we will show results of our loading and calorimetric measurements. These tests reveal that a high mean value of D/Pd has been reached in a short time and that there is a correlation between an anomalous heat emission and an electric resistivity "transition" of the overloaded palladium.

1. Introduction

1.1 Coehn effect

In electrotransport the effect on the concentration variations within the palladium can be very large[1]: the deuterons are forced to move along the Pd cathode (deuterons current) because of the voltage drop caused by the flowing electron current into the wire. In this region the stationary state will be reached when the incoming deuterons are exactly compensated by the outward diffusion of deuterons across the wire surface. The actual deuterium concentration in such equilibrium state will results higher than in absence of the Coehn effect. In other words, Coehn effect could be helpful in increasing the D/Pd ratio. The parameter which mainly controls the rising up of deuterium concentration is the potential drop along the cathode; accordingly, in our tests we used a thin (0.1 mm) and long (up to 200 cm length) palladium wire, in which a very large (up to 80 A) pulsed current is flowing.
In a stationary state, the deuterium concentration at a fixed point x is given by [2] :

$$c(x)=c_0\, e^{-eZ^* V(x) / K_B T} \qquad (1)$$

where
c_0 Initial concentration of H,D,T

e	Electron charge ($1.6\ 10^{-19}$ C)
V(x)	local electric potential
Z*	"effective charge" of H,D,T in Pd
	=1 at low concentrations (H/Pd<0.6) [1]
	=0.1 at high concentrations (>0.8) [3]
	and/or at high temperature
K_B	Boltzmann constant, $1.38\ 10^{-23} J \cdot K^{-1}$
T	Temperature (K)

1.2 Debye-Falkenhagen-Sach effect

In an electrolytic solution with finite ionic concentration, for the principle of global as well as local neutrality, each ion is surrounded by an ionic atmosphere, which is globally of the opposite sign of the ion. In absence of an electric field the system ion-ionic atmosphere is symmetric.

When an electric field is applied to the solution, the ion is driven in one direction, while its atmosphere is driven in the opposite direction; therefore new ionic atmosphere must be continuously reconstructed around the moving ion. The time for reconstruction of the ionic atmosphere is called *relaxation time* and the retarding effect of the motion of the ion is said *asymmetry effect*. A further retarding effect is due to the resistance to the backward motion of the ionic atmosphere, which, by the way, contains molecules of water. This second effect is called the *electrophoretic effect*. The third retarding effect, which affects the motion of both the ion and its atmosphere is due to the viscosity of water.

The conductivity of an electrolytic solution is given by the Onsanger equation:

$$\lambda = \lambda_0 - (a + b\lambda_0)\ c^{1/2}$$

λ = equivalent conductivity at concentration "c"
(the conductivity of a volume of solution containing an equivalent of electrolyte, when the electrodes are put at one cm distance and have a surface large enough to contain all the solution between).

λ_0 = equivalent conductivity at c=0 (infinite dilution).

a,b = constants (for H_2O, a=60.2, b=0.229)

Debye and Falkenhagen predicted in 1927, and Sack found in 1928 that, for alternating electric fields, if the period is equal or less than the relaxation time, given by:

$$T = 10^{-10}/c$$

the equivalent conductivity approaches the maximum, that is the conductivity at infinite dilution.

At c=0.001 normal (molar for 1:1 electrolytes like LiOH), the relaxation time is 10^{-7} seconds. So with frequencies

$$\nu > 1/(2\pi \cdot 10^{-7})\ \text{Hz}$$

that is

$$\nu > 1.6 \cdot 10^{6} \text{ Hz}$$

there are important effects, that is the conductivity may double with respect to the DC conductivity. Approximately the same effects can be obtained with voltage pulses of equivalent frequency.

1.3 Wien effect

Wien (1927) found that the application of strong electric fields increases appreciably the conductivity. Detectable effects can be obtained for ionic speeds that allow the ion to cover more than once the diameter of the ionic atmosphere (3.10^{-8} cm) in the relaxation time.

The speed of ionic migration is of the order of 5.10^{-4} cm/s per unit of electric field [V/cm].

The Wien effect becomes therefore detectable for fields of about 600 V/cm.

1.4 Self-biased pulsed electrolysis

In our particular case, because the final purpose of the electromigration is to overload the palladium electrode with deuterium, both effects result in a better exploitation of the applied voltage.

Nevertheless we anticipate and stress that the clue of the method resides in the employment of a very high voltage with global low average power. Which means the development of very high electrode overvoltages without damaging the electrode to be overloaded. This has been made possible by using high voltage pulses of about 100 ns of rise time at repetition rate of the order of 10^4 Hz and, to maintain into the Pd electrode the deuterium loaded during the high voltage pulses, the introduction of a proper rectifying diode between the pulser and the palladium electrode that brings the electrolysis yield factor to 95% of that of electrolysis in DC.

2. Experimental conditions selection criteria

In order to obtain a high voltage drop it is obviously necessary to apply a large current and to use very thin and long wires (to increase the resistance).

At the same time we have to reach high values of D/Pd ratio.

We have the following types of problems:

- an intrinsic *lower bound* of the diameter of the wire, due to the embrittlement phenomena occurring in D or H loading.
- increasing the *voltage* we also increase the *current* producing a higher heat dissipation along the wire (*Joule effect.*).
  High temperature causes two effects
  a) c/c_0 *decreasing* due to Z* decreasing
  b) *D/Pd decreasing,* according to usual PCT curves, at least in the exothermic region of the PdD system.

We solved both problems using current pulses with HF harmonic as large as possible.

In this way the effective conductive portion of the wire decreases because of the skin effect; it is then possible to use thicker wires, thus reducing the technological drawbacks of embrittlement and cracking of palladium.

By reducing the skin depth we also reduce the current necessary to obtain high voltage drop.
The skin depth depends on the fundamental harmonic frequency of Fourier analysis and there is a relationship between this frequency and the pulse rise time, thus we have to optimize the rise time (within the technological constrains).

- We reach the compromise of a rise time of 100 ns.

In order to reduce the Joule effect we reduce the pulse duration and the repetition rate in such a way that the mean value of the current density is quite low.

In order to reach high values of D/Pd ratio the pulses must have the following features:

- the pulse duration must be longer than the minimal time to obtain electrolysis.
  This is only 300 ns in our experimental conditions for the combined effects:
  - Debye-Falkenhagen and Wien effect.
    We found that Faradaic electrolytic efficiency is about 5% due to this effect only. This specific test was performed short circuiting the diode UFPD in fig. 2a.
  - self-polarization of cell due to a diode (fig 2a, UFPD) used as a decoupler, between power pulser and cathode.
    We made some experiments to verify the efficency of our pulsed loading technique . We saw that the electrolysis efficency raised to a value as large as 95% using this unconventional experimental set up [4].

- even if the time duty cycle of the pulse must be low (in order to minimize the mean input power) it must be high enough in order to avoid the deloading between pulses. We consider that during the electrolysis some impurities (mainly nickel from the anode and lithium) coat the cathode causing the desorption which is slower than the absorption.
  The effective pulse duration in our experiment is 750÷1500 ns, while the dead time between two pulses is about 99 μs at 10 kHz of repetition rate.

3. The experimental Set-Up

We built an apparatus whose configuration has been optimized in order to discriminate the contribution on deuterium concentration due to electrolysis from the electromigration contribution.
The electrolytic cell is made of commercial glass, the solution is LiOD-D_2O. A palladium wire (we tested different lengths, larger than 10 cm, and different diameters, less than 500 μm) is immersed in the electrolytic solution.

The electrolysis occurs between a part of the wire (effective length about 6 cm) and a coaxial nickel cylinder (internal diameter 12 mm) used as anode. This side of the wire is used mainly as a source of deuterium or hydrogen while the other long side (the sink), is used mainly to investigate the electromigration effect. Obviously, the most cathodic point of the system is the end of the long wire (named V_2), as shown in fig. 1, where the voltage (negative μs pulses) is sent to the palladium wire. The experimental apparatus is described in fig. 2.a, 2.b, 2.c, 2.d.

The system, from the point of view of calorimetry, can be described as a quasi-isoperibolic calorimeter where the heat exchanger is the environment (room temperature kept at constant temperature of 20 ± 2 °C) and the calibration heater is cyclically (every

6 hours) powered (1 Watt) in order to continuously calibrate the system and calculate the so called "cell exchange constant" ($^oC/W$) at various temperatures and overall experimental conditions (aging of solution due to glass dissolution by LiOD, different bubbling due to different electrolytic currents and so on).

The thermometer, located on the external cell wall, between the palladium wire and the electrolytic heater, is an integrated circuit silicon thermometer (AD590) with metallic case connected to ground (in order to minimize pick-up noise) and operated at quite large ratio of output voltage/input temperature (i.e. 10mV/^oC) in order to reduce systematic errors that can arise from unpredicted large variations of the "reference ground" at the input of the computer controlled multiplexed-multimeters (HP3457A).

The cell is powered μs duration, KHz repetition rate, high power regime, following, with further improvements, the procedure developed by us since march 1993[5],[6],[7]. The rise time of the input pulse is typically 100 ns, the fall time varies between 150 ns and 1500 ns (depending on electrolyte concentration, i.e. longer at lower concentration), the duration of the flat region is typically 500 ns.

The applied peak voltage (V_2-V_{GND}) varied between -80 V and -200 V. The voltage peak values at V_1, V_2, V_3 points (see fig. 2a) are acquired through an ultra-fast passive peak detector (fig. 2b).

The so called cathode-anode voltage (V_{o_pha} = out of phase voltage), when no power is applied (related to the well known overpotential) is read through a fast and simple circuit [fig. 2.c]. Obviously, this kind of simple circuitry gives information useful for comparison only at a given fixed operating frequency of the system (i.e., it is not correct to compare different values of V_{o_pha} at different operating frequencies).

The peak current injected to the wire is read through a fast rise time (20 ns) high peak current capability (5,000A) current monitor (fig. 2d) and transformed to a dc level through a fast, low-drop, low leakage, shottky diode (HP2800) and ceramic capacitor which has been acquired.

3.1 Typical operating conditions

The experiments were performed under the following operating conditions:

- Peak current density along the wire : 50,000÷300,000 A/cm^2 (1).
  Peak current density on the side of the electrolyte: 10,000÷100,000 mA/cm ^{2}
  For comparison, the typical values of mean current density in Cold Fusion experiments ranges between 64 and 1,000 mA/cm^2.
- Rise time of the pulse is in the range of 100-250 ns. When the peak current is increased, also te rise time increases; however with currents up to 25 A we still have 100 ns of rise time.
- The pulse duration is 500 ns.
- The fall time is between 100 and 1,000 ns (increases decreasing LiOD concentration).
- The pulse repetition rate is between 5,000 and 20,000 Hz.

---

(1) Some tests were performed with a current density as large as 500,000 A/cm^2. These values of current density are not too far from typical regions of pinch effect in hot fusion studies, so we can expect even the emission of soft X-rays. We are planning to build an experimental set-up to clarify this point.

- The electrolyte concentration has been varied between 0.01 and 0.3 N LiOD
- The diameter of the Pd wires studied were: 100, 250, 300, 500 μm
- The total wire lengths were : 20, 50, 100, 200 cm.
- The anode was made of Ni. We plan to study in the near future also Pt, Au, Pd.

4. Main results

The main results were obtained with a wire of 100 μm of diameter and 50 cm length , effective peak current density 100,000 A/cm^2 and repetition rate of 10,000 Hz.
We estimated the D/Pd ratio from measurements of wire resistance in each of the two sides of the wire : in the following we name ACTIVE the side coaxial to the anode and COEHN the other one (fig. 1, side V2-V3). The resistance measurements were done in two ways: in situ and also by AC bridge measurements (HP 4262 LCR METER operating at 120 Hz, 1kHz, 10 kHz) just after switching off the system .
At the same time we evaluate the excess heat production by the calibration method quoted in the previous section.
The resistance ratio reaches its maximum value in the ACTIVE side after 250 seconds from the beginning of the electrolysis. After this, the R/Ro ratio decreases until it reaches a value corresponding to an average D/Pd ratio of about 1.0.
About 200 seconds after this minimum has been reached the resistances ratio "jumps" abruptly and comes back to a value corresponding to D/Pd ratio of about 0.8 (fig. 3).
This back "phase" transition has a cyclic behavior and it is observed only when the applied potential is higher than a threshold value (about 130 V with our configuration).
We want to note that, although on the side of the wire that undergoes only electromigration effect (COEHN) there should be, *de principio* , cathodic and anodic (with nominal no loading) regions, *de facto* we have seen that the average loading was larger than 0.8 (fig. 5).
This observation leads us to conclude that the electromigration effect is even stronger than the anodic effect or , speculatively,that a new effect exists, due to the large voltage drop, that is able to keep the deuterium inside the Pd wire (as suggested by G.Preparata [8])
The excess heat seems to have a cyclic behavior and starts (at low intensity) only 250 sec after the beginning of the electrolysis and increases along the time following the behavior of bulk loading (fig. 5).
The excess energy obtained in the previously described experiment was about 50% (with a 5% accuracy) of the input power, i.e. typically about 5 W of excess heat. However in other experimental conditions we have obtained heat excess up to 150%, even though in unstable conditions.
The results show that the increase of the observed excess heat is related to :

- Decrease of the wire diameter
- Increase of the wire length
- Decrease of the pulser rise time (i.e., larger skin effect)

- Decrease of the LiOD concentrations up to a value of about 0.001 N (although quite unstable at low concentration); reproducible results have been obtained between 0.01 and 0.1 N.
- Increase of the repetition rate of pulses.
- The presence of some proper impurities (Ni, Pb, borosilicate) which cover the surface of Pd; this effect has to be fully studied.
- Increase of the mechanical stresses of the wire (cold working), mainly because this increases the resistivity

Almost all the previous experimental effects listed show that the voltage drop along the wire, together with the "overvoltage " value, could be the most important or even a *key parameter*.
Moreover we often have observed that even the application of a calibration power level at the heater (1 W) gives an increase of overall power gain. This effect can be explained, and it is a further proof, that the excess heat happens when the D/Pd system is in the endothermic region, that is when D/Pd is quite larger than 0.8.
We also notify that in some experiments we measured a R/Ro value less than 1. This can be an evidence of the possible existence of a superconducting state due to the extremely large density of the deuterium inside the palladium lattice, as suggested by prof. J.P. Vigier (Paris University).

Conclusion

We have observed that is possible to load above 0.8 almost any kind of palladium wire, once provided that some "intrinsically difficult" requirements are full-filled in a reproducible way and, overall, with a very short "waiting" time (only 200 s in some experiments).
About excess heat, if we accept that the procedure of self calibration is correct [9] in the framework of isoperibolic calorimetry, we observed that it starts when the D/PD ratio is larger than about 1 and, at least in our experimental setup, it has a cyclic behavior. We think that just electromigration is not enough to explain all the experimental phenomena we found, and that a new theoretical approach is necessary to explain our results [9].

Acknoledgments

We would like to thank prof. M.Okamoto (TIT, Tokio) and K. Matsui (IAE, Tokio) for very useful discussion, criticism and comments. Prof. J.P.Vigier (Paris, France) gave us useful comments.
The palladium wires were kindly provided from IMRA Material (Japan), Tanaka K.K. (Japan) and ORIM S.r.l. (Italy).
Dr. F.Ferrarotto (INFN,Rome), gave us strong suggestions about the behavior of pulsed electrolysis since march 1993.

References

[1] A.Coehn, Z. Elektrochem,35,676,(1929)
[2] Hydrogen in metals II, Topics in applied physics, vol 29 , Springer and Verlag, ed. G.Alefeld and J. Volkl, 277, (1978)
[3] Giuliano Preparata, private communications, November,(1994)

[4] F.Celani, M.Boutet, D. Di Gioacchino et al., "First results about hydrogen loading by means of pulsed electrolysis of YBCO pellets", Physics letters A 189, 397, (1994)
[5] F.Celani, A.Spallone, P.Tripodi et al.
Conference proceedings ICCF3, Vol.1, pag.22-1,22-14, (1994)
[6] F.Celani, A.Spallone, P.Tripodi et al.
Fusion Technology, Vol. 26, pag 127-137, (1994)
[7] F.Celani, A.Spallone, P.Tripodi et al. "Reproducible D/Pd ratio over 1 and excess heat correlation by μs pulse high current electrolysis."
Publishing on Fusion Technology, (summer 1995)
[8] G.Preparata (private communications, December 1994)
[9] G.Preparata, M.Scorletti, M.Verpelli, "Isoperibolic calorimetry on modified Fleischmann-Pons cells", Preprint of Physics Department, University of Milan, MITH 95/4 (1995)

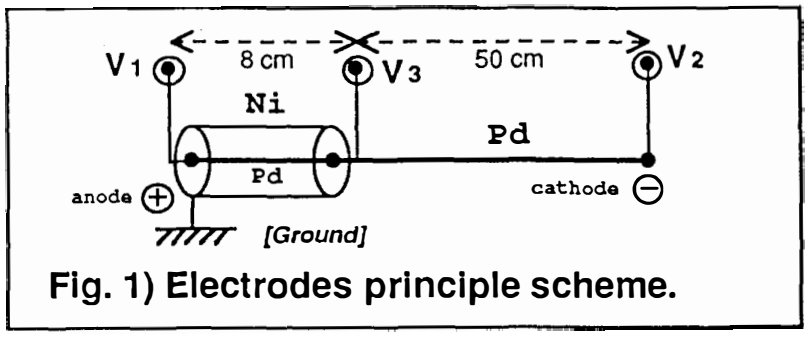

Fig. 1) Electrodes principle scheme.

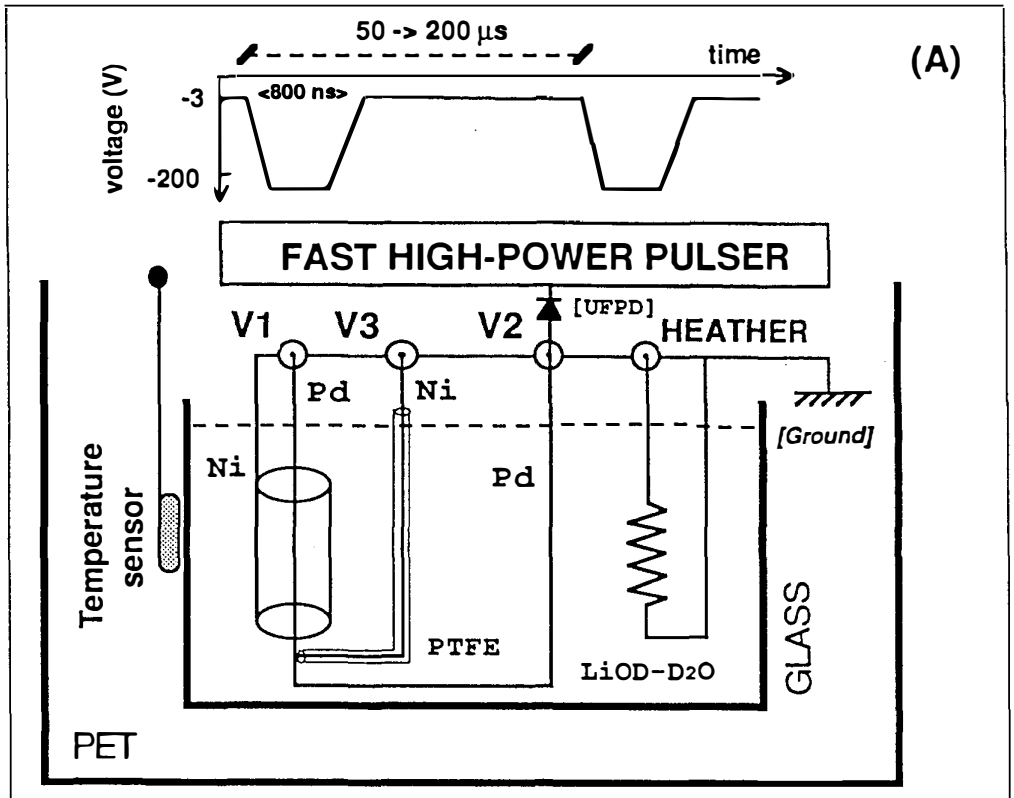

Fig. 2.a) Apparatus set-up.

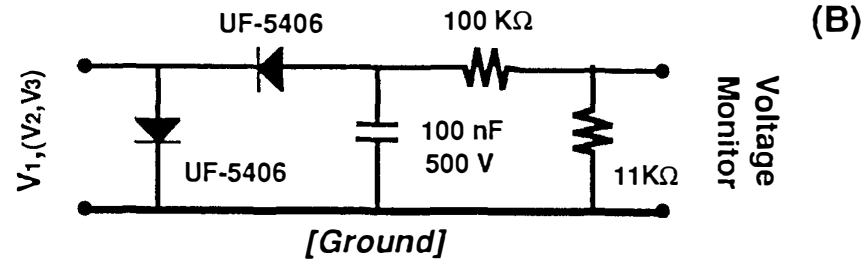

Fig. 2.b) Peak detector circuit.

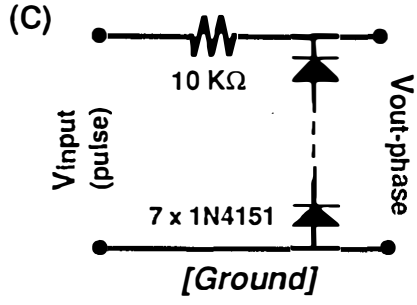

Fig. 2.c) Vout-ϕ circuit.

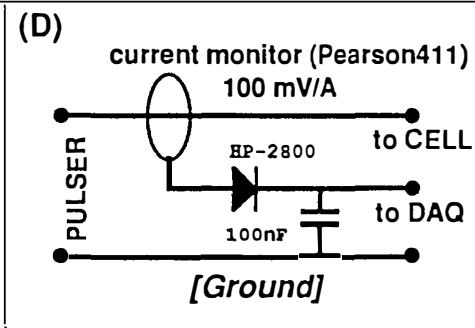

Fig. 2.d) Current circuit.

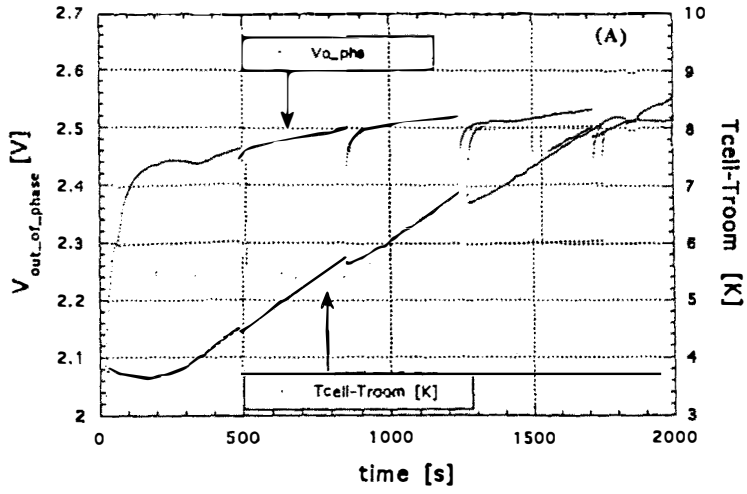

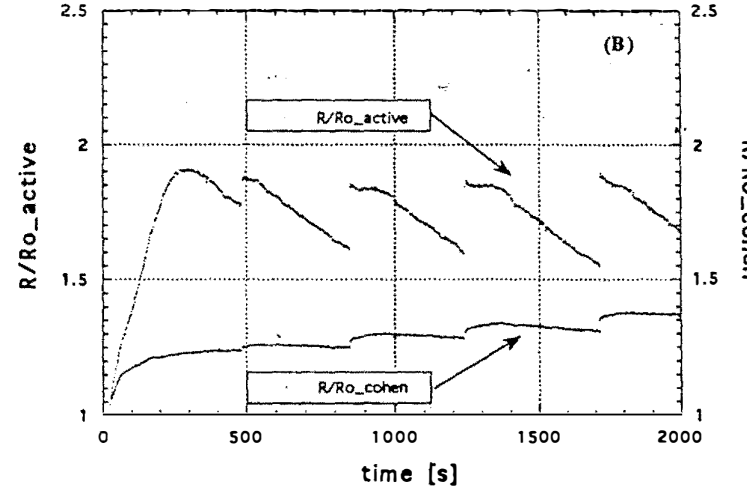

fig 3:
(a) Trend of Voltage out of phase and trend of the difference between cell and room temperature during the first 2000 seconds.
(b) Resistence ratio of the ACTIVE and the COEHN side of the wire during the first 2000 seconds.

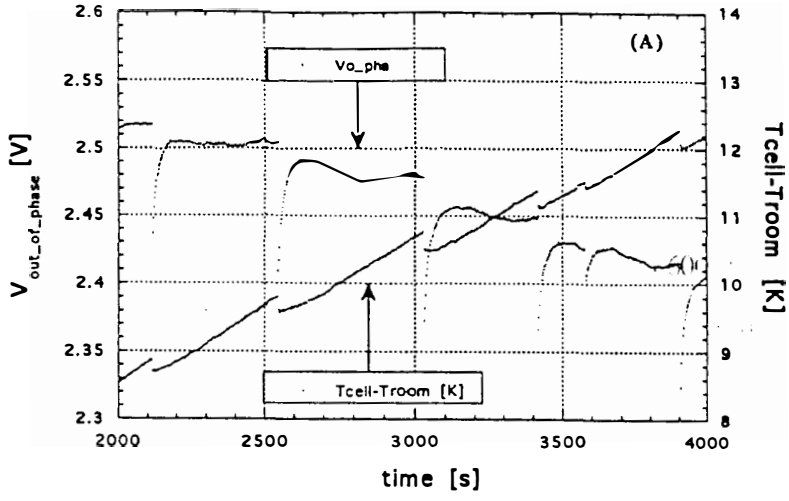

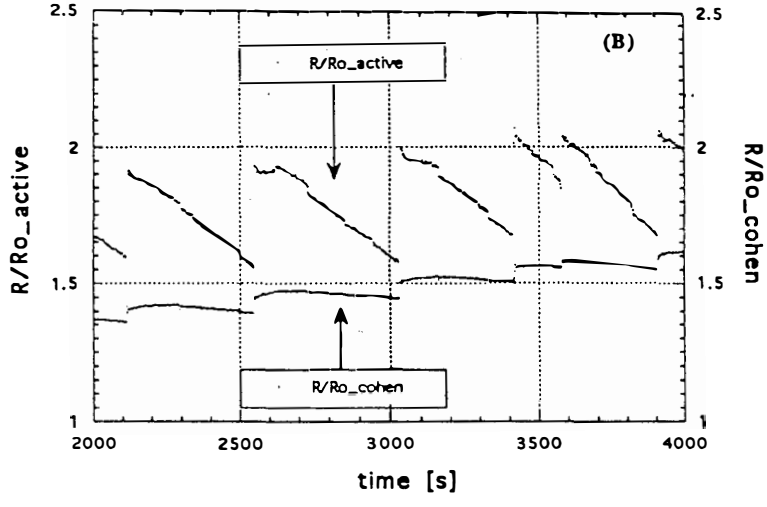

fig 4:
(**a**) Trend of Voltage out of phase and trend of the difference between cell and room temperature during the time between 2000 and 4000 seconds.
(**b**) Resistence ratio of the ACTIVE and the COEHN side of the wire during the time between 2000 and 4000 seconds.

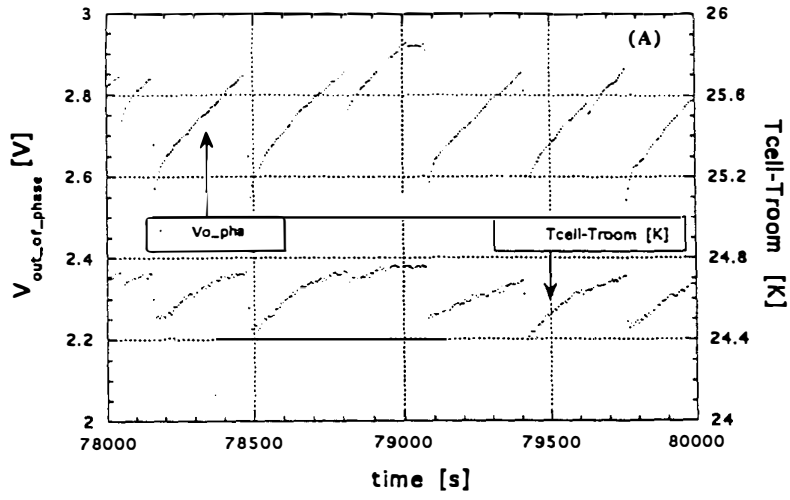

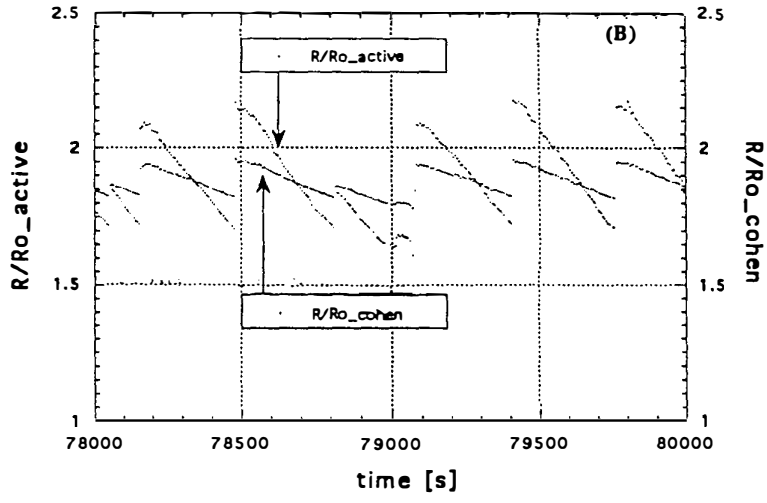

fig 5:
(a) Trend of Voltage out of phase and trend of the difference between cell and room temperature during the time between 78000 and 80000 seconds.
(b) Resistence ratio of the ACTIVE and the COEHN side of the wire during the time between 78000 and 80000 seconds.

Fifth International Conference on Cold Fusion
9-13 April, 1995 - Monte Carlo, Monaco
ICCF5 ©1995

EXPERIMENTAL CORRELATION BETWEEN EXCESS HEAT AND NUCLEAR PRODUCTS

A. TAKAHASHI, T. INOKUCHI, Y. CHIMI, T. IKEGAWA,
N. KAJI, Y. NITTA, K. KOBAYASHI and M. TANIGUCHI
Osaka University, Yamadaoka 2-1, Suita, 565 Japan

Abstract

A comparator of twin system was developed to study possible correlation between observed excess heat phenomenon and nuclear products. Simultaneous on-line measurements were done for foreground (Pd cathode) and background (Ni cathode) cells to monitor input/output powers, neutron spectra and X-ray spectra. Slight (5-7%) excess powers were observed with 99 % confidence level, only for Pd-cathode-cell, with weak neutron emission in the energy over 3 MeV. Burst events by X-ray detectors were analyzed.

1. Introduction

The aim of this work is to study experimentally the possible correlation between "excess heat phenomena" observed by cold fusion (CF) experiments with heavy water electrolysis [1,2] and theoretically modeled deuteron-related nuclear reactions in metal/deuterium systems [3]. However, it is difficult to establish the methodology for studying the correlation, because of the lack of reproducibility of the CF effect by experiments and also because of the lack of fully-reasonable theoretical models.

In this work, the authors have classified intrinsic conclusions of various theoretical models on nuclear or non-nuclear products, into 5 scenarios as mentioned in Section-2. The first scenario is the case of high energy charged particle emission as principal nuclear products and characteristic X-ray emission as the secondary products. Weak neutron emission with specified spectrum is of interest in the scenario. The second scenario presumes no high-energy charged-particle emissions, but does production of He-4 or other isotopes. Following two major scenarios, techniques and tools of measurement were prepared for calorimetry, neutron spectroscopy, X-ray spectroscopy and high-resolution mass spectroscopy.

Due to the "non-reproducible nature" of cold fusion phenomenon, simultaneous and parallel runs of test (foreground) and blank (background) experiments, using identical experimental set-ups except test materials (Pd vs. Ni, heavy water vs. light water, etc.), are needed to clarify in-situ excess power, X-ray emission and neutron emission taking place only for the foreground (FG) run. A comparator of twin system as mentioned in Section-3 was developed for this purpose. If we could observe any meaningful difference in FG and BG runs for output powers, X-ray and/or neutron emission from the comparator experiment running simultaneously for FG and BG systems, the "cold fusion" effect will become very reliable.

2. Major Scenarios

One clear thing that CF experiments since 1989 have clarified is that excess heat is not by known d-d fusion reactions, because of no observations of correspondingly intense neutron (2.45 MeV) emission. Therefore, if the excess heat were due to nuclear effect. we should have some kind of "new class of nuclear reactions in solids". So many theoretical models and ideas have been proposed[3] to resolve this issue, e.g., lattice-induced fusion, virtual-neutron transfer reaction, lattice-induced multibody fusion, proton-induced fission, alkali-proton reaction, neutron hallow nuclear reaction, etc.. The authors group has proposed multibody fusion models with intrinsic nuclear products and particle spectra[4,5]. At present, we do not know the ultimate working model. In spite of essential differences in models by different authors, it seems possible to classify the cases of resultant nuclear products, particle spectra and secondary reactions, into a small number of scenarios as shown in Table-1, since we find common factors in kind of particles, energies, secondary effects, chemical and material conditions, among the variety of intrinsic conclusions on "nuclear ash" by many different theoretical models.

Scenario-1: Nuclear excited energy of "aneutronic" reaction is considered to be released, by anyway, as kinetic energies of charged particles (α, p, t, h, d) of reaction products. Usually we consider that the emitted charged particle energies are in 1-20MeV region, and therefore one watt excess power corresponds to 10^{11} to 10^{12} reactions per second. Primary high energy charged particles interact with lattice atoms (i.e., Pd and deuterons) and electrons via ionization-and-recombination, slowing-down with knocked-on atoms and cascade displacements, and so on, to deposit thermal (vibration) energy to lattice. In the process, X-ray emission (PIXE) and secondary neutron emission can take place. X-rays will be produced by the characteristic K_α and K_β processes, the electron (scattered by high energy charged particle) bremsstrahlung and the nuclear bremsstrahlung.

For example, if 5-10 MeV α-particles are major primary products, we look for 21-22.4 keV Peaks of K_a and K_s X-rays from Pd. The α-particles will dissociate deuterons in PdDx by D (α,n) reactions. There are also D(d,n) reactions by knocked-on deuterons. Secondary neutrons by these reactions should have continuous spectra in the 0-10 MeV region (main component in 3-5 MeV region). Neutron yields by these processes are estimated, by D(α,n) and D(d,n) cross sections and averaged slowing-down spectra of α and deuterons, to be 10^{-8} to 10^{1} neutrons per α-particle. Therefore, when we see 1 watt excess power by the Scenario-1, we should have neutron yield of 10-10,000 n/source/sec from the cell.

Scenario-2: No neutrons and no high energy charged particles are produced in this scenario. We consider a special mechanism like "direct energy transfer from excited compound nucleus to lattice vibration[3] as proposed by Schwinger. Low energy charged particles (α = ^{4}He, h = ^{3}He) with less energy than 100 keV may be emitted by the primary reaction. Soft X-rays with exponentially decreasing intensity from several keV to about 50 keV may be only possible radiation from a cell. Production of secondary neutrons is negligible. Mass spectroscopy for ^{3}He, ^{4}He and other isotopes is the key tool of experiments. However, minor channel reaction by Scenario-1 might happen[4,5] to yield very weak emission of neutrons and weak emission of high energy charged particles.

Table-1: Scenarios of correlation between excess heat and nuclear products

Scenario	Excess H.	Primary Reaction	Secondary Reaction	Measurements
#1	Yes	Several Mev Charged Particles (α,p,t,h,d)	D(α,n):(n/α)=ca.10^{-9} D(d,n):(n/d)=ca.10^{-6} X-ray:22.4keV for Pd	Heat,He-4 C.P.spectrum n-spectrum X-spectrum (n/t) ratio
#2	Yes	Nuclear-Lattice Energy-transfer Fission Low-Energy C.P.	Ionization Displacement Recombination Soft X-ray	Heat,He-4 Isotope shift Fission Products X-spectrum
#3	Yes	Chemical Mechanical	Fracto-fusion D(d,n)	Heat 2.45Mev n
#4	No	Very few Rad. n,gamma	negligible	n-spectrum gamma-ray
#5	No	None	None	None

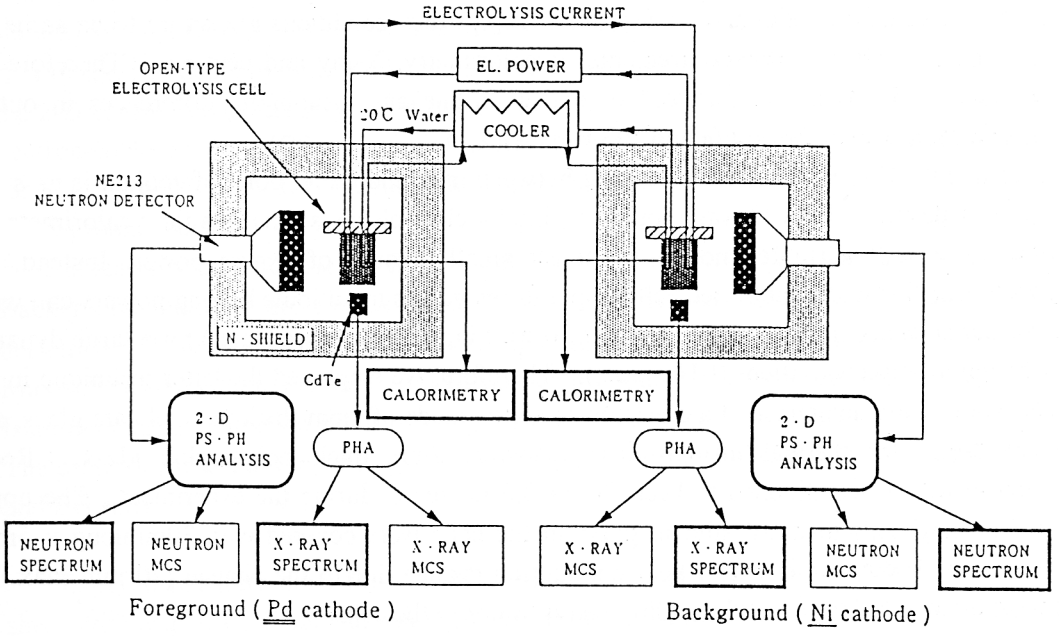

Fig. 1: A twin system of CF experiment with heavy water electrolysis, calorimetry, 2-D neutron spectroscopy and X-ray spectroscopy

Other scenarios: In Table-1 we show all the scenarios under consideration. Scenario-3 draws a possibility of "exotic" chemical or mechanical process for excess power generation, probably associating weak emission of nuclear particles and radiations. Scenario-4 belongs to S. Jones' idea. Scenario-5 belongs to Morrison/Huizinga's idea, and it will be finally proved when every thing in the CF study is proved to be due to some kind of systematic errors.

3. Comparator of Twin System

A twin system of CF experiment was designed and made as shown in Fig. 1, using two identically made open-type heavy water electrolysis cells with Takahashi type electrodes[6], two X-ray spectroscopy systems with CdTe detectors, two fast neutron spectroscopy systems with NE213 detectors, and two calorimetry monitors. One system serves for foreground (FG) runs, and the other does for background (BG) runs. In this work, the left cell for FG employs a Pd sheet cathode (25 x 25mm x lmmt), and the right cell for BG does a Ni sheet cathode (25 x 25mm x lmmt).

One power supply for electrolysis is commonly used for two cells and always the same electric current was supplied by the series connection from the FG to BG cell. Coolant (light water regulated to 20 +- 0.1 degree C by a chiller/heater) flows also by the series connection from the FG to BG cell. Two sets of electrolysis cell, CdTe detector (2x2x1 mm) and NE213 detector (13cm diam x 5cmt) are installed in each of two cavities with 30x30x30 cm size, symmetrically made in a lx2x1.5 m polyethylene pile for neutron shield.

The only difference between FG and BG systems is the difference in cathode material for the present work; i.e., Pd for FG and Ni for BG. Except this, conditions are set up to be same for electrolysis runs and on-line measurements of calorimetry, X-ray and neutrons. Therefore the twin system works as a "comparator" to detect on-line any meaningful differences in output powers and radiations between FG and BG runs.

Calorimetry: Difference of temperatures between inlet and outlet ports of coolant is as small as about 0.2 degree C for 100 watts joule heating by electrolysis, so that the flow calorimetry of the system[6] is not accurate enough to detect small amount of excess power. Instead, the calorimetry method using calibrated cell temperatures versus input joule heating powers can work with considerable accuracy (+- 0.65 watt for 50 watt input as discussed later) for a large dynamic range of input power variation (0-100 watt). Therefore, we employed the latter technique in the present work. Inner container of a electrolysis cell is made of 1mm thick pure silicate glass, and outer container for thermal insulation is made of 2mm thick polyacrylite glass. Room temperature was air-conditioned to keep 20 +- 0.5 degree C during the experiment. The upper parts of cooling coils made of silicate glass in the cells were covered with 30mmlong x 5mmt teflon pipes to isolate the effect of heat conduction change due to the change (20 mm max.) of D_2O level in the 4-5 days cycle for adding heavy water to the cells.

Calibration lines for FG and BG cells were obtained, using Ni cathode for both cells, for 5 steps (0-4 A) of electrolysis currents with 3 hours duration each step. Very straight calibration lines (input power vs. cell temperature) were obtained. Difference of calibration lines between two cells was small. Here, temperature data we retaken as average of two points, measured by

two thermocouples for each cell, in which we set up a magnetic stirrer at the bottom for mixing and homogenizing electrolyte (heavy water with 0.2 mol/l LiOD).

X-ray spectroscopy: Considering the possibility of X-ray emission in 0-50 keV region by Scenario-1, a CdTe detector was chosen because of small size (2x2x1 mm) and relatively good energy resolution (+- 2 keV) in the energy region less than 80 keV. Using an Am-241 calibration source, capability of spectroscopy for Ex > 6 keV was ascertained. Attenuation of 20 keV X-ray by heavy water layer and cell wall (silicate) was also measured with the Am-241 source. Making a hole through the outer container of cell, we set the CdTe detector on surface of the inner glass wall, from where we had 1mm silicate glass plus 15 mm electrolyte layer reaching to the Pd cathode surface. By the experiment with Am-241, we found the attenuation of about 1/30 of 21-22 keV X-rays which were supposed to be emitted from the surface of Pd cathode. Taking into account the efficiency (including geometrical factor) of CdTe detector, we may detect 22 keV X-rays, if intensity is more than 10^8 photons per second. In the later part of present work, we introduced 2-dimensional pulse-shape vs. pulse-height analysis for CdTe signals, to reject completely noise signals which gave "bremsstrahlung-like" spectra with burst events in the early part of experiments. Time-evolution of X-ray counts in 15-25keV bin was monitored by MCS systems with 4 min time width, both for FG and BG runs.

Neutron spectroscopy: The n-γ pulse shape separation technique has been utilized from the beginning of our CF study since 1989[7]. In the present work, we always used two sets of 2-D pulse-shape vs. pulse-height analyzers for FG and BG runs, so as to separate completely γ-ray events and noise events from neutron events for several months long measurements, where the stability of NE213 system became important. Because of the 2-D analyses, we can extract also γ-ray spectral data any time we want, as well as neutron spectral data. The n-γ separability in the 2-D contour map was so good that we had a wide "count-zero zone" between the γ - and the neutron-contour. For MCS counting of neutron events, we set the low energy threshold of 2 MeV for FG run, and 3 MeV for BG run, while spectroscopies were done in the 1.5-7.0 MeV range of recoil proton energy.

The reason why we chose the D_2O/Ni cell (not light water / Pd cell) for BG runs is as follows: Background neutrons are mostly produced in materials near the NE213 detector and in the detector itself by the cosmic ray induced spallation reaction and D(γ,n) reaction which emit Maxwellian-like continuous energy neutrons with about 2 MeV nuclear temperature. Therefore, from the neutron detection point of view, heavy water gives more BG neutrons than light water. The present twin condition will give exactly the same neutron BG conditions on-line both for FG and BG runs.

Experiments were done for 1) cold worked Pd sheet (NHE No.1-CW) and 2) annealed Pd sheet (900 degree C, 1 hour annealing). Experimental procedure for NHE No.1-CW and other cathodes are shown in Table-2. The pulsed L/H mode electrolysis technique[6] was fully used in the present work.

To want to have information on D/Pd ratio in the L/H mode operation, we used a separate closed cell system[8] to measure in-situ D/Pd ratios as a function of electrolysis current.

4. Results and Discussions

D/Pd ratios measured by the closed cell mostly showed about 0.90 for the L-modes (0.5 A, typically) and around 0.80 for the H-modes (4 A, typically), drew maximum for 0.5-1.0 A current and decreased for higher currents than 1 A. However, exceptionally, some Pd samples (annealed) showed increasing D/Pd ratios for the higher currents to reach 0.95. For the L/H modes general, we speculate that a slowly varying dynamic condition of repeating absorption and desorption is realized to change D/Pd ratio around 0.85. Relation of excess heat and exceptionally high D/Pd at higher current for some samples is not clear at present.

Figure-2 shows the results of powers, X-rays and neutrons in the beginning 60 hours (broken line shows interpolation of data lost by the power-off accident of the Campus). No excess power and no excess neutrons were found. However, unusual burst events of X-rays for the FG (Pd) cell was recorded in 4 successive cycles of current-off intervals of electrolysis. Pulse height spectra corresponding to these bursts show exponentially decreasing distribution from 6 keV to about 20 keV; this spectrum can be typically that of electromagnetic noise signals, but it might have some true information of X-rays since we saw coincidences with the L/H mode cycles. Possibility of soft X-ray emission by the nuclear bremsstrahlung by low energy charged particles (e.g., 46 keV α-particles[5]) should be studied in the future work.

In the following 150 hours (60-210 hours) after Fig.2, we saw no excess power for both of FG and BG runs, and no excess X-ray counts above natural BG level, though we could recognize slight increase (10-20 % at most over BG level) of neutron MCS counts and spectrum of FG run had a "structure" over 3 MeV, while BG(Ni) or cosmic neutrons has no such structure. After 18 days, we started to see a trend of excess power in the FG(Pd) cell and the trend continued for about 260 hours. Fig.3 shows the results of input/output and excess power levels for FG and BG runs, for the last 80 hours of this period. Clear excess power was observed for the FG(Pd) cell, while the BG(Ni) cell showed only fluctuated data around the "zero" excess power line. No 21-22 keV characteristic X-rays were detected by the CdTe spectroscopy in the period, though broad peaked spectra in 6-30 keV region with burst events were sometimes observed for both of FG and BG runs. Neutron (exactly speaking, recoil proton) spectrum had typical structure over 3 MeV but MCS counts were near background, while the natural BG spectrum taken with the same detector in 2 weeks after stopping electrolysis had no such structure as shown in Fig.4.

It took about an hour to reach equilibrium temperature after changing the current mode as we saw in the calorimetry calibration runs. So, we omitted calorimetry data for the beginning 1.5 hours after the mode change, and we sampled up data for later time interval than 1.5 hours, for the discussion of excess power generation. To estimate experimentally the total error width covering both of random and systematic errors, we took statistics of power balance for all the "excess power" data for BG(Ni) runs (including Ni data for annealed Pd cathode too): The results are shown in Fig.5, where solid curve shows Gaussian normal distribution with the standard deviation $\sigma = 0.65$ watt. This σ is regarded as the overall error of the present calorimetry during the long experimental period (few months), assuming the Ni cathode cell (BG cell) has no excess heat emission. The distribution of excess power data for NHE No.1-CW, compared with BG(Ni) are shown in Fig.6. Excess power data exceeding the 99 % confidence

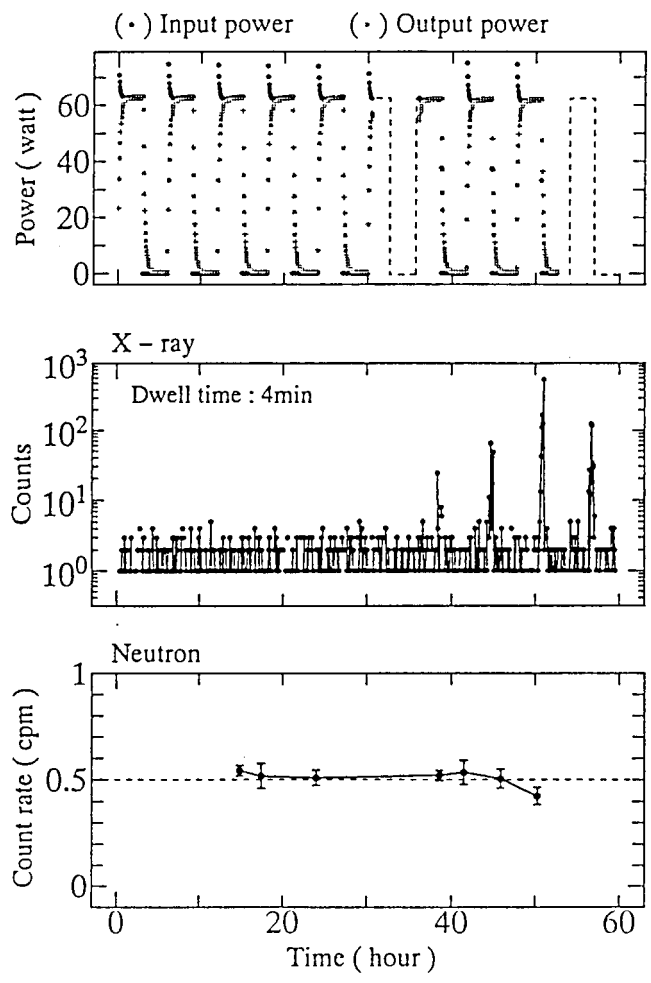

Fig.2: Results of FG run in the beginning 60 hours, for input/output, n and X—ray

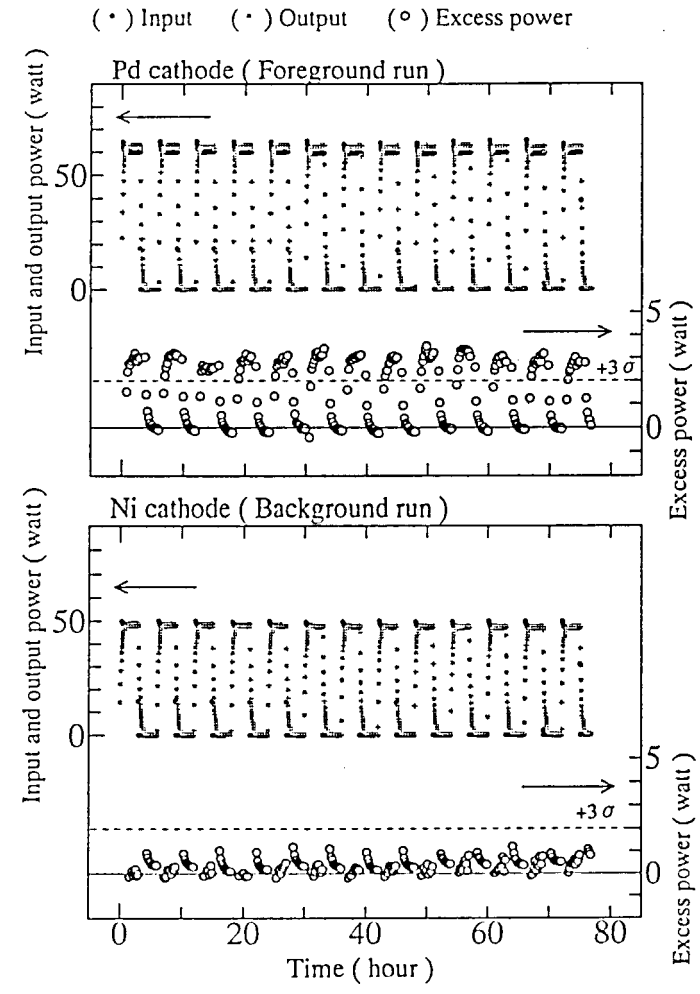

Fig.3: Results of FG and BG runs in the later period of experiments, for excess power

Table-2: Procedure of elctrolysis experiments

Date ' 4~~'05	Electrode		Mode (hour)	Mode Current
	Pd	Ni		
10/18 10/25	Tanaka 2nd batch	Nilaco No.1	On/Off (3-3)	4.5A/0.0A
10/25 10/28	〃	〃	On/Off (12-12)	4.5A/0.0A
10/31-- 11/3	NHE No.1 Cold Work	〃	On/Off (3-3)	4.5A/0.0A
11 4 11/10	〃	〃	On/Off (3-3)	4.5A/0.0A
11/10 11/17	〃	〃	Low/High (6-6)	0.5A/4.5A
11/1 11/38	〃	〃	Low/High (3-3)	0.5A/3.0A
11/20-- 12/2	〃	〃	On/Off (3-3)	3.0A/0.0A
12 1%/6	it	0	Sow-Tooth (20 min.)	0.5A--3.0A
%/7~~ 2/13	NUE No.2 Annealed	if	On/Off (3-3)	4.5A/0.0A
3/10~~ J/}7	〃	〃	Step mode (3)	

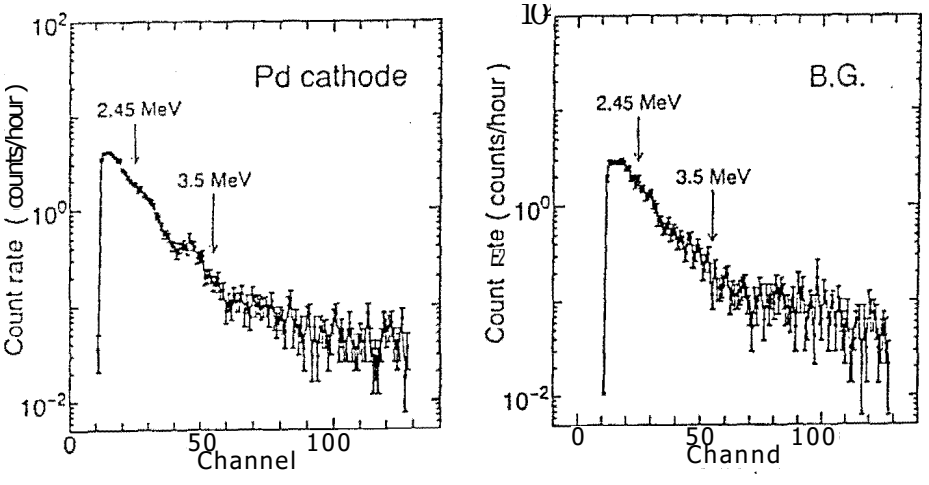

Fig.4: N[213 recoil-proton spectra, correspoding neutron spectra by unfolding, for FG(Pd) electrolysis run (left figure) and BC (elctrolysis off) run (right figure)

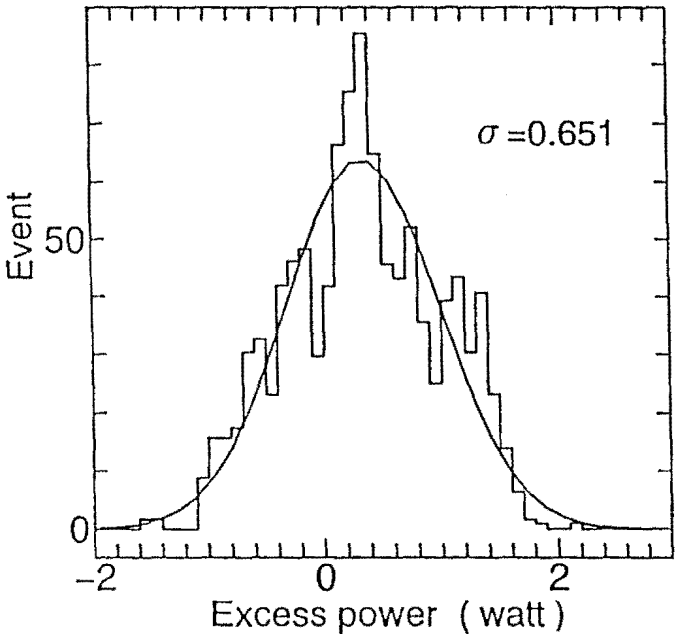

Fig.5: Distribution of power-balance data for BG(Ni) runs

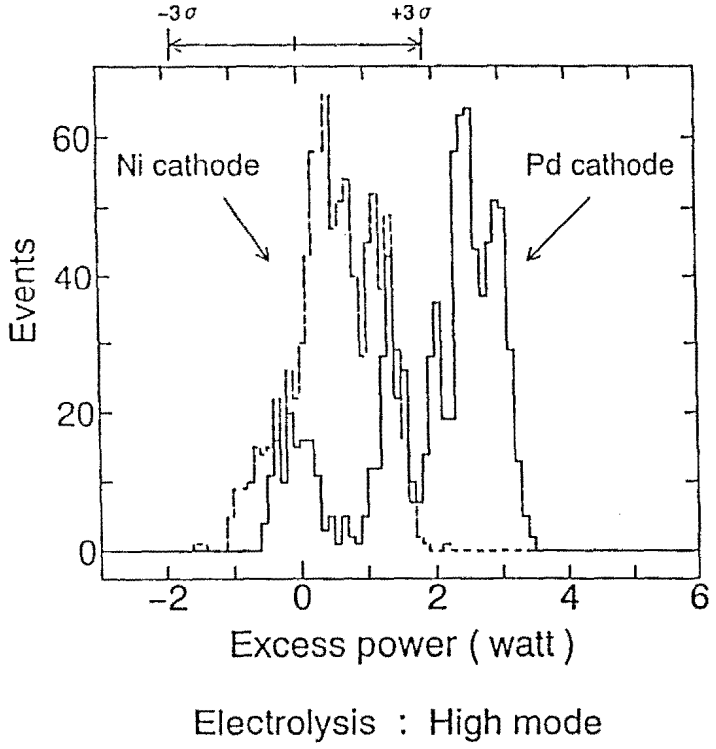

Fig.6: Distributions of excess power (power balance) data, compared for FG(Pd) and BG(Ni) runs

level (3 σ = 3 x 0.65 = 2.0 watt) are very clearly seen for the FG(Pd) cell. We had 2.3 to 3.5 watt excess power. However, excess ratio (output/input - 1.0)x100 is only 5-7 %.

The broad-peaked X-ray spectra frequently observed as bursts in 6-30 keV region was proved to be due to some noise (non-X-ray) events, based on the 2D analysis (pulse shape vs. pulse height) for CdTe signals, in the later part of the present experiment. The second series experiment for annealed Pd cathode was done using the gated condition for X-ray contour of 2-D X-ray analysis, and up to now no such broad peaked spectra in the 6-30 keV region were observed. The experiment with annealed Pd cathode is still under data processing, however we can say that a trend of excess power only for the FG(Pd) cell is also being observed.

5. Conclusion

To study the origin of excess heat and correlation with nuclear products, experimental works with a newly designed twin systems for calorimetry, X-ray and neutron 2-D spectroscopy were carried out. The twin system was proved to be very reliable and useful for the correlation study.

We observed 5-7 % (2.3-3.5 w) excess power beyond the 99 % confidence level only for the heavy water electrolysis cell with Pd cathode, while the reference heavy water cell with Ni cathode running simultaneously (in parallel with the FG run) gave no excess power data within error band 1 σ = 0.65 watt. Slight indication of neutron emission in spectra over 3 MeV was sometimes observed, but it was not tightly correlated to excess power generation, and neutron emission rates were very weak as 1 n/source or less. No characteristic X-rays, 21-22 keV for Pd were observed during the present work, though unusual burst events with continuous spectrum under 20 keV was once observed for the FG(Pd)-cell run.

We might conclude that Scenario-1 was denied because we did not see 21-22 keV X-ray when we saw excess power for the FG(Pd) cell. However, 1 mm thickness of Pd cathode plate can largely attenuate the characteristic X-rays if produced at the central zone and we should estimate scattered X-ray spectra in that case. The level of observed excess heat is still weak, so that we might not reject unforeseen systematic errors. Therefore, to draw definite conclusion on Scenarios, we need further a number of experiments with different cathode materials and different electrolysis conditions so as to statistically assure the excess heat, X-ray and neutron data.

References

1) Proc. ICCF3: Frontiers of Cold Fusion, H. Ikegami ed., Universal Academy Press (1993)
2) Proc. ICCF4: Trans. Fusion Tech., 25, Am Nucl. Soc., (1994)
3) V.A. Chechin, et al.: Int. J. Theor. Phys., 33(3), 617-670, (1994)
4) A. Takahashi, et al.: Fusion Tech., 27(Jan), 71-85, (1995)
5) A. Takahashi, et al.: Trans. Fusion Tech., 25, 451-454, (1994)
6) A. Takahashi, et al.: Ref. 1, pp.79-92
7) A. Takahashi, et al.: Fusion Tech., 19, 380-390, (1991)
8) H. Miyamaru, et al.: Ref.2, pp.151-155

Fifth International Conference on Cold Fusion
9-13 April, 1995 - Monte Carlo, Monaco
ICCF5 ©1995

FLOWING ELECTROLYTE CALORIMETRY

DENNIS CRAVENS
ENECO, Vernon Region Junior College, Vernon, Texas 76384
May 1, 1995

ABSTRACT

When the specific heat and flow rate of the electrolyte are known, the thermal output of cells using circulating electrolytes can be determined. An independent evaluation of the "Patterson Power Cell™" was conducted using the circulating electrolyte as a heat transfer medium. This allows for real time measurements and alteration of the electrolyte. The cell was found to give measurements consistent with claims of excess power. Suggestions for the improvement of the calorimetry are given. A simplified version of the system was demonstrated during the first 3 days of the International Conference on Cold Fusion - 5 (ICCF-5) and made available to those requesting its examination.

INTRODUCTION

The "Patterson Power Cell™" [1,2] has been claimed as both a light and heavy water system producing "excess heat". Before conclusions can be drawn, however, its unique calorimetry must be investigated. The system uses its electrolyte in a flow calorimetry approach. This allows greater and more rapid adjustment of internal cell conditions, while also permitting real time measurements of reaction products. It is one of few cold fusion systems which has been granted a U.S. Patent. This author was requested to evaluate the system.

The evaluation consisted of three parts- 1) observation of the cell being operated at its original site by its inventor, 2) personally operating the device at its original site [3], and 3) independently reproducing the device at a local site and testing it. All of these gave compatible results. This indicates that the device does give the observable measurements as claimed. However, ruling out systematic or equipment errors required redesign of certain components.

The initial cell design presented to the author used a thick plaster of paris insulation around the cell. The calibration resistor was embedded in the plaster and external to the cell. The overall efficiency, as measured by heat gained by the electrolyte from the resistor, varied from 20 to 70%. Such variability complicated any detailed analysis. The calibration resistor was replaced
insided the cell. The cell was wrapped with glass wool, housed inside side two dewer flasks set mouth to mouth, and sealed from humidity changes with parafilm. This raised the thermal efficiency of the calorimeter to 86 to 93%- depending on the cell packing and sealing. This lowered the thermal mass and shortened the response time of the cell. Additional sensors were added so that all measurements could be checked by secondary instruments. An quantitative investigation of the cell took place by this author after these modifications were made.

DESIGN

The modified cell is shown in figure 1. The use of plated beads as the cathode is the most unique feature of this design. These beads were supplied by Clean Energy Technologies, Inc. [4] and are produced and used in accordance to existing Patents [5]. The microspheres were originally designed for work as density gradient markers for protein analysis. They were then used in amino acid analysis and ion exchange systems. The spherical construction of the beads allows for uniform expansion and contraction without the development of large stresses and cracks. Current work [6-8] has indicated that, for at least nickel, normal water systems, the cold fusion effects are a surface or near surface effect. Thus, the use of many small spheres provides a large surface area that maintains structural integrity.

The base of the bead is a stable cross-linked copolymer made of styrene divinyl benzene. The beads are first sulfated with chlorosulfonic acid to provide a conductive surface. A copper chloride solution is then fixed to the surface. This allows the beads to withstand higher temperatures while avoiding hot spots that would otherwise blow the metal coatings off. Uniform metal plates are then layered accordingly. First with nickel, then with palladium, and than an outer coating of nickel. These multiple layers of nickel/palladium/nickel on beads thus far have out performed single coatings. Others [9] have investigated such multilayer thin films on plates which eventually detached from the surface. The plated beads have performed continually in cells for over one hundred hours without observable changes. It is estimated that 40 mg of metal (a total of about 2 micron thickness of all layers) and about 1200 beads are used within the cell. It is important to note that the small amount of metal used should be beneficial for searches of isotopic shifts.

The electrolyte outlet temperature, T2, is measured at the top of the cell as it reaches the height of the lower dewer containment lid. The inlet temperature, T1, is measured 5 cm from the lid as the electrolyte flows into the cell. The initial designs used thermocouples (K-type) coated with epoxy. After extended runs, it was determined that the lithium ions from the electrolyte were causing "decalibration errors" in the thermocouples. Furthermore, the thermocouples were not completely electrically isolated from the electrolyte. Thus, the electrolyte current could interfere with the temperature measurements.

The thermocouples were moved to stainless steel wells and insulated with teflon tape and heat sink compound. The two stainless steel wells were connected to a common ground. This increased the thermal response time but prevented additional electrical interference. The upper portion of the thermocouple wells were lightly insulated by tygon tubing. It has been pointed out that the length of the thermocouple well outside the electrolyte may cause the inlet thermocouple to see a weighted average of the temperature between the electrolyte and the environment. Such "wicking effects" have been known to produce errors of 10 to 20%. It is recommended that future designs avoid wells which extend beyond the tubing and employ thick insulation at the site of the measurements. In most experimental runs, the inlet sensor region was also located within the upper dewer and within the glass wool insulation. The physical location of the well was in a region of large flow gradients (i.e. cross sectional areas changed from $1mm^2$ to $10mm^2$ back to $1mm^2$). This provides some mixing. It is recommended that any redesigns use a commercial in-line mixer just up-stream from the temperature sensor.

The overall system is shown in figure 2. The electrolyte flows in a closed loop 1) from the reservoir 2) to the pump 3) through the flow sensor 4) through the cell 5) to a gas splitter and 6) returns to the reservoir. The input power is calculated from total voltage and current supplied to the cell. The voltage was not corrected for the gas production. The output power was obtained by the heat absorbed by electrolyte flow. The electrolyte is prepared from a one molar lithium sulfate solution of normal water. The electrolyte also serves as the heat transfer fluid. It has an apparent specific heat of approximately 0.95 within the overall system. The output heat can be arrived at via calibration curves of the cells or from first principles using the specific heat of the electrolyte. In practice, both were used and found to agree within 15%.

CALIBRATION

The system was first calibrated using distilled water for the working solution and the internal calibration resistor for its heat source. This produced overall efficiencies for the calorimeter within the range of 86 to 92%. The exact value is dependent on the sealing method (parafilm or silicon rubber) and the packing of the glass wool. The data sets given later (figure 4) are based on the 88% configuration using parafilm to seal the gaps against air flow. A series of calibration runs were conducted by varying both the flow rate and input power independently. Figure 3 shows the relationship between input power and temperature differential for a fixed flow rate and current setting. The efficiency was found to be stable (88% +/- 2%) over all practical flow rates or resistor inputs.

Next, the 1 M lithium sulfate electrolyte was used as the working solution. Its apparent specific heat within the unit was approximately 0.95 based on the above water calibration. It should be noticed lower specific heats of the working fluid could lead to overestimates of the heat generation. However, saturated lithium sulfate solutions are about 3 molar. A 100 ml volume of a saturated solution at the working temperature contains only 88 g of water. Thus, the specific heat of the electrolyte should never be lower than about 0.88. A second calibration series was conducted using the lithium sulfate solution and the calibration resistor.

At the beginning and end of each experimental run, a calibration pulse of 15 minutes was used to check the system's performance. During some runs, a calibration pulse was delivered as the system was generating anomalous heat. In those cases, it was noticed that power delivered to the calibration resistor gave additional heat output greater than can be expected by simple additive processes. This is seen as either a) the heat producing mechanism has a positive temperature coefficient or b) the instrumentation and sensors over estimates the heat generation. All physical mechanisms proposed (gas bubbles at sensors, heat gain and loss via sensor sheaths, etc.) in support of the second alternative appear to be an order of magnitude smaller than the observed effects. To test the first premise, an auxiliary heater was added to the electrolyte's reservoir. Pre-heating of the electrolyte to 40 to 60 degrees C before entry into the cell apparently enhances the power generation. Due to limited time, only a few runs at elevated temperatures were conducted. Further investigation has clearly indicated and should throw light on the heat mechanism and response of the instruments. Such effects are the subject of current experimentation.

There is an initial loading period required of the beads. This is about 12 hours for fresh beads and only 1 hour for pre-loaded beads. This is conducted by using a constant current power supply set at 0.2 to 0.5 amps. The

cell's resistance gradually changes from 135 to 150 ohms. This is thought to be due to hydride production on the surface of the beads. The temperature between the inlet and outlet gradually increases toward the end of the loading period.

TYPICAL DATA POINT

There are 6 primary measurements for each data set: the electrolyte flow, F; the voltage, V; the current, I; the temperatures of the inlet, T1; and the outlet, T2; and the gas productions flow, f. The gas flow is monitored only to verify that no appreciable recombination occurs. This was found to be true to the limits of measurements, +/- 0.5 ml/min. All measurements were taken by two separate sensor systems and found to be internally consistent. All meters, except the temperature, were calibrated and traceable to national standards. A simplified demonstration system was present at ICCF-5. The following data set is one that was taken immediately prior to this authors presentation: V=3.80 V, I= 0.12 A, F=10.30 ml/min., T1=24.3 C, T2=26.9 C, f=1.2 ml/min. (average). This and similar data sets were witnessed by some ICCF-5 participants. This specific data point represents an input power of: P=VI = 0.46 W. It represents a thermal output of: d[mc(T2-T1)]/dt = 1.77 W. The gas production represents an additional power production of 0.18 W. The heat loss from the cell is estimated at an additional 14 % of the heat production or 0.25 W. Such a point would appear as power ratio of 1.77/.46 = 384%. Notice that the thermal power production exceeds the electrical input power even without addition of the gas production or heat loss terms.

A series of data sets were taken and the results represented in figure 4. The points in this figure were taken with the complete laboratory device and under environmentally controlled conditions. The power ratio of: power out / power in, is in the range of 1 to 5 when neither gas production or heat loss are added to the output figures. The ratios are slightly higher when those terms are added. It is interesting that the cell gave values of between 1 and 2 for those ratios at high currents (>1 amps.). This is consistent with other studies [10] of nickel based systems showing a higher power ratios at low currents. At low current (< 0.2 amps) there is more scatter in the data. This is because any errors or uncertainties of measurements are exaggerated by the ratio at low power levels. However, the ratios are consistently above 2 to 1 even with the most pessimistic data sets. The high current regions of the chart are on firmer experimental grounds. However, it is the low current regions that are the most intriguing for future engineering projects.

During the conference, a simplified version was demonstrated. This used hand meters instead of bench meters, minimum insulation for visibility and other low weight alterations. The demonstration device was displayed and run for 3 days (minus about 3 hours due to transport to nightly storage). Power ratios of between 2 to 6 to 1 were demonstrated for most of that time as represented by the typical data set given above. Conference participants were invited to take data, their data is summarized in table A. The demonstration was run in the low current ranges (< 0.5 amps). The device was for demonstration purposes only and was designed to illustrate the reproducibility and reliability of the basic design. The goal was to introduce the unique features of this relatively unknown system to conference participants.

CONCLUSION

The system does appear to be worth further study. Nothing discovered during the evaluation of the cell is inconsistent with the production of excess heat within the cell assembly provided that there is a positive temperature rate coefficient. This evaluation has concentrated on increasing the thermal efficiency of the calorimeter, consistency between measurements, better placement of the calibration resistor, measurement of the gas production in real time, use of calibrated and traceable electrical meters and alternative measurements of key values. It is advised that further study is required to limit uncertainties due to temperature measurement of liquid flow. Additional independent experimentation with "inert beads" as controls and the use of in-line mixers should be considered. The high power ratios at the low current levels need to be revisited using measurements with tighter error bounds. However, regardless of the cause, the system does give repeatable results at substantial levels. If, as expected, the power levels persist with tighter experimental bounds in the low current levels, then the system should have important practical and commercial applications.

REFERENCES

[1] Patterson, James, "Method for Electrolysis to Form Metal Hydride", U.S. Patent 5,318,675

[2] Patterson, James, "System for Electrolysis of Liquid Electrolyte", U.S. Patent 5,372,688

[3] Klein, Bruce, "Cold Fusion Testing at Clean Energy Technologies Inc.", Cold Fusion, 9(1995), p21.

[4] Clean Energy Technologies, Inc., bead batch #116, 14332 Montfort, Suite 6302, Dallas, Texas 75240

[5] Patterson, James, "Metal Plated Microsphere Catalyst", U.S. Patent 5,036,031
Patterson, James, "Process For Producing Uniformly Plated Microspheres", U.S. Patent 4,943,355

[6] Bush, P.T. and R.D. Eagleton, Calorimetric Studies for Several Light Water Electrolytic Cells With Nickel Fibrex Cathodes and Electrolytes with Alkali Salts of Potassium, Rubidium, and Cesium", Proc. ICCF-4, 1993, EPRI TR-104188-V2 (1994), p13

[7] Notoya, R. and M. Enyo, "Excess Heat Production during electrolysis of H2O on Ni, Au, Ag and Sn Electrodes in Alkaline Media", Proc. ICCF-3 (1992).

[8] Mills, R. and S.P. Kneizys. "Excess Heat Production by the Electrolysis of an Aqueous Potassium Carbonate Electrolyte and the Implications for Cold Fusion", Fusion Technology, 20 (1991) p65.

[9] Miley, G.H., H. Hora, E.G. Batyrbekov, and R.L. Zich, "Electrolytic Cell with Multilayer Thin-film Electrodes", Fusion Technology, 26 (1994) p313.

[10] Ramamurthy, H., M. Seinivasan, U.K. Mukherjee, and P. Adibabu, "Further Studies on Excess Heat Generation in Ni-H2O Electrolytic Cells", Proc. ICCF-4, (1993) vol. 2, p15-1

Figure 1
Patterson Power Cell
Design

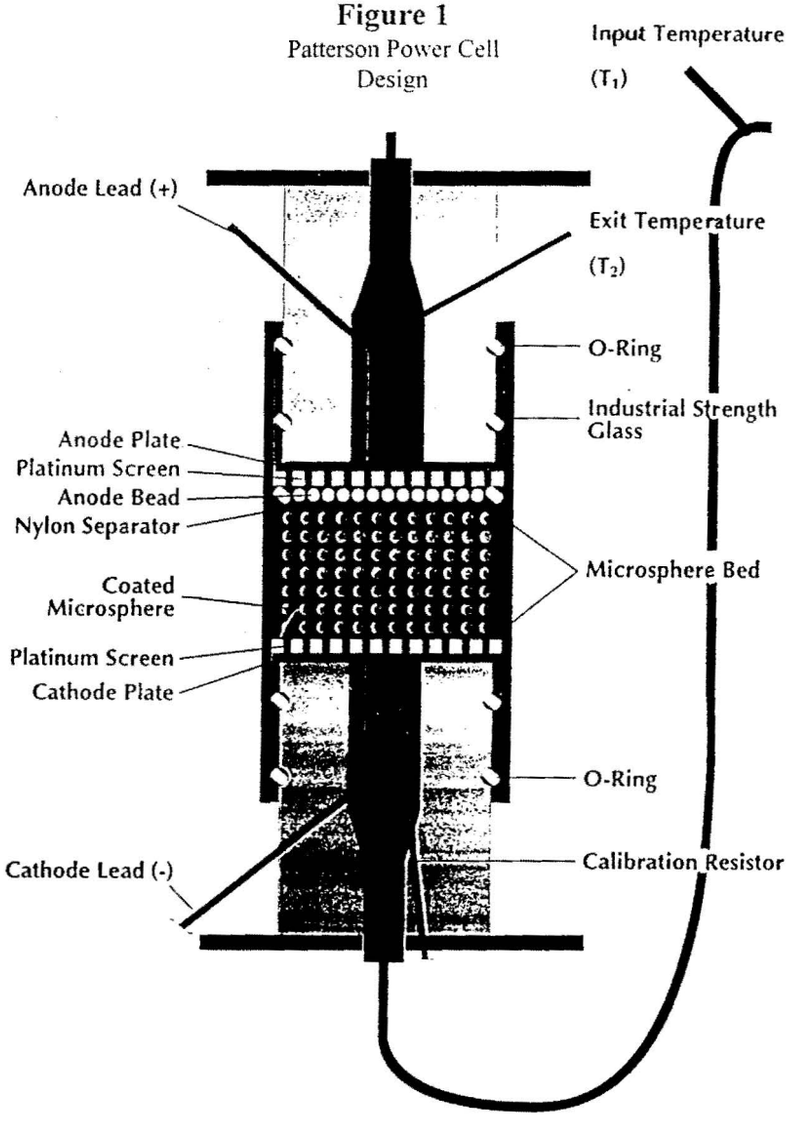

Figure 2

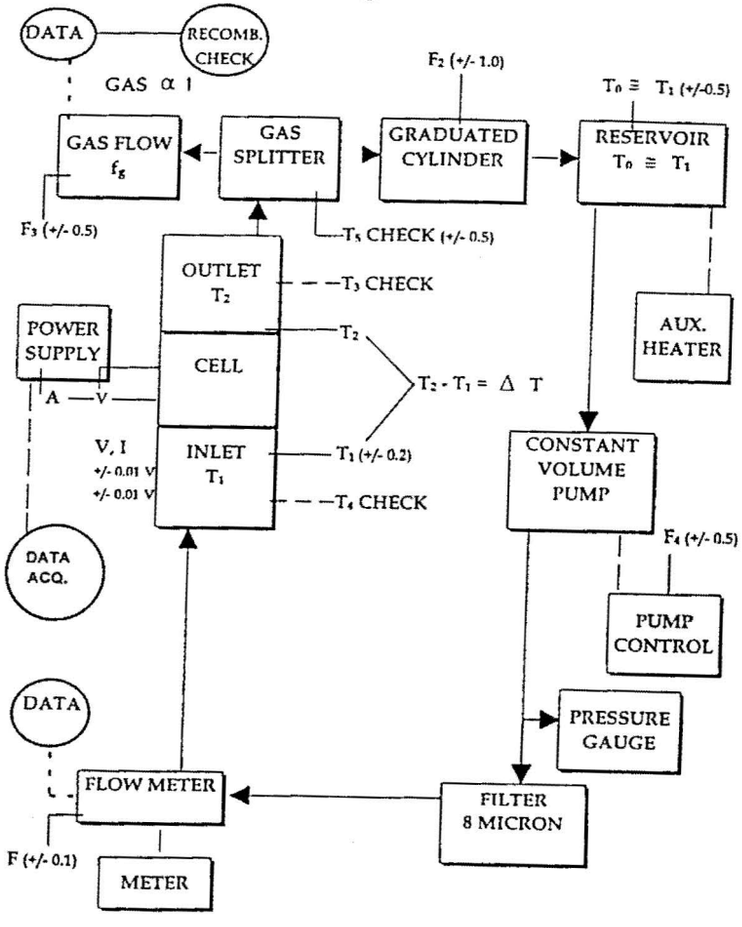

System Diagram

Figure 3

Calibration

delta T vs. input power(resistor)

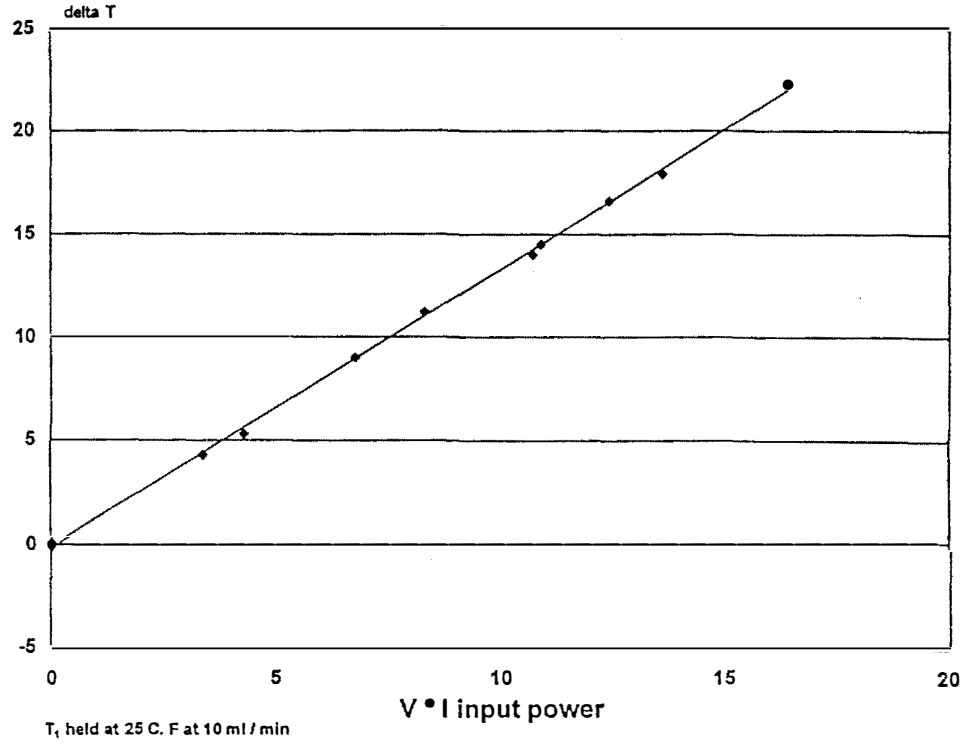

Figure 4

Power Run

excess power vs. current

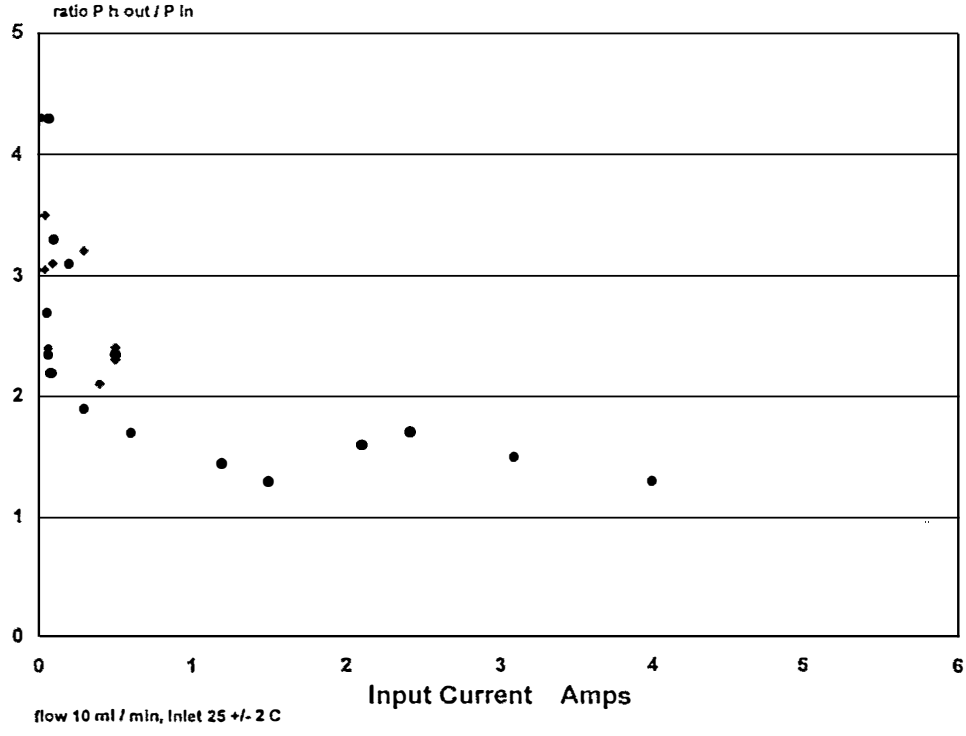

Table A

Patterson Power Cell Demonstration

Data taken by conference attendees at ICCF-5

Date	Time	Voltage (V)	Amp (I)	Flow Rate L/min	ΔT (°C)	Raw Heat Yield (a) (%)	Heat Yield - Correction (b) (%)	Heat Yield w/ Correction (c) (%)
4/9/95	21:10	3.29	.07	10.28	1.1	326	379	688
4/10/95	9:45	3.80	.12	10.08	2.6	381	443	726
4/10/95	14:38	3.80	.12	10.04	3.5	511	594	973
4/10/95	14:45	3.80	.12	10.11	3.6	529	615	1008
4/10/95	15:15	3.80	.13	10.01	3.3	443	516	844
4/11/95	12:28	3.74	.15	10.00	2.4	284	330	546
4/11/95	14:05	3.74	.13	10.00	2.5	341	396	656
4/11/95	18:30	3.43	.10	9.38	2.5	453	527	927
4/11/95	18:50	3.43	.09	10.00	2.4	516	599	1054
4/12/95	12:00	4.15	.21	10.00	3.0	228	265	413
4/12/95	14:10	4.15	.21	10.00	3.2	243	283	440
4/12/95	16:20	4.15	.21	10.00	3.4	259	301	468

Note: Yield calculations assume specific heat of electrolyte of .95.
(a) Raw heat yields without gas or thermal heat loss corrections.
(b) Heat yields with thermal heat loss correction (cell is 86% thermally efficient).
(c) Heat yields with thermal heat loss correction and gas correction (1.48); assuming no recombination.

Fifth International Conference on Cold Fusion
9-13 April, 1995 - Monte Carlo, Monaco
ICCF5 ©1995

Present Status and the Perspective of New Hydrogen Energy Project

Naoto. ASAMI, Kazuaki. MATSUI and Fumihiko. HASEGAWA *

R&D Center for New Hydrogen Energy, The Insititute of Applied Energy
3-5, Techno Park 2-Chome, Shimonopporo, Atsubetsu-ku, Sapporo , Hokkaido-004, Japan
* New Energy and Industrial Technology Development Organization
1-1, 3-Chome, Higashi Ikebukuro Toshima-ku, Tokyo-170, Japan
(Presented at ICCF-5, Monaco; April 10-13, 1995)

Abstract

A research and development project, named as 'New Hydrogen Energy', has started in Japan in November, 1993, to confirm the excess heat generation during electrolysis with Pd-LiODsystem as the first priority objective. The Project has been supported by the Ministry of International Trade and Industry(MITI) and major industries in Japan, and new laboratory was established in Sapporo.

Present status and the perspectives of the project will be reported together with main technical results. Two types of electrolysis cells, namely, open type cell system from IMRA-Europe, Inc. and the fuel cell type cell systems from IMRA-Japan, Inc., were installed in NHE Sapporo laboratory and the experiments have started from February 1994 to demonstrate the NHE-phenomena.

Correlationships among maximum attainable D/Pd ratio, deuterium absorption and desorption and the characteristics of various palladium sources and treatments have been studied and analysed based on the resultsof the material observations and instrumentational analysis such as O/M, SEM, XRD, AES , SIMS and EPMA.

The laboratory will be reinforced by introducing of mass flow calorimetry systems, and reaction products detection systems towards an interim review scheduled in late 1995.

This R&D program has been conducted under the consignment of New Energy and Industrial Technology Development Organization(NEDO).

1. Introduction

Fleischmann and Pons revealed the excess heat generation phenomena by electrolysis of heavy water using a palladium electrode in 1989. Since then, there have been many researchers who observed this heat generation and the amount of heat sometimes cannot be explained by chemical reaction, and there are some theoretical models which may possibly explain the phenomena. Since the heat generation is essentially based on abundant deuterium, there arose an expectation to develop this phenomena as a non-oil energy source.

A R&D project has started in Japan on November 1993, in which the excess heat generation is regarded as "New Hydrogen Energy". The aim of this R&D project is to clarify the potentiality and possibility to use a future energy source and to control heat generation quantitatively by its demonstration and understanding of the reaction mechanism.

This "NHE-Project" had been first announced and introduced at ICCF-4 held in Maui by one of the author, Matsui.

2. Organization Structure

Ministry of International Trade and Industry (MITI) has decided to subsidize New Energy and Industrial Technology Development Organization (NEDO). NEDO have contracted with the Institute

of Applied Energy (IAE) to conduct this research and development project of four years as period from late 1993. Figure 1 shows the R&D execution structure.

Three committees were established in NEDO with noticeable experts, some from the academic world and the other from industries; the first committee is responsible to determine a basic plan and action programs, the second to evaluate R&D results and the third to plan and manage the action programs.

The NHE R&D project consist of a national project and multi-client industry supported project. The national project conducts mainly to examine excess heat generation for confirmation and demonstration. The latter project conducts basic researches. The framework of the NHE R&D project is illustrated in figure 2. These two projects keep close relationships and are mutually supported and cooperated. Details of latter project will be described later by Prof. Okamoto of Tokyo Institute of Technology.

The guidelines of the NHE-R&D project are as follows,

(1) The NHE research and development program is to be recognized as one of national basic research plans of industrial science and technology in long term energy issues, and to be executed in focal point manner with researchers of private sector who have significant experiences in related fields.

(2) The researches by universities with financial support from private sector will concentrate more basic researches, such as clarification of reaction mechanisms in order to support the national project.

(3) Furthermore, reinforcement of international networking with foreign research institutes and exchange of basic research information through international symposiums and exchange program to support identification of possibility for future energy source.

3. Research and Development Programs

(1) Demonstration of excess heat generation

1) Measurement of excess heat during electrolysis

Based on several prior arts of experiments, measurements of excess heat are to be demonstrated to confirm the NHE phenomena, and the excess heat generation is to be quantified together with its reproducibility, controllability, amplification and durability.

2) Reaction products accompanied with excess heat

The specifications of kinds and amount of reaction products is to be instrumented with in-situ observation, and correlation with heat generated is to be surveyed to support reaction modeling.

3) Conjunction of electrolysis and vacuum method

To take advantages of both electrolysis(wet) and vacuum method(dry), electrode material and reaction products are to be analyzed during excess heat generation at high deuterium loading to find out the control factor of the reaction.

(2) Material analysis and development

1) Material analysis

At first, it is essential to find out basic features of electrode material required to generate excess heat. Two types of materials; one with excess heat generation and the other without, and another with high loading and the other with low, are to be observed and analyzed to identify the differences.

2) Material development

Controlled factors of material characteristics are to be found out for the high loading and the heat generation, and guidelines for material development are to be formulated.

(3) Information exchange

Information and data exchange are to be encouraged to formulate developmental guidelines in order to conduct effectively research and development programs of which master schedule and research items are shown in figure 3.

4. Progress of NHE-Project.

The milestones of this national project are shown as follows,

FY1993

Nov. 01, 1993: Establish R&D Center for NHE(Tokyo)
Dec. 01, 1993: 1st NHE Steering Committee(Start of the Project)
Dec. 01, 1993: Establish NHE Laboratory(Sapporo) in NHE Center
Dec. 06, 1993: ICCF-4(Maui, Hawaii), 1st announcement of the project
Feb. mid., 1994: Start of Excess Heat Experiments with Two Electrolysis Systems
Feb. 23, 1994: 1st NHE National Symposium in Sapporo
Mar. end, 1994: Annual Report(FY1993)

FY1994

May. 17, 1994: 2nd NHE Steering Committee
Sep. 05, 1994: 1st International NHE Workshop(Lake Kawaguchi)
Oct. mid., 1994: Start Development of Mass Flow Calorimetry Components and System
Dec. 13, 1994: 3rd NHE Steering Committee
Mar. end, 1995: Annual Report(FY1994)

FY1995

Apr. 10, 1995: ICCF-5, 3 Presentations from NHE Project.
Jun. 02, 1995: 4th NHE Steering Committee
Oct. mid, 1995: 2nd International NHE Workshop(Trino)
Dec. mid, 1995: Interim Review of NHE Project
Mar. end, 1996: Annual Report(FY1995)

5. Major Activities and the Results

According to the basic plan which is described above, R&D activities have been conducted in NHE-Center. Major experimental activities and the results which have been performed hitherto, substantially during FY 1994, in NHE-Laboratory are summerized. Figure 4 shows the milestone chart of NHE-R&D items in FY1993 and FY1994.

5-1 Demonstration of excess heat generation

(1) Experiments on fuel cell type electrolysis system

Measurement of the D/Pd ratio and excess heat of Pd from various sources have been carried out using fuel cell type electrolysis systems. Various Pd include 3-nine and 4-nine purity, meltedin atmosphere and vacuum, as cold worked and annealed, polycrystal and single crystallized, and Pd-5%Rh and -10%Rh alloys were examined to seize the suitable material characteristics.

Major results are followings

a) Measurement of Excess heat of 9～15% have been reproduced in 2 cases with vacuum

annealed pure Pd, however reproducibility issue still remained.

b) D/Pd ratio of 0.89 and H/Pd ratio of 0.93 have been attained with vacuum annealed pure Pd and single crystallized Pd.

c) Low D/Pd ratio of 0.79～0.82 have been measured in as cold worked Pd having surface defects such as micro-crack.

d) High D/Pd ratio of 0.9～0.94 have been attained with Pd-10at%Rh alloys, however excess heat has not observed.

(2) Experiments on open type electrolysis system

The open type cell systems, namely ICARUS-1 system which was developed by Fleischmann and Pons originally, have been introduced in NHE-Laboratory at the end of Jan. 1994, and started electrolysis with pure Pd and Pd-10%Ag.

ICARUS-1system is capable to measure the phenomena with relatively low current(～200mA) electrolysis and then negligible region of evaporation effect. Necessity of the improvement on cell components and instrumentation had been recognized to reduce the measurement noise and improve precise calorimetry.

Version up to ICARUS-2 system from ICARUS-1 system to measure near boiling region phenomena and to eliminate ambiguity by accuracy and precision, has been completed in Feb. 1995.

(3)Development of mass flow calorimetry system(FCS)

A mass flow calorimrtry to confirm the excess heat generation measurement in above 2 prior systems has been developed from middle 1994. Figure 5 shows the conceptual system flow of NHE- FCS. Although various electrolysis cell types are considerable, at the first step, fuel cell type electrolysis cells which is illustrated in figure 6, has been developed.

As a result of careful modification of the FCS components, fluctuation of flow rate of <0.5% and heat recovery rate of >98% has been attained .

On the other hand, mass flow calorimetry systems with a cell having recombiner which had been developedby SRI was also introduced and installed in NHE Laboratory in Mar. 1995.

5-2) Material analysis and material developments

Microstructural observations and analysis on various source Pd have been performed to compare and evaluate the material characteristics. Surface and inner microstructure using O/M and SEM, surface impurity analysis using AES, SIMS, and EPMA, and crystal structure analysis using XRD have been carried out for Pd electrodes. And also, chemical composition analysis of electrolytes using ICP-AES, ICP-MS and isotopic composition analysis using NMR have been conducted.

As a results of the analysis and observation, understandings of correlation among material characteristics such as exisistence of surface defects and impurities, effect of annealing and annealing conditions, D/Pd loading factors, have been deepened.

From the overall evaluation of excess heat measurement, material analysis , and loading rate, standardized Pd material specifications and treating processes have been proposed as follows;

1) Source Pd: Vacuum melting pure Pd (Typically >3 nine) and cold working uniformly

2) Processing: Machining surface layer(～0.2mm) to remove surface defects and impurities

3) Annealing: Annealing in high vacuum(<10^{-5} torr) environment at 850℃ after chemically etched

6. Perspectives

This FY1995 is the 3rd fiscal year from the start of NHE-Project, and about 15 monthes has been passedfrom the beginning of actual experimental works. The project is now at the most important and interesting stage. There are many issues to pursue and to clarify the correlation between the heat generation and material characteristics, and excess heat and nuclear products. From this view point, the domestic and international collaboration should be emphasized to conduct effective research and development of this new scientific field because isolated research effort has its limit in human and ideas, and financial resources.

Major activities to be conducted in FY1995 are as follows;

(1) Improvement of reproducibility for excess heat measurement in fuel cell type electrolysis systems with high loading material
(2) Reproduce Fleischmann & Pons Phenomena at nearly boiling point of electrolyte using ICARUS-2 systems.
(3) Confirmation of heat generation using both newly developed and SRI type mass flow calorimetry systems
(4) Material analysis and development to attain high loading and reproducibility, and development of in-situ X-ray diffraction measurement to investigate the crystallographic change during electrolysis.
(5) Development of reaction products detection systems and the measurement of γ -ray, tritium, and He etc. at high deuterium loading.

The NHE research activities will be reinforced by introducing of mass flow calorimetry and reaction productsdetection systems toward an interim review scheduled in late 1995.

7. Acknowledgement

New Hydrogen Energy Project has been supported by the Ministry of International Trade and Industry(MITI), and by New Energy and Industrial Technology Development Organization(NEDO). The authors would like to acknowledge those contracting parties and the persons concerned for their continuous support.

The authors are indebted to Prof. Okamoto, Prof. Ikegami, Prof. Takahashi, Prof. Ohta and all of NHE committees members for their guidance and valuable advices in promoting this NHE-Project.

The authors greatly appreciate to Prof. Fleischmann and Pons, Dr. McKubre and his collaborators, and Dr. Kunimatsu and his coworkers for supply their electrolysis systems to NHE-Laboratory and their continuous cooperation to the NHE-Project.

We would also like to thank all members of NHE-Centre and Laboratories for their collaboration and sincere research efforts.

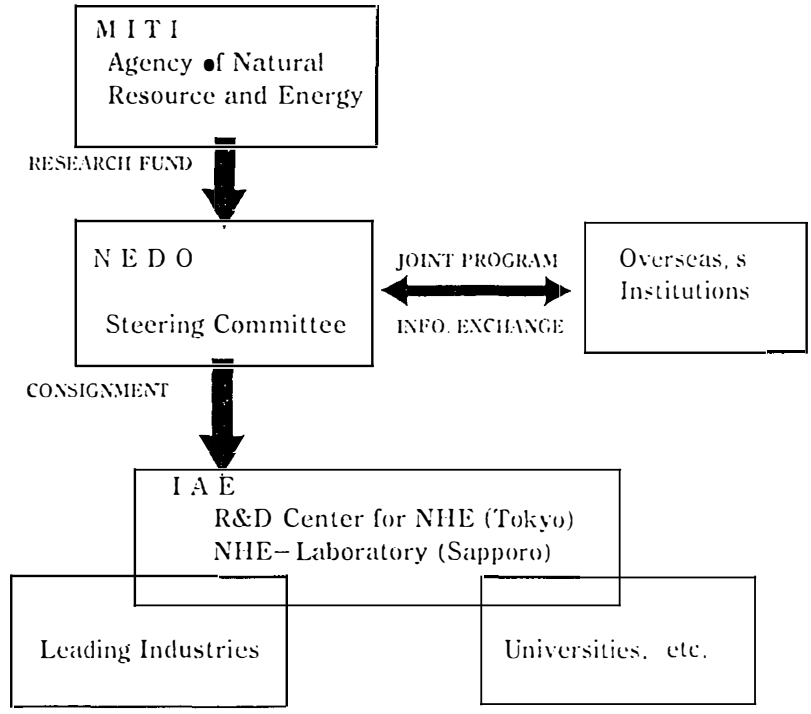

Figure 1 Organizational Structure of NHE Project

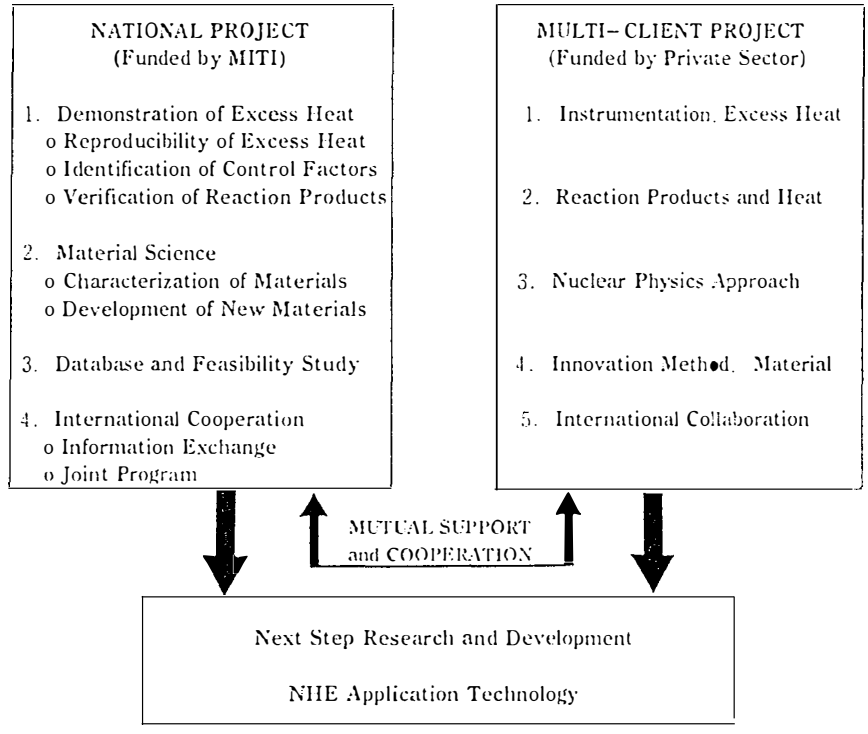

Figure 2. Framework of NHE Research and Development

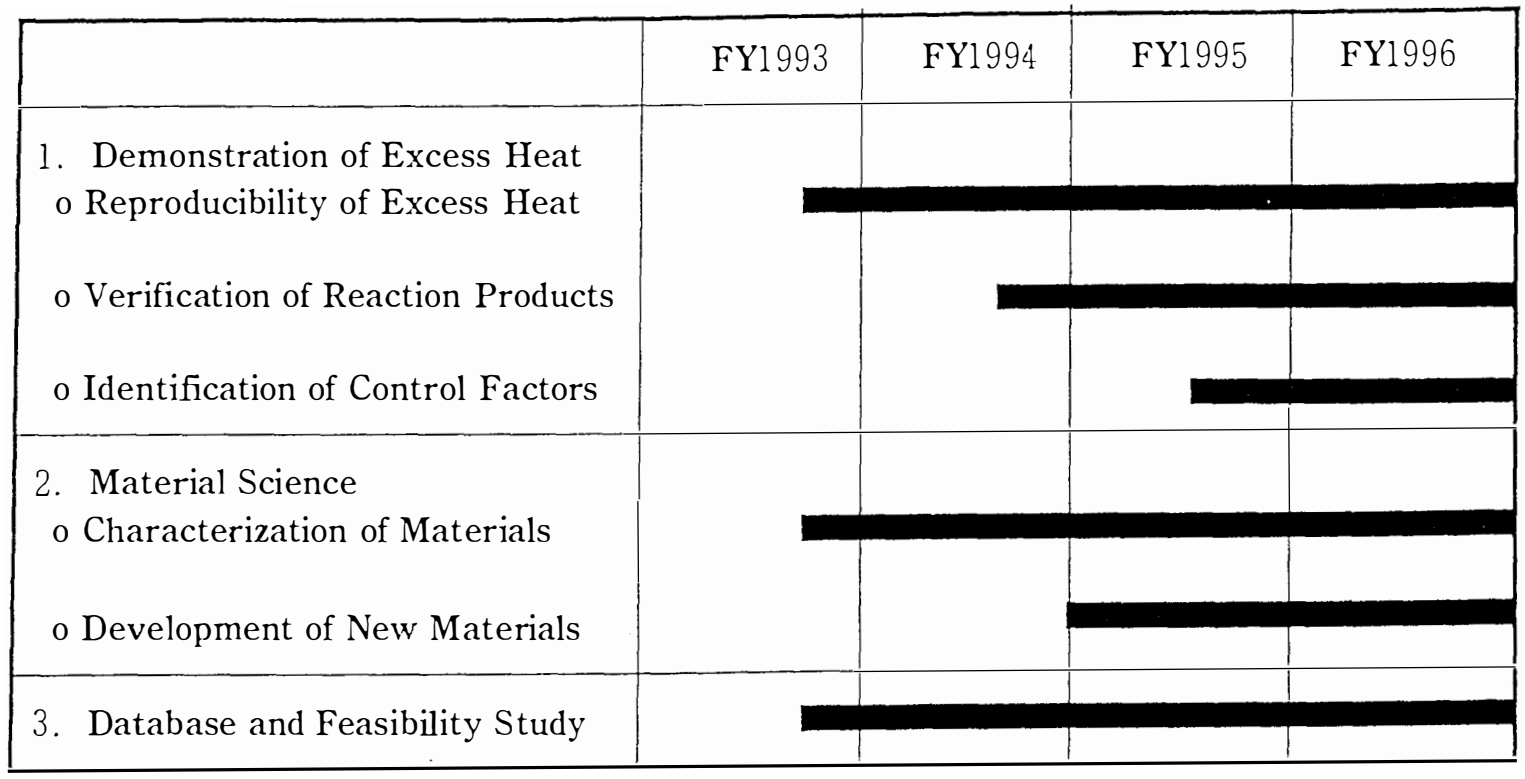

Figure 3 Master Schedule and R&D Items of NHE Project

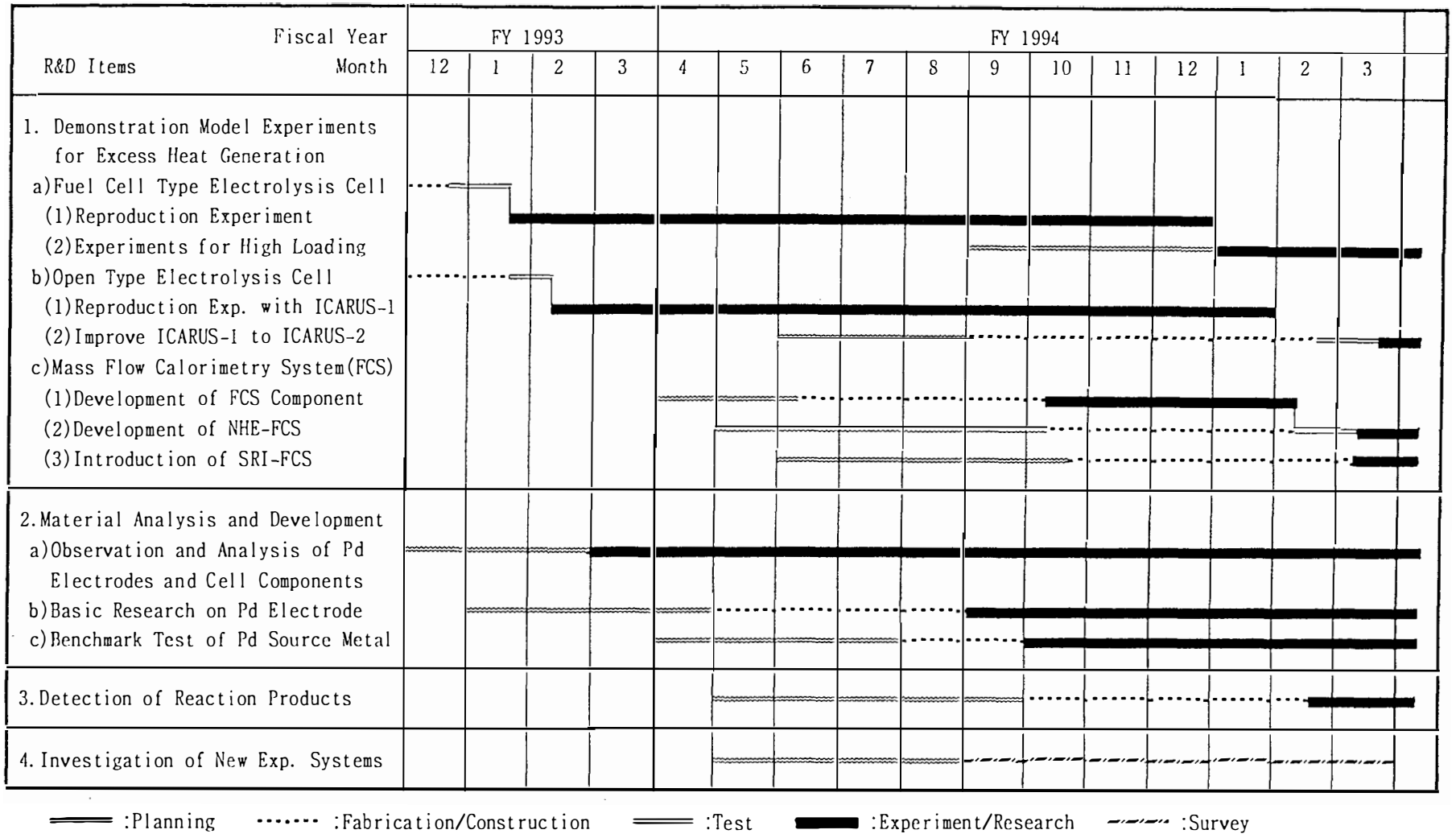

Figure 4. Milestone Chart of NHE R&D Items in FY 1993 and FY 1994

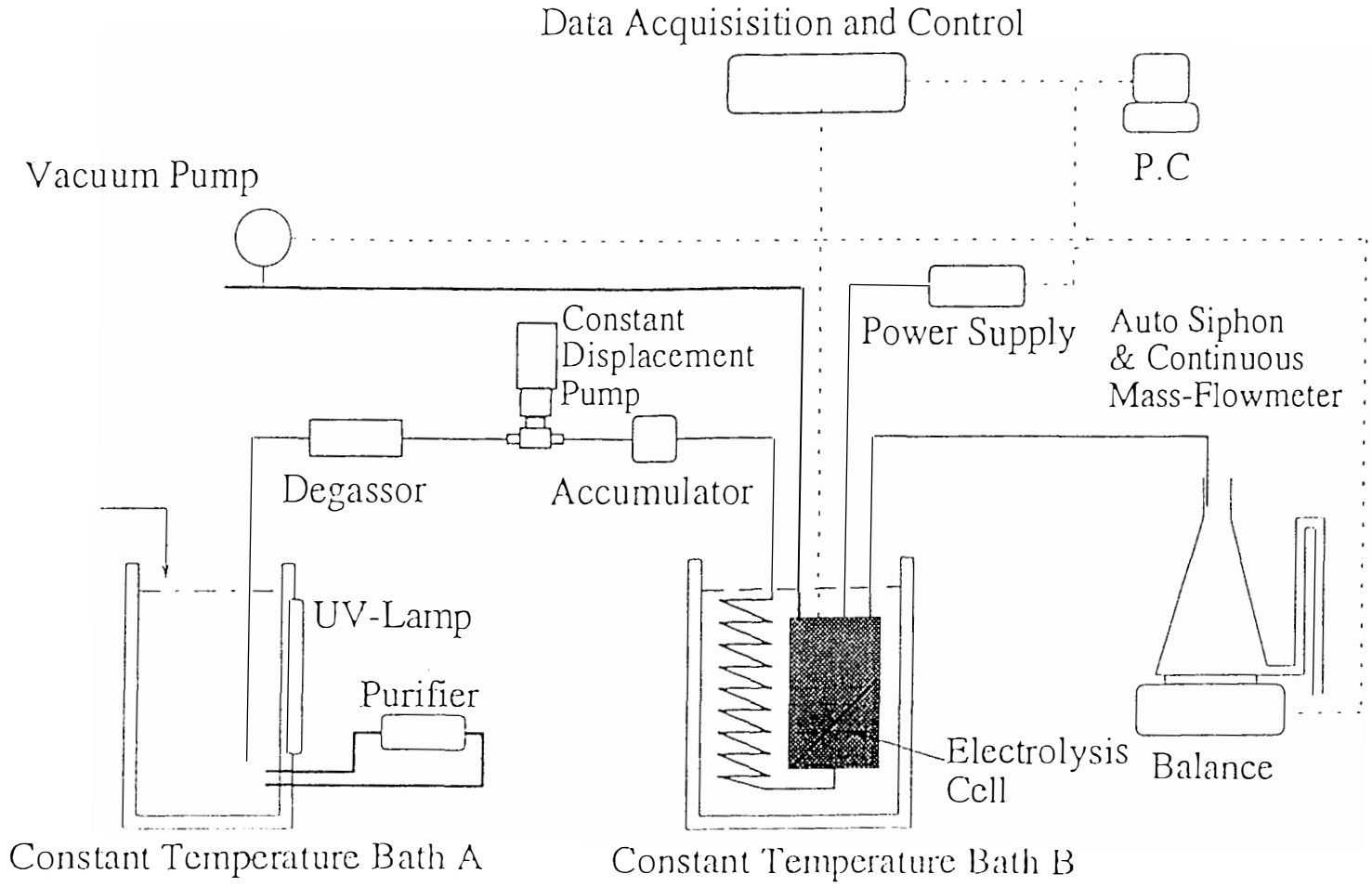

Figure 5. The Concept of Mass Flow Calorimetry System

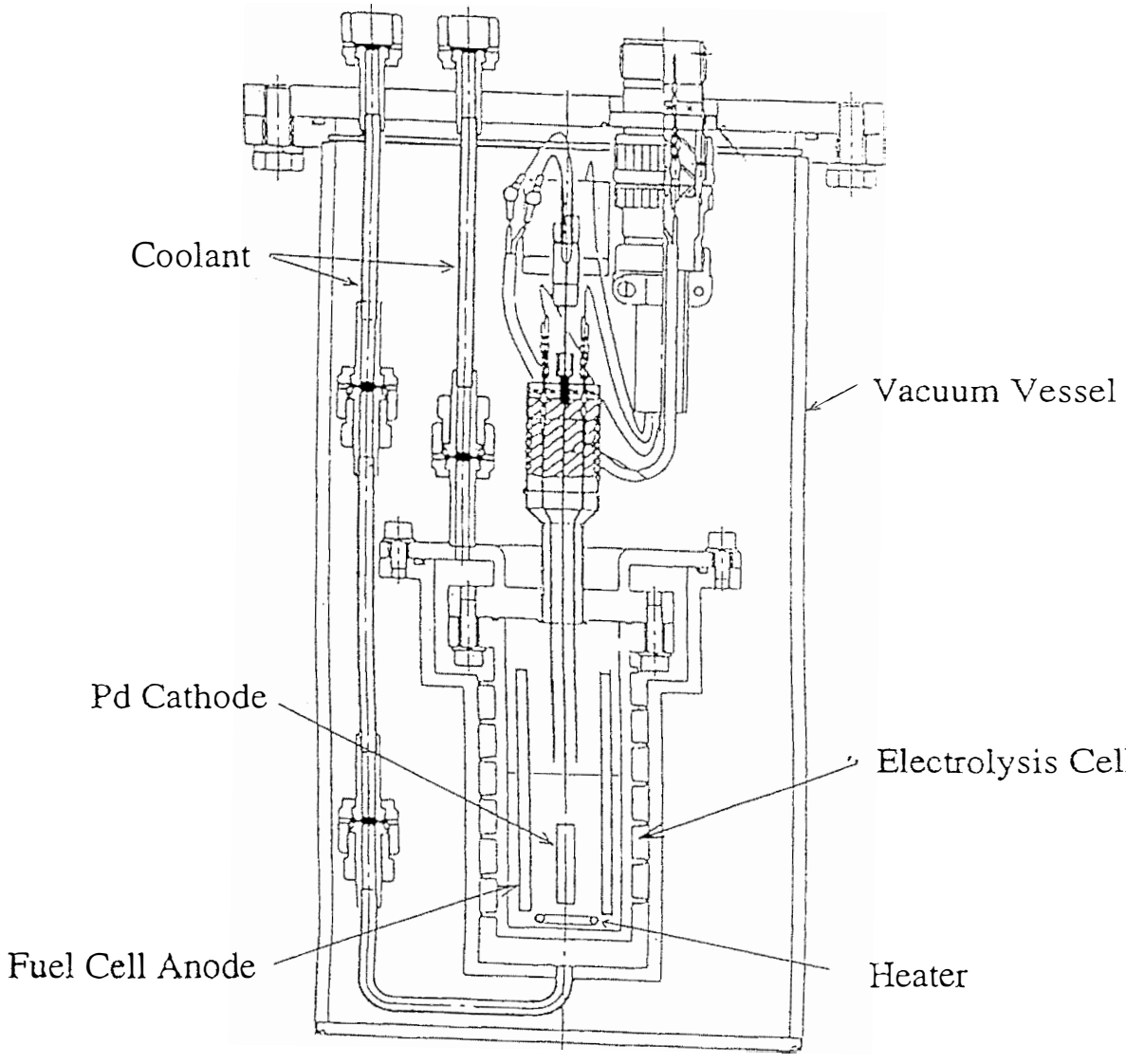

Figure 6. Schematic Figure of Fuel Cell Type NHE–FCS Cell

Fifth International Conference on Cold Fusion
9-13 April, 1995 - Monte Carlo, Monaco
ICCF5 ©1995

The Extraction of Information From an Integrating Open Calorimeter in Fleischmann-Pons Effect Experiments

Melvin H. MILES
Chemistry & Materials Branch, Research & Technology Division
Naval Air Warfare Center Weapons Division
China Lake, CA 93555-6001 USA

Abstract

Our first 5 months of investigating the Fleischmann-Pons effect in 1989 experiments produced no significant excess enthalpy. The November 1989 report of the Energy Research Advisory Board to the U.S. Department of Energy listed China Lake with MIT, Caltech, Harwell, and other laboratories as one of the groups not observing excess heat. Later experiments using palladium from another source (Johnson-Matthey), however, produced up to 30% excess power and 1,400 kJ of excess enthalpy. This amount of excess enthalpy is difficult to explain by any chemical reaction. Numerous experiments have shown that there is no recombination of the D_2 and O_2 electrolysis gases when fully-submerged palladium cathodes are used. Recombination can occur when palladium particles are exposed to the gas phase. In this case, our experiments prove that this recombination can be readily detected and easily corrected. In general, only about 20% of our experiments have produced measurable amounts of excess enthalpy. The cathode material used is apparently a major factor since successful experiments cluster around Johnson-Matthey supplied palladium.

1. Introduction

A previous paper has discussed the principles and problems of open isoperibolic electrochemical calorimetric systems (1). This includes the pronounced effect of the electrolyte level when the temperature is measured directly in the electrochemical cell (1,2). The measurement of the temperature in a secondary fluid or solid surrounding the cell provides an integration of the total cell power and minimizes the effect of the electrolyte level within the electrochemical cell itself.

2. Methods

Our first set of experiments in 1989 involved two different types of calorimetric cell designs: 1. the measurement of the temperature within the electrolyte of the cell and 2. the measurement of the temperature in a secondary compartment filled with H_2O and surrounding the cell (2). The second design providing an integrating open calorimeter proved to be more accurate (2). Both types of calorimeters were used in early 1989 experiments to investigate a palladium wire (Wesgo, d = 0.14 cm) and produced no evidence for any excess enthalpy production (2).

An improved calorimetry design involving temperature measurements by two thermistors (±0.01 K) rather than by a single thermometer (±0.05 K) evolved from these experiments as shown in Fig. 1. This calorimetric cell design and calibrations are reported in detail in previous publications (3,4).

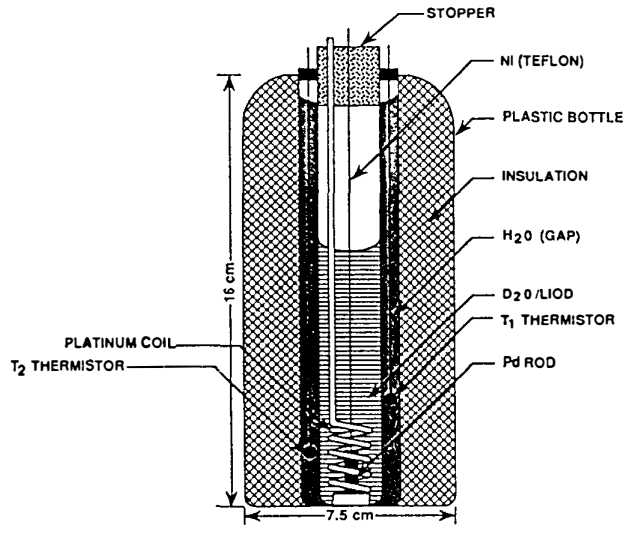

Figure 1. Electrochemical Calorimetric Cell Design.

A summary of general experimental procedures is given in Table I. Low currents (25-100 mA) are typically used for 7-10 days of electrolysis. The cell

Table I. General Experimental Procedures.

Electrodes
Pd polished with #600 silicon-carbide paper (dry)
Pd spot welded to 1 mm diameter Ni wire
Ni lead covered by shrink-Teflon
Epoxy used to mask spot-weld
Pt-coil counter electrode (symmetry important)
Cell
Pyrex glass test tubes (1.8 x 15 cm)
0.1 M LiOD (16 cm^3)
Rubber stopper sealed with silicon rubber
Calorimeter
Vermiculite and Styrofoam insulation (heat conduction)
Isoperibolic (constant surroundings)
Operations
Low currents (25-100 mA) used for 7-10 days
Cell temperatures usually 40-60°C (400-600 mA)

current is then increased to 400-600 mA that raises the cell temperature to about 40-60°C when 0.1 M LiOD is used. Any excess enthalpy will generally be measurable within 2-3 weeks of the start of the experiment. However, some experiments required 6 weeks of electrolysis before any excess enthalpy was detected. Most experiments (80%) failed to produce any significant excess heat effects. The excess power was generally in the range of 1-5 W per cm^3 of palladium. The design of any calorimetric experiment should consider the size of the palladium cathode and the expected magnitude of the excess power. This is illustrated by Table II for palladium rods of 1.5 cm lengths. The cathode size should be sufficient to yield an excess power effect that can be readily measured.

Table II. Excess Power as a Volume Effect
($P_X \approx 1$ W/cm^3).*
(Palladium rods length = 1.5 cm)

Diameter (mm)	Area (cm^2)	Px (W)
1	0.48	0.012
2	0.97	0.047
3	1.48	0.106
4	2.01	0.188
6	3.11	0.424
Caltech Study: V = 0.073 cm^3 (0.21 x 2.1 cm)		
MIT Study: V = 0.071 cm^3 (0.1 x 9 cm)		

* Must scale cathode to yield P_X of 3 σ or larger above calorimetric error. (NAWCWPNS, 1 $\sigma = \pm 0.020$ W).

3. Results

Our first set of experiments conducted over a 5-month period (April-September 1989) produced no significant evidence for any excess enthalpy production. For example, a palladium cathode (Wesgo, d = 0.14 cm) in D_2O-LiOD produced a ratio (X) of power out/power in of $X = 1.00 \pm 0.04$ while a platinum cathode control in a similar solution yielded $X = 0.97 \pm 0.06$ (2).

The early experiments at China Lake were listed in the Energy Research Advisory Board report to the U.S. Department of Energy as one of the groups not observing excess heat (5). The groups from MIT, Caltech, and Harwell also reported no evidence for excess heat (5) and discontinued their experiments after a few months of investigation. We continued to investigate other palladium samples and eventually observed significant evidence for excess enthalpy from the use of Johnson-Matthey palladium rods (3, 4). In fact, for electrodes cut from one particular palladium rod, 7 out of 8 experiments produced the excess enthalpy effect. The level of excess power observed in our experiments (1 W/cm^3 Pd) was very similar to that reported by Fleischmann and Pons for the current densities (100-200 mA/cm^2) that were used (3, 4, 6).

Most experiments have failed to produce any significant evidence for excess enthalpy production. A typical experiment producing no excess enthalpy is shown in Fig. 2. For the two cells run in series, the mean X-values were 0.993 ±0.014 for cell A and 0.982±0.022 for cell B. We have encountered long time periods lasting almost a year (January 1991 to December 1991) where no significant excess enthalpy was detectable. This makes progress very slow in this field. Approximately 20% of our experiments have produced significant levels of excess enthalpies.

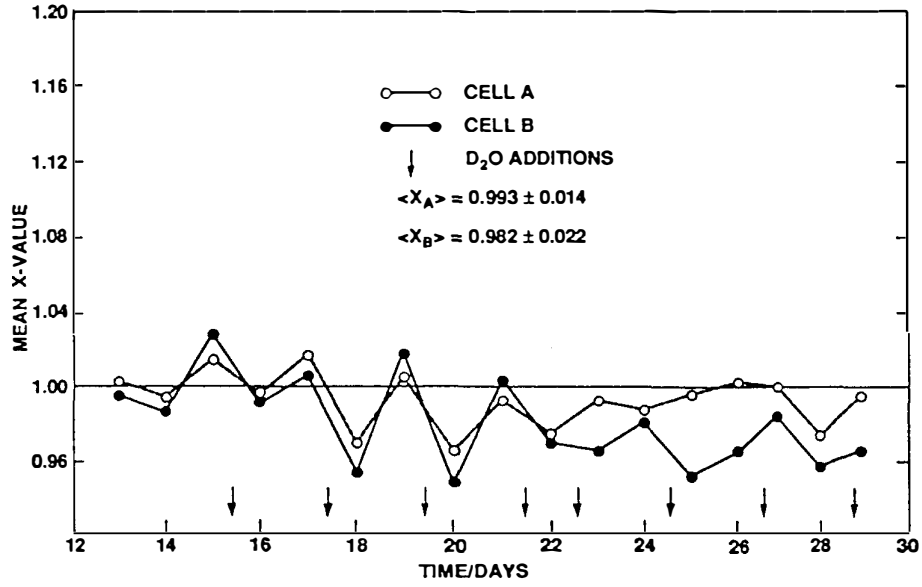

Figure 2. Calorimetric Studies Showing No Excess Power (3-19 August 1992)

Many experiments have proved that the recombination of D_2 and O_2 electrolysis gases does not occur to any significant level for experiments using a fully-submerged palladium cathode (4, 7). Some scientists, however, ignore this evidence and continue to claim that the excess heat effect can be explained by recombination (8). The extent of any recombination can be determined by measuring the rate of evolution of the $D_2 + O_2$ electrolysis gases (4). In addition, the volume of D_2O added to replenish the cell each day provides a secondary check of any significant recombination effect. We have never detected any significant recombination of the D_2 and O_2 electrolysis gases when fully-submerged palladium cathodes are used.

There are completely different types of electrolysis experiments where recombination can occur such as the co-deposition of palladium metal and deuterium from a D_2O-$PdCl_2$-LiCl solution onto a copper substrate. This method reported by Szpak et al. (9) provides for a high-purity palladium deposit that is simultaneously loaded with deuterium. However, this palladium deposit is often dendritic in nature, hence the palladium becomes detached from the electrode, floats in the solution, and adheres to the cell wall above the D_2O electrolyte level. This

finely-divided palladium acts as an excellent catalyst for recombination and sometimes yields loud explosions. Recombination in the gas phase is quite likely in this co-deposition experiment. The extent of this recombination can be readily determined by measuring the current efficiency (γ) for the D_2O electrolysis. This is determined by the rate of evolution of the $D_2 + O_2$ electrolysis gases. The resulting γ can be easily applied to the calorimetric equations (1) to correct for any apparent excess enthalpy produced by recombination .

A typical co-deposition experiment where significant recombination occurs is shown in Fig. 3. The apparent excess power reaching levels up to 18% could be readily corrected for recombination by the simultaneous measurement of the rate of evolution of the $D_2 + O_2$ electrolysis gases used to determine the current efficiency (γ). The corrected values for X were then close to unity, and the overall ratio of power out/power in was $X = 1.0005 \pm 0.022$; i.e., no significant excess power was observed after applying the correction for recombination. The results in Fig. 3 show that recombination can be readily detected and easily corrected.

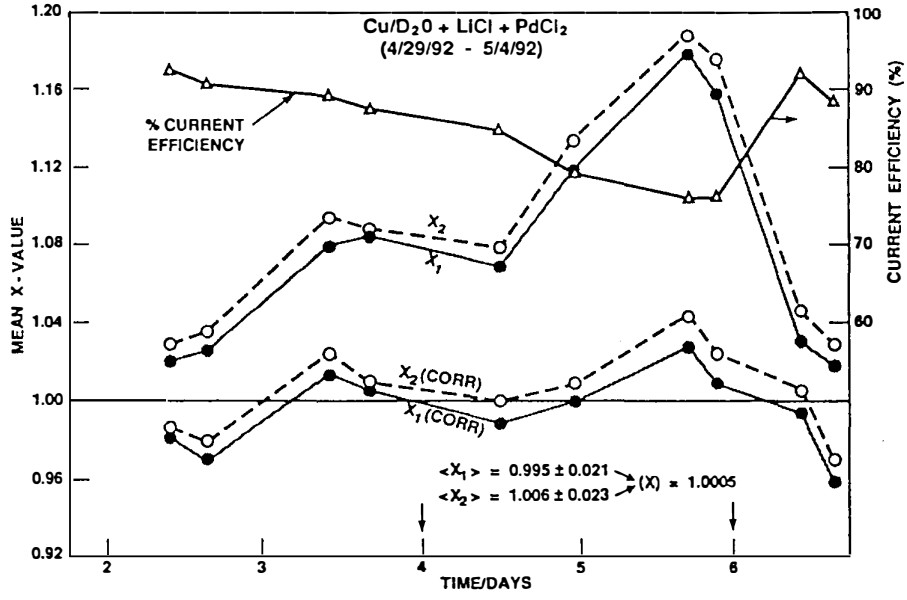

Figure 3. Effect of Deuterium-Oxygen Recombination in a Palladium Deposition Experiment.

Table III presents the total excess enthalpy observed in various experiments. These values range from 248 kJ for the shortest excess enthalpy period (11 days) up to 1,400 kJ for the longest period of excess heat (83 days). The complete combustion of all palladium within the cell to PdO and all the absorbed deuterium to D_2O would only yield about 6-7 kJ for the mass of palladium used (4.3 g). Thus chemical reactions cannot explain the total excess enthalpy that was measured. There was also evidence for ^4He production in the 1990, 1991, and 1993 experiments (4, 10, 11).

Table III. Total Excess Enthalpy in Various Experiments.

Year	Cathode	Excess enthalpy	Days/cell	Comments
1989	JM Pd (6.35 mm)	210 kJ	26/B	
1989	JM Pd (6.35 mm)	220 kJ	26/A	
1989	JM Pd (6.35 mm)	300 kJ	38/A	
1990	JM Pd (6.35 mm)	1,400 kJ	83/A	Helium, glass flasks, U or Texas
1991	JM Pd (6.35 mm)	48 kJ	11/B	Helium, glass flasks, Rockwell
1993	JM Pd (1 mm)	290 kJ	66/B	Helium, metal flasks, DOI[a]

$$2\ Pd_2D + 5/2\ O_2 \rightarrow 4\ PdO + D_2O,\ \Delta H = 6.2\ kJ \text{ for } 4.3\ g\ Pd$$

[a] Helium analysis by Department of Interior Laboratory, Amarillo, Texas.

4. Discussion

The palladium material used in the Fleischmann-Pons effect experiments seems to play a major role in the success rate. Some palladium sources yield a high ratio of experiments that produce excess enthalpy while other palladium sources yield no excess enthalpy in any experiments.

Table IV provides a summary of China Lake experiments for various sources of palladium. The diameter (d) and volume (V) of the palladium cathode is also shown. The first three sources (JM, F/P, JM) are all Johnson-Matthey palladium and yield a combined success rate of 12 out of 17 experiments. Many other palladium sources produce no experiments that show the Fleischmann-Pons excess enthalpy effect. This polarization of successful experiments would be very difficult to explain by random errors. These results indicate that the metallurgical preparation of the palladium is a major factor for observation of the excess enthalpy effect. Possible variables include the palladium metal grain size and the levels of impurities.

The small amount of palladium used in the co-deposition experiments would yield only 2 mW of excess power at 1 W/cm^3 of palladium. This small level of excess power would not be detectable by our calorimetry. Two of the 34 experiments, however, produced significant excess power levels that remained even after correcting for recombination. Excess enthalpy, tritium production, and the presence of some form of radiation has been reported for co-deposition experiments (9).

Table IV. Palladium Materials (March 1994 Summary).

Source[a]	d (cm)	V (cm^3)	P_x/V (W/cm^3)	Success ratio
JM	0.63	0.36	1.3	9/14
F/P	0.20	0.038	1.6	2/2
JM	0.10	0.016	2.5	1/1
Tanaka (Japan)	---	0.05	1.2	1/3
JM	0.40	0.20	0	0/1
IMRA (PdAg)	0.40	0.20	0	0/1
NRL	0.40	0.25	0	0/4
JD	---	0.04	0	0/2
Pd/Cu	(0.63)	0.02	0	0/2
Wesgo (1989)	0.14	0.09	0	0/6
Co-Deposition (1992)	(0.63)	0.002	75	2/34

[a] JM = Johnson-Matthey, F/P = Fleischmann/Pons, NRL = Naval Research Laboratory, JD = John Dash, Pd/Cu = palladium-plated copper.

5. Conclusions

Our experiments show that the patience to continue experiments over long time periods is essential to observing the excess enthalpy effect reported by Fleischmann and Pons. Our 1989 results were very similar to the reports by Caltech, Harwell, and MIT , and others over the April-September time period, i.e., no excess heat was detected. The major difference is that we continued to investigate palladium from other sources and eventually observed significant excess enthalpy production. The ratio of successful experiments, nevertheless, remains low. Apparently, some metallurgical property of palladium is a major factor for producing the Fleischmann-Pons effect.

Acknowledgments

The assistance of ONT/ASEE postdoctoral fellows was essential for our program. These postdoctoral fellows are Drs. D. E. Stilwell, K. H. Park, G. S. Ostrom, B. F. Bush, and K. B. Johnson. The assistance and encouragement of Dr. Richard A. Hollins was also appreciated. The author thanks his son, David L. Miles, for his computer analysis of the experimental data.

References

1. Miles, Bush, and Stilwell, "Calorimetric Principles and Problems in Measurements of Excess Power During Pd-D_2O Electrolysis," *J. Phys. Chem.*, **98**, 1948 (1994).
2. Stilwell, Park, and Miles, "Electrochemical Calorimetric Studies on the Electrolysis of Water and Heavy Water (D_2O)," *J. Fusion Energy*, **9**, 333 (1990).

3. Miles, Park, and Stilwell, "Electrochemical Calorimetric Evidence for Cold Fusion in the Palladium-Deuterium System," *J. Electroanal. Chem.*, **296**, 241 (1990).
4. Miles, Hollins, Bush, Lagowski, and Miles, "Correlation of Excess Power and Helium Production During D_2O and H_2O Electrolysis Using Palladium Cathodes," *J. Electroanal. Chem.*, **346**, 99 (1993).
5. Landis and Huizenga, "Cold Fusion Research—A Report of the Energy Research Advisory Board to the U.S. Department of Energy," November 1989, pp. 11-14, DOE/S-0073 (1989).
6. Fleischmann, Pons, Anderson, Li, and Hawkins, "Calorimetry of the Palladium-Deuterium-Heavy Water System," *J. Electroanal. Chem.*, **287**, 293 (1990).
7. Storms, "Review of Experimental Observations About the Cold Fusion Effect," *Fusion Technol.*, **20**, 433 (1991).
8. Jones, Hansen, Jones, Shelton, and Thorne, "Faradaic Efficiencies Less Than 100% During Electrolysis of Water Can Account for Reports of Excess Heat in Cold Fusion Cells," *J. Phys. Chem.* (in press).
9. Szpak, Mosier-Boss and Smith, "On the Behavior of Pd Deposited in the Presence of Evolving Deuterium," *J. Electroanal. Chem.*, **302**, 255 (1991).
10. Miles, Bush, and Lagowski," Anomalous Effects Involving Excess Power, Radiation, and Helium Production during D_2O Electrolysis Using Palladium Cathodes," *Fusion Technol.*, **25**, 478 (1994).
11. Miles and Bush, "Heat and Helium Measurements in Deuterated Palladium," *Fusion Technol.*, **26**, 156 (1994).

Fifth International Conference on Cold Fusion
9-13 April, 1995 - Monte Carlo, Monaco
ICCF5 ©1995

Studies on Fleischmann-Pons Calorimetry with ICARUS 1

Toshiya Saito, Masao Sumi, Naoto Asami, and Hideo Ikegami*
New Hydrogen Energy Laboratory , The Institute of Applied Energy
3-5 Techno Park 2, Shimonopporo, Atubetu-ku, Sapporo 004, Japan

*National Institute for Fusion Science, Nagoya 464-01, Japan
(Presented at ICCF5, Monaco; April 10 - 13, 1995)

Abstract

The Fleischmann-Pons calorimetry (FPC) is examined with the ICARUS 1 system, which is identical to the original cells which they designed for their calorimetry. In the present experimental studies, a critical evaluation is made of their original method (FPC) and a modified version of FPC is proposed. Its usefulness and validity is experimentally examined by detecting and regenerating artificial heat pulses regarded as heat excess.

1. Introduction

The calorimetry which M. Fleischmann and S. Pons developed and have used with their cold fusion cells has been considered to determine the absolute power of heat excess, without any degradation of the time response caused by the heat capacity of the system. Their method depends entirely upon a mathematical analysis of the heat balance equation which is designed for their electrochemical calorimetry[1]. The method may be applied to various calorimetric systems other than electrochemical cells. The validity of their method has, however, seemingly not well been accepted, a possible reason of which will be discussed later on, in particular concerning their claim of excess heat from cold fusion.

Controversy on the Fleischmann-Pons Calorimetry (FPC) centers on the effective radiative heat transfer coefficient (k_R). With any electrochemical calorimetry, when temperatures are measured, the temperature inhomogeneity in the cells is always a matter of great concern, and is normally observed in the present experiments to be less than a percent. With the FPC method, the temperature inhomogeneity, as well as conductive heat losses, is automatically woven into the effective radiative

heat transfer coefficient (k_R) in the process of its determination. In their papers Fleischmann and Pons give a detailed description of their calorimetry; however, it is not clear how they actually estimated excess heat production. They seem to be too concerned with the precise determination of k_R to the exclusion of other factors. This leads one to wonder, on analyzing actual experimental data, how accurately and precisely the heat excess can be detected by' their method, with the use of such a carefully determined k_R.

This is the context, in which the evaluation was made on FPC with the ICARUS 1 system (Fig.1), which was installed in February 1994 at the New Hydrogen Energy (NHE) Laboratory in Sapporo, in a close collaboration with Dr. S. Pons, IMRA Europe S. A..

2. The Principle of Fleischmann-Pons Calorimetry (FPC)[1]

Their basic power balance equation determines the cell temperature θ, which is the temperature of the electrolyte in the cell, to be given by

$$MC\frac{\partial\theta}{\partial t} = E - H + Q - k_R\left(\theta^4 - \theta_{bath}^4\right) \qquad (1)$$

where CM is the heat capacity, E denotes the ohmic part of the electric power input, H gives the enthalpy carried away by the gas stream consisting of water vapor and electrolysis products. Any other generated heat in the cell is given by' Q, and the last term represents radiative heat losses from the cell to the surrounding bath water across the vacuum gap of the Dewar in the unsilvered lower part of the cell (Fig.1), where k_R is the effective radiation heat transfer coefficient into which any other unknown heat losses, positive or negative, are considered to be woven. With the Dewar cell structure employed in the present experiments, conductive losses are assumed to be negligibly' smaller than the radiative loss, but they do influence k_R, as will be discussed in the later section.

There are two unknowns in Eq.(1), namely MC and k_R, which can be simultaneously determined experimentally by introducing a square test heat pulse into the cell. Integrating Eq.(1) from the front time (t = 0) of the square heat pulse input (ΔQ) to the time t and rearranging it with respect to MC and k_R, we will obtain the following equation.

$$\frac{\int_0^t (E - H + \Delta Q)\, dt}{\int_0^t (\theta^4 - \theta_{bath}^4)\, dt} = k_R + CM \frac{\theta(t) - \theta(0)}{\int_0^t (\theta^4 - \theta_{bath}^4)\, dt} \qquad (2)$$

It will be easily seen that using two quantities, X (t) and Y (t), defined by

$$X(t) = [\,\theta(t) - \theta(0)] \Big/ \int_0^t (\theta^4 - \theta_{bath}^4)\, dt \qquad (3)$$

$$Y(t) = \int_0^t (E - H + Q)\, dt \Big/ \int_0^t (\theta^4 - \theta_{bath}^4)\, dt \qquad (4)$$

we can rewrite Eq.(2) as

$$Y(t) = k_R + CM\, X(t). \qquad (5)$$

At each time of t, Y (t) and X (t) are calculated to show a linear relation as given by Eq. (5), where the slope indicates the heat capacity, CM, and the intercept of the linear line on the Y axis gives the effective radiative heat transfer coefficient, k_R.

Inserting the values of MC and k_R, thus determined, into Eq.(1), we can obtain the heat generation Q (t) in the cell simply by rewriting Eq.(1) as

$$Q(t) = CM \frac{d\theta}{dt} - E(t) + H(t) + k_R \{\theta(t)^4 - \theta_{bath}^4\} \qquad (6)$$

Now, if we artificially assume that no excess heat is generated within the cell under the condition where the excess heat is actually present, i.e. with Q(t) > 0, the "imaginary" radiative heat transfer coefficient (denoted by k_{R1} hereafter) should be observed to be smaller than the "real" radiative heat transfer coefficient (denoted by k_{R2}). Then the excess heat must be given by

$$Q(t) = (k_{R2} - k_{R1})\{\theta(t)^4 - \theta_{bath}^4\} \quad (7)$$

The problem is how the "real" radiative heat transfer coefficient $k_{w)}$ can be determined. For this, Fleischmann and Pons use the following technique. At time t = - 0, just before the test heat pulse is applied, they assume that Eq.(1) should satisfy the following condition,

$$\left[CM\frac{d\theta}{dt}\right]_{t=0} = 0 = E(0) - H(0) - k_{R2}\{\theta(0)^4 - \theta_{bath}^4\} + Q_f \quad (8)$$

Putting $Q = Q_f + \Delta Q$ in Eqs.(1) and (8), where Q_f denotes unknown heat excess, and integrating Eq.(1) in time from the front time (t = 0) of the test heat pulse, ΔQ, we will obtain the following expression for k_{R2}, by canceling Q_f in combination with Eq.(8) with the assumption that $Q_f(t)$ is constant.

$$k_{R2} = \frac{\int_0^t [\{E(t) - E(0)\} - \{H(t) - H(0)\}]\,dt - CM\{\theta(t) - \theta(0)\} + \Delta Qt}{\int_0^t \{\theta(t)^4 - \theta(0)^4\}\,dt} \quad (9)$$

where ΔQ is also constant in the time period [0, t]. Putting the thus determined k_{R2}, into Eq.(7) together with k_{R1} determined by Eq.(2), one should be able to detect the averaged excess heat Q_f, only in each time period during which the test heat pulse is applied, under the further assumption that the excess heat Q_f is constant in time, — something which would be difficult to tell.

3. Experimental Evaluation of FPC

In the present experiments, efforts were made first to determine both k_{R1} and k_{R2} with a platinum rod cathode (2ø) x 12.5 mm) electrolyzing 0.1 M LiOD electrolyte in the identical cell (Fig.1) as used and operated by Pons and Fleischmann, which they named ICARUS 1. Since there would be no so-called excess heat anticipated in this blank experiment with the use of the platinum cathode, we should expect $k_{R1} = k_{R2}$, and the difference between them is considered to give a measure of errors, that is, a minimum detectable amount of heat output. Normally in the present experiment, those radiative heat transfer coefficients, determined by the method described in the previous section, were observed to scatter to give $|k_{R1} - k_{R2}|/k_{R2} = 10\%$ as shown in Fig.2. A minimum detectable power may be estimated from

$$\delta Q = \delta k_R \, T_{bath}^{\,4}$$

to be unexpectedly as large as approximately ± 0.3W, since the principle assumes the radiative heat loss to be a dominant loss. The main error source was found to be generated in the process of determining k_{R2} as would be anticipated from its way of deduction with Eq.(9).

Furthermore, as also shown in Fig. 2, another serious problem is found in the fact that in some cases k_{R1} was estimated to be larger than k_{R2}, which should not occur by any means according to their definition, unless Q(t) is negative, so that this casts a doubt on the validity of FPC.

After careful analysis of the FPC method, we had to devise our own alternative method of calorimetry by modifying FPC. Our method examines how the test heat pulse is regenerated, which could then be regarded as a pulse of artificial heat excess. This entails using an MC and k_R that have been predetermined by another test heat pulse in the manner described in the previous section [Eqs.(2) - (5)], that is, aside from FPC, what validity Eq.(6) would have in detecting the excess heat with the use of an MC and k_R, which have been predetermined under an assumption that no heat excess is then present. Should there already exist any unknown heat excess in the base line, it will not be directly detected by this method; however, the regenerated test heat pulse will be observed as a heat pulse with a smaller amplitude, since k_R then will have been estimated to be a smaller value than the "real" radiative heat transfer coefficient for $Q_f = 0$.

With the use of our modified method, each test heat pulse of 0.25W was detected and regenerated as a heat pulse of 0.25 ± 0.002 W, as shown in Fig.3, for all 5 test pulses over 10 days of continuous electrolytic operation at 200 mA with a cathode rod (21) x 12.5 mm) of $Pd_{90}Ag_{10}$. Those values, $k_R = 0.7706 \times 10^{-9}$ W/K⁴ and MC = 490.0 J/K, were determined at the time of 2×10^5 seconds from the initiation of the electrolysis. The upward and downward spikes at the both edges of every regenerated pulse indicate errors due to MC dθ/dt , that is, combined errors in determining both MC and dθ/dt.

At the initiation of the electrolysis, a triangular decay of heat output may indicate the absorption heat of deuterium into the palladium cathode. One may also claim that some excess heat at a level of 10 mW was continuously generated during the period of 2.7×10^5 seconds (from 1×10^5 to 3.7×10^5 seconds), where the integrated heat excess amounted to 2.7 kJ, or 94.3 kJ / cm³. This sort of excess heat generation may be overlooked by FPC which uses k_{R1} and k_{R2}, to detect an averaged heat excess only during the period of test heat pulses. However, such amount of heat excess as in the

level of 10 mW can be explained by a possible recombination of diffused deuteriums onto the anode surface. The observed power of 10 mW amounts to approximately 3% of the power spent to electrolyze the heavy water ($E_{\text{thermoneutral potential}} \times I$), which is estimated in the present case to be ~300 mW. This power has been taken care of in Eci.(1) by subtracting it from the total electric power input to leave only the ohmic power as denoted by E, however, the recombination (oxidization) has been neglected.

Repeated downward spikes indicate cooling (approximately - 300 J), by a supply of heavy water (approximately 4 cc) every 48 hours (172,800 sec.) of electrolysis and evaporation, at 200 mA. The spikes at the edges again indicate errors from the first term in the right hand side of Eq.(6), that is, combined errors in determining both MC and $d\theta/dt$.

A repeated change of slope in the base line in each period between the water filling time, indicates a change of k_R influenced by a change in conductive heat losses which have not been taken into consideration in Eq.(1). As the water decreases due to the electrolysis and evaporation, the water level descends and the distance of heat conduction through the glass wall, i.e. the distance from the electrolyte surface to the top of the cell increases, which turns out to suppress the conductive heat transfer, and there appears a periodic apparent heat generation. With the electrolytic currents of 400mA, the rate of descent of the water- surface level is faster than in the case of 200 mA, showing a larger apparent heat generation, with a steeper slope of sawtooth in the base line, as shown in Fig.4.

When the electrolytic currents increased from 200 mA to 400 mA, an additional change was observed that the base line stepped down by 0.07 W as also shown in Fig.4, as if a heat sink appeared in the cell. This could be explained as being caused either by lifting of the electrolyte surface level associated with a volume increase due to deuterium gas bubbles produced in the electrolyte, or by a voltage drop in the thin lead wire (0.25 mmø) of platinum to the cathode. Both are estimated to come in the same order of magnitude, sufficient to explain the loss of 70 mW, which is the amount of the base line down shift that was observed to be proportional to the electrolytic currents. In order to perform a proper calorimetry, the effective radiative heat transfer coefficient k_R must be re-estimated at each critical point such as when the electrolytic currents are changed. When the electrolyte boils, the surface level will change rather violently and the present method cannot be applied anymore.

Taking into consideration this experimental evaluation, we can claim that our modification of the FPC method makes it possible to detect any heat excess, by simply determining Eq.(6) with a properly determined k_R. With our modified method, we could easily detect any positive / negative amount of heat excess above approximately 30 mW over longer than a two month period, with the continuous use of the same k_R which has been determined at the initial stage of the electrolysis, when we could assume there to be no heat excess present. More precisely we may be able to claim from Fig.3 that

the power detectability with this method, under a low constant current operation, is better than a few mW during the first 10^6 seconds (approximately 10 days) after the determination of k_R.

4. Conclusion

The Fleischmann-Pons calorimetry (FPC) was examined with the ICARUS 1 system, which is identical to the original cells which they designed for their calorimetry. In our present experiments, their original method (FPC) could not reveal any satisfactory detectability to meet our expectation.

The most serious problem of FPC was found that in some cases k_{R1} was estimated to be larger than k_{R2}. This should not occur by any means according to the principle of the FPC method.

Our modified version of FPC proposes to use the basic power balance equation, Eq.(1), and to estimate any heat excess with the use of an MC and k_R which have been predetermined in the earlier stage of the electrolysis under an assumption that no heat excess was present. The validity of our method is confirmed by regenerating a test heat pulse of 0.25W regarding it as an artificial heat excess. It was detected and regenerated as a heat pulse of 0.25 ± 0.002 W for all 5 test heat pulses over 10 days of continuous electrolytic operation.

Our modified method of FPC could detect any excess heat, exceeding 30 mW under a low constant current operation for over a two month period with a continuous use of the same k_R, which was determined at the initial stage of the electrolysis, assuming that no heat excess was generated then. More precisely, the method was confirmed to show a power detectability as good as a few mW during the first 10^6 seconds (approximately 10 days) from the time of determination of k_R.

The authors would like to acknowledge Dr. Stanley Pons and Dr. Martin Fleischmann for their cooperation and valuable suggestions in operating the ICARUS 1 system at the NHE laboratory, in Sapporo, Japan.

Reference

(1) M. Fleischmann and S. Pons, Phys. Letters A 176 (1993) 118

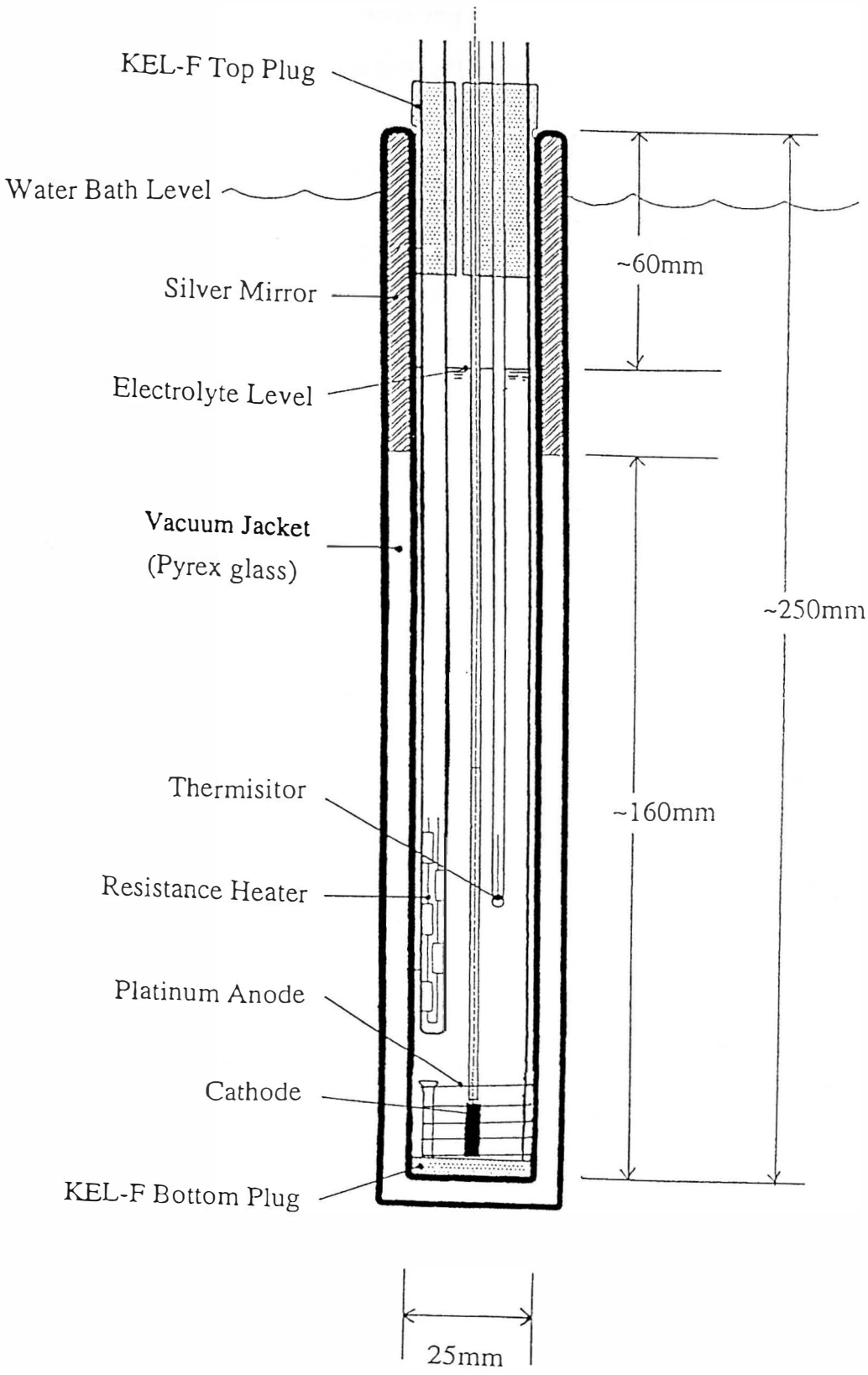

Fig. 1 Fleischmann - Pons Type Open Cell

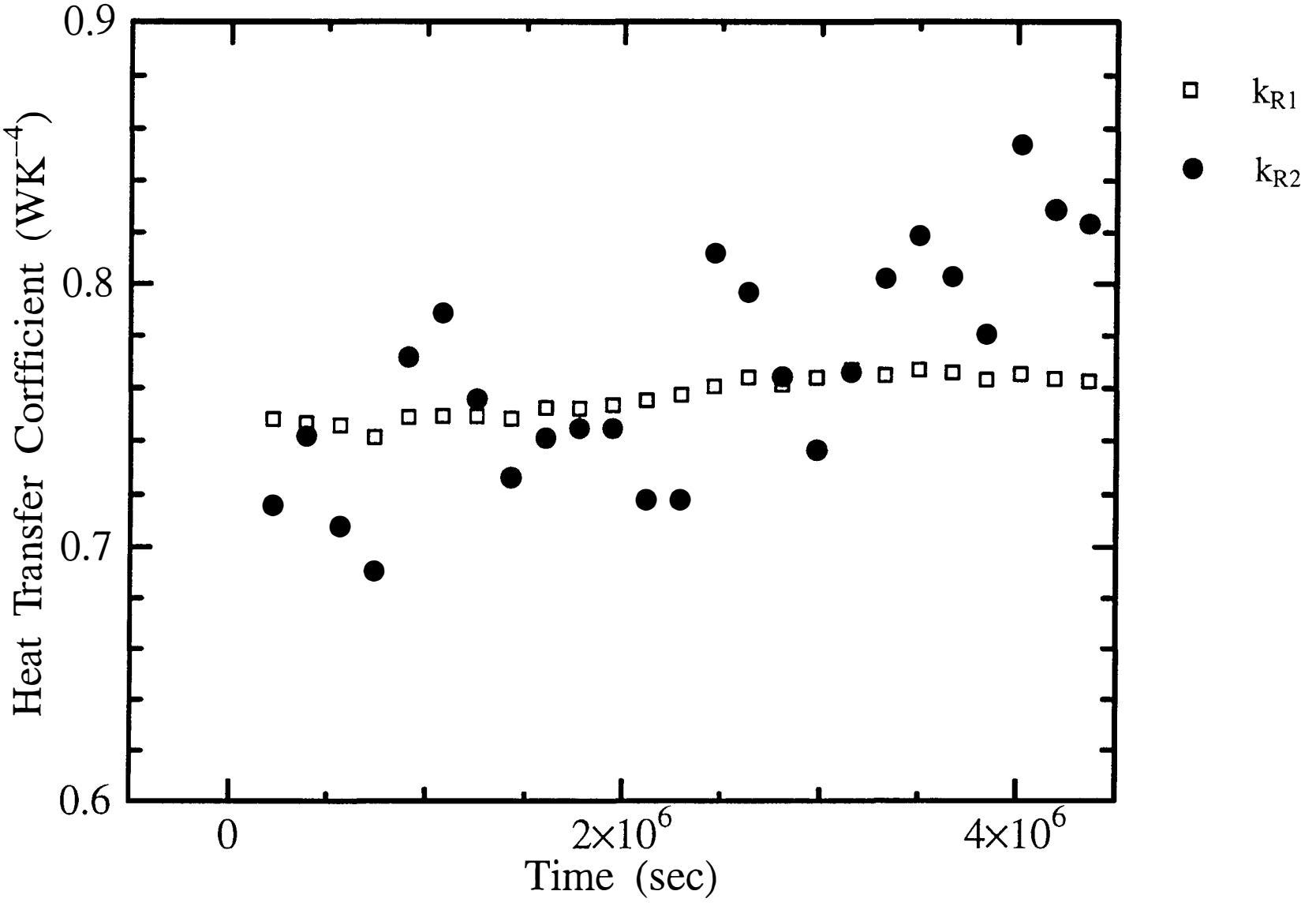

Fig.2 Heat Transffer Coefficient of exp.4711
Electrode : Pd (J/M Bt.8023 ϕ 2x12.5) Electrolyte : 0.1M LiOD

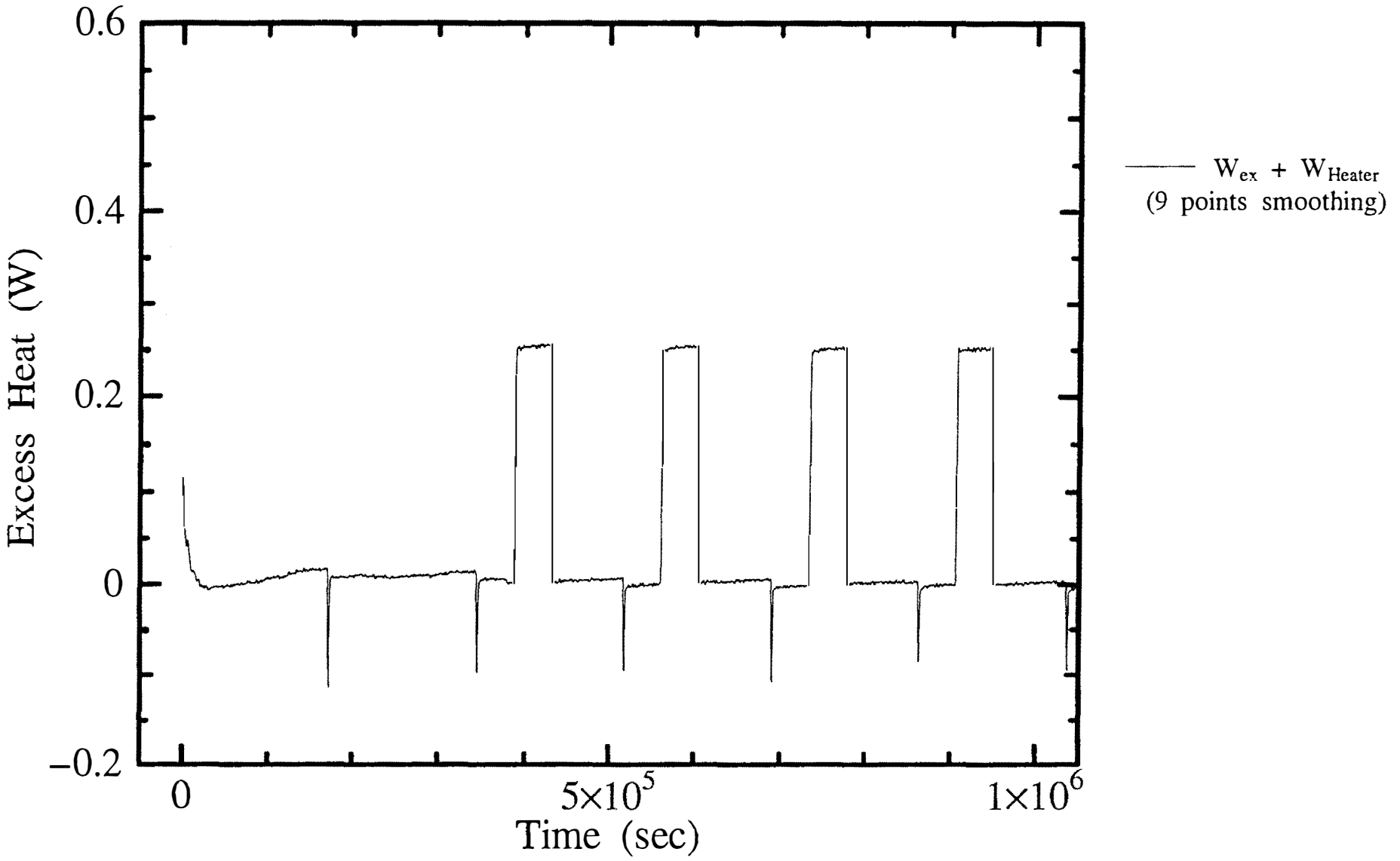

Fig.3 Change of Excess Heat (include Heater Input) of exp.4251

Heater inputs are reproduced as square pulses.
Electrode : 10%Ag–Pd (J/M Bt.0.549 ϕ 4x12.5) Electrolyte : 0.1M LiOD
k_R = 0.7706x10^{-9} (WK^{-4}), CM = 490.0 (J/K), W_{Heater} = 0.2506

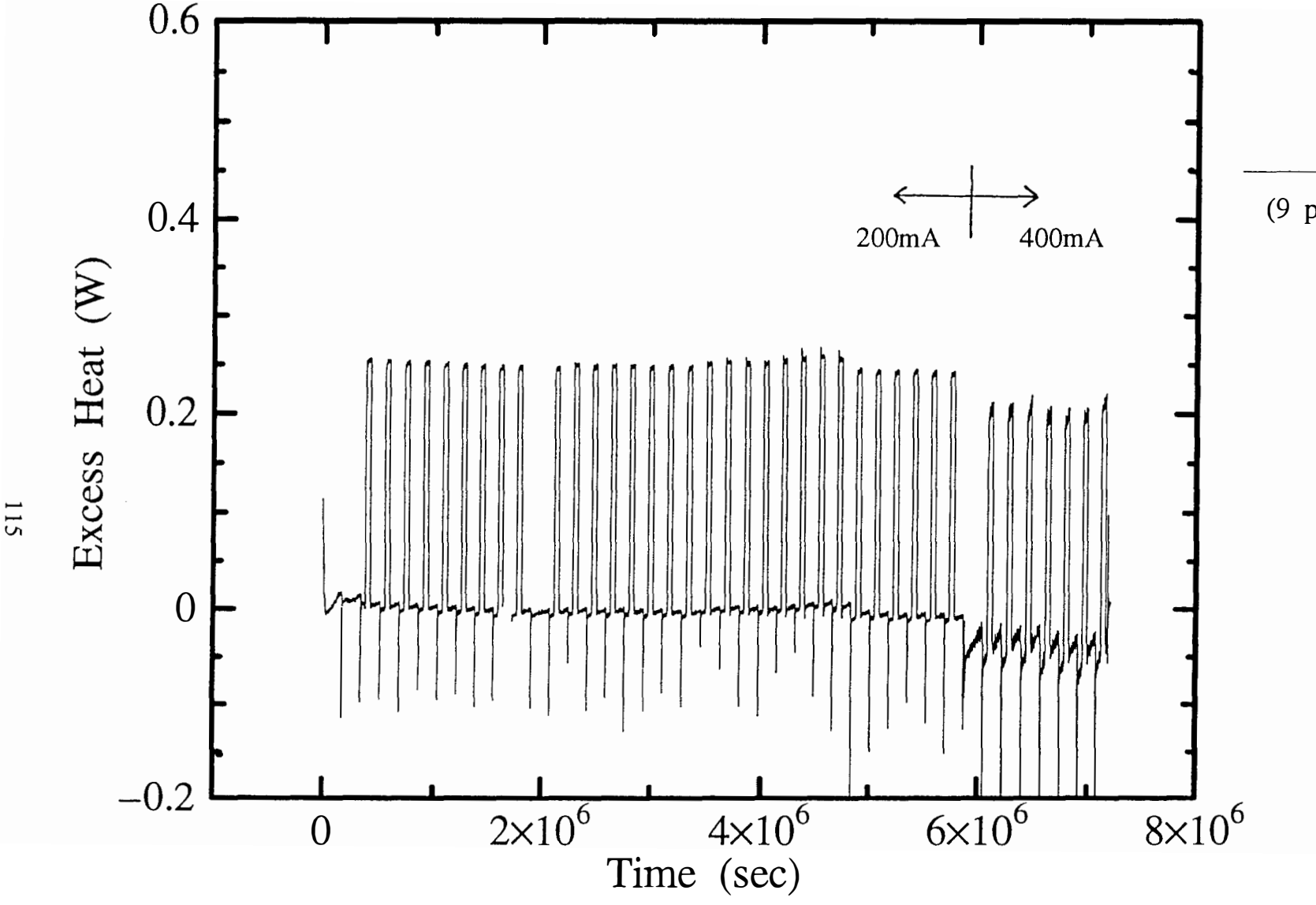

Fig.4 Change of Excess Heat (include Heater Input) of exp.4251

Electrode : 10%Ag–Pd (J/M Bt.0.549 ϕ 4x12.5) Electrolyte : 0.1M LiOD

k_R = 0.7706x10^{-9} (WK^{-4}), CM = 490.0 (J/K), W_{Heater} = 0.2506

Fifth International Conference on Cold Fusion
9-13 April, 1995 - Monte Carlo, Monaco
ICCF5 ©1995

Correlation of Excess Heat and Neutron Emission in Pd-Li-D Electrolysis

H. Ogawa, S. Yoshida, Y. Yoshinaga, M. Aida, and M.OKAMOTO
Research Laboratory for Nuclear Reactors
Tokyo Institute of Technology
2-12-1, Ookayama, Meguro-city, Tokyo 152 Japan

Abstract

To investigate the dominant factors for the reproducible occurrence of the nuclear reaction in D-Pd systems, the initial electric resistance and the hardness of the Pd cathode have been examined in terms of the excess heat generation and the excess neutron emission in the LiOD-Pd electrolysis cells. The two background runs and one foreground run with the Pd cathode of high electric resistance and high hardness gave no nuclear effects, while one foreground run with low electric resistance and low hardness gave appreciable excess neutron emission and the excess heat generation. The reversal correlation was found between the two nuclear effects.

1. Introduction

The dominant factors to reproduce the cold fusion phenomena should be clarified firstly to elucidate the mechanism of the cold phenomena and to find the new nuclear energy system based on the deutrium nuclear reaction in the condensed matters. A series of basic researches had been carried out to realize the anomalous distribution of deuterium with high concentration in the surface of Pd cathode by means of high/low pulse mode electrolysis. The reproducibility of the occurrence of the cold fusion phenomena became appreciably higher than the cases of the constant current electrolysis.[1] In the present study, we have examined the effects of the initial electric resistance and the hardness of the Pd electrode to the reproducibility of the cold fusion phenomena in a series of heavy water electrolysis with high/low pulse mode.

2. Experimental

The Pd cathodes used were prepared from a Pd plate of 1mm thickness by cutting

into plates with the size of 10mm×25mm. After washing in a ultrasonic bath of acetone and drying in the ambient, their Vicars-hardness were measured and then their electric resistance were evaluated as the cell voltage in Pd-Pt pair in LiOD electrolyte. We selected two pairs of Pd electrodes, one of them is a pair of high electric resistance and high hardness, and the another one is a pair of low electric resistance and low hardness. By use of one pair, a couple of the background runs with LiOD-Pd system and another pair was used in a couple of foreground runs with LiOD-Pd system.

The electrolysis cells used here were the same cells used in the previous studies reported by the present authors. [1,2,3] The details of an excess heat monitoring system and a NE213 liquid scintillation neutron detector were described in the previous papers.[1,2,3]

The electric current of high density of 800mA/cm^2 was applied for 1 hours and the low density of 20mA/cm^2 was applied for 3 hours repeatedly for about 25 days. The temperature of the electrolyte was measured by the three thermocouples and the data were stored into a computer in every 30sec, and the counting rate from the NE213 neutron detector was stored into the computer in every 3 min. The experimental conditions are listed in Table1.

3. Results and Discussion

3-1. Excess heat generation

The electrolyte temperatures obtained in the couple of background run (Run 3) and foreground run (Run 1) by use of the Pd cathodes with low electric resistance and low hardness are plotted in Fig.1 and Fig.2 as a function of the input power. In Fig.2, we can find the appreciable upper deviation of the plots from the calibration line. From the upper deviation, we can conclude that the excess heat was generated in this foreground run. As has been reported , we have no excess heat detection in the all cases of LiOH-Pd electrolysis as same as in the present study, while more than 60% of LiOD-Pd electrolysis with high/low pulse mode gave the excess heat as shown in Fig.2. According to our data, the excess heat generation should be recognized to be specific to deuterium in the LiOD-Pd electrolysis.

The averaged electrolyte temperature is plotted as a function of the input power in Fig.3 for background run (Run 4) and Fig.4 for foreground run (Run 2) obtained with the couple of the Pd electrodes of high electric resistance and high hardness,

respectively. The solid lines in these figures represent the calibration lines for each runs. In these runs, there are no clear upper deviations of the plots of the electrolyte temperatures, so it is concluded that we had no excess heat in these runs.

3-2. Excess neutron emission and its correlation with the excess heat generation

The details of the evaluation of the excess neutron emission was described in the previous papers. In the present study, the correlation between the excess heat generation obtained in Run 1 (F.G.) and the excess neutron emission obtained from Run 1 and Run 3 (B.G.)is demonstrated for the electrolysis time. It may be very clear that the correlation between excess neutron emission and the excess heat generation is just reversal correlation in each other, as illustrated in Fig.2 and Fig.5.

In Fig.6, we can find the neutron energy spectra from the ratio of the neutron emission rate obtained in Run 1 and that in Run 3 . The result is very similar to the many other data obtained and reported previously by the present authors. It can be said that the neutron emission rate is very low and the energy of the emitted neutrons varied so wide from 1MeV to 7MeV, and the neutrons in the higher energy region may be dominant relatively, as discussed by us[3] and by Takahashi et al[4].

4. Conclusion

The Pd plates characterized in terms of their initial electric resistance and the hardness were examined as the cathodes in the cold fusion test cell. The Pd cathodes with high electric resistance and high hardness gave no excess heat and also no excess neutron, even in the foreground run in LiOD-Pd electrolysis, while the Pd cathode with low initial electric-resistance and low hardness gave the excess heat generation and the excess neutron emission. The correlation between the excess heat generation and the excess neutron emission was found to be just reversal with respect to the operation time.

The further examinations should be carried out on the characteristics of Pd electrodes to clarify the key factors for the satisfied reproducibility of the occurrence of the cold fusion phenomena.

Acknowledgements

The present study has been carried out as a part of the Basic Research Project of New Hydrogen Energy financially supported 20 industries of Japan

Table.1 Experimental Condition

		Hardness (Hz)	Cell Voltage (V)	Electrolyte (1M)	Sustained Electrolysis	Pulse mode Electrolysis	Measurement System
F.G. (D_2O)	Run.1	low (118)	low (7.5)	LiOD	7	52	I
	Run.2	high (138)	high (8.6)	LiOD	7	43	II
B.G. (H_2O)	Run.3	low (119)	low (7.5)	LiOH	9	29	I
	Run.4	high (136)	high (8.6)	LiOH	8	34	II

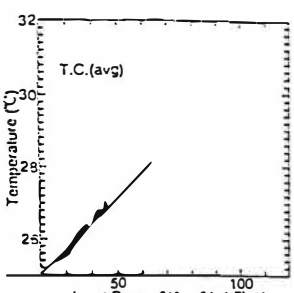

Fig.1 Run.3 (B.G.)

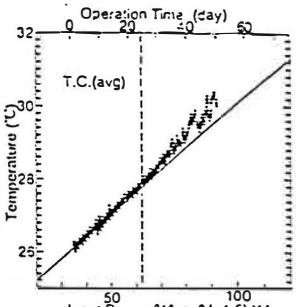

Fig.2 Run.1 (F.G.)

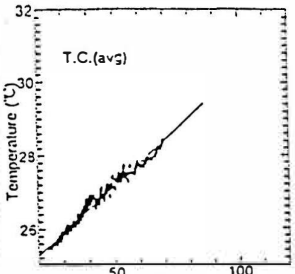

Fig.3 Run.4 (B.G.)

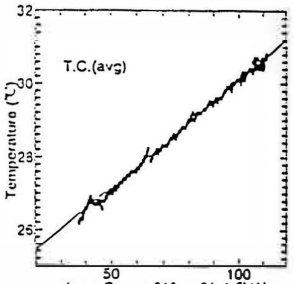

Fig.4 Run.2 (F.G.)

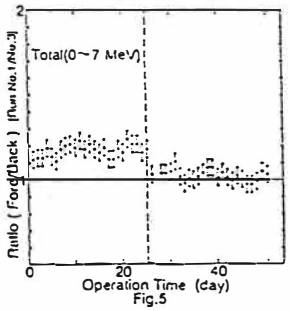

Fig.5

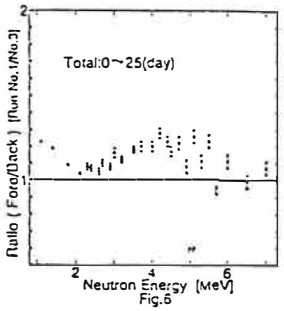

Fig.6

References

[1]M.Nakada, T.Kusunoki and M.Okamoto. Energy of the Neutrons Emitted in Heavy Water Electrolysis. Frontiers of Cold Fusion, Tokyo: Universal Academy Press, 1992, pp.173-178. [book]

[2]M.Okamoto, Y.Yoshinaga, M.Aida and T.Kusuniki. Excess Heat Generation, Voltage Deviation and Neutron Emission in D_2O-LiOD Systems. Proceedings of Fourth International Conference on Cold Fusion Vol.2: EPRI, 1994, pp.3-1~3-6

[3] M.Okamoto, H.Ogawa, Y.Yoshinaga, T.Kusunoki, and O.Odawara. Behavior of Key Elements in Pd for the Solid State Nuclear Phenomena Occurred in Heavy Electrolysis. Proceedings of Fourth International Conference on Cold Fusion Vol.3: EPRI, 1994, pp14-1~14-8

[4]A.Takahashi, A.Mega, T.Takeuchi, H.Miyamaru and T.Iida. Anomalous Excess Heat by D_2O/Pd Cell under L-H Mode Electrolysis. Frontiers of Cold Fusion, Tokyo: Universal Academy Press, 1992, pp.79-91.[book]

Fifth International Conference on Cold Fusion
9-13 April, 1995 - Monte Carlo, Monaco
ICCF5 ©1995

Simultaneous Measurement Device of Heat and Neutron of Heavy Water Electrolysis with Palladium Cathode.

Y. ASAOKA, T. ICHIJI, T. FUJITA and T. MATSUMURA
CRIEPI, Central Research Institute of Electric Power Industry
2-11-1, Iwato-kita, Komae, Tokyo 201, JAPAN

Abstract

An experimental device of cold fusion phenomena has been developed. Feature of the device is precise calorimetry and simultaneous measurement of excess heat, neutron and gamma-ray emitted from the electrolysis cell. The deuterium loading ratio of the palladium cathode can be measured simultaneously.

The galvanostatic electrolysis of heavy water with Pd cathode and Pt anode has been carried out in a closed cell with recombination catalyst. For precise excess heat measurement, the flow calorimetry method were adopted. Obtained accuracy of the calorimetry system was $\pm$0.2W at up to 10W of applied power. The electrolysis cell was set in shielding and neutron emission was detected by an NE-213 liquid scintillation counter and a He-3 proportional detector. Gamma-ray emission was measured with the Ge(Li) semiconductor detector. Electric resistance of the palladium cathode and pressure of the gas phase in the electrolytic cell were measured simultaneously to evaluate the deuterium loading ratio. D/Pd ratio evaluated by each method has reached approximately 0.87.

With these in-situ measurements of heat, neutron and gamma-ray, no remarkable cold fusion phenomena have been observed up to the present time.

1. Introduction

To reproduce the cold fusion phenomena, high loading ratio of deuterium in palladium cathode, that is considered to be one of the most important factors, is required[1,2]. Simultaneous and precise measurements of excess heat and nuclear products, such as neutron, tritium, helium and gamma-ray, are required to obtain the relationship of them in the investigation of the cold fusion phenomena.

An experimental device of cold fusion phenomena has been developed under consideration of these requirements. Objectives of the experimental device are reproducing cold fusion phenomena with attention to the deuterium loading ratio and measuring excess heat, neutron and gamma-ray simultaneously.

In the present study, characterization of the device was performed and preliminary results of the experiments are also discussed.

2. Experimental Methods

Galvanostatic electrolysis of D_2O-LiOD solution with Pd cathode and Pt anode has been carried out in a closed cell with recombination catalyst. Palladium cathode

materials obtained from Tanaka Kikinzoku Kogyo(TKK) was cut to sheets of 12mm×12mm×1mm or rods of 3mmϕ×15mm. Platinum anode wire is rolled round the cathode as in the device of Takahashi et al.[3] for the sheet-shaped cathode; and mesh type anode is used for the rod-shaped cathode. A stainless steel electrolysis cell has volume of 140cm^3,which is coated by Teflon in inner wall. The cell includes a cathode, an anode, a resistance heater, a thermocouple, about 70cm^3 electrolyte and recombination catalyst. The pressure of the electrolysis cell is monitored by pressure transmitter located near the top of cell.

Cross section of the calorimeter and the electrolysis cell is shown in Fig. 1. For precise excess power measurement, flow calorimetry method was adopted. The calorimeter is consists of a water bath, thermal insulation, and a Dewar bottle. Flow rate of coolant is controlled to be constant in about 14g/min. Calibration was done with an internal resistance heater before and after electrolysis. Temperatures were measured at five points, near the top of the water bath, near the bottom of the bath, at the water inlet tube, at the outlet tube and in the electrolyte. The difference between the inlet and outlet temperatures is used to calculate the output power.

Fig.2 shows top view of the neutron and gamma detectors together with shielding. The electrolysis cell was set in the shielding which consists of polyethylene, cadmium and low background (Co-60 free) iron. Neutron emission was detected by an NE-213 liquid scintillation counter and a He-3 proportional detector. Gamma-ray emission was measured with a Ge(Li) semiconductor detector. The radiation measurement system is able to monitor back ground neutron count rate simultaneously with another He-3 detector set out of the shielding, measure continuously for two weeks and identify the energy of neutron and gamma ray. The detection efficiency for each detector was measured with a neutron source of Cf-252 and gamma-ray sources of Cs-137, Co-60, Na-22 and K-40. Back ground count rate decreased about 30% for the He-3 proportional counter, about 35% for the NE-213 liquid scintillation counter, and about 65% for the Ge(Li) semiconductor detector with shielding. The performance of the radiation measurement system is shown in table 1.

Deuterium loading ratio was evaluated with the electric resistance of palladium cathode measured by means of the 4 lead method and

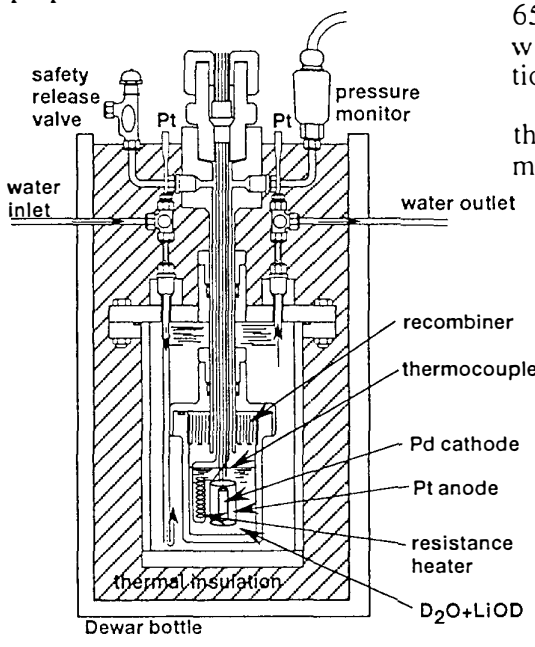

Fig. 1 Cross section of the electrolytic cell and calorimeter.

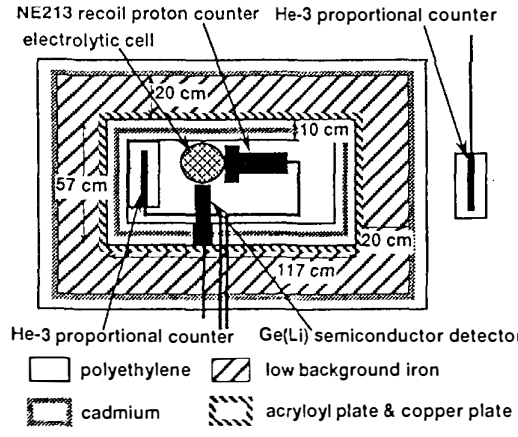

Fig. 2 Top view of the neutron and gamma detectors together with shielding.

Table 1. The performance of the radiation measurement system.

detectors	detection efficiency (%)	back ground count rate (s^{-1})	minimum detectable count rate (s^{-1})
He-3 proportional counter	0.89	1.5×10^{-2}	1.01×10^{-2}
NE-213 liquid scintillation counter	0.32	6.38×10^{-2}	1.94×10^{-2}
Ge(Li) semiconductor detector			
5.49MeV	0.027	2.60×10^{-2}	1.29×10^{-2}
6.26MeV	0.026	2.60×10^{-2}	1.29×10^{-2}
23.8MeV	0.014	4.56×10^{-1}	4.97×10^{-2}

the calibration curve of the R/Ro-D/Pd relationship[4]. D/Pd ratio was also evaluated with monitored pressure of the gas phase in the Pd cathode electrolysis cell compared with that of the reference experiments of Pt cathode electrolysis.

3. Results and Discussion

Fig. 3 shows the typical results of energy balance of heavy water electrolysis with a sheet-shaped palladium cathode and resistance heater calibration. The ordinate represents the difference between the calibrated value with the resistance heater before and after the electrolysis. The output power was calculated with the inlet and outlet temperatures and flow rate of coolant. The period of 0 to 75 hours and that of 700 to 800 hours represent the energy balance of heater calibration. The calibration curve was determined with these data. The period of the 75 to 700hours is for electrolysis. Input power changed several times from 1W to 9W, according to the electrolysis current was changed from 300mA to 900mA. The energy balance of the electrolysis seems to be almost zero except the sharp peaks due to step wise change of input power, that means the output power is always equivalent to the calibrated value calculated from the input power. From the data of non-excess heat electrolysis, the accuracy for the

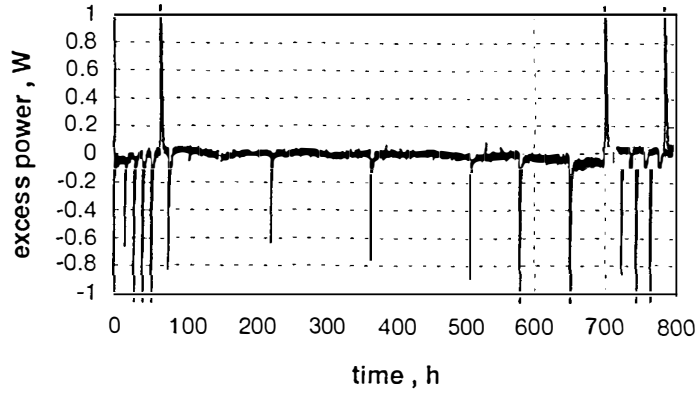

Fig. 3 Energy balance for heavy water electrolysis.

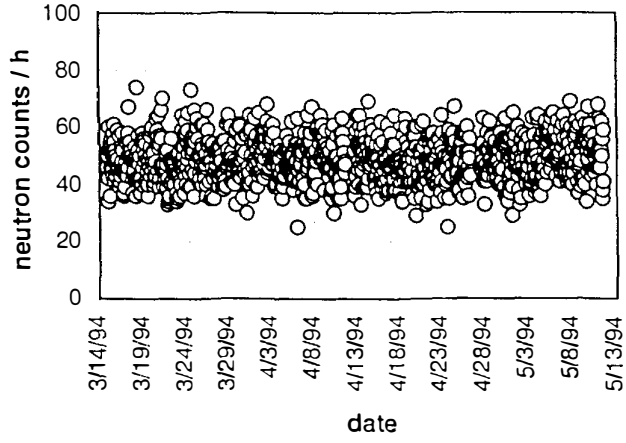

Fig. 4 Neutron count rate of He-3 counter in the shielding.

excess power measurement of the system was obtained to be ±0.2W at up to 10W of applied power.

Fig. 4 shows the count rate of the He-3 proportional counters in the shielding. The count rate seems to be almost constant during the electrolysis. No anomalous counts was observed for the other experiments. The data of the NE-213 counter and those of the Ge(Li) detector showed similar results.

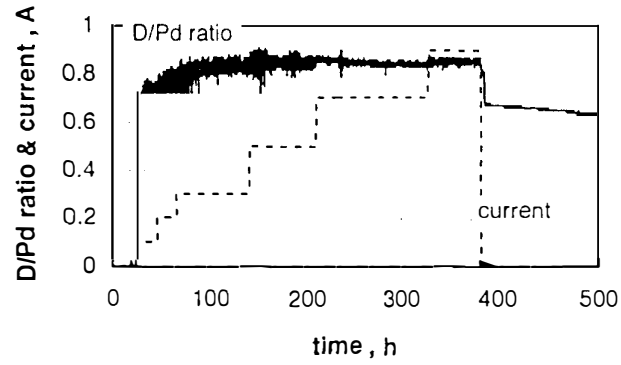

Fig. 5 Deuterium loading ratio in palladium cahtode.

D/Pd ratio of rod-shaped palladium cathode evaluated by the electric resistance together with the electrolysis current is shown in Fig. 5. When the electrolysis started, the loading ratio increased immediately and reached saturation in a day. Maximum D/Pd ratio was seems to reach 0.87. D/Pd ratio determined with cell pressure showed the similar results.

The performance of developed device was enough to detect the reported cold fusion phenomena. However, the results of all experiments showed no excess heat and no excess neutron and gamma-ray. One of the reasons for undetectable cold fusion phenomena is considered that the D/Pd ratio is not high enough for the phenomena.

4. Summary

Simultaneous measurement device of heat, neutron and gamma-ray of heavy water electrolysis with palladium cathode was developed. The device is able to monitor the deuterium loading ratio in palladium cathode simultaneously. As the result of the characterization of the developed device, the performance was enough for detection of the reported cold fusion phenomena.

With these in-situ measurements of heat, neutron, gamma-ray, no remarkable cold fusion phenomena, as excess heat or higher neutron count rate than back ground have not observed up to the present time. One of the reasons for undetectable cold fusion phenomena is considered to be low deuterium loading ratio.

Reproduction of the cold fusion phenomena with various cathode materials with attention to the D/Pd ratio, simultaneous measurement of heat, neutron, gamma-ray, helium and deuterium loading ratio, analysis of the palladium cathode are to be conducted.

References

1. M. McKubre, S. Crouch-Baker, A. Riley, S. Smedley and F. Tanzella, "Excess Power Observations in Electrochemical Studies of the D/Pd System; the Influence of Loading" *Frontiers of Cold Fusion*, ed. H. Ikegami, Universal Academy Press, Inc., Tokyo (1993) p.5
2. K. Kunimatsu, N. Hasegawa, A. Kubota, N. Imai, M. Ishikawa, H. Akita and Y. Tsuchida. "Deuterium Loading Ratio and Excess Heat Generation during Electrolysis of Heavy Water by a Palladium Cathode in a Closed Cell Using a Partially Immersed Fuel Cell Anode" ibid. p.31
3. A. Takahashi, A. Mega, T. Takeuchi, H. Miyamaru and T. Iida, "Anomalous Excess Heat by D_2O/Pd Cell under L-H Mode Electrolysis" ibid. p.79
4. M. McKubre, B. Bush, S. Crouch-Baker, A. Hauser, N. Jevtic, S. Smedley, M. Srinivasan, F. Tanzella, M. Williams, S. Wing and T. Passell, "Loading Calorimetric, and Nuclear Investigation of D/Pd System" *Proc. of ICCF-4*, Dec 1993, Hawaii, USA., EPRI TR-104188-V1 (1994)

Fifth International Conference on Cold Fusion
9-13 April, 1995 - Monte Carlo, Monaco
ICCF5 ©1995

Heat Production and Trial to Detect Nuclear Products from Palladium-Deuterium Electrolysis Cells

Shigeru ISAGAWA, Yukio KANDA and Takenori SUZUKI
National Laboratory for High Energy Physics, KEK,
1-1 Oho, Tsukuba-shi, Ibaraki-ken, 305 Japan

Abstract

A burst-like excess heat release, equivalent to 110% of the input electric power, was clearly observed for the first time in our newly built open type electrolysis cell using Pd/0.1MLiOD/Pt. After being precharged, the cell was driven to boiling three times the last of which continued for about 16 hours to almost dryness. The burst occurred just during the calm period about 6 hours after the first boiling. The temperature of the cell, about 100 ml in volume, increased by 7.5 K in 13 minutes. A palladium cathode, 2mmϕ × 7.05mm, was a heat source, although the mechanism of the heat generation is still uncertain. During the whole period of this run, however, the phenomenon took place only once. Neither increase of neutron emission nor that of tritium concentration has been detected. Mass analysis showed that any traces of D_2 as well as ^4He have not remained in the Pd sample used. Detection of γ ray emission as well as ^3He and ^4He in off gas during or just after release of excess power should be yet to be pursued further.

1. Introduction

The most important issue about the cold fusion research is to reproduce the claimed large amount of excess heat experimentally. The question of whether it is nuclear origin or not, can be clarified only by repetition of the heat phenomena. Among many experimental results, we have thus been particularly interested in observing with our own eyes a "burst" of excess enthalpy as originally reported by Fleischman, Pons and Hawkins [1]. Until very recently, however, no clear-cut heat bursts have been observed in our open type cell experiments. On the other hand, aiming to explain the lack of neutron (n) or tritium (T) consistent with the heat excess, new nuclear reaction mechanism in solid has been conjectured. Coincidental determination of the presence or absence of nuclear products like ^3He, ^4He and γ as well as n and T became essential. In order to accomplish a complete experiment, several improvements have been made so far: 1)A new cell was designed and prepared; 2)A new method of sample preparation was invented; 3)Mass spectroscopy of ^3He and ^4He was made possible; 4)High energy *in situ* γ ray spectroscopy system was prepared.

2. Electrochemical Cells

A new cell as illustrated in Fig.1 was designed and prepared whose heat insulation was reinforced by silver mirror, super insulation muffler and thick TFE inner flange. Palladium cathode (99.80% pure, Johnson Matthey) is screwed together with

1mmϕ Pt wire that is enclosed with FEP shrinkable tubing and 1.5/4mmϕ Pyrex glass tubing. Pt wire for anode (1mm in diameter and 3m in length) is symmetrically wound around 6 Pyrex glass supports with rather coarse pitch for upper 7 turns but with dense pitch for lower 29 turns. As the reference electrode a palladium wire of 1mm in diameter is immersed outside the anode spiral. Special care has been taken so that cathode may be centered by virtue of TFE bead and thick perforated flange.

No metal surface, Pt in particular, is exposed to gas phase with the aid of teflon coverage, which avoids spontaneous recombination between D_2 and O_2. A cartridge resistance heater of 10W is used for heat calibration. Temperature was measured with a chromel-alumel thermocouple also covered with teflon. Electrolytic current, voltage and temperature of the cell were continuously monitored. Two identical cells were prepared and installed in positions of 5 (VI05) and 6 (VI06) in a constant temperature bath kept at 20.0±0.01°C (see Fig.3 in the reference [2]). Evolved gas was passed through a 250ml buffer bottle and escaped to the air through 100ml D_2O and Si oil bubblers in series.

Two Pd cathodes were prepared. One for VI05 was 2mmϕ×7.05mm, mass and surface area of which are 0.227g and 0.435cm^2, respectively. It was cut from a 2ϕ×100 rod, shaped round with diamond files, polished with W wool and degreased. The other for VI06 was 3.2mmϕ×5.25mm, mass and surface area of which are 0.388g and 0.60cm^2, respectively. This sample had been remelt *in vacuo* using an Al_2O_3 crucible and stored in D_2O. The surface was filed, shaped and degreased. Both were annealed *in vacuo* up to about 800°C and charged with D_2 gas in the furnace just before installed in the cell. The electrolyte used was 0.1M LiOD solution, prepared by the addition of lithium metal to D_2O (99.9at.%, Aldrich Chemical Company). A different batch of electrolyte was used: an old one for VI05; and a new one for VI06, which means that the former contains more Si dissolved from glass container whose teflon lining peeled off after long storage of the solution. Electrolysis has been done in constant current mode. After precharging period of 28 and 8 days, the current density was increased from 35 to 920mA/cm^2 and 22 to 663mA/cm^2 for VI05 and VI06 cells, respectively. Heavy water of about 12ml was added twice a week to make up for losses due to electrolysis.

3. Measurement of Nuclear Products and Mass Spectroscopy

Neutron measurements were performed by positioning two different types of counter, BF_3 and ^3He, next to the electrolysis cells and another BF_3 counter about 3m apart for BG monitoring [2]. A fourth one, ^3He type, was also set below the furnace to check the abnormal emission during D_2 gas charging in Pd. Tritium concentrations, before, during and after electrolysis, were measured with a liquid scintillation counter by an external standard method. A γ ray survey meter using a 1"ϕ×1"NaI(Tl) scintillator and an MCA system using a 3"ϕ×3"NaI(Tl) scintillator were prepared. In the updated system γ ray signals up to 32 MeV can be accumulated every two hours and processed for anomalies in energy spectra. These scintillator detectors can be placed on top of the bath, but unfortunately could not be ready for the measurements when the boiling and the heat burst phenomena of the cells were observed.

Samples of Pd after electrolysis were degassed up to 770°C in a closed vacuum furnace. The extruded gas was analyzed in a high-resolution mass spectrometer system that was specially designed and prepared [3]. Off gas collected in bottles was also analyzed, but results were only preliminary. After these analyses the Pd samples were carefully observed and photographed through microscope. Although 3 months had already passed after the heat burst phenomenon, γ ray radiation from the sample VI05(941016) was measured by the use of a Ge(Li)-spectrometer. Chemical analyses of the solution or the solid precipitates in the cell after electrolysis were also done by ion chromatography, X-ray diffraction, X-ray fluorescence method and so on.

4. Results and Discussions

Under the constant current conditions the cell potential and the cell temperature increased gradually. Owing to improved heat insulation, electrolysis continued at relatively higher cell temperatures, even the higher as the addition of D_2O repeated. At the early stage of high current density up to 920mA/cm^2 (VI05 cell) or 663mA/cm^2 (VI06 cell), the electrolysis was rather calm, but after a few weeks it became astable and fluctuating. Cell resistance measured across reference electrode and anode showed similar but asynchronous fluctuations.

In case of VI05 cell sudden rise-up and fall-down of cell potential were found as the first symptom. At the next stage sudden step-ups like **A** and **B** in Fig.2 appeared. Decrease of liquid conductance due to Li escape, however, cannot account for these effects, as it should be more gradual, if any. All of a sudden the cell potential sharply increased and thus the cell temperature reached to boiling at **C** [4]. Due to voltage limitation of the power supply used, the current is lowered and boiling stopped again all of a sudden at a point **D** owing to some unknown delicate factors.

It was just during the calm period about 6 hours after the first boiling that an enormous heat release was observed (between **E** and **F**). The temperature of the cell, about 100 ml in volume, increased by 7.5 K (from 83.4°C to 90.9°C) in 13 minutes. The cell potential showed a dip correspondingly. Enlarged view is shown in Fig.3. As two cells were made almost identically, they obey the same calibration curves (see Fig.4 and Fig.5). By applying an electric current to a heater in a twin cell, VI06, we could simulate the heat burst phenomenon as shown in Fig.6. From this simulation, assuming no stored energy is released, the excess heat can be estimated to be 6.8 W, about 110% as compared with the input electric power. It amounts to 360 W per 1 cm^3 Pd bulk. Although a mechanism of heat generation is still uncertain, the cathode can be assumed to be a heat source due to following reasons. First the cell potential showed an abrupt partial recovery as shown by **B**$\rightarrow$ **C** in Fig.3, when the heat release stopped. It can be assumed to be caused by fast cooling of the Brunner-Nernst layer bearing a large potion of potential drop near the cathode. Secondly the Pyrex glass was found to be cracked near the end of the cathode due to heat, which may justify the sudden stoppage of the heat release phenomenon at **B**.

Boiling occurred 3 times the last of which continued for about 16 hours, in the former period violent but in the prolonged later period rather gentle, and the cell was driven to almost dryness. No *heat after death* [5] was observed in this case. During the whole period of this run the heat burst phenomenon took place only once. In case of the cell VI06, boiling due to sharp increase of cell potential also occurred but only once. A large number of candidates of small heat release were, however, observed in this cell. This is why the calibration curve shows a wider spread than in the cell VI05 (see Fig.5).

No increase of neutron emission as observed before [2] has been detected during whole process of D_2 gas charging and electrolysis (see Fig.7). Only one exception was an accidental increase up to 19 counts/30min of ^{3}He type detector at time t_1 (see Fig.3), but it was not coincidental in BF_3 ones. No abnormal increase of tritium has been found either as shown in Table I. Measurement of γ during electrolysis after boiling and heat burst has shown no anomalies in counting rate and energy spectrum up to 32 MeV.

Owing to possible contamination from air (5.24ppm) as well as from standard gas used before, whether ^{4}He exists in the off gas or not could not be conclusively determined this time. According to the mass analysis of gases dissolved in Pd samples, not only ^{4}He but also any traces of D_2 could not be detected in case of VI05. ^{4}He was not detected for the sample VI06, either. In this case, however, a smaller amount of D_2 which is equivalent to $PdD_{0.1}$ was found. VI06 cell was not dried as VI05 cell during electrolysis. This means all occluded gases removed from Pd bulk during the violent boiling process. The heat burst in VI05 might happen in the deuteron reoccluding stage.

The heat of combustion of hydrogen, assuming $PdH_{0.9}$, is equal to about 232J for 0.227g of Pd. Furthermore the heat of absorption of deuterium in $PdD_{0.9}$ only amounts to about 16J. These values from chemical reactions can never account for the excess enthalpy of 5300J that comes from 6.8W lasting for 13min. Observation through microscope clarified that Pt as well as Pd, near their interface in particular, had been seriously eroded. No such erosion could be found in case of another sample that had been electrolyzed for 4 months without showing any heat excess and was degassed up to 500°C. Pt anodes were both covered with much white brittle material abundant in Si mainly composing of $Li(Al)SiO_4 \cdot D_2O$. Dark brittle scab was found on Pd surface that also consists of Si › Pt › Zr and so on. On the other hand, no special γ ray radiation except the natural one was observed in the γ spectroscopy performed on the Pt/Pd cathode sample of VI05 although peaks of ^{228}Ac (338.4keV) and ^{214}Bi (1764.5keV) were enhanced a little in a sample run (see Tables II and III).

The low intensity of neutrons and the poor enrichment of tritium in so-called cold fusion experiments have prompted proposals of nuclear processes that yield only heat and helium as products. If the nuclear reactions were assumed as: 1) $D + D \rightarrow {}^4He + \gamma$ (23.8MeV), 2) $D + D + D \rightarrow D + {}^4He + \gamma$ (23.8MeV), the number of nuclear products should be 2.62×10^{11} s^{-1} per Watt, that is, totally 1.39×10^{15} in case of the heat excess of VI05(941016) cell. Although many difficulties are met with in ^4He detection [6, 7], measurements of these products should be accomplished coincidentally with the heat burst as we observed. Detection of γ ray emission as well as ^3He and ^4He in off gas during or just after release of excess power would be ardently pursued further.

Acknowledgments

Continuing encouragement of Professors H. Hirabayashi, Y. Kimura, H. Sugawara and K. Takata are gratefully acknowledged. Thanks are also due to Dr. D. R. O. Morrison who kindly commented on this manuscript.

References

1. Fleischmann, M., Pons, S. and Hawkins, M., "Electrochemically induced nuclear fusion of deuterium," *J. Electroanal. Chem.*, **261**, 301 (1989) and **263**, 187 (1989).
2. Isagawa, S., Kanda, Y. and Suzuki, T., "Search for Excess Heat, Neutron Emission and Tritium Yield from Electrochemically Charged Palladium in D_2O," *Proc. 3rd International Conf. on Cold Fusion,* Nagoya, October 21-25, 1992, p.477. Universal Academy Press, Inc., Tokyo (1993).
3. Isagawa, S., "Mass spectroscopic Search for ^4He Contaminated with Large Amount of D_2 Produced in Electrolysis Using Palladium Cathode," to be presented at *13th International Vacuum Conf. 9th International Conf. on Solid Surfaces,* Yokohama, September 25-29, 1995.
4. Fleischmann, M. and Pons, S., "Calorimetry of the Pd-D_2O system: from simplicity via complications to simplicity," *Phys. Lett.*, **A176**, 118 (1993).
5. Pons, S. and Fleischmann, M.,"Heat after Death," *Proc. 4th International Conf. on Cold Fusion,* Maui, December 6-9, 1993, vol **2**, p.8-1. Electric Power Research Institute, Palo Alto (1994).
6. Miles, M. H. and Bush, B. F., "Heat and Helium Measurements in Deuterated Palladium," *ibid.*, vol **2**, p.6-1 (1994).
7. Gozzi, D. et al., "Helium-4 Quantitative Measurements in the Gas Phase of Cold Fusion Electrochemical Cells," *ibid.*, vol **1**, p.6-1 (1994).

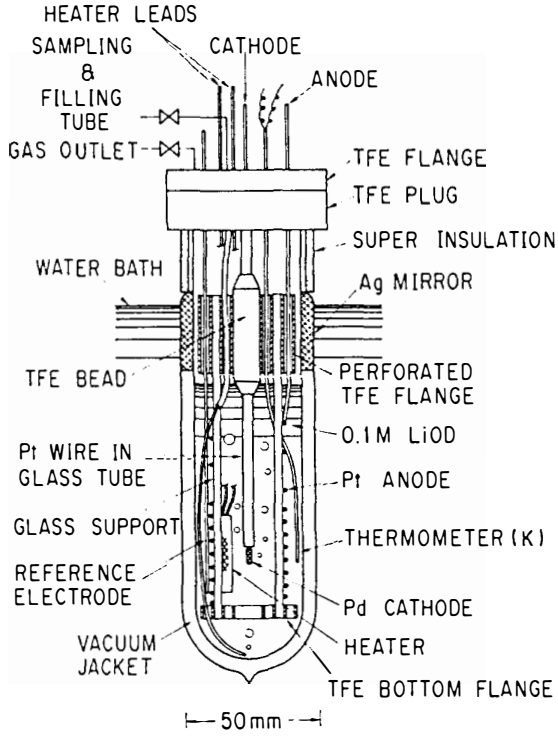

Figure 1. New vacuum insulated (VI) dewar-type cell. Level of electrolyte was kept below bottoms of perforated TFE flange and Ag mirror.

Table I.

TRITIUM CONCENTRATION

Sample No.	Sampling Date	^3H Conc. (Bq/cc)	Comment
1	930305	2.93	0.1MLIOO Original
2	"	3.40	"
29	941209	5.14	VI-05 Cell
37	950123	5.89	"
28	941209	4.83	VI-06 Cell
33	950123	5.93	"
35	950123	4.51	VI-05 D_2O Bubbler
36	950123	5.68	" Buffer bottle
32	941230	4.01	" TFE tubing
34	950123	5.62	VI-06 Buffer bottle
21	930522	4.15	D_2O bottle (99.9 atom%)
26	941118	3.73	"
27	941202	4.46	"
30	941216	3.80	"

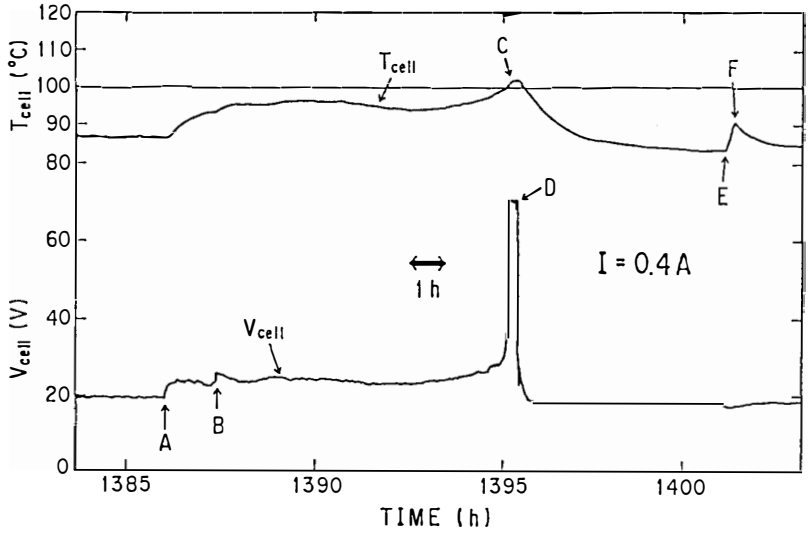

Figure 2. Temperature-time and potential-time profiles for a $2\phi \times 7.05$mm Pd electrode polarized in 0.1M LiOD for a period during which the cell went to 1st boiling and then to heat burst. The current was kept constant at 0.4A. The cell No. is VI05(941016). The time scale is in hours, the origin of which is the starting point of electrolysis.

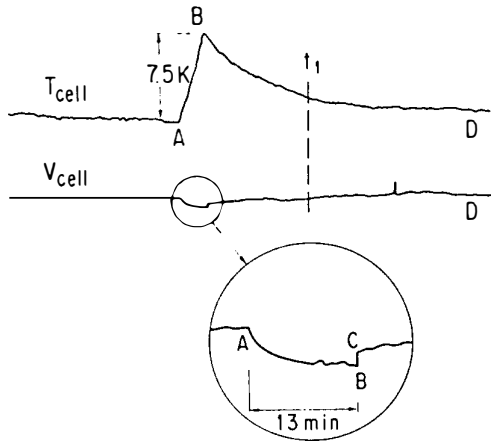

Point	T_{cell} (°C)	V_{cell} (V)	P_{in} (W)
A	83.4	17.85	6.51
B	90.9	17.0	6.17
C	90.9	17.35	6.31
D	84.0	18.2	6.65

P_{in} is input joule power (W).

Figure 3. Enlarged view of temperature-time (upper) and potential-time (lower) profiles of the cell VI05(941016) during a period of heat burst. A dip in cell potential shows a temperature rise of the electrolyte independently.

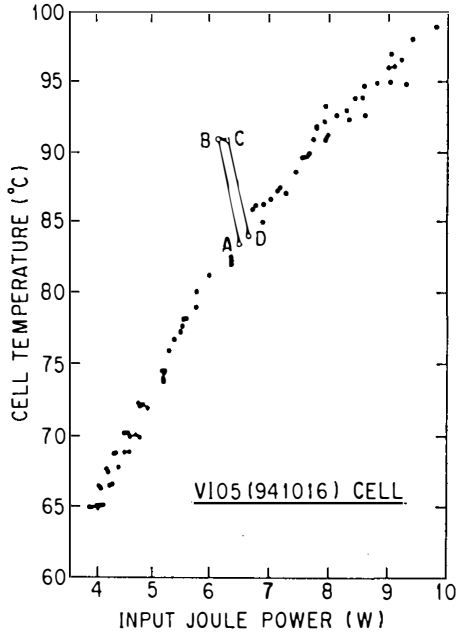

Figure 4. Calibration plots for cell VI05. Data (filled circles) were collected during electrolysis in which no heat excess was found. Empty circles represent the data during heat burst illustrated in Fig.3. Alphabets correspond to each other.

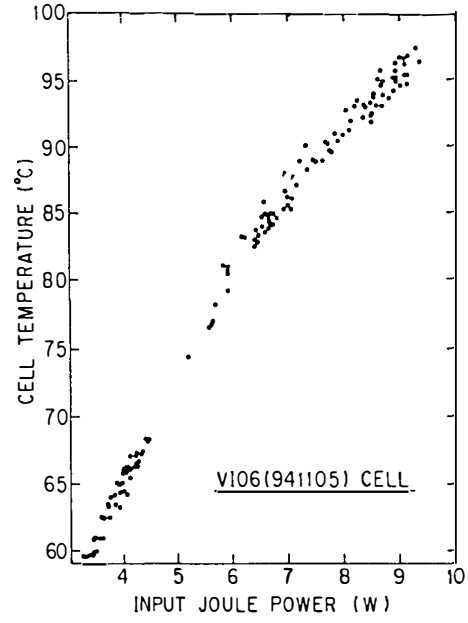

Figure 5. Calibration plots for cell VI06. Data were collected during electrolysis. Abscissa of Fig.4 and Fig.5 denotes the input joule power

$\{V_{cell}$ (V) - 1.54$\}\cdot I_{cell}$ (A) (W).

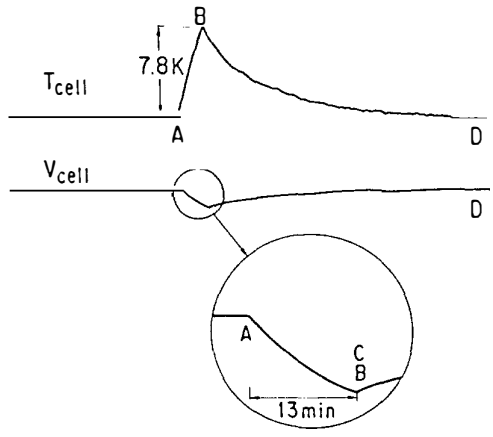

Point	T_{cell} (°C)	V_{cell} (V)	P_{In} (W)
A	82.5	21.79	6.49
B	90.3	20.1	5.94
C	90.3	20.1	5.94
D	82.9	21.79	6.49

P_{In} is input joule power (W).

Applied heater power was 6.8W (V_h = 10V and I_h = 0.68A).

Figure 6. Enlarged view of temperature-time (upper) and potential-time (lower) profiles of the cell VI06(941105) during a period of simulation run using a calibration heater. The electrolysis was kept continued with a current of 0.32A. And so the bubbles were formed continuously in the electrolyte. The base cell temperature at A (≈ 82.5°C) was almost the same value as that in Fig.3. A dip in cell potential shows a temperature rise of the electrolyte independently. A fast recovery of cell potential like B → C as observed in Fig.3 can not be found in this case.

Table II.

Gamma Spectroscopy with Ge(LI)-Detector

BG Run

Peak No.	Peak Channel (CH)	Back Area	Peak Area	Count Rate (Count/s)
1	62.27	1152.4	1078.6	1.30E-2
2	73.20	1726.4	813.2	9.83E-3
3	84.05	1489.9	131.4	1.59E-2
4	91.68	1699.7	398.1	4.81E-3
5	184.88	967.2	474.3	5.73E-3
6	237.72	914.3	159.4	1.93E-3
7	293.88	449.1	123.6	1.49E-3
8				
9	350.63	452.6	84.6	1.02E-3
10	509.59	595.0	108.0	1.30E-3
11	581.65	245.2	77.4	9.35E-4
12	607.69	236.8	96.9	1.17E-3
13	909.45	104.3	110.3	1.33E-3
14	961.87	88.0	28.9	3.50E-4
15	1118.25	75.7	56.8	6.86E-4
16	1458.09	38.7	325.4	3.93E-3
17	1761.51	44.0	5.6	6.77E-4
18	1844.50	24.3	0.8	1.02E-5
19	2200.52	11.8	13.3	1.61E-4
20	2610.69	10.8	98.7	1.19E-3

1000 CH / 1000keV Searched Region : 50 - 4050 CH
Counting Live Time : 3 1h (Normalized to 23h)

Table III.

Gamma Spectroscopy with Ge(LI)-Detector

Sample Run Sample : VI05(941016) Pd

Peak No.	Peak Channel (CH)	Back Area	Peak Area	Count Rate (Count/s)
1	62.24	1163.4	1119.6	1.35E-2
2	73.34	1629.1	929.9	1.12E-2
3	84.05	1560.6	77.4	9.35E-2
4	91.71	1699.3	427.7	5.17E-3
5	184.89	992.6	421.4	5.09E-3
6	237.90	873.0	209.0	2.53E-3
7	294.38	454.9	153.1	1.85E-3
8	336.73	377.1	87.9	1.06E-3
9	350.94	430.1	176.9	2.14E-3
10	509.59	576.9	142.1	1.72E-3
11	581.92	248.1	91.9	1.11E-3
12	607.80	258.0	76.0	9.18E-4
13	909.28	116.7	100.3	1.21E-3
14	967.06	110.6	33.4	4.04E-4
15	1118.77	91.6	11.4	1.38E-4
16	1458.09	40.3	337.7	4.08E-3
17	1761.47	25.3	45.7	5.52E-4
18				
19				
20	2610.69	10.3	107.7	1.30E-3

1000 CH / 1000keV Searched Region : 50 - 4050 CH
Counting Live Time : 23h

(a)

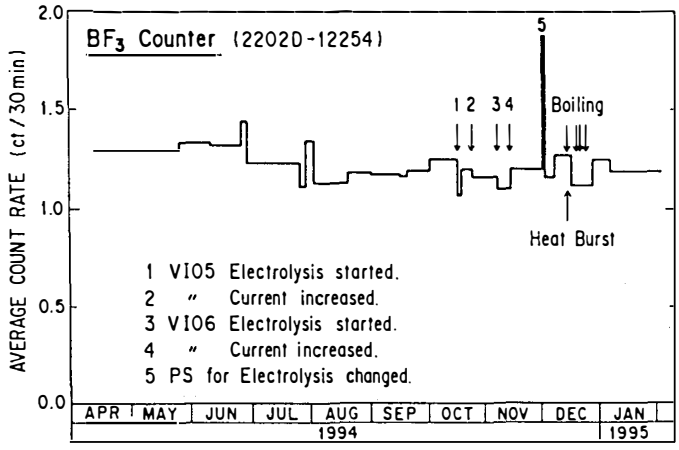

(b)

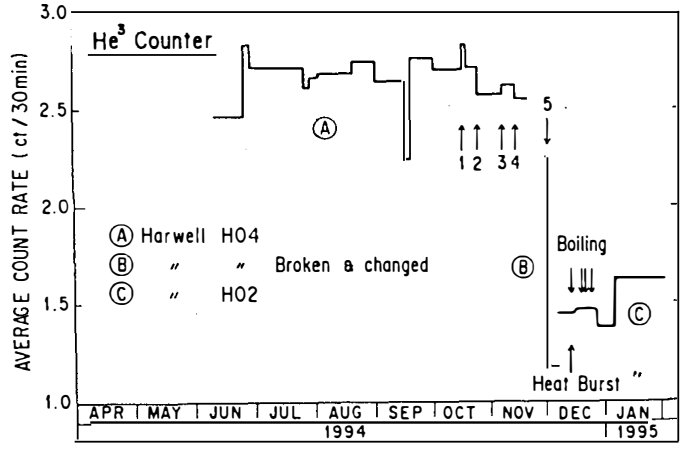

(c)

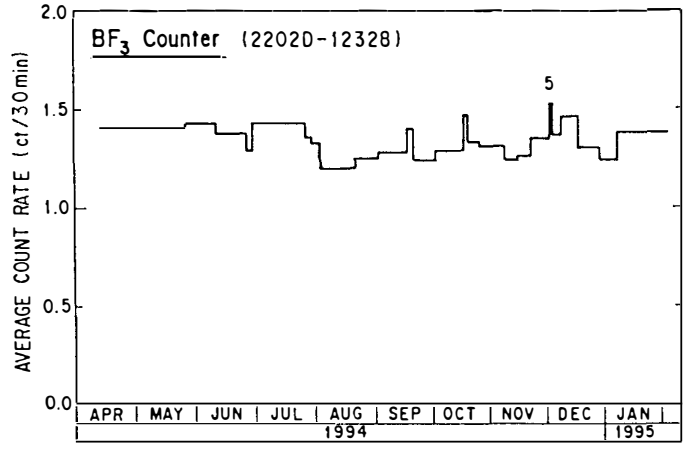

Figure 7. Deviations of average count rate per 30 min. during BG run and electrolysis run of (a) BF_3 counter near the bath, (b) ^3He counter near the bath, and (c) BF_3 counter about 3m apart from the bath [2].

Fifth International Conference on Cold Fusion
9-13 April, 1995 - Monte Carlo, Monaco
ICCF5 ©1995

EFFECT OF BORON FOR THE HEAT PRODUCTION AT THE HEAVY WATER ELECTROLYSIS USING PALLADIUM CATHODE

Ken-ichiro OTA, Kazuhiko YAMAKI, Shinji TANABE,
Hideaki YOSHITAKE and Nobuyuki KAMIYA
Department of Energy Engineering
Yokohama National University
156 Tokiwadai, Hodogaya-ku
Yokohama 240, JAPAN

Abstract

The heat balance during the electrolysis of 1M LiOD heavy water solution using Pd cathode has been measured using the flow calorimeter with the constant power supply and the thermochemically closed cell. The special attention was paied on the concentration of B in the palladium cathode. The B concentration was controlled from 127 to 1000ppm.

Using Pd that contained 127ppm and 1000ppm B, the excess heat was not observed. While, using Pd that contained 267ppm and 500ppm B, the small excess heat was observed at 3 runs out of 5 runs. The excess heat appeared continuously from the begining of the electrolysis. These concentration of B might be effective for the excess heat genaration.

1. Introduction

The excess enthalpy during the heavy water electrolysis using Pd cathode mainly in LiOD solution has been reported by the many groups[1-4]. However, the excess enthalpy is not well reproduced in most of the groups. In order to get a good reproducibility, the materials science of Pd cathode should be promoted more. The history of Pd processing and the composition of Pd metal are the interesting factors. In this study the attention was paied on the B impurity in Pd cathode.

Another point for the cold fusion study is how to measure the excess heat precisely. There is no fixed method for heat production during the electrolysis. In our group the heat balances during the heavy water electrolysis using Pd cathodes have been measured by the flow calorimeter using the constant power electrolysis in the thermochemically closed cell. In this system the input electrical energy completely converted to the thermal energy at the output. We can compare the input and the output energy very easily.

In this paper the effect of B concentration in Pd cathode on the excess heat generation during the heavy water electrolysis has been studied using our flow calorimeter system.

2. Experimental

The heat balance measurements have been carried out in an acrylic electrolysis cell with the recombination catalyst on top where the recombination reaction proceeds completely up to 4A. The recombination catalyst is fine Pd powder on Al_2O_3. Figure 1 shows the schematic

drawing of the electrolysis cell. The flow calorimetry was applied with copper tubing surrounded the cell where cooling water flows with picking up the generated heat by the electrolysis and the recombination reaction. The increase of cooling water temperature was measured by the CA thermocouples and the heat output was calculated. We adopted the constant power genarator for the electrolysis(genarally 5W) and controlled the cooling water temperature 296±0.05K at the entrance. The electrolysis was conducted up to 1500~2000 h at each run, if possible.

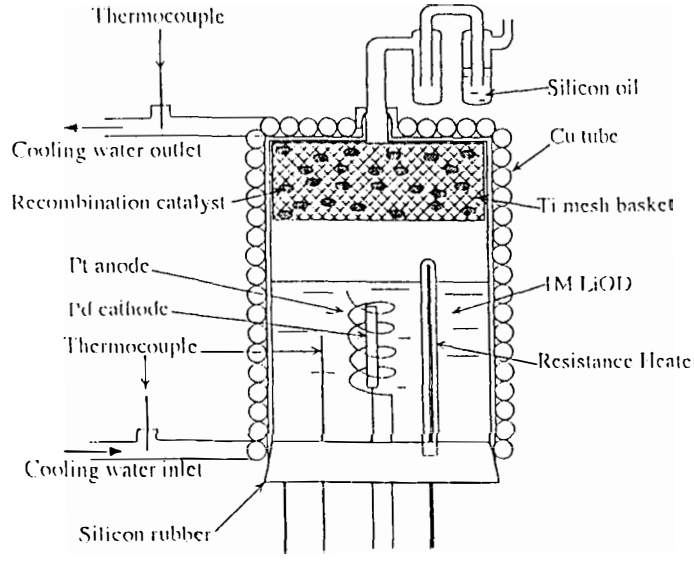

Fig.1 Electrolysis cell.

The cathodes were Pd rods(4mmØx20mm) or Pd plates(1x2x20mm) which contained the controlled concentration of B. These materials are obtained from Tanaka Kikinzoku Kogyo(TNK) and IMRA Material(IM). The B concentration was changed from 127 to 1000 wt.ppm. The anode was Pt wire(1mmØ) which surrounded the Pd cathode. The electrolyte was 1M LiOD heavy water solution which was made by solid LiOD·D_2O(99 at.%D).

3. Results and Discussion

Table 1. Heat balance of heavy water electrolysis with B-controlled Pd cathode

Run	Palladium sample		Win (W)	C.D. (mA/cm2)	Heat balance max(%)	Av.(%)
23	B 267ppm	TNK	5	750~300	107	103
25	B 127ppm	TNK	5	850~440	99	97
29	B 500ppm	IM	5	750~360	105	101
31	B 267ppm	TNK	5	900~540	103	100
33	B 500ppm	IM	5	740~660	104	103
34	B 500ppm	IM	5,10	1180~500	103	100
37	B 1000ppm	TNK	5	1040~945	101	100

Table 1 shows the summary of the results of the heat measurements at the electrolysis in heavy water. During these days the light water electrolyses were carried out 2 times using Pt cathode(Run 32 and 36) in order to check the performance of the calorimeter. In light water system the excess heat could not be observed. Although the heat output was fractuated a little bit around 100%, the average output heat was balanced with input power. We detected in average 100% of input power at the output.

At these runs(Table 1) the large excess heat that exceeded 10% of input power observed neither in continuous form nor in burst. The Pd cathodes those contained low(127ppm) and high(1000ppm) concenration of B did not produce the excess heat. However, the small excess heats in average were observed at the electrolyses using the Pd cathodes that contained 267ppm and 500ppm B at 3 runs(Run 23, 29 and 33) out of 5 runs. Most excess heat appeared continuously during the electrolysis, not in burst.

Figure 2 shows the heat balance of Run 23, where the 267ppm B containing Pd cathode was used. Most of the data points are above 100%. The excess heat appeared continuously throughout this run. The highest excess heat is 7% and the average excess heat is 3.5%. The total excess heat was calculated to be 0.6MJ. This value can not be explained by any chemical reactions that might occur in this system. Figure 3 shows the trends of the electrolysis current and the cell voltage at Run 23. Since we used the constant power electrolysis, the current and the cell voltage changed simultaneously. Generally, the cell voltage increased as the electrolysis reaction proceeded.

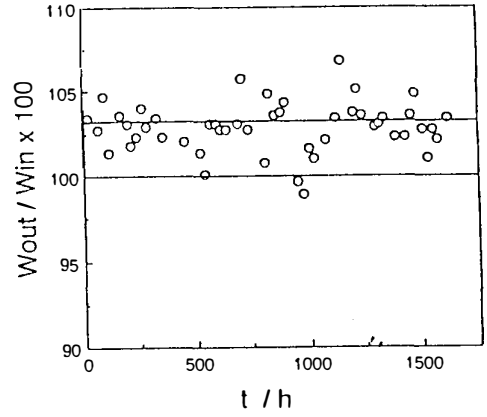

Fig.2 Heat balance at Run 23(267ppm B)

Figure 4 shows the heat balance of Run 29, where 500ppm B containing Pd cathode was used The trend of the heat balance is same as that of Run 23, although the absolute value is relatively small compared to Run 23. After this run the surface of the Pd cathode was analyzed by EPMA, Auger Electron Spectroscopy and X-ray Fluoresence. Pt was found up to 1000Å from the surface in relatively high concentration compared to the surface of Pd that could not produce excess heat.

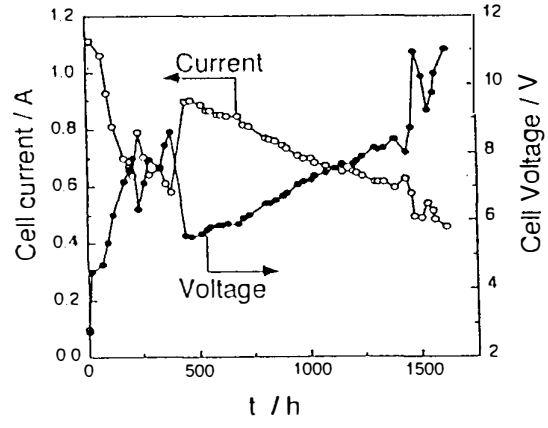

Fig.3 Cell current and cell voltage at Run-23

At Run 34 the input power was changed periodically(12h

interval) from 5W to 10W or vice versa in order to see the effect of the change of electrolysis condition. No excess heat was observed during this run. Such a long time interval might not be effective for the excess heat production.

The largest excess heat in this study was obtained at the 267ppm B containing Pd and the 500ppm B containing Pd was next. No excess heat was observed at 167 and 1000ppm B. There is no correlation between B content and the excess heat. Although our experiments are very limited and needs more data to confirm the effect of B, a suitable concentration (200~500ppm) of B in Pd might exist to produce the excess heat.

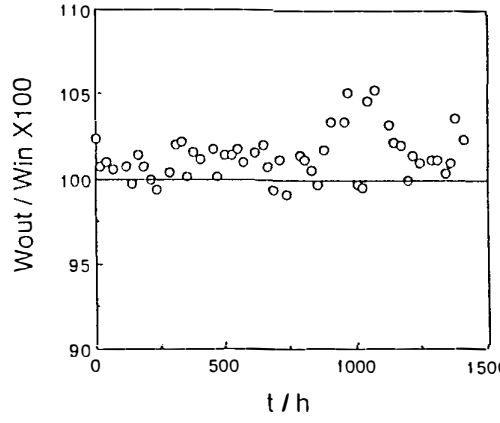

Fig.4 Heat balance at Run-29(500ppm B)

4. Conclusion

The heat balance was measured by the flow calorimetry during the heavy water electrolysis using the Pd cathode that contained the controlled concentration of B. Large excess heat that exceeded 10% of input power was not observed. The small excess heat looks appeared continuously during the electrolysis using the Pd cathode that contained 200~500ppm B. However, the excess value is so small that more precise measurement is necessary in order to confirm this results as well as the repeated studies.

The new heat measurement system is developing in our group. Using this system more precise heat measurement will be possible and the effect of B for the excess heat production will be confirmed.

Acknowledgement

The authors greatly appreciate for the financial support from the New Hydrogen Project of Japan.

References

1) Proc. 1st Annual Conf. on Cold Fusion, March 28-31, Salt Lake City (1990)
2) "The Science of Cold Fusion" (Proc. 2nd Annual Conf. on Cold Fusion) T.Bressani, E.D.Giudice, G.Preparata Eds., (1991) Italian Physical Society
3) "Frontiers of Cold Fusion"(Proc. 3rd Internat. Conf. Cold Fusion) H.Ikegami Ed., (1993) Universal Academy Press, Tokyo
4) Proc. 4th Internat. Conf. on Cold Fusion, Dec. 6-9, Lahaina (1993)

Fifth International Conference on Cold Fusion
9-13 April, 1995 - Monte Carlo, Monaco
ICCF5 ©1995

ELECTROLYSIS OF HEAVY WATER WITH A PALLADIUM AND SULFATE COMPOSITE

G.NOBLE, J.DASH, M.BREILING, and L.McNASSER
Physics Dept., Portland State University
Box 751, Portland, OR 97207

Abstract

It appears excess heat can be produced during the electrolysis of heavy water with a palladium and sulfate composite. Experiments seem to show that when this composite is coated on Platinum, and used as a cathode, excess heat similar to that generated with solid Pd results.

1. Introduction

During the summer of 1994, electrolysis experiments were conducted using small [about 25 ml] glass electrolytic cells with Teflon caps and connected in electrical series. The C [control} cell had a Pt foil anode and cathode, a recombination catalyst, and an electrolyte containing light water with 0.06 mol fraction sulfuric acid. The D cell was the experimental cell. It had a Pt foil anode, a cold rolled Pd cathode 0.35 mm thick, a recombination catalyst, and an electrolyte containing heavy water with 0.06 mol fraction sulfuric acid. Thermocouples on the outside of the cells were used to measure cell temperatures during electrolysis. A constant current source was used, and cell voltages were monitored. The schematic arrangement is shown in Fig. 1.

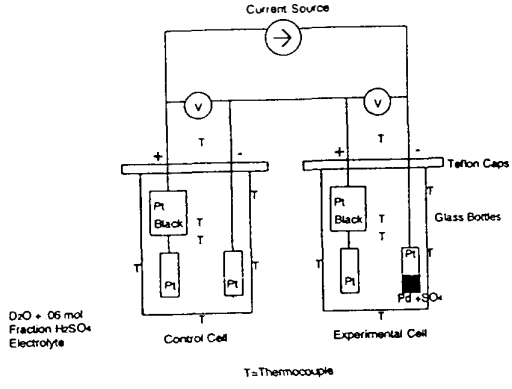

Figure 1. Heavy water electrolysis experimental arrangement.

2. Methods and Results

A series of three to five hour experiments was conducted in which a significantly higher average temperature was observed for the D cell. This occurred even though the power input to the C cell was greater. The

experiment dated 6-29-94 was the third experiment of the series, and the results are shown in Fig. 2. The average temperature was 9 C higher for the D cell with 0.52 W greater average power input to the C cell. Both cells lost electrolyte through the escape of vapor. The loses were identical for the two cells in the experiments preceding 6-29-94.

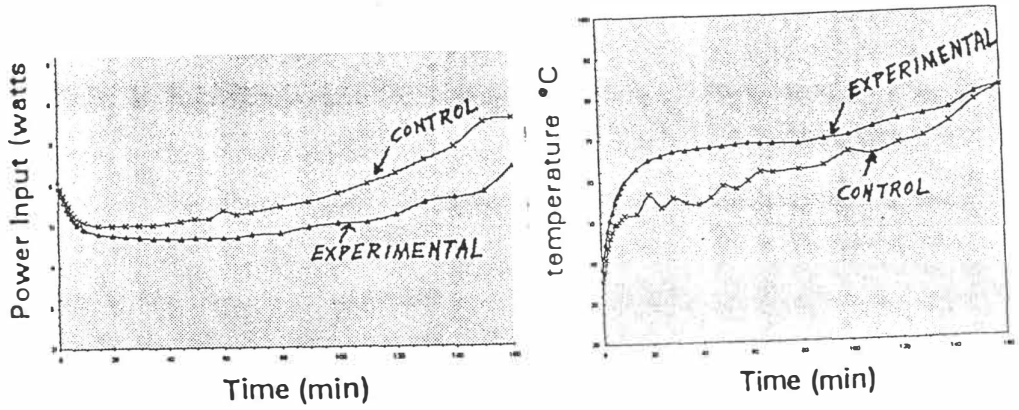

Figure 2. Power input and temperature for the experiment dated 6-29-94.

During the 6-29-94 experiment, the electrolyte turned black and a dark material collected on the Pt electrode. The Pd electrode lost 0.1 g from the electrolyzed portion, which appeared to have melted. However, it was later realized that the polarity of the cell was inadvertently reversed making the Pd electrode the anode and causing it to dissolve. The Pt was then the cathode. The black substance that deposited on the cathode is shown in Fig. 3.

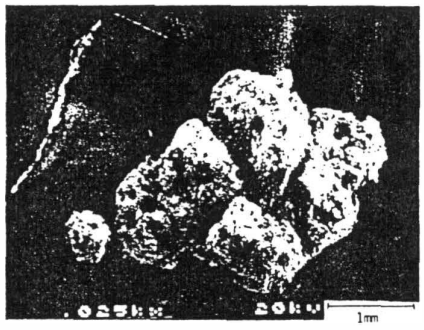

Figure 3. Sample of material that collected on the Pt cathode during experiment 6-29-94.

The spectra in Figs. 4a and 4b were taken with an energy dispersive spectrometer. Both show the presence of Pd, S, and O.

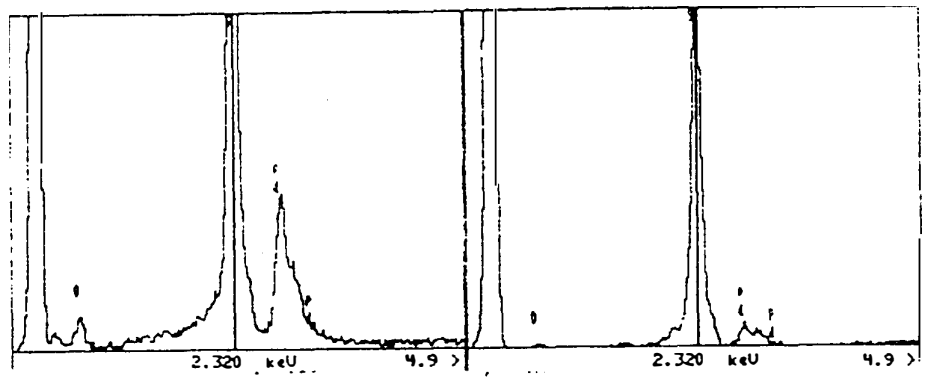

Figure 4. EDS area spectra of black substance show Pd,S, and O.

X-ray diffraction patterns were taken for the black substance and commercially available $PdSO_4$. The patterns do not match. The black substance appears to be hygroscopic but not to the same extent as the $PdSO_4$. Although believed to be palladium and sulfate composite, full characterization is not yet complete.

In another series of experiments, Pt foil cathodes were coated with palladium and sulfate by electrolyzing in a cell with a Pd anode. These cathodes were then electrolyzed with a Pt anode, a heavy water electrolyte with 0.06 mol fraction sulfuric acid, and a recombination catalyst. A control cell was connected in series, as described above. Fig. 5 shows the results of an experiment performed on 2-17-95. Each point on the graph represents the average of six thermocouple readings at the locations shown in Fig. 1. The average power input to the [C] control cell was 0.15,W greater than to the experimental [D] cell but the average temperature was more than 1 C greater on the D cell. The electrolyte loss was the same for both cells.

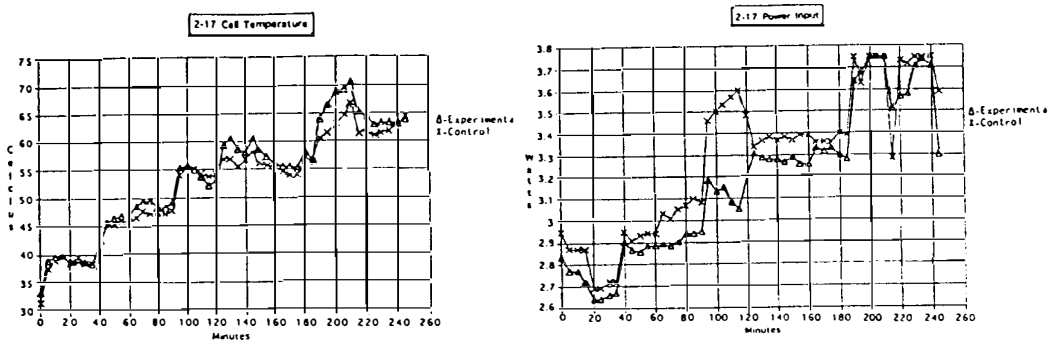

Figure 5. Temperature and power for experiment 2-17-95.

Fig. 6 shows the results for an experiment performed on 3-16-95. There was a 0.7 g greater electrolyte loss from the C cell than from the D cell. The power input to the C cell averaged 0.32 W more than to the D cell but the D

cell temperature averaged 2 C higher than the C cell.

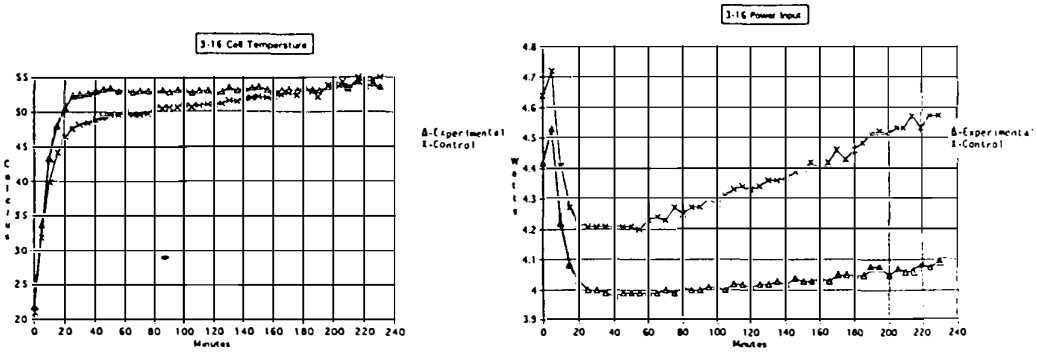

Figure 6. Temperature and power input for experiment 3-16-95.

In the final experiment in the series, the cell tops were interchanged. This resulted in the D cell losing 0.7 g more electrolyte than the C cell. Fig. 7 shows the results of this experiment performed on 3-29-95. The power input to the C cell averaged 0.062 W higher than to the D cell and the C cell averaged 1 C higher temperature than the D cell.

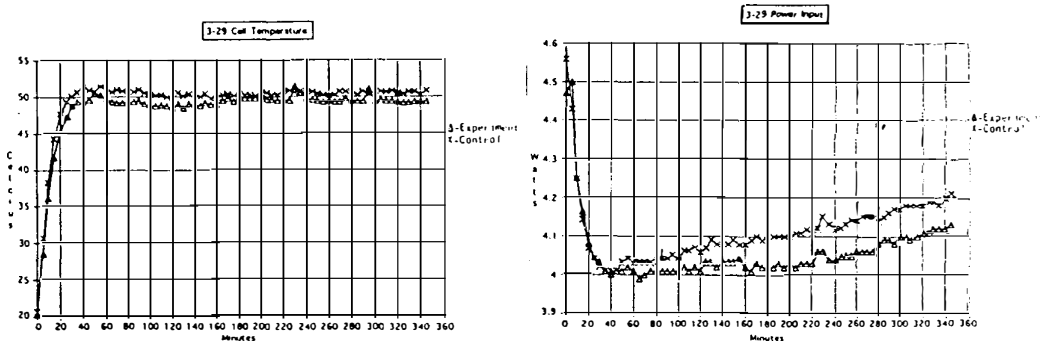

Figure 7. Temperature and power input for experiment 3-29-95.

It appears that excess heat in this experiment was carried with the net vapor loss from the D cell. The amount of excess heat may have been about 5000 J, depending on the composition of the vapor which escaped.

4. Conclusion

It appears that excess heat is produced during the electrolysis of heavy water with a palladium and sulfate coated cathode. The amount of this excess heat seems comparable to that produced with a pure palladium cathode.

Fifth International Conference on Cold Fusion
9-13 April, 1995 - Monte Carlo, Monaco
ICCF5 ©1995

More about Positive Feedback; more about Boiling

M. FLEISCHMANN
IMRA S.A., Science Center, 220 Rue Albert Caquot, Sophia Antipolis, 06560 Valbonne, France.

Introduction

We have already described elsewhere (1,2) some of the principles which have guided our search for the generation of high rates of excess enthalpy generation at elevated temperatures, say, up to the boiling points of the electrolytes (3,4). One of these principles has been the prediction that the partial molar enthalpy of absorption of hydrogen (or deuterium) in palladium (5) will become positive at the high charging ratios (X = D/Pd) required for excess enthalpy generation (6,7), see Fig 1.

Although a transition from exothermic to endothermic absorption is probably not a necessary condition for achieving excess enthalpy generation at elevated temperatures[1], such a transition will certainly facilitate the achievement of high charging ratios. For example, increases of temperature will then themselves lead to increases in X and thereby in the rates of excess enthalpy generation. These are the conditions required for the development of "positive feedback" and, in this paper, we report on two lines of investigation which have indicated the presence of these effects[2]. We then outline the way in which our understanding of this phenomenon has guided our investigation of excess enthalpy generation at elevated temperatures.

"Positive Feedback"

The most direct and systematic evidence for the presence of "positive feedback" can be obtained from the routine calibrations at long experiment times of the Pd/D_2O system in the isoperibolic calorimeters which we use in parts of our investigations (for an illustration see Fig 4A (8)). As we have described elsewhere (1,2,3,4), we have laid considerable stress on the "lower bound heat transfer coefficient $(k_R')_{11}$", obtained from the experimental data by assuming that there is no source of excess enthalpy in the cell, $Q_f(t) = 0$. Rearrangement of the differential equation governing the behaviour of the cell gives

[1]Thus the application of a sufficiently large difference in Galvani potential (either between a Pd-cathode and the electrolyte or within the metal phase itself) will always be able to counteract the effects of the heat of absorption if this remains exothermic.

[2]We obtained the first evidence for the presence of "positive feedback" during 1986, a phenomenon which we later described under the euphemistic heading "uncontrolled releases of thermal energy". Our subsequent work has been carried out under narrowly and tightly controlled conditions to limit the consequences of these effects.

$$\left(k_R'\right)_{11} = \frac{\left\{\begin{array}{l}\left[E_{cell}(t) - E_{thermoneutral,bath}\right]I \\ + \Delta\mathrm{QH}(\mathrm{t} - \mathrm{t}_{1}) - \Delta QH(t - t_2) \\ -\dfrac{3I}{4F}\left[\dfrac{P(t)}{P^* - P(t)}\right]\left[\left(C_{P,D_2O,g} - C_{P,D_2O,\ell}\right)\Delta\theta(t) + L_{D_2O}\right] \\ -C_{P,D_2O,\ell}M^0\dfrac{d\Delta\theta}{dt}\end{array}\right\}}{\left[\left(\theta_{\mathrm{bath}} + \Delta\theta(t)\right)^4 - \theta_{\mathrm{bath}}^4\right]} \qquad (1)$$

Here we have assumed that any small conductive contribution to heat transfer, $k_c\Delta\theta$, can be lumped into the radiative term by increasing the true radiative heat transfer coefficient from k_R to k_R'. The reason why $(k_R')_{11}$ is a lower bound is because the inclusion of any excess enthalpy term must inevitably increase the derived heat transfer coefficient. $(k_R')_{11}$ can be evaluated at any point of the coupled temperature-time and cell potential-time series, such as the points t_1, just before the application of the heater calibration pulse (with neglect of $\Delta\theta$) or the time t_2 at the completion of this pulse (with inclusion of $\Delta\theta$): see the schematic Fig 2.

For appropriate blank experiments (Pt in H_2O or D_2O), $(k_R')_{11}$ rapidly approaches a constant value and the standard deviation of these values is 0.1-0.2% of the mean (see also Fig 4B below). We regard this standard deviation as a measure of the precision of the experiments. The reason why it cannot be regarded as a measure of the accuracy (even for blank experiments) is because the possible reduction of electrogenerated oxygen would contribute an extra rate of enthalpy generation (electrogenerated hydrogen or deuterium cannot be re-oxidised at oxide-coated Pt anodes). It is necessary, therefore, to calibrate the system so as to compare the precision of $(k_R')_{11}$ with the accuracy of (k_R'). The simplest way of achieving such calibrations is to make a thermal balance at a single point in time, just before the termination of the calibration pulse, $t = t_2$, Fig 2. We have designated the heat transfer coefficient derived in this way as $(k_R')_2$:

$$(k_R')_2 = \frac{\left\{\begin{array}{l}\left\{\left[E_{cell}(\Delta\theta_1, t_2) - E_{cell}(\Delta\theta_2, t_2)\right]I + \Delta Q\right. \\ \quad -\dfrac{3I}{4F}\left[\dfrac{P(\Delta\theta_2, t_2)}{P^* - P(\Delta\theta_2, t_2)}\right]\left[\left(C_{P,D_2O,g} - C_{P,D_2O,\ell}\right)(\Delta\theta_2)_{t_2} + L_{D_2O}\right] \\ \quad +\dfrac{3I}{4F}\left[\dfrac{P(\Delta\theta_1, t_2)}{P^* - P(\Delta\theta_1, t_2)}\right]\left[\left(C_{P,D_2O,g} - C_{P,D_2O,\ell}\right)(\Delta\theta_1)_{t_2} + L_{D_2O}\right] \\ \quad \left. -C_{P,D_2O,\ell}M^0\left(\dfrac{d\Delta\theta}{dt}\right)_{\Delta\theta_2,t_2} + C_{P,D_2O,\ell}M^0\left(\dfrac{d\Delta\theta}{dt}\right)_{\Delta\theta_1,t_2}\right\}\end{array}\right.}{\left[\left(\theta_{bath} + (\Delta\theta_2)_{t_2}\right)^4 - \left(\theta_{bath} + (\Delta\theta_1)_{t_2}\right)^4\right]} \qquad (2)$$

The relative standard deviations of $(k_R')_2$ are in the range 1-2% of the mean and these standard deviations are measures of the accuracy which can be achieved by

making thermal balances at a single point in time. The principal reason for the order of magnitude difference between the precision of $(k_R')_{11}$ and the accuracy of $(k_R')_2$ is the fact that the denominator of (2) is determined by the difference of two comparably large terms, whereas that of (1) is determined by one of the terms alone[3].

For the investigation of blank experiments (Pt in H_2O or D_2O), we find that the heat transfer coefficients related to $(k_R')_{11}$ are somewhat smaller than those related to $(k_R')_2$ (we describe these heat transfer coefficients with the generic designations $(k_R')_{i,1}$ and $(k_R')_{i,2}$. We believe that the reason for this small difference is the contribution of a small rate of excess enthalpy generation due to the reduction of electrogenerated oxygen, see above (1,2). By contrast to these blank experiments, $(k_R')_{11}$ for the Pd-H_2O system is initially markedly reduced, so much so that under suitable conditions $(k_R')_{11}$ may be negative at short times. The reason for this reduction in $(k_R')_{11}$ is the exothermic dissolution of H in Pd. However, this phenomenon decays with the diffusional relaxation time and at longer times $(k_R')_{11}$ is again closely similar to the true value of the heat transfer coefficient, $(k_R')_2$.

The condition $(k_R')_{11} < (k_R')_2$ is maintained for prolonged periods of time, typically 2-6 weeks. However, at sufficiently long times we frequently observe a strange reversal of behaviour in that $(k_R')_2$ apparently becomes smaller than $(k_R')_{11}$. Such behaviour must have a quite special explanation because the condition $(k_R')_2 < (k_R')_{11}$ is forbidden by the Second Law of Thermodynamics (taken at its face value, the cell would have to behave as a spontaneous refrigerator to explain the result). The condition $(k_R')_2 < (k_R')_{11}$ is maintained for a limited period of time but eventually the system reverts to the expected behaviour, $(k_R')_{11} < (k_R')_2$.

We illustrate this transition with three calibration cycles taken from the results accumulated under the Japanese New Hydrogen Energy Project[4], Figs 3A-C. It will be seen that the transition is associated with further peculiarities. The temperature-time series both before and after the transition show the expected approach to a quasi-steady-state following the application of the heater calibration pulse and a relaxation to the base line following the termination of this pulse[5], Figs 3A and C. By contrast, during the transition, Fig 3B, the temperature does not approach a quasi-steady-state at the end of the calibration pulse, nor does the temperature relax to the base line at

---

[3]We have described elsewhere (1,2,3,4) changes in the methods of data processing which allow us to increase the precision of $(k_R')_{11}$ and the accuracy of $(k_R')_2$ by factors of ≅10. These methods rely on the use of the integrals of the experimental quantities rather than on evaluations at single points in time as for $(k_R')_{11}$ and $(k_R')_2$. These enhancements of the precision and accuracy are not required for the discussion of the topics considered in the present paper except for the comparison outlined in the following paragraph.

[4]We are greatly indebted to NHE for permission to use this illustration, as well as that in Fig 4A.

[5]As the temperature-time and cell potential-time series are coupled, see equations (1) and (2), the thermal relaxation times depend on both time series. A rough approximation is (9)

$$\tau = \frac{C_{P\,D_2O,t}\,M^0}{\left[4k_R'\theta_{bath}^3 - \left(\frac{dE_{cell}}{d\Delta\theta}\right)I\right]} \qquad (3)$$

A more exact result based on a series-type solution of the differential equation governing the behaviour of the calorimeters is available as an internal Technova Report. As $(dE_{cell}/d\Delta\theta)$ is negative (see Figs 3A-C), the temperature dependence of E_{cell} shortens τ from the external value. Indeed, the two terms in the denominator of (3) are of comparable magnitudes and we expect that the cells should show "negative feedback" under normal conditions.

the end of this pulse (compare the behaviour of the cells investigated by the group at Harwell, Figs 2A and B (8)). We have to conclude that the temperature rise induced by the heater calibration pulse itself induces an increase in the rate of generation excess enthalpy both during the application of the calibration pulse as well as after its termination. These are the conditions required for "positive feedback" which is evidently sufficiently marked to outweigh the normal "negative feedback" shown by the cells.

It is a consequence of the "positive feedback" that the temperature at the end of the calibration pulse is higher that it would be in the absence of such feedback. As a result, $(k_R')_2$ is smaller than expected so that we can reach the condition $(k_R')_2 < (k_R')_{11}$.

A possible explanation of the onset of "positive feedback" is a reversal in the heat of absorption at sufficiently high charging ratios, Fig 1. Although other explanations could be invoked (and should be explored), it is natural to search for direct evidence of changes in the heat of absorption - a matter of some difficulty. A possible approach is the detailed examination of the variation of $(k_R')_{11}$ with time in the region of the calibration pulses because transient sources of excess enthalpy in the cell affect $(k_R')_{11}$ directly. Fig 4A shows one such example: we see that the application of the heater pulse leads to a transient increase in $(k_R')_{11}$ which must be interpreted as a transient endothermic process in the cell. We observe this positive excursion in $(k_R')_{11}$, although the longer-term effect of the application of the calibration pulse is a decrease of $(k_R')_{11}$ which must be due to an increase in the rate of excess enthalpy generation. We note also that if the effects of "positive feedback" are not fully established, we would expect to see a transient decrease in $(k_R')_{11}$ at the termination of the heater calibration pulse due to the reversal of endothermic absorption, i.e. the establishment of transient exothermic desorption. Such effects can, indeed, sometimes be observed as in the example shown in Fig 4A.

The behaviour of $(k_R')_{11}$ shown in Fig 4A should be judged in the context of the variability of $(k_R')_{11}$ observed in typical blank experiments, Fig 4B (see also above). In the interpretation of such data it should be borne in mind that about one-third of the standard deviation of the measurements is due to the systematic decrease of $(k_R')_{11}$ with time during any given two-day period[6].

We note finally that the experiments give other evidence for the presence of a reversal of the heat of absorption. Thus in the region where we observe "positive feedback", we also observe fluctuations in the cell temperature and cell potential (3,4). These fluctuations may be quite small (as for the Pd-systems) or marked (as, especially, for Pd-Rh alloys), regular or, in the limit, chaotic. We observe that such oscillations would be expected in the region where $\Delta H = 0$ because the fluctuations in entropy will become unbounded. However, it is likely that the reversal in the heat of absorption is itself due to a complex phenomenon such as the formation of the proposed third γ -phase (10). Phase transitions would also lead to oscillatory behaviour.

More about Boiling

The explanation of the effects of "positive feedback" in terms of a reversal of sign of the partial molar enthalpy of absorption with increasing charging ratio, Fig 1,

[6]This period is set by the time interval between the "topping-up" of the cells to make up for losses of D_2O due to electrolysis and, at temperatures approaching the boiling point, due to evaporation.

also provides us with a rationale for other features of the behaviour of the Pd-D_2O system. Thus, it is likely that the achievement of pronounced levels of the rates of excess enthalpy generation requires the attainment of the regime of "positive feedback", which in turn requires the use of prolonged periods of polarisation, a matter to which attention has been drawn repeatedly. However, the attainment of the condition of "positive feedback" is not sufficient to ensure sustained, high, levels of the rates of excess enthalpy generation. Maintenance of the systems in the region giving pronounced oscillations will eventually diminish or even destroy excess enthalpy generation. The explanation of "positive feedback" in terms of the reversal of the sign of the partial molar enthalpy of absorption indicates that the attainment of this regime needs to be coupled to sustained increases in temperature to ensure that the charging ratio will show the necessary increases required to achieve increases in the rates of excess enthalpy generation. It follows that the use of essentially isothermal calorimetry (a strategy which has been followed in most investigations) is ill-advised, indeed self-defeating.

It is desirable therefore to examine the extent to which the reported achievement of boiling conditions (1,2) fits into this overall pattern. The routine calibration of the cells, Figs 5A and B, allows us to monitor the system behaviour and it is certainly true that the rapid increases in temperature towards the boiling point are only achieved following the detection of "positive feedback", as has been indicated in Fig 3B. The rates of excess enthalpy generation can become very high under these conditions, so much so that the cells are "driven to dryness" in relatively short periods of time (the last half of the cell contents (45 ml) may be evaporated in 11-15 min). The particular cells used (see Fig 4A (8)) are not suitable for accurate measurements and we therefore adopt conservative approaches to the interpretation of the experimental data (1,2). The simplest first step is to calculate the amount of energy available for evaporation of D_2O, Fig 6. Here we have used the true value of the heat transfer coefficient to calculate the radiative output. The total energy available is $\cong$70.5 kJ, sufficient to evaporate $\cong$1.7 M of D_2O. This leaves a deficit of 127 kJ required for the evaporation of the remaining 3.05 M D_2O.

In the absence of excess enthalpy generation, we reach a further impossible conclusion. As Fig 6 shows, the cumulative energy would then need to be negative for the first $\cong$7.7 hours of operation of the cell during the last period of operation. This again contravenes the Second Law of Thermodynamics. We conclude, therefore, that we must necessarily invoke excess enthalpy generation to explain the thermal balancing of the cell. However, our explanation of the behaviour must also be extended to give an account of the time dependence of the cell contents. The simplest assumption which we can make is that which has been used as a basis of the construction of Fig 6. This gives us curve A on Fig 7 and is clearly inadmissible. An alternative assumption is that the total cell contents in D_2O (5 M) are evaporated during the last period of operation, i.e. we rule out that the cell has been driven to boiling (1,2). We can derive such a "force fit" by regarding the atmospheric pressure, P*, as an adjustable parameter. We obtain curve C in Fig 7 and need to postulate the variation of the rate of excess enthalpy generation with time shown in Fig 8. However, such an explanation is again in conflict with other aspects of the experimental evidence. In the first place, we need to assume a value of P* which is below that of the recorded atmospheric pressure. Secondly, we conclude that the cell would then have to have been half-empty some 2.5 hours before achieving "boiling to dryness",

whereas video recordings show that this point was reached some 11 minutes before "boiling to dryness"[7]. The third assumption which we can make is that the rate of excess enthalpy generation can be calculated using the actual atmospheric pressure. This gives us the lower curve in Fig 8 for the rate of excess enthalpy generation in Fig 8 and the time course, curve B, for the cell contents in Fig 7. We conclude that we must now assume a period of intense boiling to account for the removal of the last half of the cell contents. This is in line with our visual observations and in turn leads to high final rates of excess enthalpy generation shown in Fig 8. The two plots in Fig 8 give the extrema of the behaviour: the actual behaviour must lie between the two limits but clearly closer to that given by the scenario leading to curve B in Fig 7 than that leading to curve C (1,2).

Conclusion

Prolonged polarization of cells containing Pd-based cathodes leads to "positive feedback", which can be attributed (at least in part) to a change from exothermic to endothermic absorption with increasing charging ratio. Increase of the cell temperature then leads to marked increases in the rates of excess enthalpy generation and enthalpy generation at the boiling point can be achieved.

References

1. M. Fleischmann and S. Pons in "Frontiers of Cold Fusion: Proceedings of the Third International Conference on Cold Fusion", Nagoya, Japan (21-25 October 1992) ed. H. Ikegami, Frontiers of Science Series No. 4, Universal Academy Press, Tokyo (1993) page 47; ISSN 0915-8502.
2. Martin Fleischmann and Stanley Pons, Phys. Lett. A, 176, 118 (1993).
3. M. Fleischmann, S. Pons, Monique Le Roux and Jeanne Roulette in: Proceedings of the Fourth International Conference on Cold Fusion, Lahaina, Maui, Hawaii, U.S.A. (6-9 December 1993) T.E. Passell, Editor, Volume 1 page 1-1, EPRI TR-104188-VI.
4. M. Fleischmann, S. Pons, Monique Le Roux and Jeanne Roulette, Trans. Fusion Technology, 26, 323 (1994).
5. T.B. Flanagan and J. F. Lynch, J. Phys. Chem., 79, 444 (1975).
6. M. C. H. McKubre, S. Crouch-Baker, A. M. Riley, S. I. Smedley and F. L. Tanzella, in "Frontiers of Cold Fusion: Proceedings of the 3rd International Conference on Cold Fusion", Nagoya, Japan, October 21-25 (1992) ed. H. Ikegami, Frontiers of Science Series No. 4, Universal Academy Press, Tokyo (1993) page 5; ISSN 0915-8502.
7. K. Kunimatsu, H. Hasegawa, A. Kubota, N. Imai, M. Ishikawa, H. Akita and Y. Tsuchida, in "Frontiers of Cold Fusion: Proceedings of the 3rd International Conference on Cold Fusion", Nagoya, Japan, October 21-25 (1992) ed. H. Ikegami, Frontiers of Science Series No. 4, Universal Academy Press, Tokyo (1993) page 31; ISSN 0915-8502.
8. M. Fleischmann, "The Experimenters' Regress", see these Proceedings of the Fifth International Conference on Cold Fusion, Monte Carlo (9-13 April 1995).
9. M. Fleischmann, S. Pons, M. W. Anderson, L.J. Li and M. Hawkins, J. Electroanal. Chem., 287, 293 (1990).
10. G. Preparata, "Cold Fusion '93: Some Theoretical Ideas", paper T1.2 presented at the Fourth International Conference on Cold Fusion, Maui, Hawaii, U.S.A. (6-9 December 1993).

[7]Although our use of video recordings to time the cell contents has been criticised, we note that it is hardly possible to confuse 11 minutes with 2.5 hours.

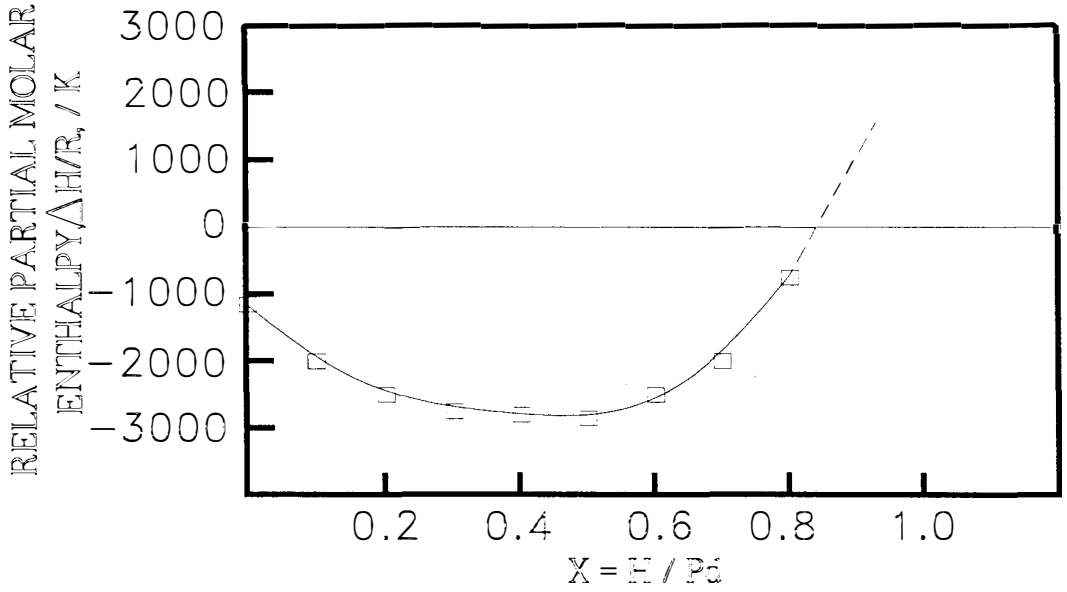

Fig 1. The variation of the relative partial molar enthalpy of hydrogen in palladium as a function of the charging ratio.

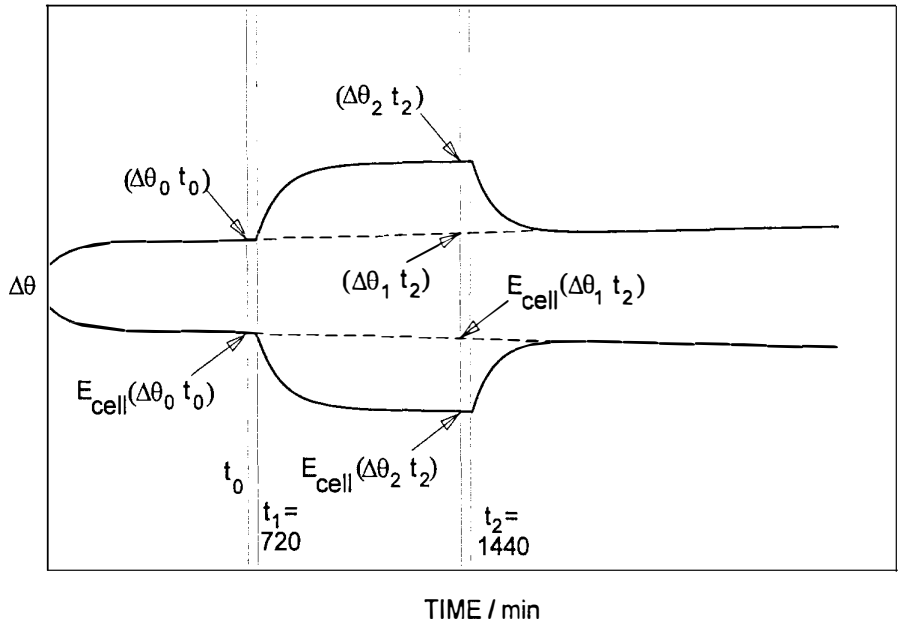

Fig 2. Schematic diagram of the methodology used in the calculations.

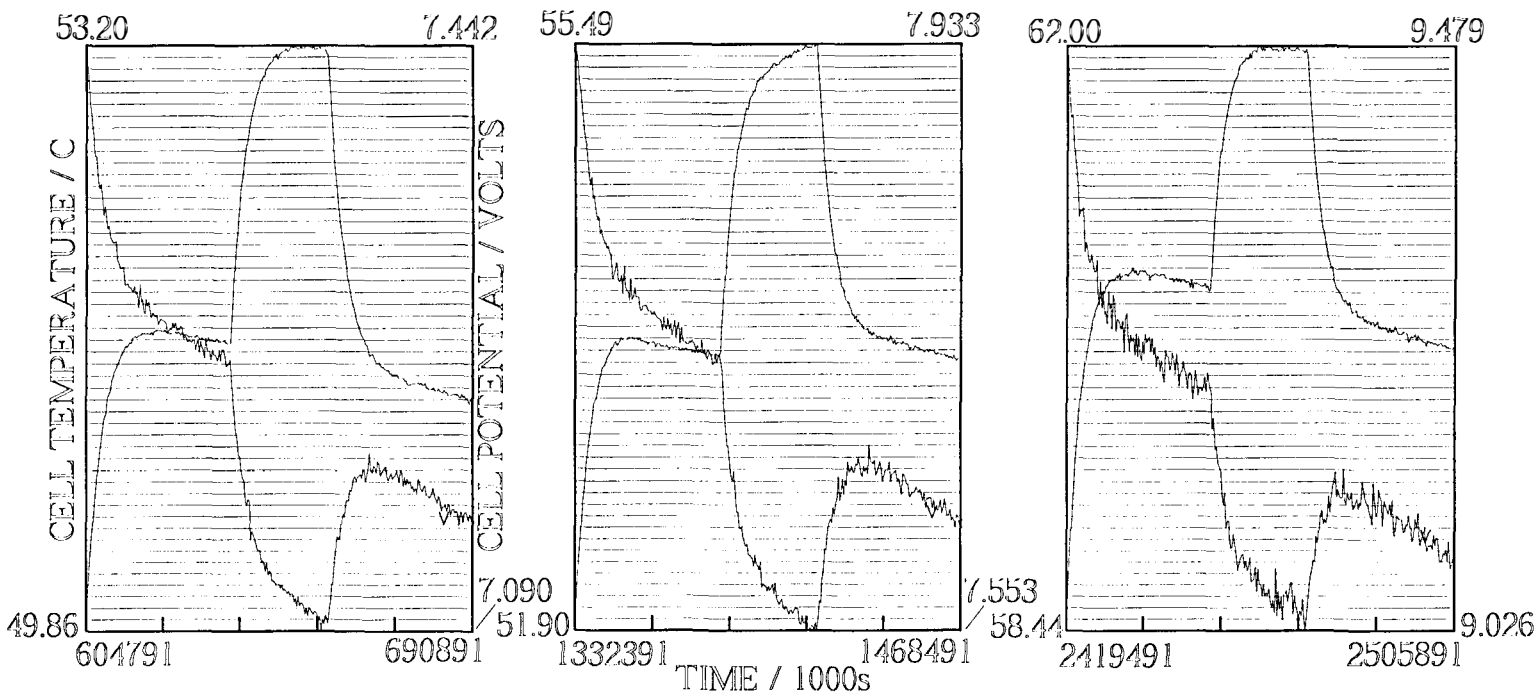

Fig 3. Experiment 4661 of the N.H.E. data sets. Pd 90 Ag10 cathode, 0.4 cm diameter, 1.25 cm length polarized in 0.1 M LiOD in D_2O; cell current = 0.5A, ΔQ = 0.2504W; the "raw data" of the cell temperature and cell potential as a function of time

A: a calibration before the onset of "positive feedback"

B: a calibration in the region of "positive feedback"

C: a calibration after the region of "positive feedback".

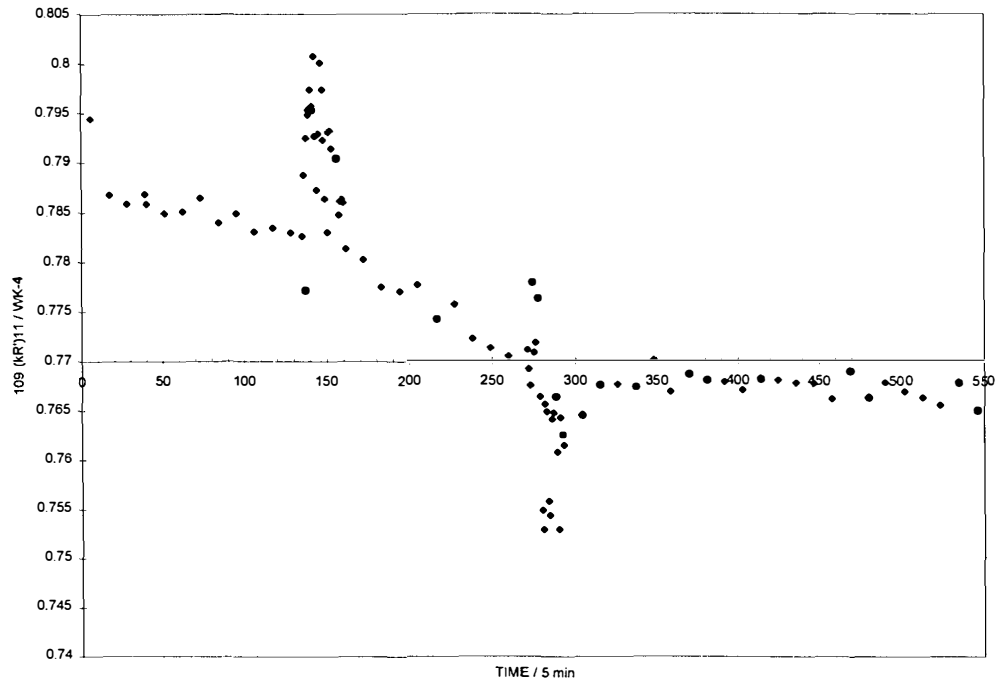

Fig 4A. Experiment 4731 of the N.H.E. data sets. Pd 90 Ag 10 cathode, 0.4 cm diameter, 1.25 cm length polarized in 0.1 M LiOD in D_2O; cell current = 0.2A, $\Delta Q = 0.2504W$; the variation of $(k_R')_{11}$ with time during days 33 and 34 of polarization. The start and end of the heater calibration pulse are shown by the positive and negative excursions of $(k_R')_{11}$.

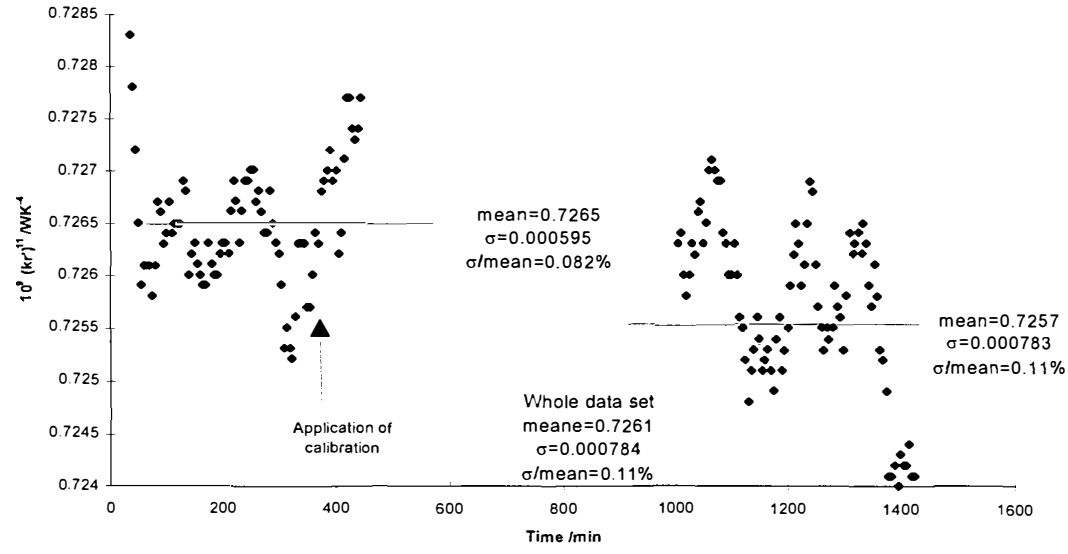

Fig 4B. Variation of $(k_R')_{11}$ with time for a blank experiment. Pt cathode 0.125 cm diameter, 1.25 cm length polarized in 0.1 M LiOD in D_2O; cell current = 0.2A. The region before and after completion of the calibration pulse.

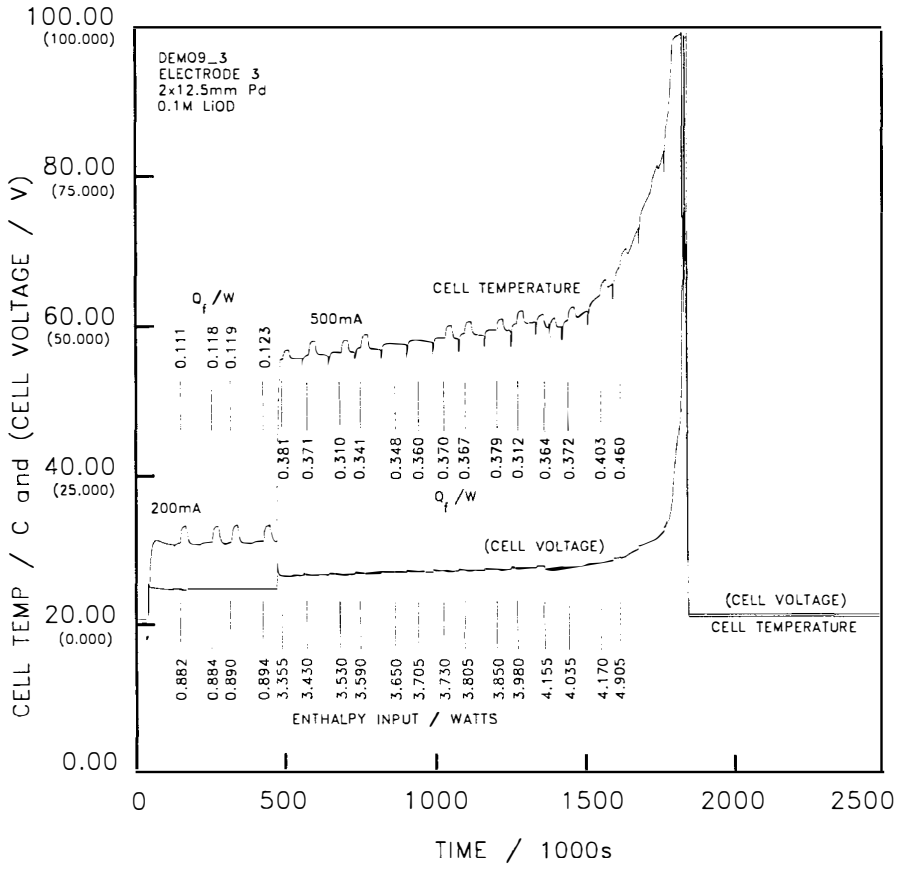

Fig 5A. The cell temperature and cell voltage for a cell driven to boiling. Pd cathode 0.2 cm diameter, 1.25 cm length polarized in 0.1 M LiOD in D_2O; cell current = 0.2A and then 0.5A.

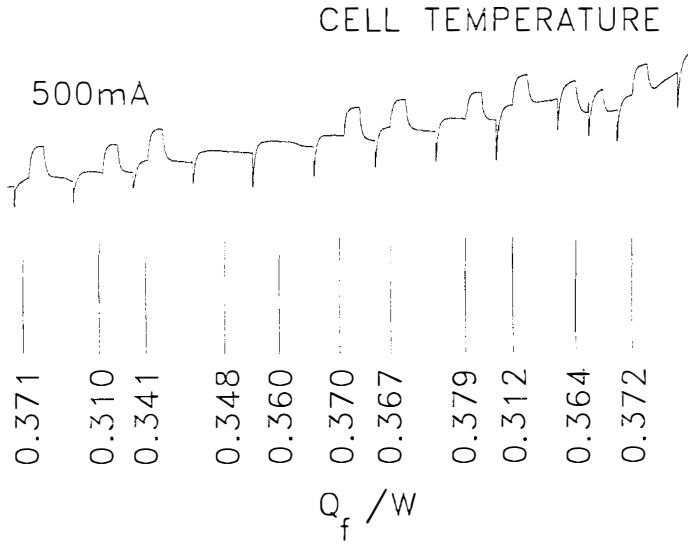

Fig 5B. Enlargement of a section of Fig 5A.

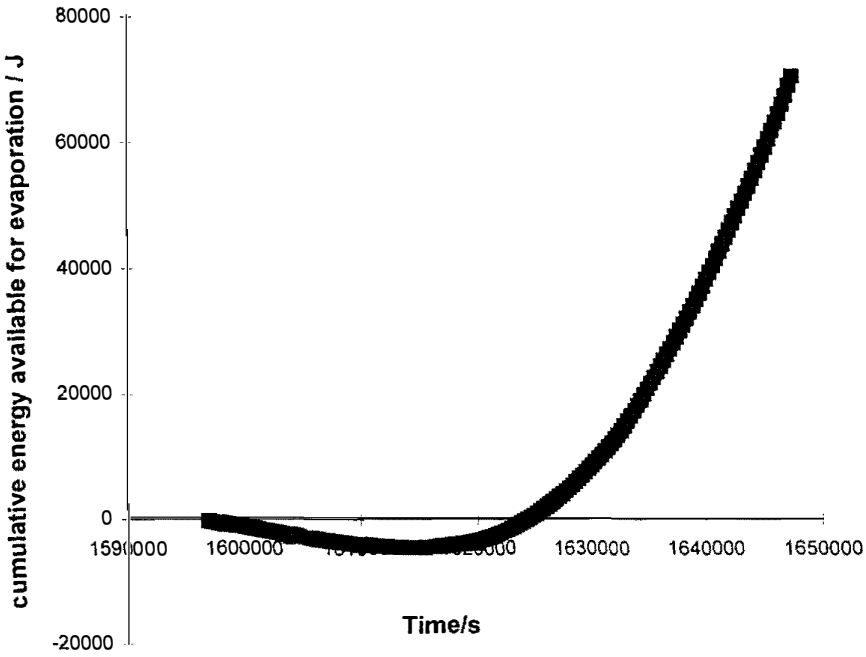

Fig 6. The cumulative energy available for evaporation of D_2O for the last period of operation of the experiment illustrated in Fig. 5A based on the assumption that there is no generation of excess enthalpy.

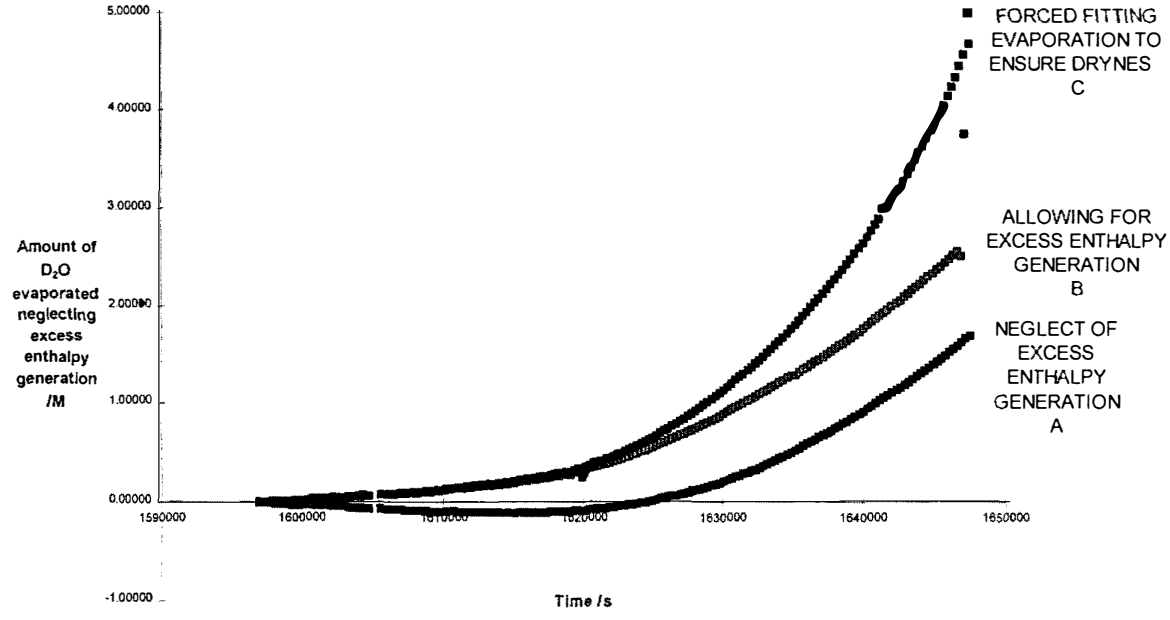

Fig 7. The variation of the evaporated D_2O with time for the last period of operation of the experiment illustrated in Fig 5A.
A: assuming that there is no generation of excess enthalpy
B: including the excess enthalpy calculated from the temperature-time and cell potential-time curves with P* given by the atmospheric pressure
C: as B but with P* reduced to 0.953 bar to force fit the evaporation to be completed during the last period of operation of the experiment.

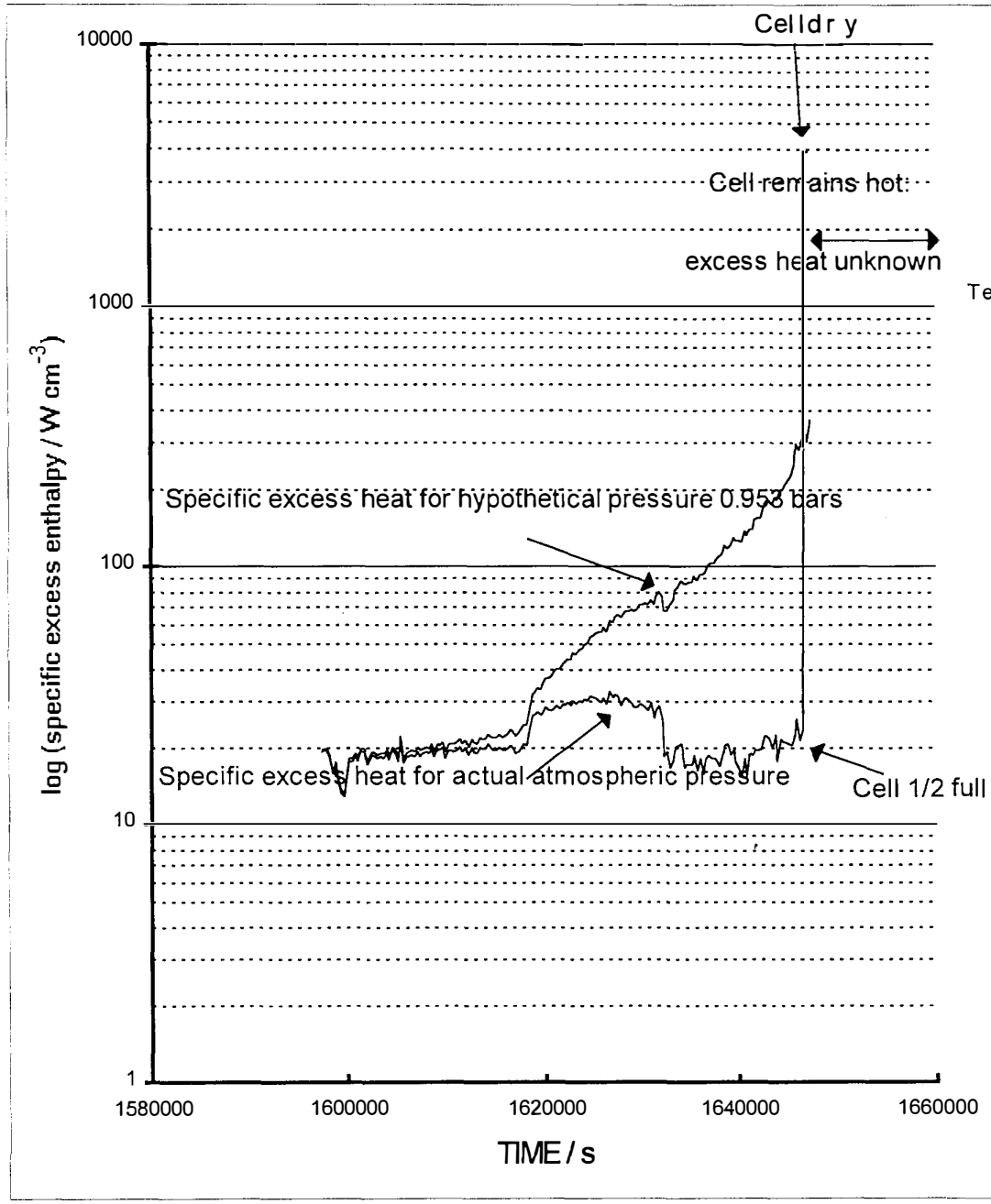

Fig 8. The variation of the rate of excess enthalpy generation with time for the assumptions B and C used in the construction of Fig 7.

Fifth International Conference on Cold Fusion
9-13 April, 1995 - Monte Carlo, Monaco
ICCF5 ©1995

The Experimenters' Regress

M. FLEISCHMANN
IMRA S.A. Science Center, 220 Rue Albert Caquot, Sophia Antipolis, 06560 Valbonne, France

Introduction

At the beginning of any new and controversial field of investigation, we cannot tell which of the following two statements is true:

A. "Positive" conclusions are correct; "negative" results are due to bad experimentation.
B. "Negative" conclusions are correct; "positive" results are due to bad experimentation.

This is the basis of the Experimenters' Regress, a concept drawn from the field of the Sociology of Science, e.g. see (1). As scientists, we also need to examine the possible validity of the following statement (as well as its corollary):

C. Key "negative" conclusions have been due to incorrect evaluations/interpretations; the results in fact point to "positive" conclusions.

If statement C applies, then the Experimenters' Regress should be seen to be substantially broken (Sociologists would not agree with this view because their judgements are made in terms of the public perception of fields of study).

Sociologists of Science also express the following view, e.g. see (1):

D. A discovery is not made at a single point in time.

As Scientists, we might again wish to add some further statements, such as:

E. Interpretations are not completed at a single point in time.
F. Interpretations (and calibrations) are affected by our knowledge of the system being studied[1].

[1] Unfortunately, the process of data evaluation is frequently curtailed, partly because of the costs involved and partly because of the loss of the "raw data".

We can investigate the applicability of these ideas by considering some of the experimental results obtained by the research group based at Harwell (2) (this has been the key study which has been generally perceived to fall into category B.). Figs 1A and B are sections of experimental temperature-time plots for Cell 3 of the data sets (Cell containing a 6 mm diameter by 1 cm length Pd-cathode polarized at 0.298A in 0.1M $NaOD/D_2O$) and for Cell 4 (Cell containing a similar cathode polarized at 0.298A in 0.1M $NaOH/H_2O$); see also (3). Figs 2A and B are enlargements of the section containing the application of a heater calibration pulse (denoted by H in Fig 1A). The data for Cells 3 and 4 can be evaluated to give the "lower bound heat transfer coefficients, $(k_R')_{11}$" (4,5,6,7,8) such as those shown in Figs 3A and B. The decrease of $(k_R')_{11}$ with time shown in Fig 3B is expected because of the progressive falling level of the electrolyte (caused by the electrolysis) in the cell, Fig 4B, used in the Harwell study (these cells were not silvered in their top portions; contrast the cell design, Fig 4A, used in our current studies). We draw attention especially to the fact that superposition of the heater calibration pulse on the Joule heating due to electrolysis does not give any anomalous changes in $(k_R')_{11}$ indicating correct thermal balancing for this cell (i.e. no generation excess enthalpy). By contrast, $(k_R')_{11}$ for Cell 3, Fig 4A, does not show the expected decrease with time. We have to interpret this by assuming an overall decrease of a rate of excess enthalpy generation with time (4,5,6,7). However, we also see that the temperature-time curve for Cell 3, Fig 3A, shows one of the tell-tale signatures of "positive feedback" in the region of the heater calibration pulse. The temperature does not relax to the expected baseline following the completion of the calibration; the calibration pulse therefore increases the thermal output (compare (3)). Transient development and loss of "positive feedback" would be expected to lead to "bursts" in the rates of excess enthalpy generation. Evidence for such "bursts" is seen in the temperature-time record for Cell 3, as is shown by comparison of Figs 1A and B.

In view of the presence of these "bursts" as well as of "positive feedback", Fig 3A, we cannot obtain a valid calibration for Cell 3 from the heater calibration pulse (see especially (8)). For further evaluation of the data, we therefore have to search for special ways of calibrating this cell. One possible approach is to evaluate $(k_R')_{11}$ at the series of temperature minima, Fig 1A and B, and to use the decrease of $(k_R')_{11}$ with time determined for Cell 4, Fig 3B, to make estimates of $(k_R')_{11}$ for Cell 3 at times other than those of the minima. Fig 5B shows that this procedure evidently overestimates the decrease of $(k_R')_{11}$ with time because the cell becomes progressively endothermic (which contravenes the Second Law of Thermodynamics). Application of the same procedure to Cell 4 must therefore lead to an underestimate of the rate of excess enthalpy generation, Fig 5A. Moreover, this procedure necessarily resets the rate of excess enthalpy generation to zero at each successive minimum, i.e. we cannot detect any underlying progressive changes in these rates.

Discussion

We can consider the particular section of the results obtained in the Harwell study illustrated in this paper both from the qualitative and the quantitative point of view. As far as the qualitative interpretation is concerned, we observe that it is not

possible to observe increases in the cell temperature, Fig 1A, without invoking the presence of a source of excess enthalpy. Evidently statement C applies[2].

In view of the difficulties of achieving calibrations of the cells used in the Harwell study, we can at present achieve at best a semi-quantitative evaluation of the datasets. Such an evaluation shows that the "bursts" in the rates of excess enthalpy generation shown in Fig 5A are of the same order of magnitude as the steady-state rates we observed at comparable current densities in our first studies ( ). In those early studies we also observed prolonged "bursts" in the rates of excess enthalpy generation ( ). One possible reason for the persistence of these "bursts" in the Harwell study is that the electrodes were made of sintered metal of high purity (2). By contrast, the material which we have used in our ongoing programme has been cast from metal of somewhat lower purity. We believe that electrodes made of sintered metal may be especially liable to crack; formation of cracks must lead to deloading of the lattice (10).

We observe that the conclusion that there was no excess enthalpy generation in the Pd/D_2O system was reached in the Harwell study in the absence of any detailed evaluation of the temperature-time and cell potential-time series, even though the complexities posed by the particular cell design, Fig 4B, were recognised (2). The present and other more detailed investigations of the Harwell data sets (10), however, shows that excess enthalpy generation was in fact observed in that study, contrary to the conclusions reached by the authors (2). Evidently, it is necessary to take into account the statements E and F made above: interpretations of a given set of results are not completed at a single point in time and these interpretations are inevitably affected by our state of knowledge of the systems under study. It is this reinterpretation which leads us to C: the "negative" conclusion reached in the Harwell study was due to incorrect interpretations and the results in fact pointed to "positive" conclusions.

Acknowledgement

It is greatly to the credit of the research group at Harwell that they have made their "raw data" available for further study.

[2] The only alternative is to assume that there were malfunctions in the instrumentation. It is not possible to conclude that the instrumentation was operating correctly yet that there was no generation of excess enthalpy, which was the conclusion reached in the Harwell study (2).

References

1. H. Collins and T. Pinch, *The Golem*, Cambridge University Press, Cambridge, UK (1993).

2. D. E. Williams, D. J. S. Findlay, D. W. Gaston, M. R. Sene, M. Bailey, S. Croft, B. W. Hooten, C. P. Jones, A. R. J. Kucernak, J. A. Mason and R. I. Taylor, Nature, 342, 375 (1989).

3. M. Melich and W. Hansen in "Frontiers of Cold Fusion: Proceedings of the Third International Conference on Cold Fusion", Nagoya, Japan (21-25 October 1992) ed. H Ikegami, Frontiers of Science Series No. 4 (FSS-4) p397.

4. M. Fleischmann and S. Pons in "Frontiers of Cold Fusion: Proceedings of the Third International Conference on Cold Fusion", Nagoya, Japan (21-25 October 1992) ed. H Ikegami, Frontiers of Science Series No. 4 (FSS-4) p47.

5. Martin Fleischmann and Stanley Pons, Phys. Lett. A, 176, 118 (1993).

6. M. Fleischmann, S. Pons, Monique Le Roux and Jeanne Roulette in: Proceedings of the Fourth International Conference on Cold Fusion, Lahaina, Maui, Hawaii, U.S.A. (6-9 December 1993) T.E. Passell, Editor, Volume 1 page 1-1, EPRI TR-104188-VI.

7. M. Fleischmann, S. Pons, Monique Le Roux and Jeanne Roulette, Trans. Fusion Technology, 26, 323 (1994).

8. M. Fleischmann, "More about positive feedback; more about boiling", see the Proceedings of the Fifth International Conference on Cold Fusion, Monte Carlo (9-13 April 1995).

9. M. Fleischmann, S. Pons and M. Hawkins, J. Electroanal. Chem., 261, 301 (1989); 263, 187 (1989).

10. M. Fleischmann, S. Pons, M. W. Anderson, L. J. Li and M. Hawkins, J. Electroanal. Chem., 287, 293 (1990).

11. to be published.

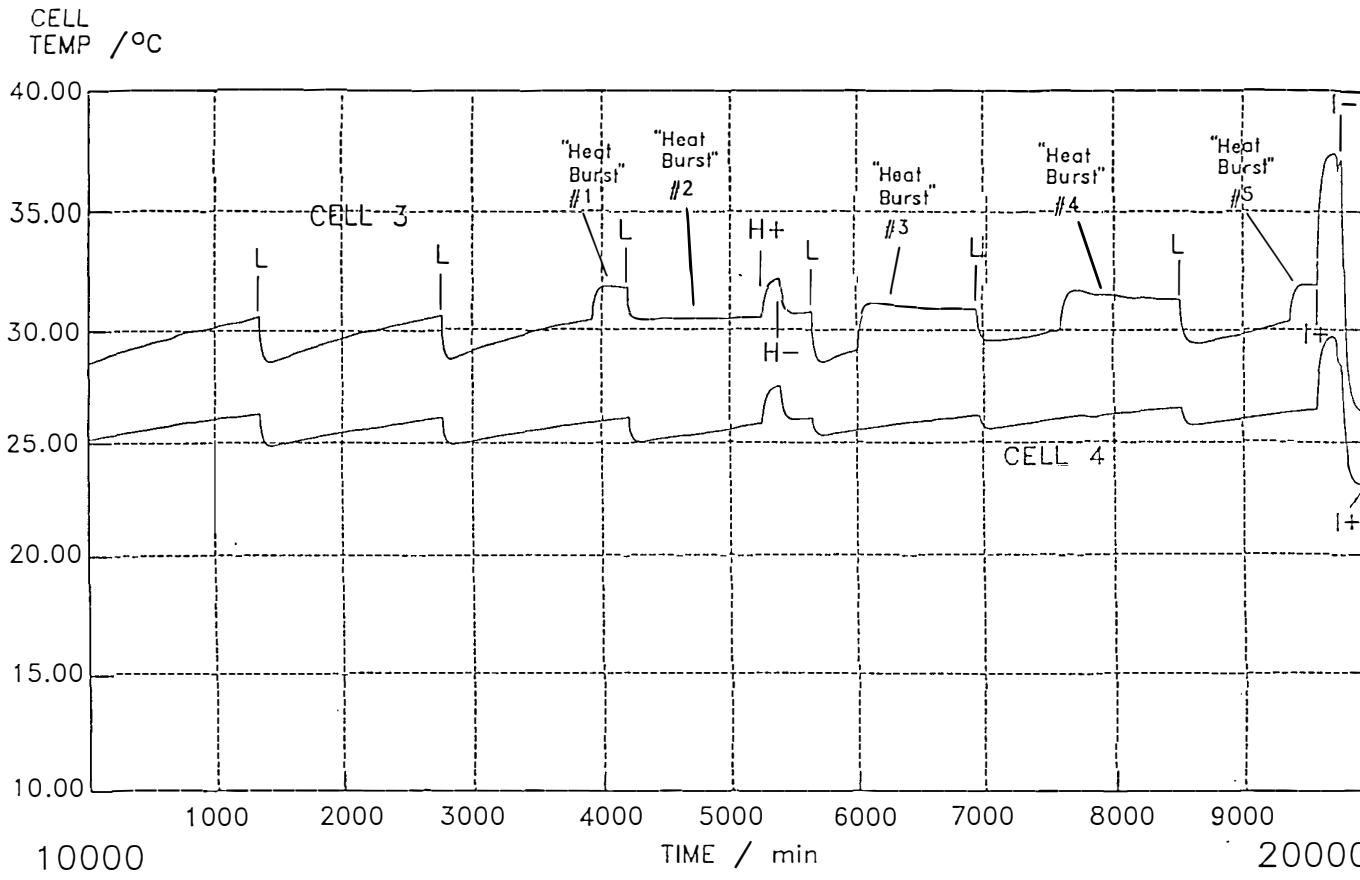

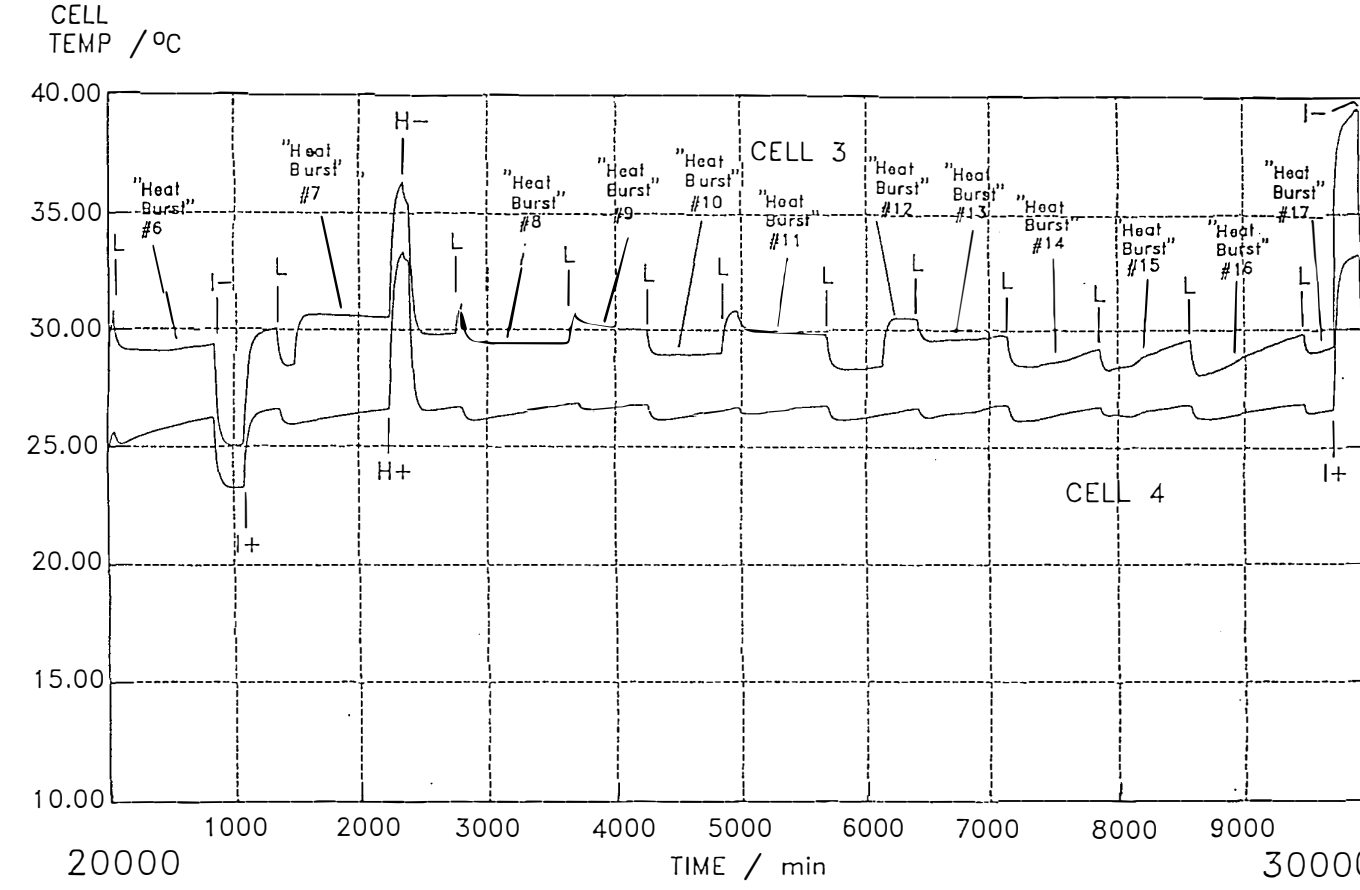

Figs 1A and B. Sections of the temperature-time plots for Cell 3 (containing a 6 mm diameter by 1cm length Pd-cathode polarized at 0.298A in 0.298A in 0.1M $NaOD/D_2O$) and Cell 4 (containing similar cathode polarized in 0.1M $NaOH/H_2O$).

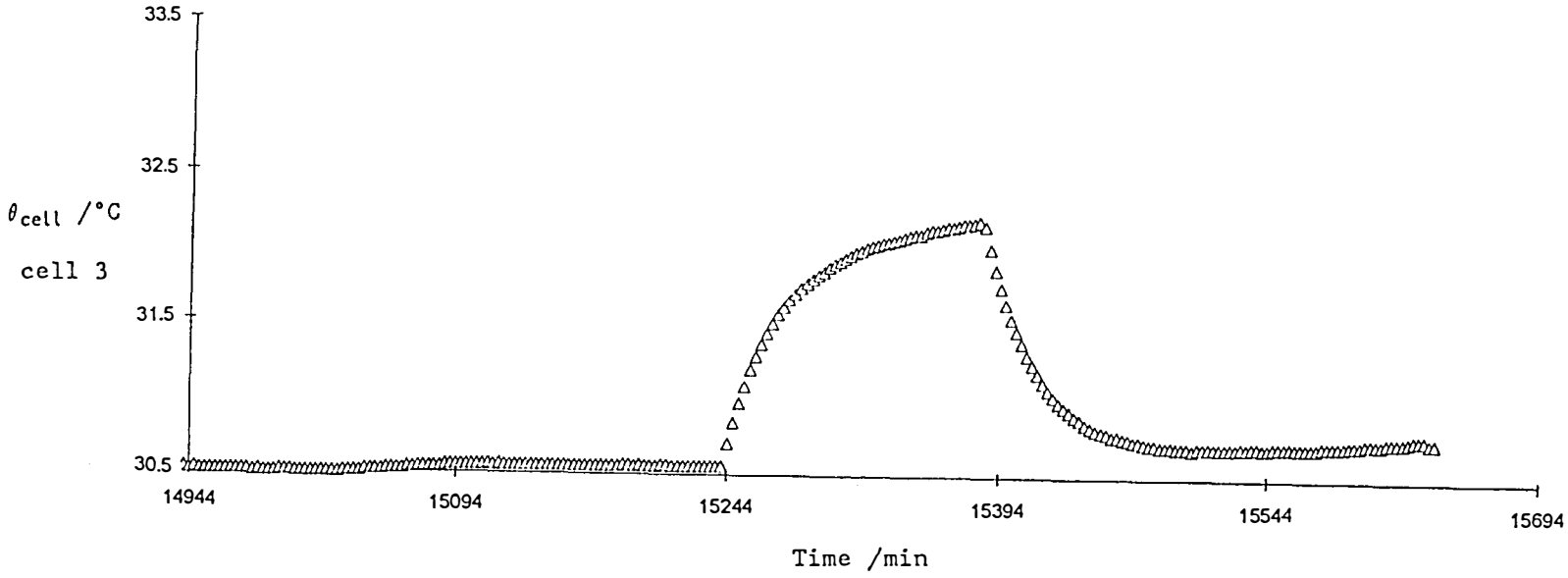

Fig 2A. Enlargement of the section covering the application of an heater calibration pulse to Cell 3 (denoted by H in Fig 1A).

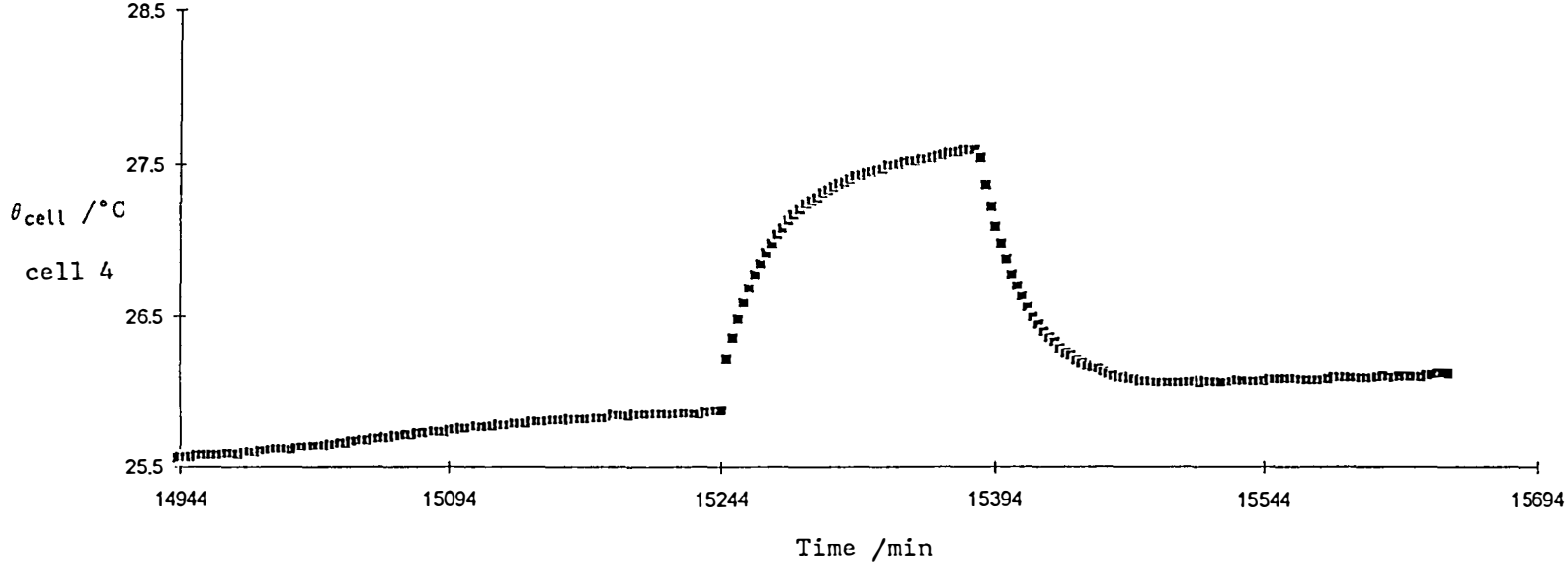

Fig 2B. Enlargement of the section covering the application of an heater calibration pulse to Cell 4 (denoted by H in Fig 1A).

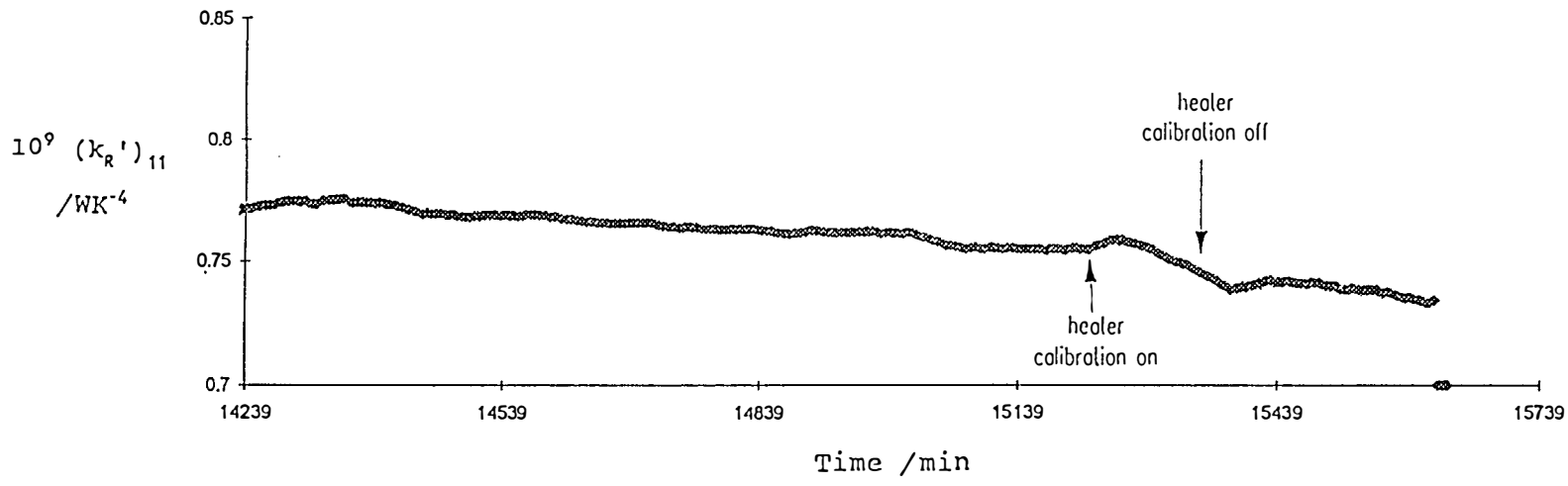

Fig 3A. The lower bound heat transfer coefficient, $(k_R')_{11}$, as a function of time for the section of data for Cell 3 illustrated in Fig 2A.

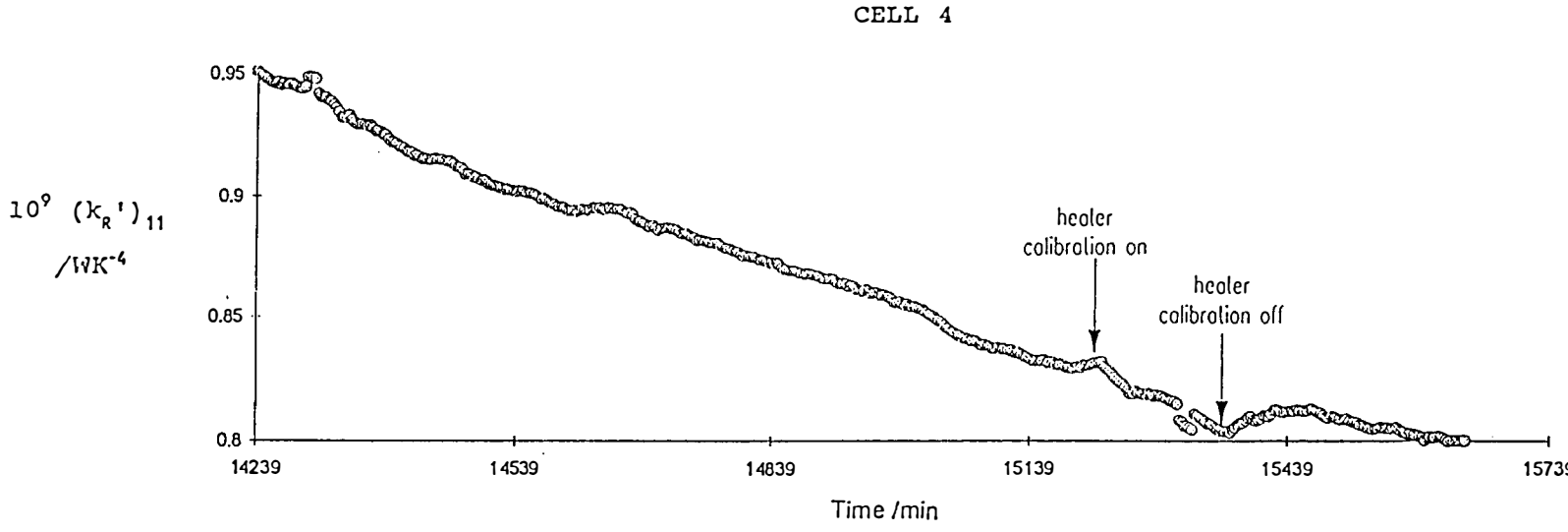

Fig 3B. The lower bound heat transfer coefficient, $(k_R')_{11}$, as a function of time for the section of data for Cell 4 illustrated in Fig 2B.

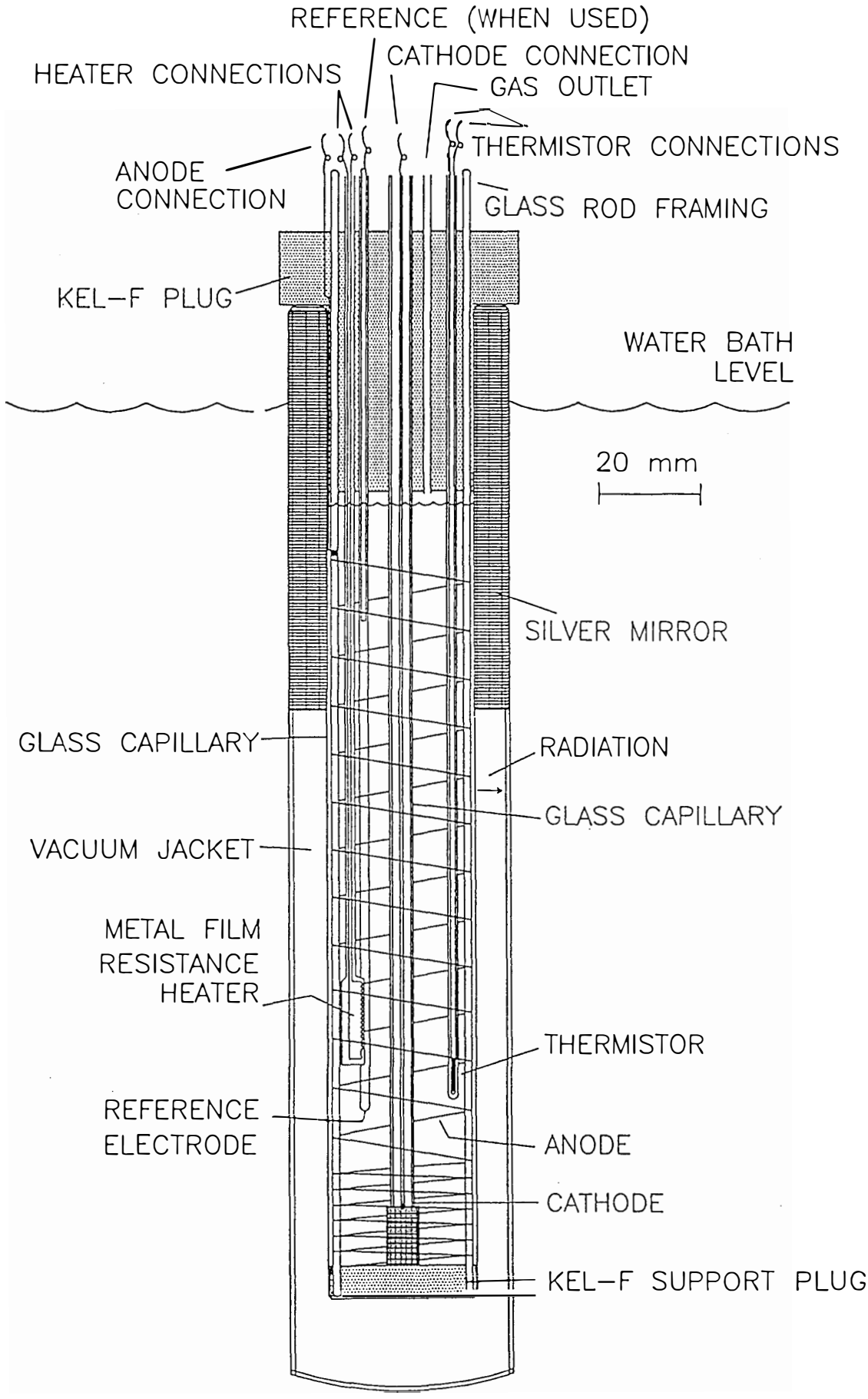

Fig 4A. The cell design used in current investigations at IMRA, Europe.

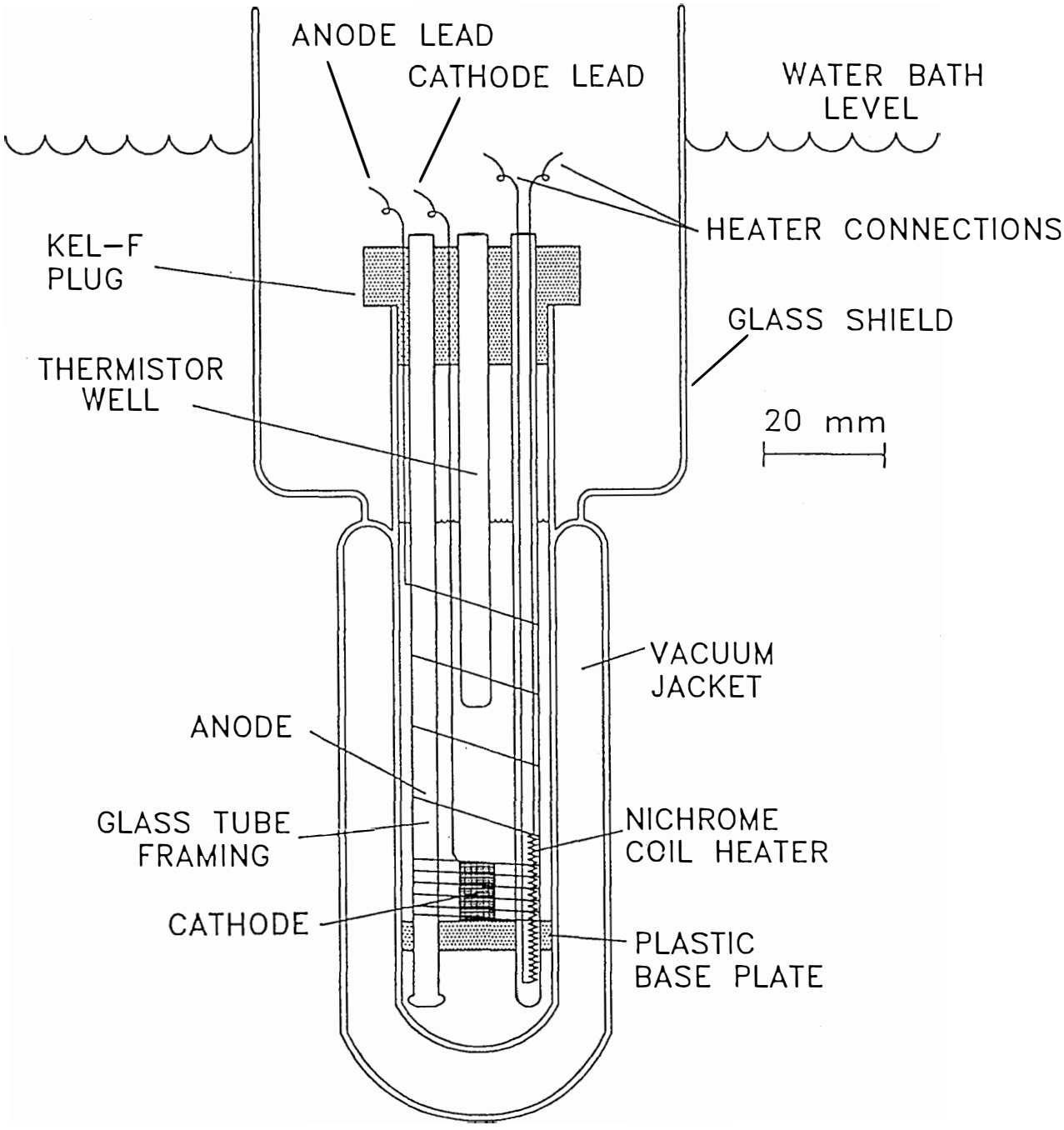

Fig 4B. The cell design used in the investigations at Harwell.

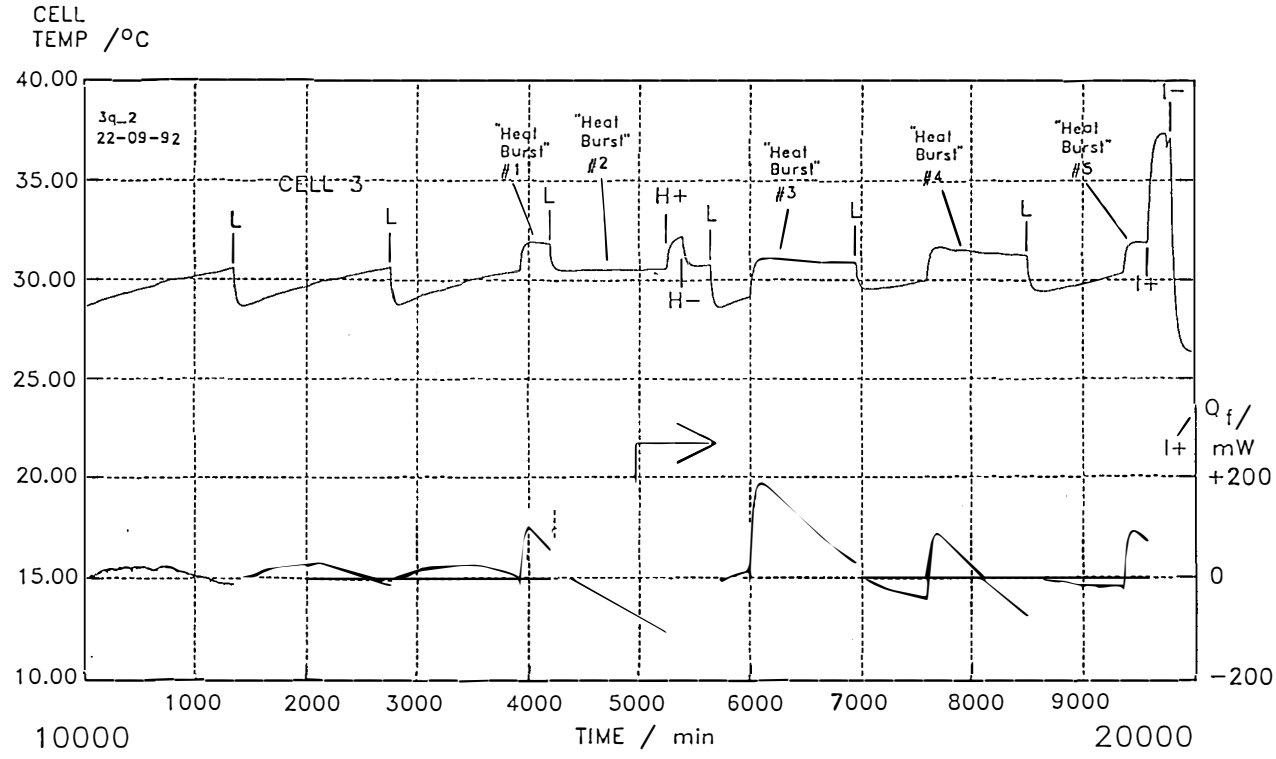

Fig 5A. The rate of excess enthalpy generation in Cell 3 derived using the lower bound heat transfer coefficients calculated according to the procedure outlined in the main text.

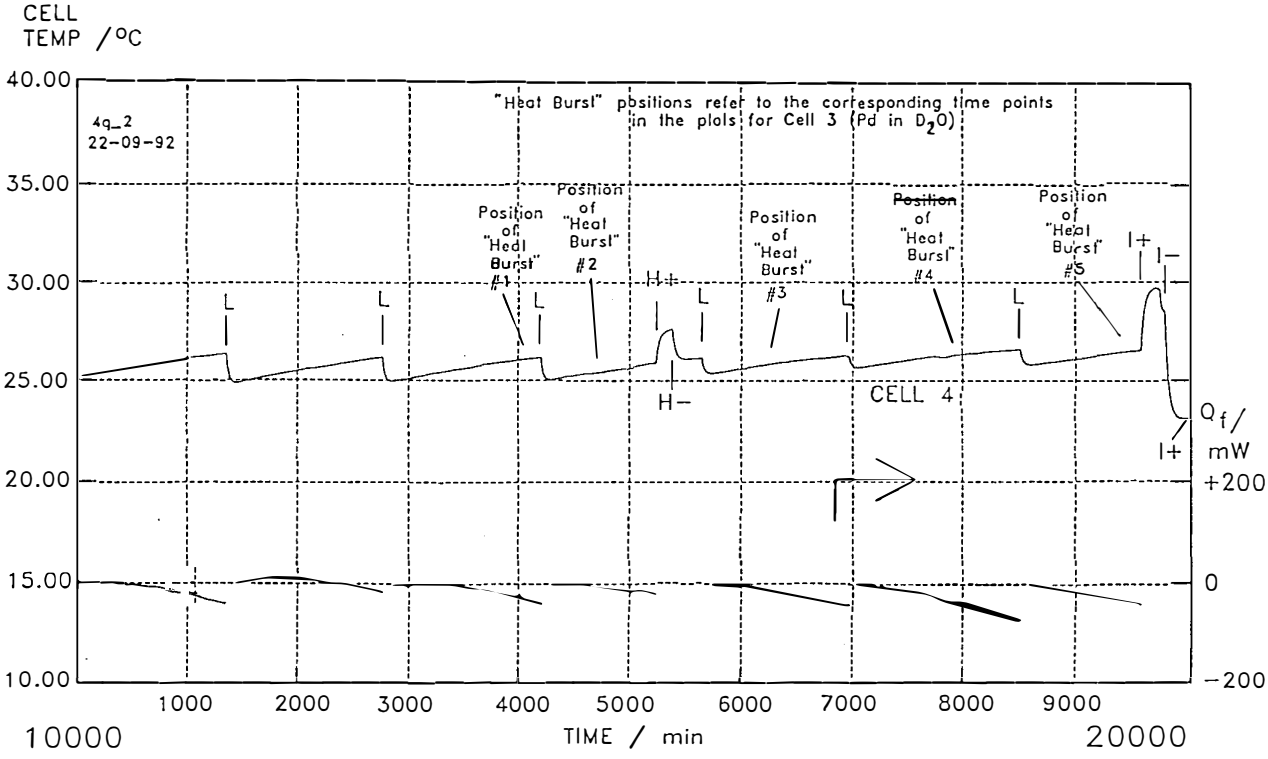

Fig 5B. The rate of excess enthalpy generation in Cell 4 derived using the lower bound heat transfer coefficients calculated according to the procedure outlined in the main text.

Session 3

Nuclear Measurements and Instrumentation

Fifth International Conference on Cold Fusion
9-13 April, 1995 - Monte Carlo, Monaco
ICCF5 ©1995

Some Experiments on the Decrease of the Radioactivity of Tritium Sorbed by Titanium

Otto REIFENSCHWEILER
Philips Research Laboratories, Eindhoven,
The Netherlands

Abstract

A sharp decrease of the radioactivity of tritium was observed when the hydrogen isotope is sorbed by small monocrystalline particles of titanium and the preparation is heated to several hundred degrees centigrade. In other experiments the concentration of tritium in such preparations was varied, showing that the radioactivity of the tritium increased less than proportionally to its concentration. A first attempt is presented to explain these remarkable effects in terms of a "nuclear pair hypothesis".

1. Introduction

In a recent letter [1] the author has given a short description and preliminary interpretation of experiments where a sharp decrease of the radioactivity of tritium was observed. The present paper describes these and additional experiments in more detail. By this procedure a high degree of evidence was obtained for the strange effect of the decrease of the radioactivity of tritium. I should like to recall that the experiments have been done many years ago in the course of technological projects.

2. Experimental

As described in ref. [1] titanium preparations were made by evaporation of the metal in argon at a pressure of 1 up to 2 cm Hg. By homogeneous nucleation small monocrystalline particles of titanium are obtained which are arranged in chains with many ramifications. By this procedure a very loose soot-like deposit is obtained. After pumping out the argon tritium is introduced and is sorbed with a time constant of about 10 s.

Two different measuring procedures are applied to determine the radioactivity of tritium. In one part of the experiments, the heating experiments described in this paper, a thin stainless steel or nickel window enables measurement of the x-radiation accompanying the β-decay by a GM tube (fig.1). In some other experiments the β-emission current is measured directly by a vibrating reed electrometer. While the first measuring procedure is applied for thick preparations, e.g. on an average about 80 Ti-particles thick, the second one can only be

applied for thin preparations, about one particle thick. An analysis of the measuring procedures is given in ref. [1]

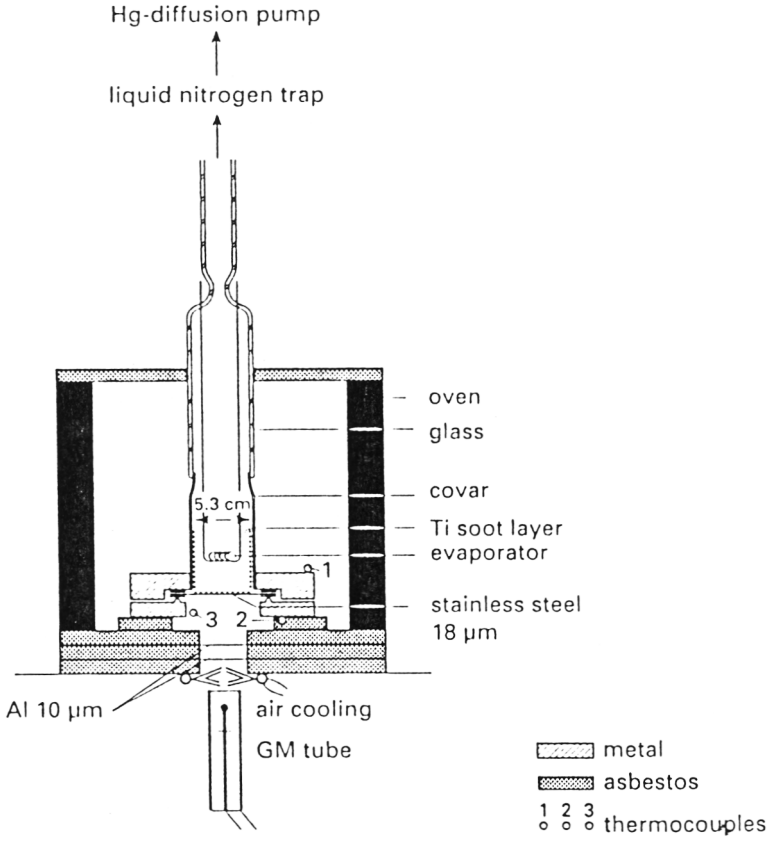

Fig.1. Experimental arrangement for measuring the β-radioactivity as a function of temperature via the x-radiation by a GM-tube.

3. Heating Experiments

The heating experiment presented in ref. [1] is described and evaluated in more detail in this paper.

In a preliminary experiment the pressure rise of tritium by heating a $TiT_{0,0035}$-preparation (48 mg Ti, 100 mC T_2) twice in a closed system was determined. Fig. 2 shows the result. With a first rise of temperature the tritium pressure (graph B) shows no increase at temperatures below about 350°C and then increases. With the second rise of temperature the tritium pressure (graph C) increases very much earlier at about 250°C. A possible explanation of this important phenomenon may be that the release of the tritium at the first rise of temperature is prevented by surface contamination [2], above all titanium oxide, which is dissolved in the metal during the heating up to 480°C at the first rise of temperature. This preliminary explanation has to be carefully investigated applying UHV-technique and definitely determined oxide layers. Such investigations should support our preliminary conclusion

that the pressure rise upon the second rise of temperature indicates the release of tritium atoms from their bonds to the titanium lattice.

In a most important heating experiment [1] an identical preparation is heated in the arrangement shown in fig. 1. Fig 2 graph A gives the count rate as a function of temperature. As stated in ref. [1] it is very strange that the count rate decreases sharply between 115°C and 160°C by 28% followed by a further slower decrease, reaching 60% of the initial value at 275°C and then rises to about the initial .value at 360°C. With a further increase of temperature the count rate decreases fast, which is due to decomposition of the preparation.

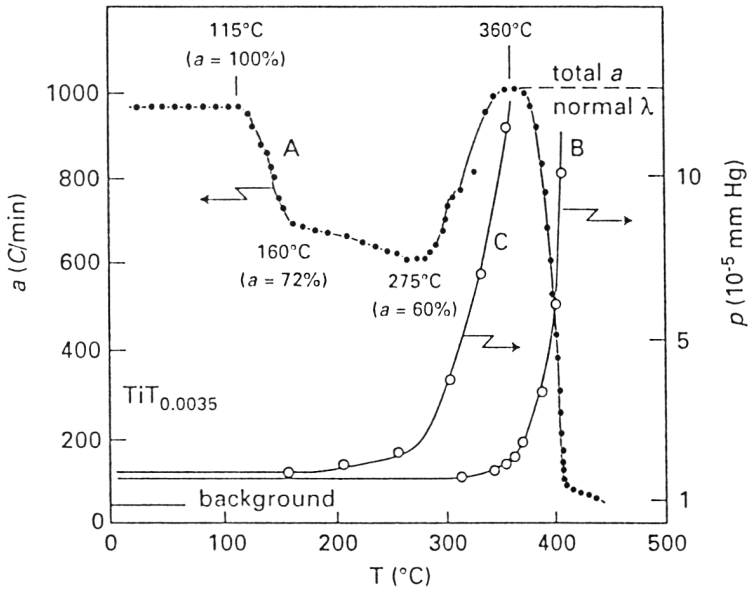

Fig. 2. As a function of temperature, $TiT_{0.0035}$-preparation:
Graph A: Count rate, pumped system.
Graph B: Tritium pressure at the first rise of temperature, closed system.
Graph C: Tritium pressure at the second rise of temperature, closed system.

The sharp decrease of the radioactivity above all between 115°C and 160°C, but also the further slower decrease between 160°C and 275°C, cannot be explained by decomposition of the preparation. This is clearly shown by graph B which represents the increase of the tritium pressure and hence the release of tritium upon a first rise of temperature: in such a preparation there is no measurable release of tritium below about 350°C, which is confirmed by many experiments. But the strongest argument that no tritium is lost at the first decrease of count rate between 115°C and 275°C is the fact that the radioactivity increases again between 275°C and 360°C to the initial value before decomposition of the preparation. Thus we arrive at the following preliminary conclusion:

In the temperature region between 115°C and 275°C a new compound of tritium is formed with a lower λ_T and with further increase of temperature this lower emitting compound is destroyed.

The re-increase of the count rate begins at the same temperature as the increase of tritium pressure at the second rise of temperature. This leads to the preliminary conclusion that the binding of the tritium atoms (nuclei) to the titanium lattice is a necessary condition for the decrease of the radioactivity. However the tritium atoms released from their bonds to the titanium lattice which exhibit normal λ cannot leave the titanium particles, as shown by graph B.

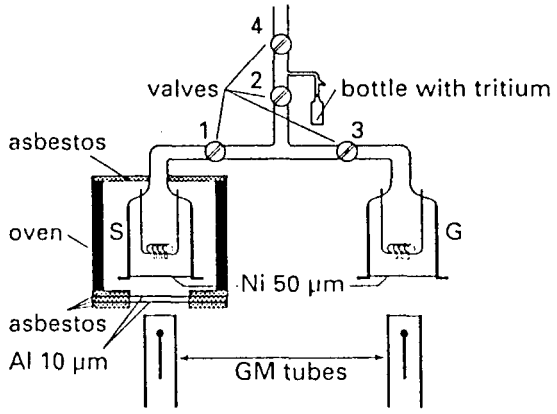

Fig. 3. Experimental arrangement with two tubes. Tube S contains a $TiT_{0.035}$-preparation at the beginning of the experiment and is heated in an oven. Tube G contains a finely divided Ti-preparation which absorbs the tritium released from preparation S.

In a further heating experiment a preparation with a 10 times higher concentration of the tritium (48 mg Ti,1 Ci tritium) is investigated. In this experiment the tritium is desorbed from the TiT0.035-preparation during heating on account of the higher concentration. Fig. 3 shows the experimental arrangement. The tritium which is released from the preparation in tube S (solid) is absorbed by an identical titanium preparation in a second tube G (gas) maintained at room temperature and the radioactivity is measured by a second GM tube. Fig. 4a shows the result. Graph S gives the count rate of tube S which is heated and graph g that of the second tube G remaining at room temperature which determines the amount of the released tritium gas. The count rate of tube S is constant up to about 210°C and then decreases steeply. This led to the preliminary conclusion that the tritium is desorbed from preparation S during heating.

To proceed to a more complete evaluation of this experiment we normalize the count rate of tube G to the same sensitivity as count rate S (fig. 4b). The count rate G gives the radioactivity of the tritium gas released from tube S and S+G is a measure of the total radioactivity. As can be seen a similar decrease and re-increase of the total radioactivity takes place as in fig.2, and the minimum of the radioactivity is attained at the same temperature of 275°C. If we attribute the decrease of the radioactivity only to the solid preparation of tube S we obtain graph S'.

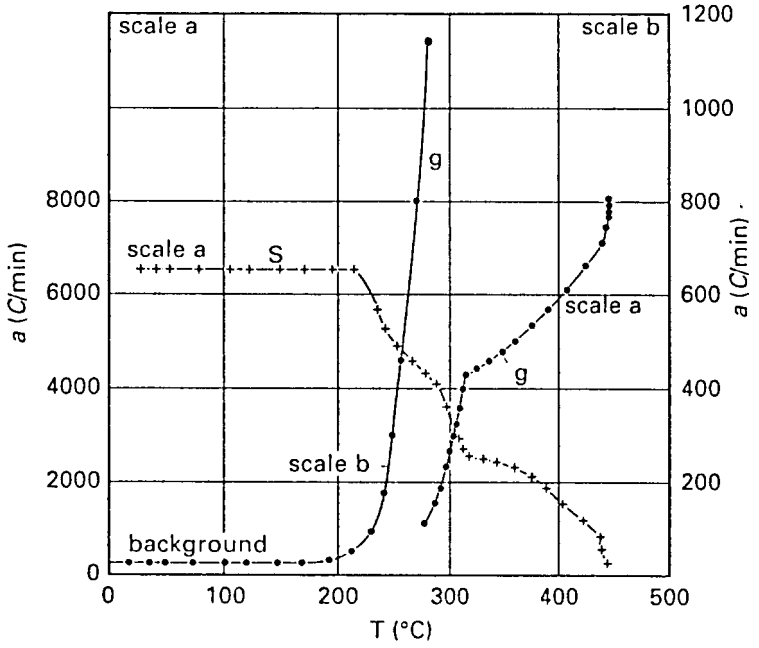

Fig. 4a. Count rate as a function of temperature
S: for tube S
g: for tube G

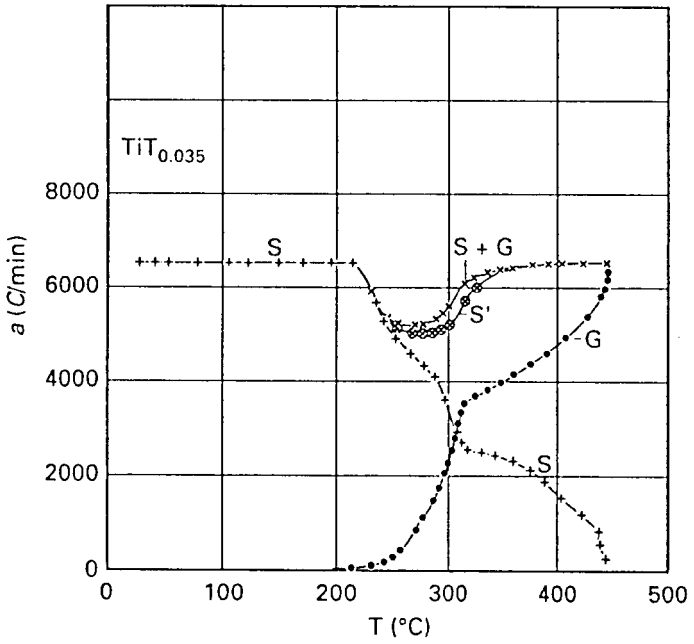

Fig. 4b. Radioactivity as a function of temperature
S: for tube S
G: for tube G
S + G: total radioactivity
S': remaining radioactivity in the preparation of tube S

Most interesting is the evaluation of the decrease of the radioactivity above 210°C. Between 210°C and 230°C the decrease of the radioactivity is 12.5 times higher than the amount of the released tritium and between 210°C and 242°C the corresponding value is 10.5 times higher. Thus the strong decrease of the radioactivity S above 210°C cannot be caused by the release of tritium from the preparation. This is a further strong argument for the decrease of the radioactivity during heating of our preparation above 210°C. That is just the beginning of the pure α-phase [3]. Then monocrystallinity of the small particles is regained which was disturbed by extremely small hydrid particles precipitated in the small TiT-α phase particles.

It can be shown that the course of $a = f(T)$ for the two heating experiments done under quite different conditions is equivalent. By evaluation of our first heating experiment we arrived at the preliminary conclusion that T-atoms (nuclei) must be bound to the titanium lattice to get a decrease of the radioactivity. In the first experiment (fig.2) the tritium atoms released from their bonds to the titanium lattice cannot leave the small titanium particles probably on account of surface contamination, above all oxidation. They have normal λ and the re-increase of the radioactivity above 275°C is due to these liberated tritium atoms remaining in the preparation. With the second experiment (fig 4) the tritium atoms released from their bonds to the titanium lattice leave the small titanium particles on account of the higher concentration. The total radioactivity re-increases in the same manner as with the first experiment. The only difference is that with the first experiment the tritium atoms which regain normal λ remain in the preparation and with the second experiment they leave the small titanium particles as a gas on account of the higher concentration.

It is most important to apply an oxide layer to the titanium particles or another means to prevent release of tritium from the Ti-particles in a heating experiment of the kind described in ref. [1] and fig.2 of this paper when working with UHV technique. It may be possible to distinguish between bulk absorption and chemisorption at the surface of the Ti-particles by performing experiments with a different degree of surface oxidation. It is recommended to apply in all experiments a second tube or another means to determine a possible release of tritium gas from the preparation.

Two other heating experiments, where the surface of the TiT_c-particles is oxidized by exposing the preparations to ambient air before heating, also distinctly show the effect. However the diminution of the radioactivity was not so strong as with the "clean" preparations (fig. 5). Especially interesting is the experiment with a $TiT_{0.065}$-preparation, with

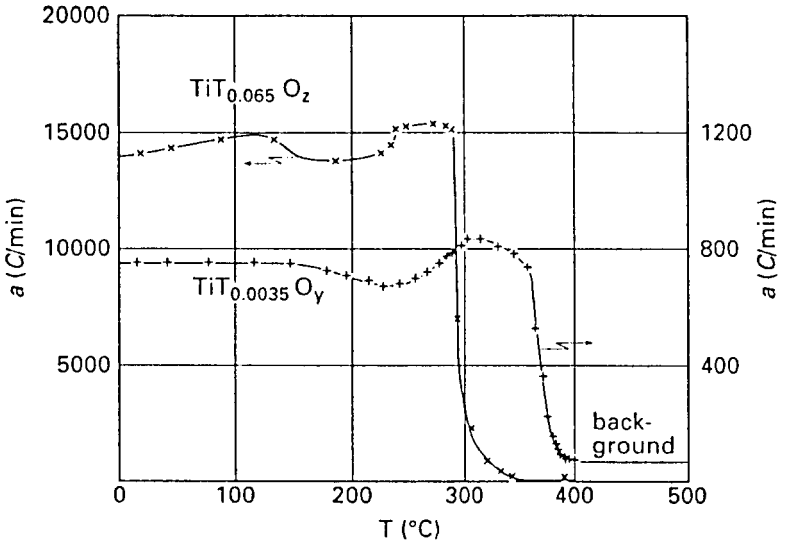

Fig.5. Count rate as a function of temperature for oxidized preparations.

a tritium concentration nearly twice as high as that of the experiment where the tritium was desorbed during heating. In this experiment the tritium remained in the preparation until the re-increase of the radioactivity occurred. Obviously the release of tritium was prevented by a strong oxide layer on the surface of the titanium particles. It seems furthermore that the oxidized surface layer (about 4 nm) of the small Ti-particles does not participate in the decrease of λ_T.

The release of the tritium atoms from their bonds to the titanium lattice can be prevented by maintaining an equilibrium pressure of tritium above the preparation. With this mode of operation we may expect a further decrease of the radioactivity. Such experiments provide confirmation or our preliminary conclusion that the binding of the tritium atoms to the titanium lattice is a necessary condition for the decrease of the radioactivity.

Up till now in all heating experiments the formation of the lower emitting compound occurred in the α-phase of the titanium-tritium system, thus with very low concentrations. It is extremely interesting to perform such experiments with higher tritium concentration, with the hydride phase TiT_c.

For a theoretical interpretation of the effect it may be important that the tritium atoms (nuclei) are bound in harmonic oscillator potential wells.

In a recent opposing note E. Wicke [4] argued that the decrease of the radioactivity *a* in fig. 2 is caused by migration of the tritium atoms from chemisorption at the surface to bulk absorption when the radioactivity decreased and conversely that it returns to the surface

upon the re-increase of the radioactivity. However the effect proposed in ref. [4] cannot explain the course of $a = f(T)$ presented in figs. 2 of this paper and of ref. [1]. On average about 80 Ti-particles are piled up in our titanium layer and the β-electrons are either completely stopped in the layer, or those which leave the layer enter it at another part of the tube wall. Thus the Ti layer and the upper part of the tube wall supporting the layer are a homogeneous source of x-radiation whose' intensity is proportional to the β-radioactivity of the preparation. Furthermore Wicke's argument cannot apply to the second heating experiment where the concentration of tritium strongly decreased during re-increase of the total radioactivity. A contra-note will be submitted for publication in the near future.

4. TiT_x.-Experiments

By our heating experiments we arrive at the conclusion that by heating TiT_c-preparations (c=0.0035; 0.035 and 0.065) a new compound of the tritium in the small titanium particles with a lower λ_T is formed. However there is no physical effect known that can account for the observed decrease of radioactivity.

It has been speculated that the decrease of λ_T in the small titanium particles may have something to do with the different phases of the TiT_c-system (a suspicion which has so far not been confirmed). Therefore experiments were undertaken to measure the radioactivity as a function of the concentration in such systems. The concentration was taken as independent variable x and the relating experiments are therefore indicated as TiT_x-experiments. In these experiments small accurately determind quantities of tritium were added successively to a thin finely divided titanium preparation and the increase of the emission current Δi was measured by a vibrating reed electrometer. The result of the most important experiment is shown in fig. 3 of ref. [1]. With increasing $x\,\Delta a/\Delta x$ first decreased reaching a minimum at $x \approx 3\times10^{-4}$ and then increased again to the initial value at $x \approx 5\times10^{-4}$. From this and further TiT_x-experiments a "nuclear pair hypothesis" was derived which reads explicitly:

Two tritium nuclei (identical nuclei with half integer spin) under certain conditions (in our case by embedding in small particles of titanium) arrange themselves in pairs with nuclear spin zero. Such a nuclear pair acts for the decay to a certain extent as the parent nucleus, so that the radioactive decay changes to a certain extent into a higher forbidden one.

The author would like to emphasize that the "nuclear pair hypothesis" is a *hyphothesis.* This implies that it is a first attempt to explain the strange effect of the decrease of λ_T. It is to be proved

or disproved by further experiments. Furthermore nothing has yet been said about the nature of the hypothetical nuclear pairs.

5. Concluding Remarks

There is a strong suspicion that the two different effects, cold DD-fusion and decrease of tritium radioactivity are caused by the same or a related fundamental principle: hydrogen isotopes, D or T, are sorbed in suitable metals and nuclear properties are changed in .a quite incomprehensible manner. It should be investigated if cold DD-fusion happens in preparations as used in our experiments at elevated temperatures. If so thermodynamic analysis may lead to a deeper understanding of the effect. The fact that sometimes cold fusion experiments with a positive result are not reproducible points to the existence of a hidden necessary condition. For the effect of λ-decrease of tritium such a condition may be monocrystallinity or another may be smallness of the metal particles. Both can be investigated experimentally. Also compact layers have to be investigated.

It may be interesting that in the experiment of M. Fleischmann and S. Pons [5] where excess enthalpy production was observed with deuterium absorbed in palladium analogous conditions for the formation of small $PdD_{0.6}$-particles (hydride phase) are present as for the formation of our monocrystalline particles: Increasing the concentration of deuterium above the end of the α-phase ($PdD_{0.01}$) one gets supersaturation of the α-phase, which results in homogeneous nucleation. This brings about formation of small monocrystalline particles of Pd-hydride. To get homogeneous nucleation the Pd-metal has to be very pure, a condition which is also necessary for the production of excess enthalpy as reported by the authors of ref. [5]. Otherwise one gets inhomogeneous nucleation with the formation of bigger and non-monocrystalline hydride particles. It is suggested that the microstructure and possible monocrystallinity of the palladium hydride suspended in the Pd-matrix should be investigated by metallographic techniques at different states of saturation.

With both effects, cold DD-fusion and decrease of tritium radioactivity, identical particles interact. The cold DD-fusion gives the possibility to check if such interactions are only possible between identical particles (indicated as "homo-interactions") or also between non-identical ones (indicated as "hetero-interactions"). If one gets neutron production in a cold fusion experiment by DD-reaction one has to repeat the experiment with a mixture of e.g. 50% deuterium and 50% tritium. If the reaction occurs between non-identical particles one has then to observe a high intensivity of 14 MeV neutrons from the DT-reaction. The result of such an experiment is very important for the

theoretical interpretation of the cold fusion effect. If the reaction happens only between identical particles many theories are ruled out.

Acknowledgments

I am gratefull to Professors H.B.G. Casimir, M.J. Steenland and M.J.A. de Voigt for their interest and encouragement and usefull comments. Special thanks are due to Dr. J.F. van de Vate, who collaborated with me on the heating experiments during a stay in my laboratory as a part of his scientific education.

References

1. O. Reifenschweiler, Phys. Lett. A., 184, 149 (1994).
2. H. Peisl in G. Alefeld and J. Völkl, editors, Hydrogen in Metals, Topics in Applied Physics Vol.1 (Springer, Berlin, Heidelberg, New York) 28, 63 (1978).
3. N.A. Galaktinova, Hydrogen-Metal Systems Databook, Ordentlich Holon (1980).
4. E. Wicke, Z. Naturforsch. 49a, 1259 (1994).
5. M. Fleischmann and S. Pons, Phys. Lett. A, 176, 118 (1993).

Fifth International Conference on Cold Fusion
9-13 April, 1995 - Monte Carlo, Monaco
ICCF5 ©1995

Evidence for Tritium genration in Self-heated Nickel Wires Subjected To Hydrogen Gas Absroption/Desorption Cycles

T.K. SANKARANARAYANAN, M. SRINIVASAN*
M.B. BAJPAI & D.S. GUPTA
Chemical Engineering Division, * Neutron Physics Division
Bhabha Atomic Research Centre
Trombay, Bombay - 400 085, India

Abstract

The loading characteristics of hydrogen gas in electrically self-heated nickel wires was investigated with a view to maximise hydrogen absorption and thereafter "trigger" it to generate anomalous excess heat as reported by Focardi et. al in early 1994. The nickel wires were found to absorb substantial quantity of hydrogen following several alternate cycles of absorption/desorption. But calorimetric studies conducted with the system so far indicate that we have not succeeded in triggering excess heat generation. However on dissolution and counting using standard liquid scintillation techniques, a number of hydrogen loaded nickel wires were found to contain tritium in the range of 3 Bq to 2333 Bq. This finding corroborates the detection of tritium in light water solutions electrolysed by nickel cathodes reported by the authors first at ICCF - 3 (Nagoya, 1992) and again at ICCF - 4 (Hawaii, 1993), confirming the occurrence of anomalous nuclear reactions in nickel-hydrogen systems.

Introduction

Focardi et al have reported[1-4] observation of anomalous "excess heat" generation in a "reproducible" manner, in a nickel rod (5mm dia x 90 mm long) subjected to repeated cycles of hydrogen gas absorption/desorption. In their experiments the nickel sample was heated by means of a platinum heater coil mounted around it. We report here attempts to replicate this so called "Piantelli experiment". In our experiments the nickel sample was taken in the form of an electrically self-heated wire (either 125 um or 380 um dia), 35 to 50 cm long. The self-heated wire method has the significant advantage that the wire temperature can be easily and precisely controlled through its resistance ratio (Rt/Ro), where Ro is the initial room temperature resistance.

For calorimetric measurements a double walled glass cell was employed. Coolant water was passed through the outer jacket in a once through fashion. A pair of RTDs mounted at the inlet and outlet of the water jacket measured the Delta T rise across the cell. Knowing the water flow rate in millilitres per minute, the heat dissipated in the cell could be easily measured and compared with the power input (product of voltage and current) to the nickel wire coil for detecting "anomalous" excess power production, if any.

Experimental Set up and Methodology

The apparatus comprised of a glass vacuum line provided with a rotary vacuum pump and a gas handling system incorporating a Toepler pump, intermediate gas storage reservoir etc. The cell in which the nickel wire was mounted in the form of a spring was made either of Pyrex or Quartz glass and was provided with a pair of tungsten electrical connecting leads. Iolar grade hydrogen gas was used for the absorption experiments. The absolute pressure of H_2 gas in the system was measured by a mercury manometer. The quantity of hydrogen gas absorbed/desorbed during a given cycle could be accurately measured by means of a sensitive silicone oil differential manometer. Fig.1 is a schematic diagram of the experimental set up.

At the outset the voltage-current characteristics of the nickel wires was studied both in vacuum and in H_2 gas. All the wire samples displayed a unique and characteristic shape for the V-I curve (See Fig.2), composed of three distinct regions :

Region I : $1.0 < (Rt/Ro) < 1.9$

Region II : $1.9 < (Rt/Ro) < 3.5$ (upto curie point)

Region III : $3.5 < (Rt/Ro)$ (above curie point)

Interestingly above the curie point the V-I curve was remarkably linear giving a normalised incremental resistance ratio ((dV/dI)/Ro, a dimensionless number) of ~(9.0 ± 1.0) in all cases.

Hydrogen Absorption Characteristics of Nickel

The first objective of the experiments was to study the hydrogen loading characteristics of nickel samples and optimise the procedure which will lead to maximum amount of net H_2 absorption. It is generally known that repeated cycles of loading/unloading has to be resorted to, to obtain high loading values. The procedure arrived at for this, after several trial runs, was as follows:

After degassing / annealing the Ni wire under dynamic vacuum at glow hot condition for about 5 minutes, Ro the initial resistance at room temperature is recorded. The surface of the wire is then "activated" by first annealing in air at low pressure and then introducing hydrogen gas under glow hot condition. After noting the initial H_2 gas filling pressure at room temperature, the wire is allowed to absorb hydrogen for about 10 to 15 hrs. As pointed out by Focardi et. al[1] we also find that the rate of gas absorption is somewhat faster if the nickel wire temperature is set at about 200°C to 300°C corresponding to Region II of the V-I characteristics. When the absorption has reached a saturation value, a cycle of desorption is commenced by evacuating the system and taking the wire to glow hot condition. The quantum of absorption or desorption is measured using the silicone oil manometer. Fig.3 shows a typical variation of the net amount of H_2 gas absorbed by a nickel wire as a function of the absorption/desorption cycle number. In Fig.3 odd numbers on the X-axis correspond to absorption cycles (open circle points) and even numbers to desorption cycles (crosses). It was generally observed that during 4 to 5 hours of desorption, approximately a third of the quantity of gas intake of the previous absorption cycle is released. Table I summarises the quantum of hydrogen gas absorbed, in units of centimetres of silicone oil, in some of the nickel wire samples studied by us. Only data for those wires which gave tritium are included in this table.

The quantity of H_2 gas absorbed in units of cm of oil can be converted into mass of H_2 gas loaded into the nickel wire, provided the volume of the cell plus the dead volume of the system are known. In our experiments for the case of a 60 ml volume cell, the effective system volume was measured to be ~68 ml, and hence 1 cm of pressure drop in the silicone oil manometer corresponds to ~5.3 μg of H_2 gas absorption in the nickel wire. Thus for the case of wire # Ni-27 (48.6 mg weight) for example, the net absorption as per silicone oil manometer reading of 436 cm of oil (see Table I) implies 2.3 mg of H_2 gas absorption. This corresponds to an average H/Ni loading ratio of 2.6 which is even higher than in NiH_2! Such a large loading ratio is obviously very difficult to believe.

In order to verify the exact magnitude of hydrogen loading in the Ni wires, some samples were got analyzed by an "inert gas fusion method". (This instrument melts the nickel and measures the quantum of hydrogen released into the flowing argon cover gas, through a calibrated conductivity technique). The inert gas fusion measurement however indicated a much lower value of H/Ni, in the region of a few hundred ppm only. We are currently investigating the possible causes for the large discrepancy in loading ratio between oil manometer and inert gas fusion results.That there is no basic flaw in the silicone oil manometer measurement was independently confirmed by loading hydrogen in Pd wires[5]. In the case of Pd, three different techniques of assessing the H/Pd loading ratio, namely resistivity method, oil manometer method and inert gas fusion method have all given comparable results.

However, it must be pointed out that even the several hundred ppm level of loading in nickel, indicated by the inert gas fusion set up, is much higher than the 10 ppm value quoted by D.P. Smith[6] for nickel, presumably obtained using "conventional gas loading" techniques. We speculate that the electrically self-heated wire method, is probably helpful in obtaining higher loading values.

Measurement of Tritium Content of Hydrogen Loaded Nickel Samples

The authors have earlier reported[7,8] observation of tritium in light water solutions of K_2CO_3, Li_2CO_3 etc electrolysed by nickel cathodes wherein hydrogen is loaded electrolytically into the nickel. As such it was suspected that tritium may also be generated during gas phase loading of hydrogen into nickel. To investigate this possibility, the loaded nickel wires in the present experiments were cut into 3 or 4 pieces of 8 to 12 cm length each and dissolved seperately in 5 ml of dilute (10%) HNO_3. At least 24 hours time was given to enable complete dissolution. Excess acid was then neutralised by adding AR grade anhydrous Na_2CO_3, and the solution distilled under partial vacuum using a microdistillation set up.

Standard liquid scintillation counting technique was adopted for measuring the tritium content of the distilled sample. For this 1 ml of the distilled water sample (derived from the nickel solution) was added to 10 ml of scintillation cocktail (mixture of toluene + Triton X-100 + scintillation chemicals) and counted in a scintillation counting unit, after allowing about 16 ~ 20 hrs for "chemiluminiscence" effects to decay.

So far 6 out of 9 loaded wires have indicated generation of tritium. However not all the cut pieces from a given wire showed tritium, suggesting that tritium production is not uniform over the length of the wire. For example, out of 27 cut pieces which have been dissolved and counted upto now, only 14 pieces were found to contain tritium. Table II summarises the tritium content of these cut wire samples. The

measured tritium activities range from 3 Bq to 2333 Bq. For the lowest activity case of 3 Bq (in 5ml of dissolved solution) the count rate was ~30% above the background value of ~250 counts/10 mins. The maximum tritium activity was observed in a 11 cm segment of Ni-27 wire which displayed exceptional absorption/desorption characteristics in terms of both rate as well as quantity of H_2 absorption (see Table I).

In the case of one of the cut pieces of wire # Ni-504 wherein the surface layers were leached out seperately prior to dissolving the balance portion, both the solutions (sample nos 504/5/I and 504/5/II) indicated presence of tritium. Blank (or control) samples cut from the two nickel stock spools (125 μm dia and 380 μm dia) dissolved and counted following an identical procedure have not given any counts above background levels.

Two cut pieces from two different loaded nickel wires when exposed sandwiched between a pair of medical X-ray films gave clear autoradiographic images. The images on the upper and lower photographic films were identical. The sample from one wire gave identical but weak spotty images, while the sample from the other wire gave images which were more intense though diffused.

At present we are not in a position to state whether these images are due to presence of tritium or some luminiscence type of phenomena observed in PdH_x [10].

Summary and Conclusions

Hydrogen loading characteristics of self-heated nickel wires have been investigated with a view to try and replicate the anomalous production of excess heat, first reported by Focardi et. al[1]. We seem to be obtaining bulk loading ratios of atleast a few hundred ppm. The loading ratio in the near surface region may be somewhat higher. We have however not been able to obtain the conditions necessary for the production of excess heat. About two thirds of the loaded nickel wires indicated presence of tritium on dissolution and counting in a liquid scintillation countinig set up, using standard procedures. Tritium generation is however found to be non-uniform along the length of the wire. The quantum of tritium in individual cut wire pieces was in the range of 3 to 63 Bq except for one wire segment which gave an unduly large amount of 2333 Bq. These results corroborate the generation of tritium reported earlier by us[7,8] as well as Notoya et al[9] during electrolytic loading of hydrogen in nickel cathodes. It is possible that a significant amount of tritium is getting lost from the wires during the desorption phase and hence it may be worthwhile to search for tritium in the gas phase also. A couple of loaded nickel wires have given clear autoradiographic images on medical X-ray film.

Although no excess heat has been detected by us to date, the occurrence of some anomalous nuclear process in hydrogen loaded nickel wires stands confirmed in view of the observation of tritium in several samples.

References

(1) Focardi, S. et. al "Anomalous Heat Production in Ni-H Systems", Note Brevi, Il Nuovo Cimento, Vol 107A, N.I, p153, Gennain 1994.

(2) Mallove, E.F., "News Report", Cold Fusion, Vol.1, No.1, p44, May 1994.

(3) Focardi, S., "Processi di Caricamento del Nichel, Ferromagnetici e Altrimetalli", Proc. Conf. on Status of Cold Fusion Research in Italy, Siena, Italy, March 24-25, 1995.

(4) Piantelli, F., "Evidence di Produzione di Calore e di Effetti nucleari nell'

esperimento di Siena", Proc. Conf. Status of Cold Fusion Research in Italy, Siena, Italy, March 24-25, 1995.
(5) Garg, A.B. et.al, "Protocol for Controlled and Rapid Loading /Unloading of H_2/D_2 Gas from Self-Heated Palladium Wires to Trigger Nuclear Events", Paper # 309, Proc. ICCF-5, Monte Carlo (Monaco), April 9-14, 1995.
(6) Smith, D.P., "Hydrogen in Metals", The University of Chicago Press, Chicago, USA 1948, p34.
(7) Srinivasan, M. et.al, "Tritium and Excess Heat Generation During Electrolysis of Aqueous Solutions of Alkali Salts with Nickel Cathode", Frontiers of Cold Fusion, Ed. H. Ikegami, Universal Academy Press, Inc. 1993, p123.
(8) Sankaranarayanan, T.K. et.al, "Investigation of Low Level Tritium Generation in Ni-H_2O Electrolytic Cells", Paper presented at ICCF-4, to Fusion Technology in 1994.
(9) Notoya, R. et.al, "Tritium Generation and Large Excess Heat Evolution by Electrolysis in Light and Heavy Water-Potassium Carbonate Solutions with Nickel Electrodes", Fusion Technol. Vol.26, p179, Sept. 1994.
(10) Rout, R.K. et.al, "Copious low energy emissions from Palladium loaded with hydrogen or deuterium," Indian Journal of Technology, 29, 5071, (1991)

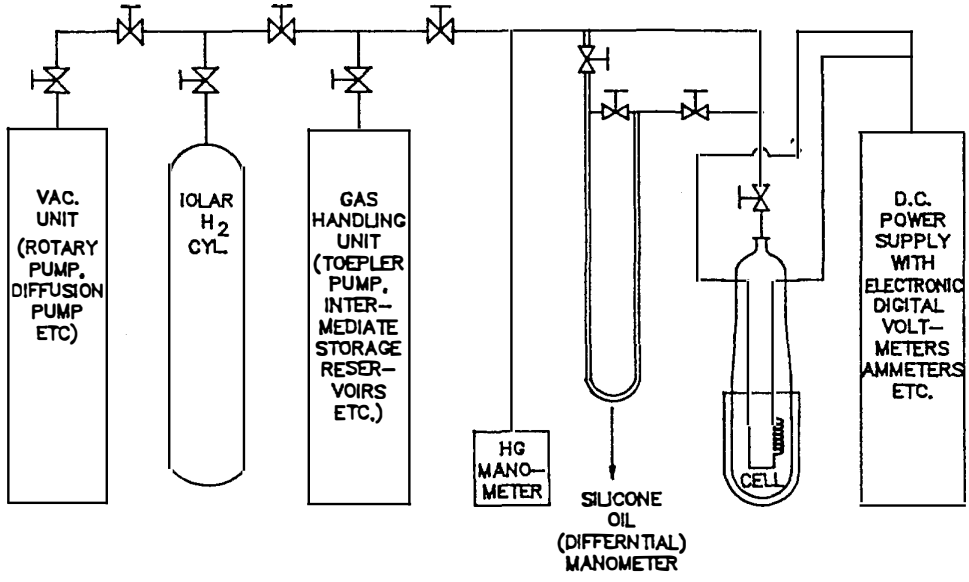

FIG.1: SCHEMATIC DIAGRAM OF THE EXPERIMENTAL SETUP

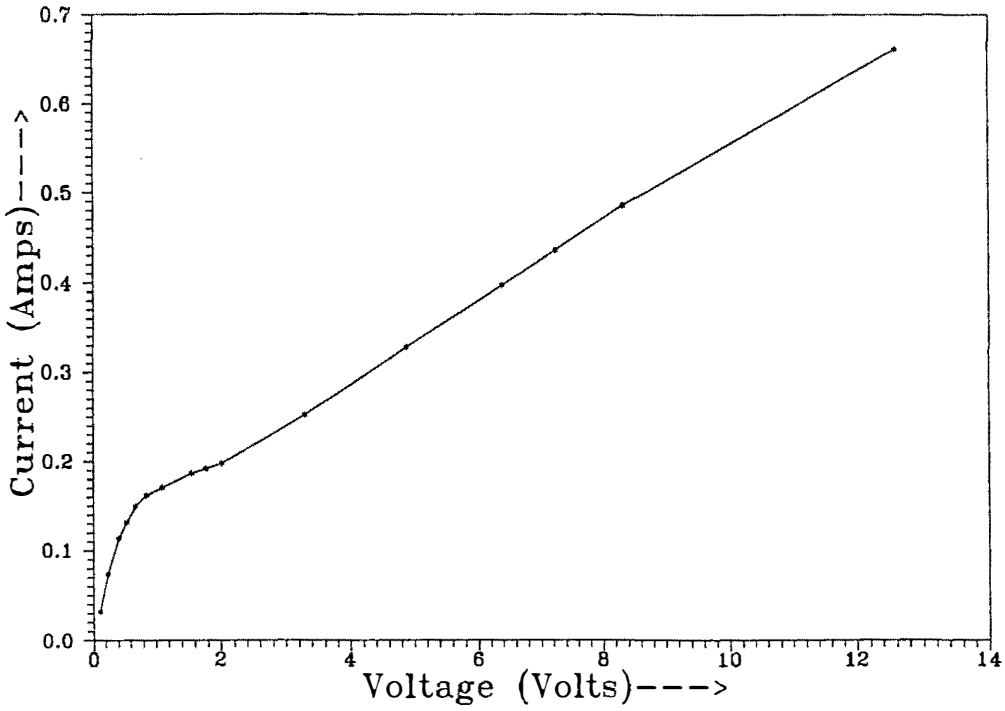

FIG.2 V–I CHARACTERISTICS OF Ni WIRE IN VACUUM

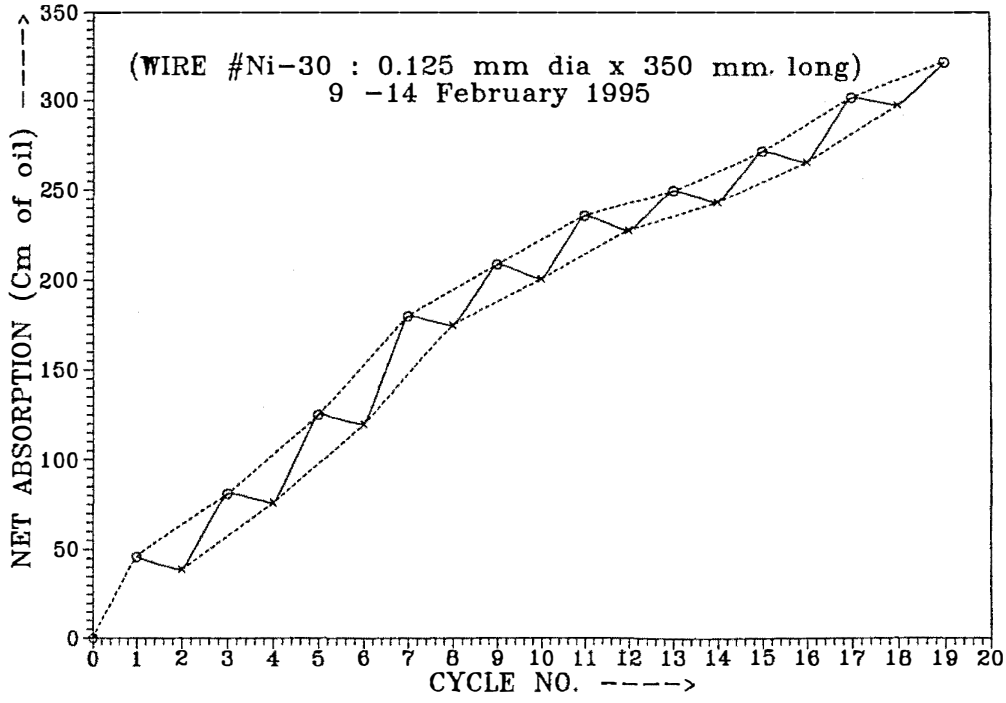

FIG.3 NET ABSORPTION OF HYDROGEN FOLLOWING REPEATED CYCLES OF ABSORTION/DESORPTION

Table 1.

QUANTUM OF HYDROGEN GAS ABSORPTION IN NICKEL WIRE SAMPLES THAT HAVE INDICATED PRESENCE OF TRITIUM

Sr. No.	Wire #	Dimensions Dia mm	length cm	Mass mg	Duration of loading	Number of cycles	Net Loading loading
1	Ni-23	.125	50	53.8	7th OCT to 13th OCT	5	*
2	Ni-501	.38	50	500	24th OCT to 27th OCT	5	125
3	Ni-504	.38	50	500	23th OCT to 9th DEC	15	203
4	Ni-24	.125	50	54.1	12th DEC to 15th DEC	5	58
5	Ni-27	.125	45	48.6	18th JAN to 25th JAN	6	436
6	Ni-30	.125	35	39.4	9th FEB to 14th FEB	10	325

* Not measured

Table 2.

OBSERVED TRITIUM ACTIVITY IN DISSOLVED CUT PIECES OF Ni WIRE SUBJECTED TO SEVERAL HYDROGEN ABSORPTION / DESORPTION CYCLES

Sr. No.	Dissolved Cut Wire Sample #	Average Excess Over Background Counts* per 10 minutes (1 ml Solution)	Total Tritium Activity in Cut Wire piece (5 ml Solution) (Bq)
1	23/1	313	13
2	501/1	532	22
3	504/4	152	6
4	504/5/I	70	3
5	504/5/II	103	4
6	24/1	440	18
7	24/2	690	28
8	24/3	1150	47
9	27/1	950	38
10	27/2	704	28
11	27/3	57650	2333
12	30/1	1560	63
13	30/2	220	9
14	30/3	550	22
15	Standard	4200	170

*Background count rate was approximately 250 counts in 10 minutes. 10 % in excess of BG represents limit of sensitivity

Fifth International Conference on Cold Fusion
9-13 April, 1995 - Monte Carlo, Monaco
ICCF5 ©1995

Observation of High Multiplicity Bursts of Neutrons During Electrolysis of Heavy Water with Palladium Cathode Using the Dead–Time Filtering Technique

A. SHYAM, M SRINIVASAN, T C KAUSHIK and L V KULKARNI
Neutron Physics Division,
Bhabha Atomic Research Centre
Trombay, Bombay 400 085, **India**.

Abstract

A series of experiments were carried out to detect production of neutrons from a commercial (Milton Roy) palladium–nickel electrolytic cell operated with 0.1 M LiOH or LiOD as the electrolyte at a current density of ≃ 80 mA/cm^2. Neutron emission was monitored using a bank of 16 BF_3 detectors embedded in a cylindrical moderator assembly. A dead–time filtering technique was employed to detect the presence of neutron "bursts" if any and characterize the multiplicity distribution of such neutron bursts. It was found that with an operating Pd–D_2O cell located in the centre of the neutron detection set–up, the daily average neutron count rate increased by about 9% throughout a one month period, over the background value of ≃ 2386 counts/day indicating an average daily neutron production of ≃ 2220 neutrons/day by the cell. In addition analysis of the dead–time filtered counts data indicated that about 6.5% of these neutrons were emitted in the form of bursts of 20 to 100 neutrons each. On an average there were an additional 6 burst events per day during electrolysis with LiOD over the daily average background burst rate of 1.7 bursts/day. The frequency of occurrence of burst events as well as their multiplicity was significantly higher with D_2O + LiOD in the cell when compared with background runs as also light water "control" runs.

1. Introduction

At the first annual conference on cold fusion[1], the authors had reported the results of multiplicity distribution analysis of neutron counts obtained from a commercial Milton Roy electrolytic cell operated with 5M NaOD. For this, counts obtained in 20 ms intervals from a bank of BF_3 counters embedded in a slab of hydrogenous moderator was statistically analysed. It was found that about 10 to 25% of the neutrons produced were in the form of bunches of 400 to 600 neutrons, the balance following Poisson statistics i.e. neutrons emitted randomly one at a time. But since the efficiency of neutron detection in those measurements was only about 1%, the probability of detecting more than one neutron out of a bunch of simultaneously emitted neutrons was extremely small for bursts of < 100 neutrons. Subsequent attempts in 1991, with a newly procured Milton Roy cell and using pulse shape discrimination method in conjunction with a proton recoil counter (threshold < 0.01 n/s), did not yield any evidence of neutron production. In this paper we report on further work carried out to detect and characterize neutron emissions from a large cathode area Pd–D_2O Milton Roy electrolytic cell using a high efficiency annular neutron detection apparatus. A novel dead–time filtering technique(1,2) was employed

this time to monitor and analyze burst neutron emission.

The experiments were carried out over a period of two months of which the first 15 days were devoted to background runs i.e. without cell. Electrolysis with LiOD was performed for the next 30 days while LiOH was used in the last 15 days to serve as "control".

2. Neutron Detection Set–up

The neutron detection system[3] comprised of a bank of 16 numbers of 50 mm dia, 300 mm long BF_3 counters embedded in a cylindrical plexiglas moderator assembly which could accommodate the electrolytic cell at its centre. An instantaneous burst of neutrons released into such a system is temporally stretched to a few tens of μs duration in the moderator owing to the statistical time spread inherent in the slowing down process. The detectors were arranged to form three independent channels as shown in Fig. 1. The outputs, from each of the preamplifiers contained in shielded boxes, was fed to spectroscopic amplifiers. A suitable window was selected in the single channel analyzers (SCA) around the peak region of the pulse height spectrum of the amplifier output. The output pulses from the SCA were passed through a dead–time unit to distinguish bunches of pulses within 100 μs of each other, by generating an output corresponding to the first such pulse and rejecting all subsequent pulses arriving during the preset dead–time of 100 μs (see Fig. 2). The data of six channels, corresponding to direct and dead–time filtered pulses from each of the three detector segments, was counted over 5s intervals and stored continuously by means of a personnel computer (PC) controlled scalar.

The neutron monitoring system had an overall detection efficiency of $\simeq$ 10% and an average background of $\simeq$ 0.048±0.002 counts/s (or $\simeq$ 172 counts/hr) which was more or less constant over a 15 day period. The preamplifiers and detector connections were hermetically sealed and specially designed to minimize electromagnetic disturbances. The entire set–up which was located inside a "Faraday cage" did not register any spurious counts even under the high humidity conditions of the Bombay monsoon season.

3. Electrolytic Cell and Experimental Protocol

The Milton Roy electrolytic cell consists of 16 numbers of tubular palladium cathodes with a total surface area of $\simeq$ 300 cm^2. A pair of outer and inner nickel tubes serve as anodes. The power supply was used in a constant current (galvanostatic) mode. For each case, the cell was run at a small current density of 20 mA/cm^2 on the first day for "conditioning", followed by operation at about 40 – 45 mA/cm^2 on the 2nd day. Thereafter the main electrolysis was carried out at a steady current of $\simeq$ 80 mA/cm^2. To compensate for losses due to electrolysis or evaporation, D_2O or H_2O, as required, was made up every morning.

4. Results and Discussion

Although data from the three segments of counters were recorded separately, prior to analysis, the counts data from all the three channels were summed up. The data of individual segments were used only to check for internal consistency. For each day, the 5s counts were totalized from all the 10,000 intervals. The total direct channel counts for each day for (a) no cell (detector set–up only) case; (b) electrolysis run using D_2O + LiOD and (c) electrolysis run using H_2O + LiOH are summarized in Tables 1(a) to 1(c). The tables also show the frequency distribution of 5s counts for multiplicities upto 8. The frequency

distribution expected for a Poisson distribution corresponding to the average background of each experiment, is indicated as Npd at the bottom of the Tables for comparison. The total counts for each day, listed in the last column of the tables, are shown plotted in Fig. 3. It is clearly evident that the average count rate has shifted up significantly during electrolysis with LiOD + D_2O, relative to the no cell case. During the experiment with light water however, there is a large variation initially and subsequently the average count rate comes down towards background level by the end of the experiments. The multiplicity distribution of 5s counts, integrated and normalized for a 30 day experimental duration for the three cases, are shown plotted in Fig. 4. While the electrolysis experiments are seen to contain counts with multiplicity of upto 8, the background run has a maximum multiplicity of 5 only.

The characteristics of burst events, obtained from the difference of direct and dead–time filtered counts of a given absolute time interval, are summarized in Tables 2(a)–2(c) for the three sets of experiments. The tables represent the multiplicity distribution of counts obtained in 100 us intervals following every neutron pulse which managed to trigger the dead–time gate. The data for the case of electrolysis using D_2O+LiOD solution (Table 2(b)) again shows several instances of high multiplicity burst events. (Data have been appropriately normalised to account for the fact that the duration of the D_2O experiment was twice that of the other two cases). The effect is more apparent when plotted (see Fig. 5) as day–wise variation of total burst counts, for all the three experiments. It is assumed here that in one 5s interval only one burst occurs (as the overall frequency is very small in comparison to the total numbers of intervals). Fig. 6 shows a plot of the number of events having a given multiplicity of counts per burst in a 100 μs interval over a 30 day period. Here again it is clear that with D_2O cell and to a lesser extent with H_2O cell, events with multiplicities as high as 4 to 7 are recorded whereas with background (no cell case) maximum multiplicity of counts observed is only 3.

5. Summary and Conclusions

The total neutron counts per day with the D_2O cell was found to be consistently $\simeq$ 9% above the background level. However in the case of the H_2O experiment, which was conducted immediately after a month long D_2O run, the average daily count rate was found to steadily decrease to background level (Fig. 3), suggesting that this behaviour can probably be attributed to the slow replacement of D by H, within the Pd cathodes over several days. The frequency distribution of 5s counts was close to Poisson distribution in case of background but contained several large multiplicity events in presence of the H_2O or D_2O cells (Fig. 4). Moreover while the background counts did not show even a single count with multiplicity of 4 or more throughout the 15 day period (Table 2(a)), there were several events with multiplicity of 6 and even 7 counts in the 100 μs duration data, in presence of H_2O or D_2O cells. On the whole the number of burst events were however very few, the average values being 1.7, 3.8 and 7.6 bursts per day for the cases of background, H_2O cell and D_2O cell respectively.

In the present experiment since the overall neutron detection efficiency was $\simeq$ 10%, one can say that approximately 10 neutrons are emitted by the electrolytic cell for every neutron detected. Likewise a multiplicity of 4 counts during a 100 μs interval implies emission of a burst of roughly 40 neutrons by the cell. Out of the 2608 neutrons detected per day (on an average) in presence of the Pd–D_2O cell, after subtracting the background of 2386, the balance of 222 counts/day can be attributed to the cell. Of this about 14.5 counts per day (see

Tables 2(a) and 2(b)) can be accounted for by high multiplicity (>20) burst neutron emission. Thus the conclusion from the present series of experiments is that about 6.5% of the neutrons produced by the Milton Roy electrolytic cell can be attributed to high multiplicity (> 20 neutrons/burst) events, and the balance 93.5% is produced either as single neutrons (with Poisson distribution) or with multiplicity of < 20 neutrons.

The present experiment thus once again confirms that a small component of the neutrons emitted by Pd–D_2O cells is produced in the form of temporally bunched neutrons. Any theoretical explanation of phenomena must account for this effect also.

References

1. Srinivasan, M., et. al, "Statistical Analysis of Neutron Emission in Cold Fusion Experiments" Proc. First Annual Conf. on Cold Fusion, March 28–31, 1990 Salt Lake City, Utah, USA, p175.
2. Degwekar, D.G. and Srinivasan, M., "A simple dead time method for measuring the fraction of bunched neutronic emission in cold fusion experiments",Ann. Nucl. Energy **17**, 583 (1990).
3. Shyam, A., et. al, "Technique to measure small burst of neutrons in presence of background of other radiations and electromagnetic interference", Ind. J. Appl. Phys. **32**, 837 (1994).

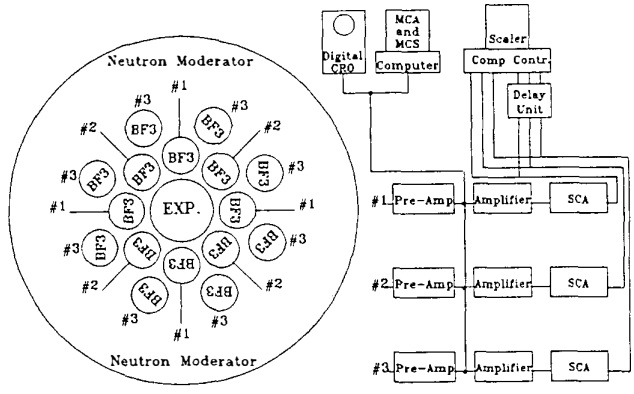

Fig.1
Schematic of Neutron Detection Set-up

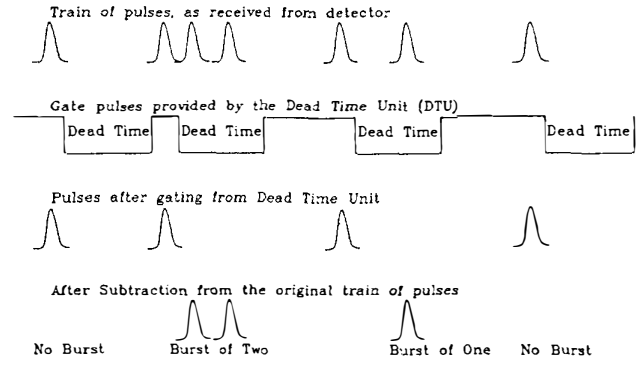

Fig.2
Principle of Burst Neutron Detection Using a Dead-Time Filter

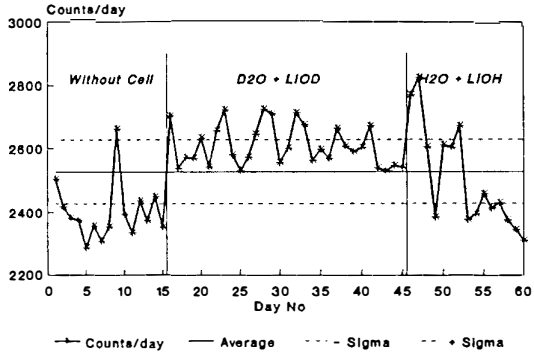

Fig.3

Day-wise Variation of Total Direct Channel Counts

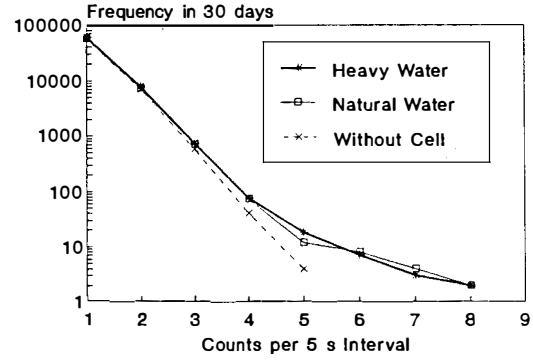

Fig.4

Frequency Distribution of 5 sec Counts Integrated (Normalised) Over 30 Day Period

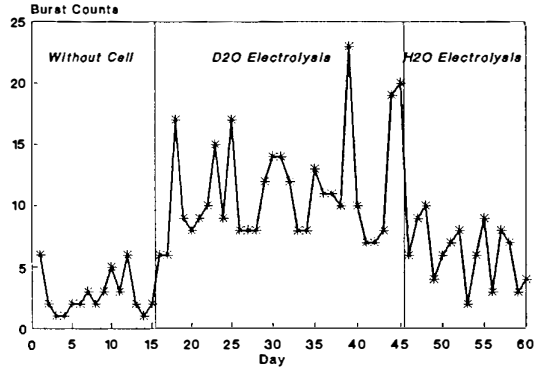

Fig.5

Day-wise Variation of Total Burst Counts

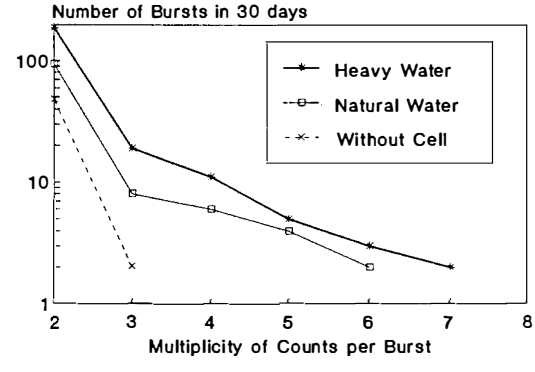

Fig.6

Frequency Distribution of Burst Counts Integrated (Normalised) Over 30 Day Period

Table 1. Direct Channel 5 sec Counts Data

1(a) : Background (No Cell) Case

Day	Frequency For Counts in 5 Second Intervals								
	1	2	3	4	5	6	7	8	Net
1	2001	228	16	0	0	0	0	0	2505
2	1877	231	25	1	0	0	0	0	2418
3	1864	222	23	1	0	0	0	0	2381
4	1808	245	20	4	0	0	0	0	2374
5	1836	195	17	1	1	0	0	0	2286
6	1800	257	13	1	0	0	0	0	2357
7	1793	222	21	2	0	0	0	0	2308
8	1816	249	10	2	0	0	0	0	2352
9	2012	280	30	0	0	0	0	0	2662
10	1847	236	21	2	1	0	0	0	2395
11	1822	229	18	0	0	0	0	0	2334
12	1883	243	20	2	0	0	0	0	2437
13	1873	220	19	1	0	0	0	0	2374
14	1895	244	21	1	0	0	0	0	2450
15	1876	207	18	2	0	0	0	0	2352
Tot.	27803	3508	292	20	2	0	0	0	35985
N_{pul}	28053	3415	277	16.9	0.82	0.033	0.001	$<10^{-4}$	

1(b) : With D_2O + LiOD

Day	Frequency For Counts in 5 Second Intervals								
	1	2	3	4	5	6	7	8	Total
1	2049	280	27	2	1	0	0	0	2703
2	1948	254	26	1	0	0	0	0	2538
4	1978	255	21	3	0	0	0	0	2572
4	1973	259	22	3	0	0	0	0	2569
5	2029	261	26	1	0	0	0	0	2633
6	1981	235	28	2	0	0	0	0	2543
7	2037	255	22	9	0	1	0	0	2655
8	2051	277	31	3	0	2	0	0	2722
9	1970	255	31	2	0	0	0	0	2581
10	1982	237	21	3	0	0	0	0	2531
11	1970	256	18	2	3	1	1	0	2572
12	1980	275	28	5	2	0	0	0	2644
13	1986	331	21	1	0	0	0	0	2724
14	2029	284	32	0	3	0	0	0	2708
15	1996	215	19	2	1	0	0	0	2556
16	1976	269	22	2	1	0	0	1	2601
17	2052	276	29	1	1	1	1	0	2713
18	1996	287	28	5	0	0	0	0	2674
19	1957	273	17	1	1	0	0	0	2563
20	1974	257	32	2	0	1	0	0	2598
21	1982	248	22	6	0	0	0	0	2568
22	2009	271	30	4	0	0	0	0	2663
23	2011	262	12	0	1	0	0	0	2606
24	1930	278	32	2	0	0	0	0	2590
25	1987	261	27	3	0	0	0	0	2602
26	1983	278	29	4	3	1	0	1	2671
27	1937	269	20	1	0	0	0	0	2539
28	1938	243	28	5	0	0	0	0	2528
29	1935	266	25	1	0	0	0	0	2546
30	1911	277	20	1	1	0	1	0	2540
Tot.	59570	7977	752	77	18	7	3	2	78253
N_{pul}	59966	7981	708	47.1	2.51	0.113	0.004	$<10^{-4}$	

1(c) : With H_2O + LiOH

Day	Frequency For Counts in 5 Second Intervals								
	1	2	3	4	5	6	7	8	Net
1	2082	302	26	0	1	0	0	0	2769
2	2100	301	32	4	2	0	0	0	2824
3	1996	242	35	3	0	0	1	0	2604
4	1836	246	17	1	0	0	0	0	2383
5	2020	249	31	0	0	0	0	0	2611
6	1930	285	30	3	0	0	0	0	2602
7	2024	271	27	6	0	0	0	0	2671
8	1894	208	18	3	0	0	0	0	2376
9	1836	226	22	6	0	1	0	1	2392
10	1824	277	23	1	0	1	0	0	2457
11	1895	223	22	1	0	0	0	0	2411
12	1913	220	19	3	0	0	1	0	2429
13	1867	223	17	1	0	1	0	0	2374
14	1822	225	21	2	0	0	0	0	2343
15	1839	195	16	3	3	1	0	0	2310
Tot.	28878	3693	356	37	6	4	2	1	37556
N_{pul}	29089	3716	316	20.2	1.033	0.044	0.002	$<10^{-4}$	

Table 2. Burst Counts Data For 100 us Intervals

2(a) : Only Counters, No Cell

Day	Frequency For Burst Counts						
	2	3	4	5	6	7	Total
1	5	0	0	0	0	0	10
2	1	0	0	0	0	0	2
3	0	0	0	0	0	0	0
4	0	0	0	0	0	0	0
5	1	0	0	0	0	0	2
6	1	0	0	0	0	0	2
7	2	0	0	0	0	0	4
8	1	0	0	0	0	0	2
9	2	0	0	0	0	0	4
10	4	0	0	0	0	0	8
11	2	0	0	0	0	0	4
12	3	1	0	0	0	0	9
13	1	0	0	0	0	0	2
14	0	0	0	0	0	0	0
15	1	0	0	0	0	0	2
Tot.	24	1	0	0	0	0	51

Total Number of Bursts 25
Average Number of Bursts/day 1.7

2(b) : With D_2O + LiOD

Day	Frequency For Burst Counts						
	2	3	4	5	6	7	Total
1	3	1	0	0	0	0	9
2	5	0	0	0	0	0	10
3	3	2	1	0	0	1	23
4	6	1	0	0	0	0	15
5	7	0	0	0	0	0	14
6	8	0	0	0	0	0	16
7	3	0	2	0	0	0	14
8	3	0	2	0	1	0	20
9	8	0	0	0	0	0	16
10	6	1	0	2	0	0	20
11	5	1	0	0	0	0	13
12	7	0	0	0	0	0	14
13	4	0	1	0	0	0	12
14	11	0	0	0	0	0	22
15	9	0	0	1	0	0	23
16	5	2	0	1	0	0	21
17	6	0	0	0	1	0	18
18	5	1	0	0	0	0	13
19	5	1	0	0	0	0	13
20	10	1	0	0	0	0	23
21	4	3	0	0	0	0	17
22	8	1	0	0	0	0	19
23	4	1	1	0	0	0	15
24	8	1	1	1	1	0	34
25	6	0	1	0	0	0	16
26	6	0	0	0	0	0	12
27	6	0	0	0	0	0	12
28	4	0	1	0	0	0	12
29	13	1	1	0	0	0	33
30	11	1	0	0	0	1	25
Tot.	189	19	11	5	3	2	529

Total Number of Bursts 229
Average Number of Bursts/day 7.6

2(c) With H_2O + LiOH

Day	Frequency For Burst Counts						
	2	3	4	5	6	7	Total
1	1	0	0	1	0	0	7
2	8	0	0	0	0	0	16
3	6	0	1	0	0	0	16
4	3	0	0	0	0	0	6
5	3	1	0	0	0	0	9
6	6	0	0	0	0	0	12
7	5	1	0	0	0	0	13
8	1	0	0	0	0	0	2
9	5	0	0	0	0	0	10
10	1	1	0	0	1	0	11
11	2	0	0	0	0	0	4
12	0	0	1	1	0	0	9
13	3	0	1	0	0	0	10
14	2	0	0	0	0	0	4
15	1	1	0	0	0	0	5
Tot	47	4	3	2	1	0	134

Total Number of Bursts 57
Average Number of Bursts/day 3.8

Fifth International Conference on Cold Fusion
9-13 April, 1995 - Monte Carlo, Monaco
ICCF5 ©1995

Observation of Nuclear Products under Vacuum Condition from Deuterated Palladium with High Loading Ratio

Takehiko ITOH, Yasuhiro IWAMURA,
Nobuaki GOTOH and Ichiro TOYODA
Advanced Technology Research Center,
Mitsubishi Heavy Industries, Ltd.
1-8-1, Sachiura, Kanazawa-ku, Yokohama, 236, Japan

Abstract

Gas release experiments with a method of heating highly deuterated palladium metals (D/Pd=0.7 ~ 0.83) in a vacuum chamber to induce anomalous nuclear effects have been performed. Neutron emission and X-ray emission were observed in some cases, and DT gas breeding with high reproducibility. DT gas breeding was correlative with D/Pd and degassing rate of deuterium gas. It shows that anomalous nuclear effects are related to D/Pd and diffusion process of deuterium atoms in palladium metals.

1. Introduction

Much research has been performed and many papers have indicated that nuclear reactions occur in deuterated palladium since the announcement of "cold fusion" phenomena by Fleischmann and Pons[1]. We previously reported performance of gas release experiments[2] in ICCF-4 and indicated neutron emissions and tritium productions from gas loading deuterated palladium samples (D/Pd≤0.66). We assume that key factors to induce the anomalous nuclear effects are as follows. First point is high D/Pd ratio. This factor is widely recognized as an important factor to cause nuclear effects. Second point is the diffusion process of deuterium atoms in palladium metals. In order to clarify the effects of these factors, we performed gas released experiments using electrochemical loading samples with high D/Pd ratio. Figure 1 demonstrates an outline

of the experiments. It consists of combined two parts. First part is the gas release experiments presented in ICCF-4. The aim of these experiments is to induce anomalous nuclear effects by the diffusion of deuterium atoms by heating deuterated palladium in a vacuum chamber. Second part is the sample preparation of deuterated palladium with high D/Pd ratio by electrochemical loading. Combining these two parts, we performed gas release experiments under the vacuum condition using deuterated palladium that has high loading ratio.

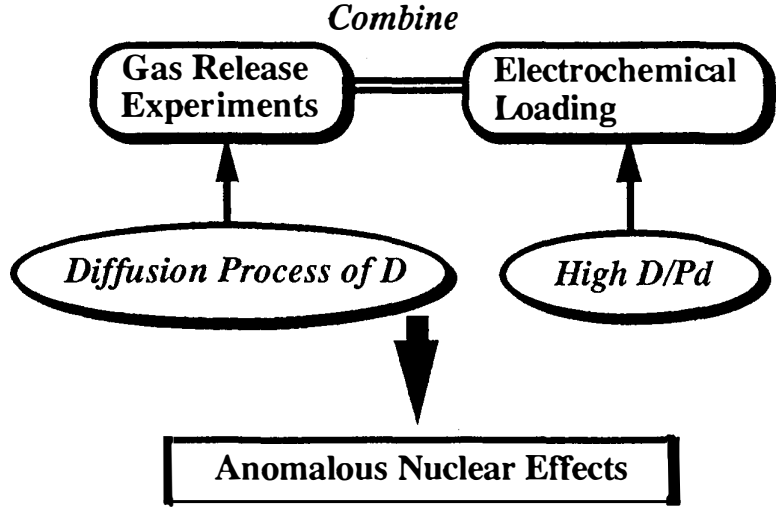

Figure 1 Outline of experiments

2. Experiment

An experimental procedure is as follows.

(1) Pre-treatment of a palladium sample.
(2) Deuterium loading
(3) Surface modification by Cu coating.
(4) Calculation of D/Pd ratio by measuring mass of the sample.
(5) Set the sample into the vacuum chamber.
(6) Evacuating the chamber (~10^{-6}Torr)
(7) Begin to measure neutron, gamma-ray, charged panicle, X-ray, pressure in the chamber, temperature of the heater and start up the quadrupole mass spectrometer.
(8) Heating the sample up to 393K
(9) Observation
(10) Heater off

Figure 2 shows an experimental device and procedure. A preparation of a deuterated palladium sample with high loading ratio was as follows. We heated a palladium rod (ø3 × 25mm: Tanaka Kikinzoku Kogyo K.K.) washed with acetone in a supersonic cleaning device in the air at 1173K for 2 hours to degrease from its surface. After that, we quenched the sample in pure water and set it in a D_2O-LiOD electrolysis cell. The cell was operated at constant current (0.1A) for 24 to 48 hours, and loading ratio of the sample reached about D/Pd=0.8. We electroplated the samples with Cu in Cu_2SO_4 electrolysis to reduce the rate of deuterium gas release and to maintain high deuterium loading ratio.

The sample was introduced into the vacuum chamber and set on a heater located in it. The chamber is equipped with two He-3 neutron detectors (EG&G Ortec: RS-P4-0806-207), two Silicon Surface Barrier Detectors (EG&G Ortec: CU-020-450-300) for charged particle spectroscopy, NaI scintillation counter (Bicron: 2M2/2) for gamma-ray spectroscopy, a CdTe (TOYO MEDIC: CDTE4BE) detector for X-ray spectroscopy and a high resolution quadrupole mass spectrometer (ULVAC: HIRESOM-2SM) for gas analysis. Neutron detectors surrounded with polyethylene modulators are used only for neutron counting. Counting system consists of preamplifiers (EG&G Ortec: 142PC), amplifier and single channel analyzer (EG&G Ortec: 590A) and counters (EG&G Ortec: 996) which are connected to a personal computer by GPIB interface. As for gamma-ray spectroscopy, we use a preamplifier (EG&G Ortec: 276), an amplifier (EG&G Ortec: 575A), and a multi-channel analyzer (SEIKO EG&G: MCA7800). X-ray spectroscopy system consists of a preamplifier (TOYO MEDIC: CT571P), an amplifier (TOYO MEDIC: 571M), and a multi-channel analyzer (SEIKO EG&G: MCA7800). We obtain energy spectra of charged particle using a preamplifier (EG&G Ortec: 142B) and amplifier (EG&G Ortec: 570), and a multi-channel analyzer (SEIKO EG&G: MCA7800).

All these devices are located in a clean-room where temperature and humidity are at constant levels (23°C±1°C,40%±5%) in order to prevent contamination and false counts induced by humidity in the air. Furthermore, we always monitor electrical signals from He-3 counters, charged particle detectors, and CdTe detector using digital oscilloscopes connected to personal computers to confirm that the signals originate from true nuclear events.

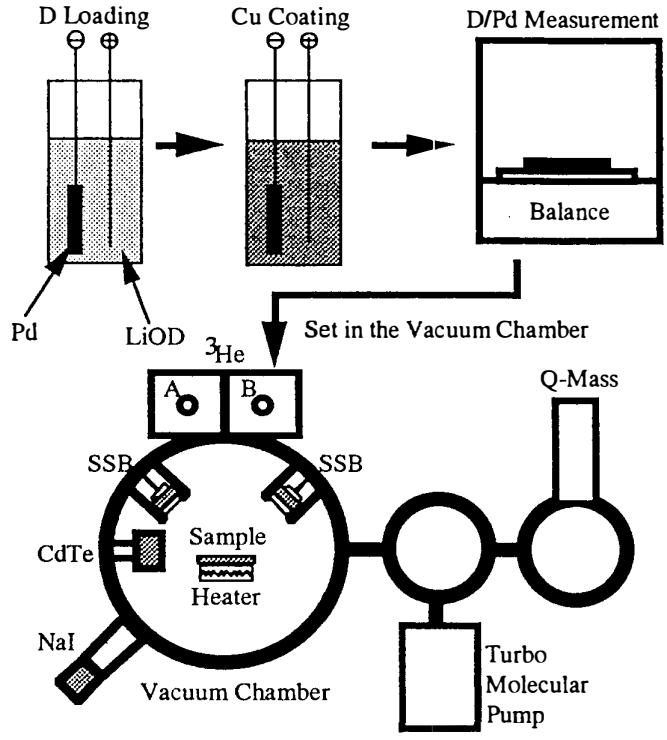

Figure 2 Experimental procedure and device

3. Results

Figure 3 shows an example (D/Pd=0.71) of experimental results of neutron emission.

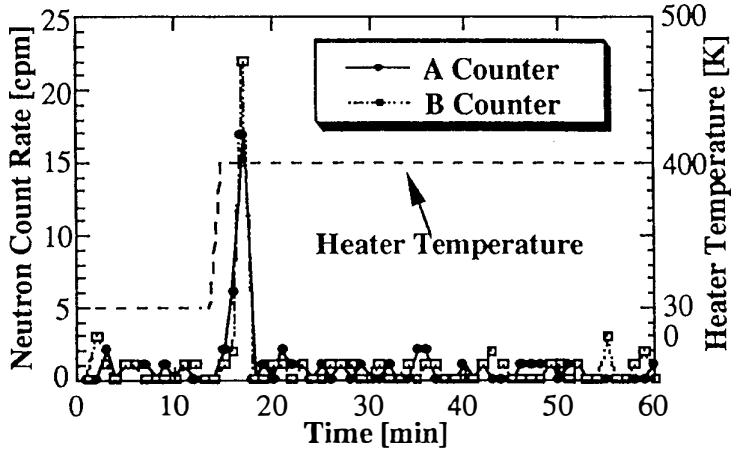

Figure 3 Neutron Emissions

At the beginning of evacuation, heater temperature equals to room temperature (296K), we can see only background neutron counting.With heating the sample up to 393K, a clear and prominent neutron emission peak is detected in both counters. If the neutron of the peak is due to fluctuation of background neutron, the probability is about 10^{-44}. Therefor, we consider that the sample emits neutron during heating.

Concerning observation of tritium production, we mainly watch behavior of mass number 5 gas by quadrpole mass spectrometer (Q-Mass). Mass number 5 gas detected by Q-Mass consists of DT and DDH^+. Regarding DDH^+, an electron attack of a filament of Q-Mass leads to formation of ion species DDH^+, and partial pressure of D_2 and H_2 determines the number of DDH^+. Figure 4 indicates DDH^+ formation in our vacuum chamber. Horizontal axis means total pressure (≈D_2 gas pressure) and vertical DDH^+ ion current, respectively. We, therefore, define DT gas breeding ratio as the ratio of mass number 5 ion current to DDH^+ ion current. If DT gas breeding ratio is larger than 1, it is considered that a sample releases DT gas. With using this breeding ratio, we can demonstrate tritium production detected by Q-Mass.

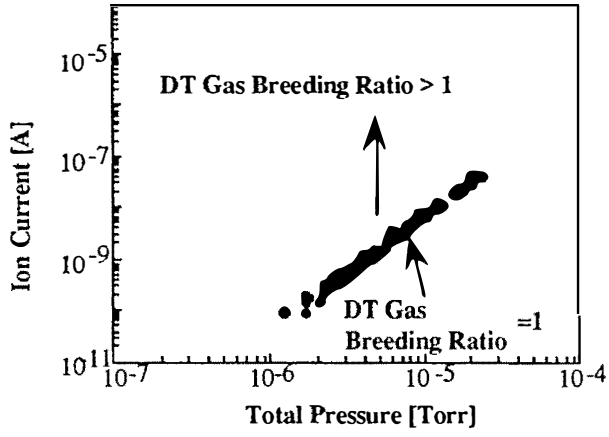

Figure 4 Formation DDH^+ in the vacuum chamber

Figure 5 shows time evolution of DT gas breeding ratio. D/Pd ratio of the sample is 0.83. At the beginning of evacuation, DT gas breeding ratio is about 1. However, we see the DT gas breeding ratio increases gradually during evacuation. At this time, it is considered that deuterium atoms in palladium diffuse toward outside, since a deuterium pressure gradient exists between inside and outside of the sample. Simultaneously, we observed X-ray emission as mentioned later. About 26 minutes after evacuating, we start heating up to 393K. Then the sample releases deuterium gas

rapidly, and DT gas breeding ratio increases at the same time. Although we cannot measure DT gas while the total pressure exceeds 3×10^{-5} torr since our mass spectrometer is not able to work, we consider that tritium atoms are produced during gas release by heating.

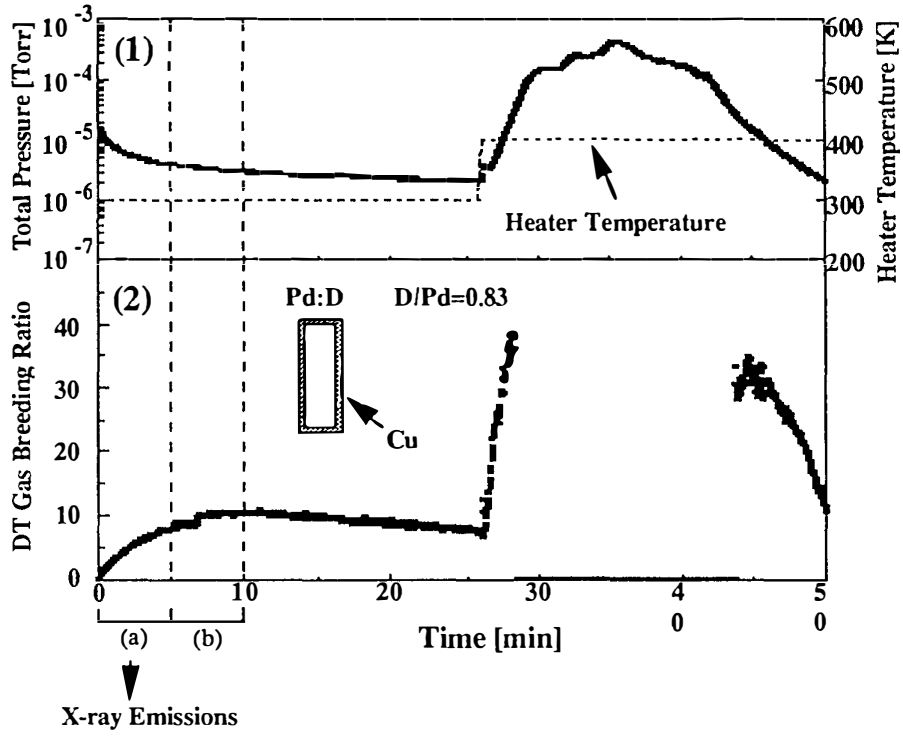

Figure 5 Tritium Production

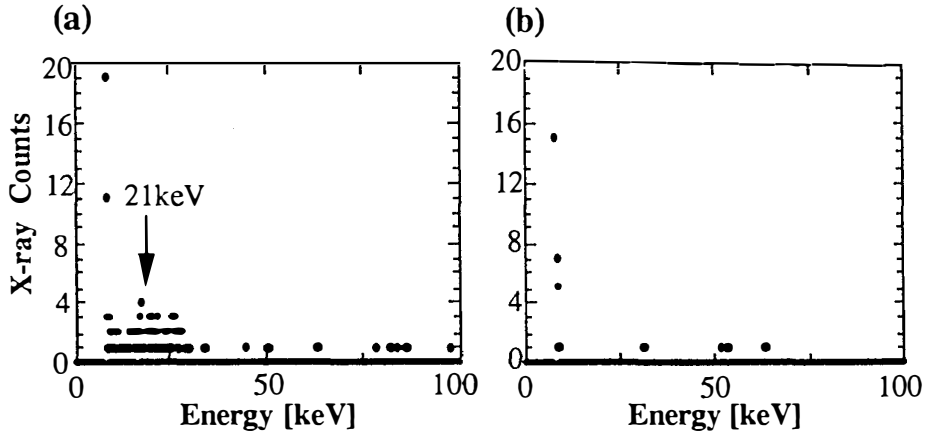

Figure 6 X-ray emission

Figure 6 demonstrates X-ray emission during evacuating. Figure 6-(a) is an energy spectrum for 5 minutes just after the beginning evacuating. This spectrum has a peak around 21keV. Figure 6-(b) is an energy spectrum from 5 to 10 minutes after evacuation. This spectrum has no peak as the spectrum of Figure 6-(a) and the sample radiates no X-ray in this period. Spectra in the other periods are similar to figure 6-(b). We consider that the deuterated palladium sample radiates X-ray that is attributed to K-α characteristic X-ray of palladium.

4. Discussions

We summarize the data of relationship between loading ratio and DT gas breeding ratio (Figure 7), since tritium production has high reproducibility in our experiment. DT gas breeding ratios are evaluated at 1.0×10^{-5} Torr of total pressure after heating. DT gas breeding ratios tend to increase as D/Pd increase and to ascend rapidly around D/Pd≈0.83. Therefore, it seems that DT gas breeding ratio is related to D/Pd; density of D atoms in palladium.

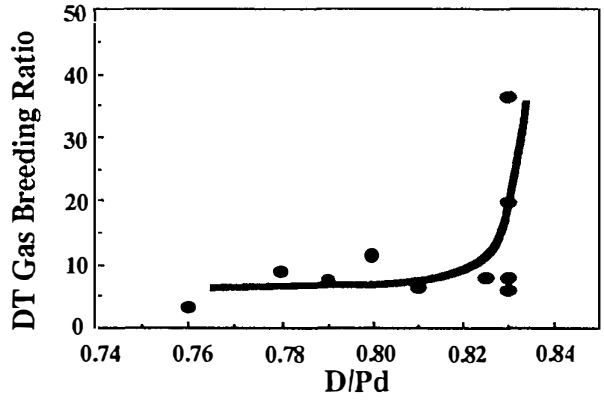

Figure 7 DT gas breeding ratio vs. D/Pd

Figure 8 shows the relation between degassing rate and DT gas breeding ratio. Degassing rate is defined as pressure equation of $Q = V\cdot dp/dt + p\cdot S$. Q; degassing rate, V; chamber volume, p; pressure, and S; the net pumping speed, respectively. The Figure indicates that DT gas breeding ratio increases as the degassing rate increases and saturated at a certain value. Though it is difficult to explain this relationship in detail, at present, degassing rate has a certain correlation with the diffusion process of deuterium

atoms in palladium metals. Therefore, it is probable that tritium production is related to the diffusion process of deuterium atoms in palladium metals.

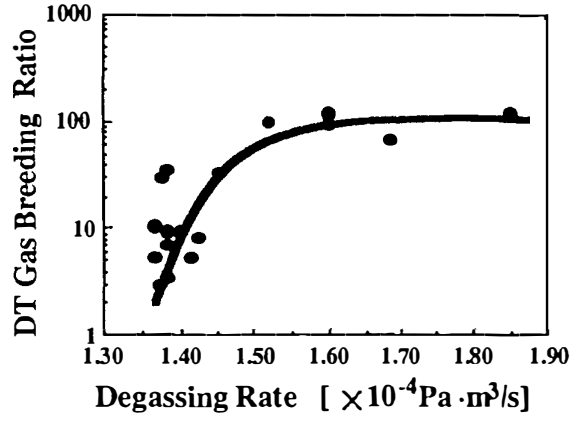

Figure 8 DT gas breeding ratio vs. Degassing rate

5. Conclusion

We performed gas release experiments under vacuum condition with high D/Pd samples obtained by electrochemical loading (D/Pd = 0.73 ~ 0.8). We observed neutron emissions and X-ray (about 21 keV) emissions several times, and tritium production with high reproducibility. DT gas breeding is related to D/Pd and degassing rate. It is considered that some of key factors to induce anomalous nuclear effects in Pd-D_2 systems are density and diffusion process of D atoms in palladium metals.

References

1. M.Fleishman, S.Pons and M.Hawkins, "Electrochemical Induced Nuclear Fusion of Deuterium,"*J.Electroanal.Chem.*, **261**, 301 (1989)

2. Y.Iwamura, T.Itoh and I.Toyoda, "Observation of Anomalous Nuclear Effects in D_2-Pd System," *Proc. of ICCF-4,* Maui, Hawaii, December 6-9,1994, vol.2, p.12. EPRI TR-104188-V3 (1994)

3. Y.Iwamura, N.Gotoh, T.Itoh and I.Toyoda, "Characteristic X-ray and Neutron Emissions from Electrochemically Deuterated Palladium," *Proc. of ICCF-5,* Monte-Carlo, MONACO, April 9-13,1995, to be published

Fifth International Conference on Cold Fusion
9-13 April, 1995 - Monte Carlo, Monaco
ICCF5 ©1995

Characteristic X-ray and Neutron Emissions from Electrochemically Deuterated Palladium

Yasuhiro IWAMURA, Nobuaki GOTOH, Takehiko ITOH and Ichiro TOYODA
Advanced Technology Research Center, Mitsubishi Heavy Industries, Ltd.
1-8-1, Sachiura, Kanazawa-ku, Yokohama, 236, Japan

Abstract

Characteristic x-ray and neutron emissions have been observed during electrochemical loading of deuterium into palladium metal. It shows that anomalous phenomena occur in deuterium-palladium system as shown in our previous paper and the others on cold fusion.

1. Introduction

As we reported in ICCF-4, we observed neutron emissions and tritium productions several times from deuterated palladium samples when the deuterium gas was released by heating them[1]. We started electrochemical loading experiments after ICCF-4, in addition to the gas release experiments with high loading ratio[2]. In this paper, experimental results on x-ray and neutron measurement of electrochemical cells are presented.

2. Experimental

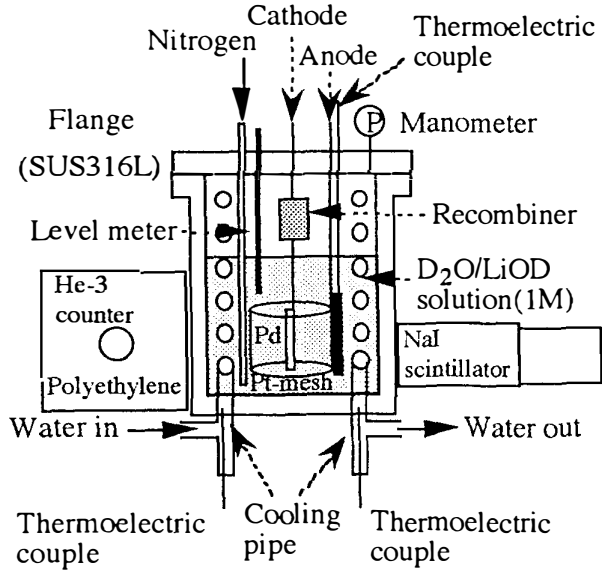

Fig.1 Schematic of Experimental Apparatus

Palladium rods (ϕ3X25mm) were heated and melted in the air by a portable propane burner and cooled down quickly to room temperature(~ 298K) in pure water. After pre-loading (D/Pd ~ 0.66) in deuterium gas, we set the deuterated palladium sample in a closed type of electrochemical cell with 1M LiOD-D_2O solution.

Figure 1 shows the schematic of experimental apparatus. The electrochemical cell consists of a cathode of palladium rod, an anode of platinum mesh, a recombiner and a cooling pipe for measuring excess heat generation. The excess heat was evaluated by the difference between input and output temperature of the water that passed through the cooling pipe. Neutron counting was performed by a He-3 detector with a polyethylene modulator. A NaI scintillation counter was used for both x-ray counting and spectroscopy. All cells and measurement systems are located in a clean-room where temperature and humidity are always kept constant.

3. Results and Discussion

Figure 2 and 3 show experimental results of sample G-10 and G-18, respectively. Horizontal axes mean elapsed time from the beginning of the experiments. X-ray and neutron counts increase clearly as shown in these figures. In Fig.3, neutron emission was observed after several hours from the end of electrolysis. Such phenomena as neutron emissions after electrolysis were observed in the other samples. It is considered that these neutron emissions occurred during diffusion process of deuterium atoms, since it takes about 20 hours to reach equilibrium state.

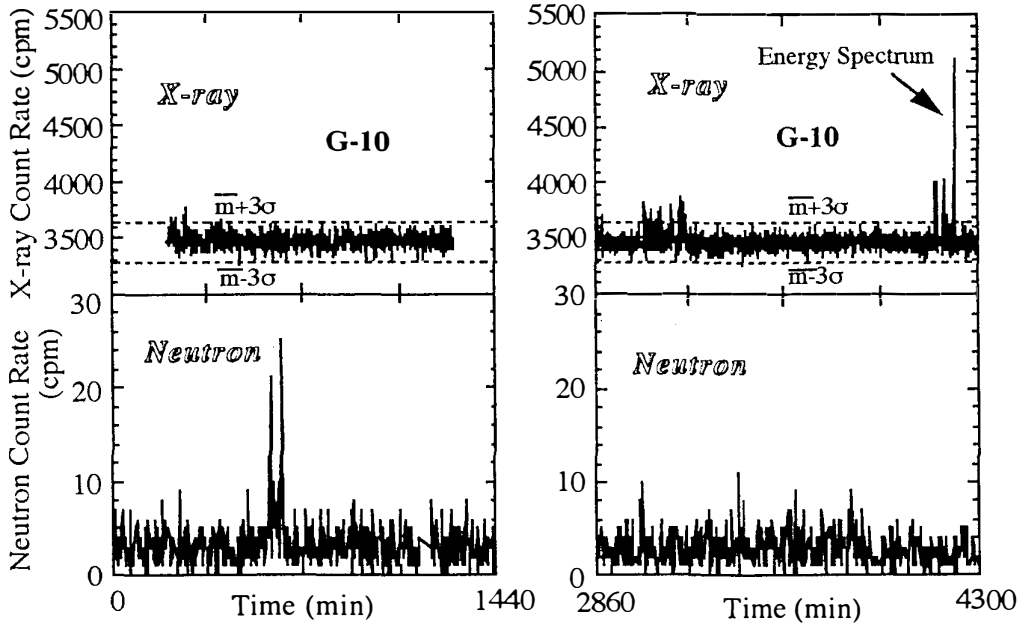

Fig.2 X-ray and neutron emissions from G-10

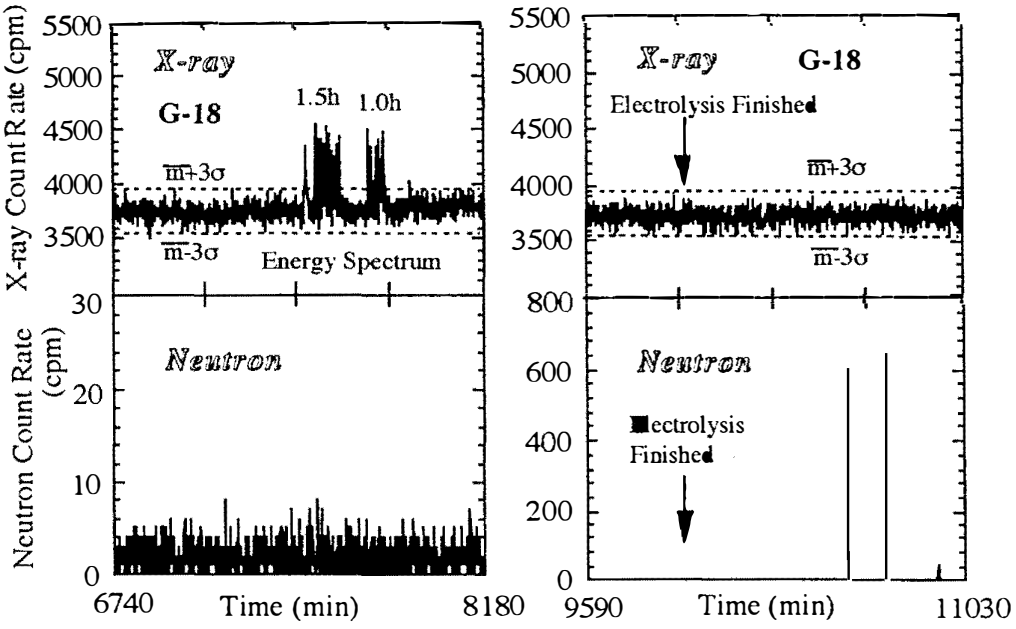

Fig.3 X-ray and neutron emissions from G-18

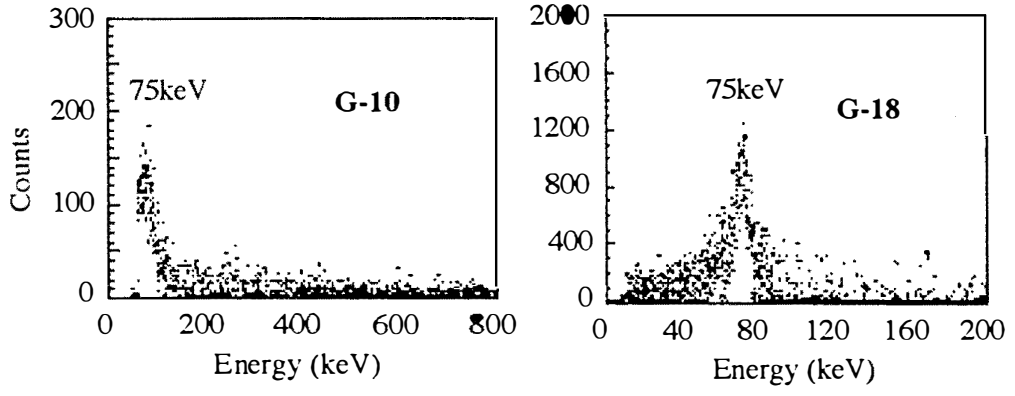

Fig.4 X-ray energy spectra for G-10 and G-18

It should be recognized that we have no correlation between x-ray and neutron emissions by our experimental data. Therefore, it can be said that x-ray and neutron are generated by different reactions.

Figure 4 shows the results of x-ray spectroscopy for the counting data in Fig.2 and 3. We subtract background x-ray data from foreground. Clear peaks can be seen around at the energy of 75keV in both cases.

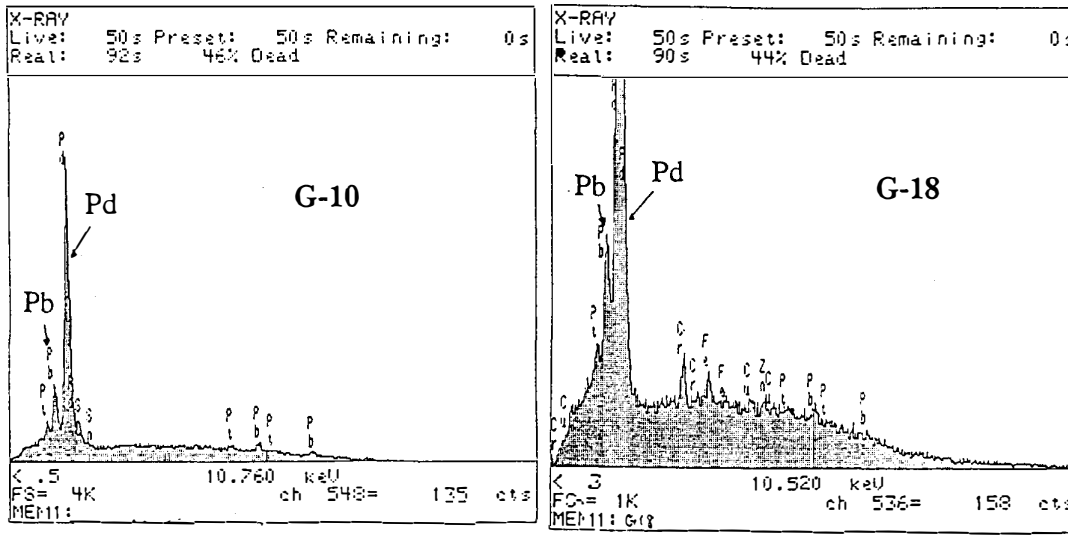

Fig.5 Analysis of electrode surfaces of G-10 and G-18 by EPMA

Figure 5 shows the results of analysis of electrode surfaces of G-10 and G-18 by EPMA. We found much Pb atoms on the palladium cathode after the electrolysis. No Pb atoms have been detected except G-10 and G-18. It should be noticed that the energy of K-α characteristic x-ray of Pb is about 75keV. Therefore Pb atoms detected on the Pd electrodes correspond to the x-ray energy observed during these experiments as shown in Fig.4.

4. Concluding Remarks

Characteristic x-ray and neutron emissions were observed during electrochemical loading of deuterium into palladium metal. We can say that anomalous nuclear reactions must occur and induce characteristic x-ray and neutron emissions in the electrochemical cells at room temperature.

References

1. Y.Iwamura,T.Itoh and I.Toyoda,"Observation of Anomalous Nuclear Effects in D_2-Pd System", *Proc. of ICCF-4,* Maui, Hawaii, December 6-9,1994, vol.2, p.12. EPRI TR-104188-V3 (1994)

2. T.Itoh, Y.Iwamura, N.Gotoh and I.Toyoda, "Observation of Nulear Products under vaccum conditon from deterated palladium with high loading ratio" , to be published in the present proceedings